

This Page Is Inserted by IFW Operations  
and is not a part of the Official Record

## **BEST AVAILABLE IMAGES**

Defective images within this document are accurate representations of the original documents submitted by the applicant.

Defects in the images may include (but are not limited to):

- BLACK BORDERS
- TEXT CUT OFF AT TOP, BOTTOM OR SIDES
- FADED TEXT
- ILLEGIBLE TEXT
- SKEWED/SLANTED IMAGES
- COLORED PHOTOS
- BLACK OR VERY BLACK AND WHITE DARK PHOTOS
- GRAY SCALE DOCUMENTS

**IMAGES ARE BEST AVAILABLE COPY.**

**As rescanning documents *will not* correct images,  
please do not report the images to the  
Image Problem Mailbox.**

GNE.2930R1C3



PATENT

**IN THE UNITED STATES PATENT AND TRADEMARK OFFICE**

Applicant : Botstein, et al.  
Appl. No. : 10/032,996  
Filed : December 27, 2001  
For : SECRETED AND  
TRANSMEMBRANE  
POLYPEPTIDES AND NUCLEIC  
ACIDS ENCODING THE SAME  
Examiner : Fredman, J.  
Group Art Unit : 1634

DECLARATION OF PAUL POLAKIS, PH.D. UNDER 37 C.F.R. § 1.132

Commissioner for Patents  
P.O. Box 1450  
Alexandria, VA 22313-1450

Dear Sir:

Attached is the Declaration of Paul Polakis, Ph.D.

Respectfully submitted,

KNOBBE, MARTENS, OLSON & BEAR, LLP

Dated: June 16, 2004

By: AnneMarie Kaiser  
AnneMarie Kaiser  
Registration No. 37,649  
Attorney of Record  
Customer No. 30,313  
(619) 235-8550

S:\DOCS\BSG\BSG-1215.DOC  
061404



## DECLARATION OF PAUL POLAKIS, Ph.D.

I, Paul Polakis, Ph.D., declare and say as follows:

1. I was awarded a Ph.D. by the Department of Biochemistry of the Michigan State University in 1984. My scientific Curriculum Vitae is attached to and forms part of this Declaration (Exhibit A).
2. I am currently employed by Genentech, Inc. where my job title is Staff Scientist. Since joining Genentech in 1999, one of my primary responsibilities has been leading Genentech's Tumor Antigen Project, which is a large research project with a primary focus on identifying tumor cell markers that find use as targets for both the diagnosis and treatment of cancer in humans.
3. As part of the Tumor Antigen Project, my laboratory has been analyzing differential expression of various genes in tumor cells relative to normal cells. The purpose of this research is to identify proteins that are abundantly expressed on certain tumor cells and that are either (i) not expressed, or (ii) expressed at lower levels, on corresponding normal cells. We call such differentially expressed proteins "tumor antigen proteins". When such a tumor antigen protein is identified, one can produce an antibody that recognizes and binds to that protein. Such an antibody finds use in the diagnosis of human cancer and may ultimately serve as an effective therapeutic in the treatment of human cancer.
4. In the course of the research conducted by Genentech's Tumor Antigen Project, we have employed a variety of scientific techniques for detecting and studying differential gene expression in human tumor cells relative to normal cells, at genomic DNA, mRNA and protein levels. An important example of one such technique is the well known and widely used technique of microarray analysis which has proven to be extremely useful for the identification of mRNA molecules that are differentially expressed in one tissue or cell type relative to another. In the course of our research using microarray analysis, we have identified approximately 200 gene transcripts that are present in human tumor cells at significantly higher levels than in corresponding normal human cells. To date, we have generated antibodies that bind to about 30 of the tumor antigen proteins expressed from these differentially expressed gene transcripts and have used these antibodies to quantitatively determine the level of production of these tumor antigen proteins in both human cancer cells and corresponding normal cells. We have then compared the levels of mRNA and protein in both the tumor and normal cells analyzed.
5. From the mRNA and protein expression analyses described in paragraph 4 above, we have observed that there is a strong correlation between changes in the level of mRNA present in any particular cell type and the level of protein

expressed from that mRNA in that cell type. In approximately 80% of our observations we have found that increases in the level of a particular mRNA correlates with changes in the level of protein expressed from that mRNA when human tumor cells are compared with their corresponding normal cells.

6. Based upon my own experience accumulated in more than 20 years of research, including the data discussed in paragraphs 4 and 5 above and my knowledge of the relevant scientific literature, it is my considered scientific opinion that for human genes, an increased level of mRNA in a tumor cell relative to a normal cell typically correlates to a similar increase in abundance of the encoded protein in the tumor cell relative to the normal cell. In fact, it remains a central dogma in molecular biology that increased mRNA levels are predictive of corresponding increased levels of the encoded protein. While there have been published reports of genes for which such a correlation does not exist, it is my opinion that such reports are exceptions to the commonly understood general rule that increased mRNA levels are predictive of corresponding increased levels of the encoded protein.

7. I hereby declare that all statements made herein of my own knowledge are true and that all statements made on information or belief are believed to be true, and further that these statements were made with the knowledge that willful false statements and the like so made are punishable by fine or imprisonment, or both, under Section 1001 of Title 18 of the United States Code and that such willful statements may jeopardize the validity of the application or any patent issued thereon.

Dated: 5/07/04

By: Paul Polakis

Paul Polakis, Ph.D.

## CURRICULUM VITAE

PAUL G. POLAKIS  
Staff Scientist  
Genentech, Inc  
1 DNA Way, MS#40  
S. San Francisco, CA 94080

### EDUCATION:

Ph.D., Biochemistry, Department of Biochemistry,  
Michigan State University (1984)

B.S., Biology. College of Natural Science, Michigan State University (1977)

### PROFESSIONAL EXPERIENCE:

2002-present	Staff Scientist, Genentech, Inc S. San Francisco, CA
1999- 2002	Senior Scientist, Genentech, Inc., S. San Francisco, CA
1997 -1999	Research Director Onyx Pharmaceuticals, Richmond, CA
1992- 1996	Senior Scientist, Project Leader, Onyx Pharmaceuticals, Richmond, CA
1991-1992	Senior Scientist, Chiron Corporation, Emeryville, CA.
1989-1991	Scientist, Cetus Corporation, Emeryville CA.
1987-1989	Postdoctoral Research Associate, Genentech, Inc., South San Francisco, CA.
1985-1987	Postdoctoral Research Associate, Department of Medicine, Duke University Medical Center, Durham, NC

1984-1985

Assistant Professor, Department of Chemistry,  
Oberlin College, Oberlin, Ohio

1980-1984

Graduate Research Assistant, Department of  
Biochemistry, Michigan State University  
East Lansing, Michigan

### **PUBLICATIONS:**

1. **Polakis, P. G.** and Wilson, J. E. 1982 Purification of a Highly Bindable Rat Brain Hexokinase by High Performance Liquid Chromatography. **Biochem. Biophys. Res. Commun.** 107, 937-943.
2. **Polakis, P.G.** and Wilson, J. E. 1984 Proteolytic Dissection of Rat Brain Hexokinase: Determination of the Cleavage Pattern during Limited Digestion with Trypsin. **Arch. Biochem. Biophys.** 234, 341-352.
3. **Polakis, P. G.** and Wilson, J. E. 1985 An Intact Hydrophobic N-Terminal Sequence is Required for the Binding Rat Brain Hexokinase to Mitochondria. **Arch. Biochem. Biophys.** 236, 328-337.
4. Uhing, R.J., **Polakis, P.G.** and Snyderman, R. 1987 Isolation of GTP-binding Proteins from Myeloid HL60 Cells. **J. Biol. Chem.** 262, 15575-15579.
5. **Polakis, P.G.**, Uhing, R.J. and Snyderman, R. 1988 The Formylpeptide Chemoattractant Receptor Copurifies with a GTP-binding Protein Containing a Distinct 40 kDa Pertussis Toxin Substrate. **J. Biol. Chem.** 263, 4969-4979.
6. Uhing, R. J., Dillon, S., **Polakis, P. G.**, Truett, A. P. and Snyderman, R. 1988 Chemoattractant Receptors and Signal Transduction Processes in Cellular and Molecular Aspects of Inflammation ( Poste, G. and Crooke, S. T. eds.) pp 335-379.
7. **Polakis, P.G.**, Evans, T. and Snyderman 1989 Multiple Chromatographic Forms of the Formylpeptide Chemoattractant Receptor and their Relationship to GTP-binding Proteins. **Biochem. Biophys. Res. Commun.** 161, 276-283.
8. **Polakis, P. G.**, Snyderman, R. and Evans, T. 1989 Characterization of G25K, a GTP-binding Protein Containing a Novel Putative Nucleotide Binding Domain. **Biochem. Biophys. Res. Commun.** 160, 25-32.
9. **Polakis, P.**, Weber, R.F., Nevins, B., Didsbury, J. Evans, T. and Snyderman, R. 1989 Identification of the ral and rac1 Gene Products, Low Molecular Mass GTP-binding Proteins from Human Platelets. **J. Biol. Chem.** 264, 16383-16389.
10. Snyderman, R., Perianin, A., Evans, T., **Polakis, P.** and Didsbury, J. 1989 G Proteins and Neutrophil Function. In ADP-Ribosylating Toxins and G Proteins: Insights into Signal Transduction. ( J. Moss and M. Vaughn, eds.) Amer. Soc. Microbiol. pp. 295-323.

11. Hart, M.J., **Polakis, P.G.**, Evans, T. and Cerrione, R.A. 1990 The Identification and Characterization of an Epidermal Growth Factor-Stimulated Phosphorylation of a Specific Low Molecular Mass GTP-binding Protein in a Reconstituted Phospholipid Vesicle System. **J. Biol. Chem.** 265, 5990-6001.
12. Yatani, A., Okabe, K., **Polakis, P.** Halenbeck, R. McCormick, F. and Brown, A. M. 1990 ras p21 and GAP Inhibit Coupling of Muscarinic Receptors to Atrial K<sup>+</sup> Channels. **Cell.** 61, 769-776.
13. Munemitsu, S., Innis, M.A., Clark, R., McCormick, F., Ullrich, A. and **Polakis, P.G.** 1990 Molecular Cloning and Expression of a G25K cDNA, the Human Homolog of the Yeast Cell Cycle Gene CDC42. **Mol. Cell. Biol.** 10, 5977-5982.
14. **Polakis, P.G.** Rubinfeld, B. Evans, T. and McCormick, F. 1991 Purification of Plasma Membrane-Associated GTPase Activating Protein (GAP) Specific for rap-1/krev-1 from HL60 Cells. **Proc. Natl. Acad. Sci. USA** 88, 239-243.
15. Moran, M. F., **Polakis, P.**, McCormick, F., Pawson, T. and Ellis, C. 1991 Protein Tyrosine Kinases Regulate the Phosphorylation, Protein Interactions, Subcellular Distribution, and Activity of p21ras GTPase Activating Protein. **Mol. Cell. Biol.** 11, 1804-1812
16. Rubinfeld, B., Wong, G., Bekesi, E. Wood, A. McCormick, F. and **Polakis, P. G.** 1991 A Synthetic Peptide Corresponding to a Sequence in the GTPase Activating Protein Inhibits p21<sup>ras</sup> Stimulation and Promotes Guanine Nucleotide Exchange. **Internatl. J. Peptide and Prot. Res.** 38, 47-53.
17. Rubinfeld, B., Munemitsu, S., Clark, R., Conroy, L., Watt, K., Crosier, W., McCormick, F., and **Polakis, P.** 1991 Molecular Cloning of a GTPase Activating Protein Specific for the Krev-1 Protein p21<sup>rap1</sup>. **Cell** 65, 1033-1042.
18. Zhang, K. Papageorge, A., G., Martin, P., Vass, W. C., Olah, Z., **Polakis, P.**, McCormick, F. and Lowy, D, R. 1991 Heterogenous Amino Acids in RAS and Rap1A Specifying Sensitivity to GAP Proteins. **Science** 254, 1630-1634.
19. Martin, G., Yatani, A., Clark, R., **Polakis, P.**, Brown, A. M. and McCormick, F. 1992 GAP Domains Responsible for p21<sup>ras</sup>-dependent Inhibition of Muscarinic Atrial K<sup>+</sup> Channel Currents. **Science** 255, 192-194.
20. McCormick, F., Martin, G. A., Clark, R., Bollag, G. and **Polakis, P.** 1992 Regulation of p21ras by GTPase Activating Proteins. Cold Spring Harbor **Symposia on Quantitative Biology**. Vol. 56, 237-241.
21. Pronk, G. B., **Polakis, P.**, Wong, G., deVries-Smits, A. M., Bos J. L. and McCormick, F. 1992 p60<sup>v-src</sup> Can Associate with and Phosphorylate the p21<sup>ras</sup> GTPase Activating Protein. **Oncogene** 7,389-394.
22. **Polakis P.** and McCormick, F. 1992 Interactions Between p21<sup>ras</sup> Proteins and Their GTPase Activating Proteins. In **Cancer Surveys** ( Franks, L. M., ed.) 12, 25-42.

23. Wong, G., Muller, O., Clark, R., Conroy, L., Moran, M., **Polakis, P.** and McCormick, F. 1992 Molecular cloning and nucleic acid binding properties of the GAP-associated tyrosine phosphoprotein p62. **Cell** 69, 551-558.
24. **Polakis, P.**, Rubinfeld, B. and McCormick, F. 1992 Phosphorylation of rap1GAP in vivo and by cAMP-dependent Kinase and the Cell Cycle p34<sup>cdc2</sup> Kinase in vitro. **J. Biol. Chem.** 267, 10780-10785.
25. McCabe, P.C., Haubrauck, H., **Polakis, P.**, McCormick, F., and Innis, M. A. 1992 Functional Interactions Between p21<sup>rap1A</sup> and Components of the Budding pathway of *Saccharomyces cerevisiae*. **Mol. Cell. Biol.** 12, 4084-4092.
26. Rubinfeld, B., Crosier, W.J., Albert, I., Conroy, L., Clark, R., McCormick, F. and **Polakis, P.** 1992 Localization of the rap1GAP Catalytic Domain and Sites of Phosphorylation by Mutational Analysis. **Mol. Cell . Biol.** 12, 4634-4642.
27. Ando, S., Kaibuchi, K., Sasaki, K., Hiraoka, T., Nishiyama, T., Mizuno, T., Asada, M., Nunoi, H., Matsuda, I., Matsuura, Y., **Polakis, P.**, McCormick, F. and Takai, Y. 1992 Post-translational processing of rac p21s is important both for their interaction with the GDP/GTP exchange proteins and for their activation of NADPH oxidase. **J. Biol. Chem.** 267, 25709-25713.
28. Janoueix-Lerosey, I., **Polakis, P.**, Tavitian, A. and deGunzberg, J. 1992 Regulation of the GTPase activity of the ras-related rap2 protein. **Biochem. Biophys. Res. Commun.** 189, 455-464.
29. **Polakis, P.** 1993 GAPs Specific for the rap1/Krev-1 Protein. in GTP-binding Proteins: the ras-superfamily. ( J.C. LaCale and F. McCormick, eds.) 445-452.
30. **Polakis, P.** and McCormick, F. 1993 Structural requirements for the interaction of p21<sup>ras</sup> with GAP, exchange factors, and its biological effector target. **J. Biol Chem.** 268, 9157-9160.
31. Rubinfeld, B., Souza, B. Albert, I., Muller, O., Chamberlain, S., Masiarz, F., Munemitsu, S. and **Polakis, P.** 1993 Association of the APC gene product with beta- catenin. **Science** 262, 1731-1734.
32. Weiss, J., Rubinfeld, B., **Polakis, P.**, McCormick, F. Cavenee, W. A. and Arden, K. 1993 The gene for human rap1-GTPase activating protein (rap1GAP) maps to chromosome 1p35-1p36.1. **Cytogenet. Cell Genet.** 66, 18-21.
33. Sato, K. Y., **Polakis, P.**, Haubruck, H., Fasching, C. L., McCormick, F. and Stanbridge, E. J. 1994 Analysis of the tumor suppressor activity of the K-rev gene in human tumor cell lines. **Cancer Res.** 54, 552-559.
34. Janoueix-Lerosey, I., Fontenay, M., Tobelem, G., Tavitian, A., **Polakis, P.** and DeGunzburg, J. 1994 Phosphorylation of rap1GAP during the cell cycle. **Biochem. Biophys. Res. Commun.** 202, 967-975
35. Munemitsu, S., Souza, B., Mueller, O., Albert, I., Rubinfeld, B., and **Polakis, P.** 1994 The APC gene product associates with microtubules in vivo and affects their assembly in vitro. **Cancer Res.** 54, 3676-3681.

36. Rubinfeld, B. and **Polakis, P.** 1995 Purification of baculovirus produced rap1GAP. **Methods Enz.** 255,31
37. **Polakis, P.** 1995 Mutations in the APC gene and their implications for protein structure and function. **Current Opinions in Genetics and Development** 5, 66-71
38. Rubinfeld, B., Souza, B., Albert, I., Munemitsu, S. and **Polakis P.** 1995 The APC protein and E-cadherin form similar but independent complexes with  $\alpha$ -catenin,  $\beta$ -catenin and Plakoglobin. **J. Biol. Chem.** 270, 5549-5555
39. Munemitsu, S., Albert, I., Souza, B., Rubinfeld, B., and **Polakis, P.** 1995 Regulation of intracellular  $\beta$ -catenin levels by the APC tumor suppressor gene. **Proc. Natl. Acad. Sci.** 92, 3046-3050.
40. Lock, P., Fumagalli, S., **Polakis, P.** McCormick, F. and Courtneidge, S. A. 1996 The human p62 cDNA encodes Sam68 and not the rasGAP-associated p62 protein. **Cell** 84, 23-24.
41. Papkoff, J., Rubinfeld, B., Schryver, B. and **Polakis, P.** 1996 Wnt-1 regulates free pools of catenins and stabilizes APC-catenin complexes. **Mol. Cell. Biol.** 16, 2128-2134.
42. Rubinfeld, B., Albert, I., Porfiri, E., Fiol, C., Munemitsu, S. and **Polakis, P.** 1996 Binding of GSK3 $\beta$  to the APC- $\beta$ -catenin complex and regulation of complex assembly. **Science** 272, 1023-1026.
43. Munemitsu, S., Albert, I., Rubinfeld, B. and **Polakis, P.** 1996 Deletion of amino-terminal structure stabilizes  $\beta$ -catenin in vivo and promotes the hyperphosphorylation of the APC tumor suppressor protein. **Mol. Cell. Biol.** 16, 4088-4094.
44. Hart, M. J., Callow, M. G., Sousa, B. and **Polakis P.** 1996 IQGAP1, a calmodulin binding protein with a rasGAP related domain, is a potential effector for cdc42Hs. **EMBO J.** 15, 2997-3005.
45. Nathke, I. S., Adams, C. L., **Polakis, P.**, Sellin, J. and Nelson, W. J. 1996 The adenomatous polyposis coli (APC) tumor suppressor protein is localized to plasma membrane sites involved in active epithelial cell migration. **J. Cell. Biol.** 134, 165-180.
46. Hart, M. J., Sharma, S., elMasry, N., Qui, R-G., McCabe, P., **Polakis, P.** and Bollag, G. 1996 Identification of a novel guanine nucleotide exchange factor for the rho GTPase. **J. Biol. Chem.** 271, 25452.
47. Thomas JE, Smith M, Rubinfeld B, Gutowski M, Beckmann RP, and **Polakis P.** 1996 Subcellular localization and analysis of apparent 180-kDa and 220-kDa proteins of the breast cancer susceptibility gene, BRCA1. **J. Biol. Chem.** 1996 271, 28630-28635
48. Hayashi, S., Rubinfeld, B., Souza, B., **Polakis, P.**, Wieschaus, E., and Levine, A. 1997 A Drosophila homolog of the tumor suppressor adenomatous polyposis coli

down-regulates  $\beta$ -catenin but its zygotic expression is not essential for the regulation of armadillo. **Proc. Natl. Acad. Sci.** 94, 242-247.

49. Vleminckx, K., Rubinfeld, B., **Polakis, P.** and Gumbiner, B. 1997 The APC tumor suppressor protein induces a new axis in *Xenopus* embryos. **J. Cell. Biol.** 136, 411-420.

50. Rubinfeld, B., Robbins, P., El-Gamil, M., Albert, I., Porfiri, P. and **Polakis, P.** 1997 Stabilization of  $\beta$ -catenin by genetic defects in melanoma cell lines. **Science** 275, 1790-1792.

51. **Polakis, P.** The adenomatous polyposis coli (APC) tumor suppressor. 1997 **Biochem. Biophys. Acta**, 1332, F127-F147.

52. Rubinfeld, B., Albert, I., Porfiri, E., Munemitsu, S., and **Polakis, P.** 1997 Loss of  $\beta$ -catenin regulation by the APC tumor suppressor protein correlates with loss of structure due to common somatic mutations of the gene. **Cancer Res.** 57, 4624-4630.

53. Porfiri, E., Rubinfeld, B., Albert, I., Hovanes, K., Waterman, M., and **Polakis, P.** 1997 Induction of a  $\beta$ -catenin-LEF-1 complex by wnt-1 and transforming mutants of  $\beta$ -catenin. **Oncogene** 15, 2833-2839.

54. Thomas JE, Smith M, Tonkinson JL, Rubinfeld B, and **Polakis P.**, 1997 Induction of phosphorylation on BRCA1 during the cell cycle and after DNA damage. **Cell Growth Differ.** 8, 801-809.

55. Hart, M., de los Santos, R., Albert, I., Rubinfeld, B., and **Polakis P.**, 1998 Down regulation of  $\beta$ -catenin by human Axin and its association with the adenomatous polyposis coli (APC) tumor suppressor,  $\beta$ -catenin and glycogen synthase kinase 3 $\beta$ . **Current Biology** 8, 573-581.

56. **Polakis, P.** 1998 The oncogenic activation of  $\beta$ -catenin. **Current Opinions in Genetics and Development** 9, 15-21

57. Matt Hart, Jean-Paul Concordet, Irina Lassot, Iris Albert, Rico del los Santos, Herve Durand, Christine Perret, Bonnee Rubinfeld, Florence Margottin, Richard Benarous and **Paul Polakis.** 1999 The F-box protein  $\beta$ -TrCP associates with phosphorylated  $\beta$ -catenin and regulates its activity in the cell. **Current Biology** 9, 207-10.

58. Howard C. Crawford, Barbara M. Fingleton, Bonnee Rubinfeld, **Paul Polakis** and Lynn M. Matrisian 1999 The metalloproteinase matrilysin is a target of  $\beta$ -catenin transactivation in intestinal tumours. **Oncogene** 18, 2883-91.

59. Meng J, Glick JL, **Polakis P.**, Casey PJ. 1999 Functional interaction between Galpha(z) and Rap1GAP suggests a novel form of cellular cross-talk. **J Biol Chem.** 17, 36663-9

60. Vijayasurian Easwaran, Virginia Song, **Paul Polakis** and Steve Byers 1999 The ubiquitin-proteosome pathway and serine kinase activity modulate APC mediated regulation of  $\beta$ -catenin-LEF signaling. **J. Biol. Chem.** 274(23):16641-5.
- 61 **Polakis P**, Hart M and Rubinfeld B. 1999 Defects in the regulation of beta-catenin in colorectal cancer. **Adv Exp Med Biol.** 470, 23-32
- 62 Shen Z, Batzer A, Koehler JA, **Polakis P**, Schlessinger J, Lydon NB, Moran MF. 1999 Evidence for SH3 domain directed binding and phosphorylation of Sam68 by Src. **Oncogene.** 18, 4647-53
64. Thomas GM, Frame S, Goedert M, Nathke I, **Polakis P**, Cohen P. 1999 A GSK3- binding peptide from FRAT1 selectively inhibits the GSK3-catalysed phosphorylation of axin and beta-catenin. **FEBS Lett.** 458, 247-51.
65. Peifer M, **Polakis P**. 2000 Wnt signaling in oncogenesis and embryogenesis--a look outside the nucleus. **Science** 287,1606-9.
66. **Polakis P**. 2000 Wnt signaling and cancer. **Genes Dev**;14, 1837-1851.
67. Spink KE, **Polakis P**, Weis WI 2000 Structural basis of the Axin-adenomatous polyposis coli interaction. **EMBO J** 19, 2270-2279.
68. Szeto , W., Jiang, W., Tice, D.A., Rubinfeld, B., Hollingshead, P.G., Fong, S.E., Dugger, D.L., Pham, T., Yansura, D.E., Wong, T.A., Grimaldi, J.C., Corpuz, R.T., Singh J.S., Frantz, G.D., Devaux, B., Crowley, C.W., Schwall, R.H., Eberhard, D.A., Rastelli, L., **Polakis, P.** and Pennica, D. 2001 Overexpression of the Retinoic Acid-Responsive Gene Stra6 in Human Cancers and its Synergistic Induction by Wnt-1 and Retinoic Acid. **Cancer Res** 61, 4197-4204.
69. Rubinfeld B, Tice DA, **Polakis P**. 2001 Axin dependent phosphorylation of the adenomatous polyposis coli protein mediated by casein kinase 1 epsilon. **J Biol Chem** 276, 39037-39045.
70. **Polakis P**. 2001 More than one way to skin a catenin. **Cell** 2001 105, 563-566.
71. Tice DA, Soloviev I, **Polakis P**. 2002 Activation of the Wnt Pathway Interferes with Serum Response Element-driven Transcription of Immediate Early Genes. **J Biol. Chem.** 277, 6118-6123.
72. Tice DA, Szeto W, Soloviev I, Rubinfeld B, Fong SE, Dugger DL, Winer J,

Williams PM, Wieand D, Smith V, Schwall RH, Pennica D, **Polakis P**. 2002 Synergistic activation of tumor antigens by wnt-1 signaling and retinoic acid revealed by gene expression profiling. **J Biol Chem**. 277,14329-14335.

73. **Polakis, P**. 2002 Casein kinase I: A wnt'er of disconnect. **Curr. Biol**. 12, R499.

74. Mao, W. , Luis, E., Ross, S., Silva, J., Tan, C., Crowley, C., Chui, C., Franz, G., Senter, P., Koeppen, H., **Polakis, P**. 2004 EphB2 as a therapeutic antibody drug target for the treatment of colorectal cancer. **Cancer Res**. 64, 781-788.

75. Shibamoto, S., Winer, J., Williams, M., Polakis, P. 2003 A Blockade in Wnt signaling is activated following the differentiation of F9 teratocarcinoma cells. **Exp. Cell Res**. 29211-20.

76. Zhang Y, Eberhard DA, Frantz GD, Dowd P, Wu TD, Zhou Y, Watanabe C, Luoh SM, **Polakis P**, Hillan KJ, Wood WI, Zhang Z. 2004 GEPIs--quantitative gene expression profiling in normal and cancer tissues. **Bioinformatics**, April 8



GNE.3230R1C1

PATENT

IN THE UNITED STATES PATENT AND TRADEMARK OFFICE

Applicant : Eaton, et al.  
Appl. No. : 10/006867  
Filed : December 6, 2001  
For : SECRETED AND  
TRANSMEMBRANE  
POLYPEPTIDES AND NUCLEIC  
ACIDS ENCODING THE SAME  
Examiner : Helms L.  
Group Art Unit : 1642

COPY

DECLARATION OF J. CHRISTOPHER GRIMALDI, UNDER 37 C.F.R. §1.132

Commissioner for Patents  
P.O. Box 1450  
Alexandria, VA 22313-1450

I, J. Christopher Grimaldi, declare and say as follows:

1. I am a Senior Research Associate in the Molecular Biology Department of Genentech, Inc., South San Francisco, CA 94080.
2. I joined Genentech in January of 1999. From 1999 to 2003, I directed the Cloning Laboratory in the Molecular Biology Department. During this time I directed or performed numerous molecular biology techniques including qualitative Polymerase Chain Reaction (PCR) analyses. I am currently involved, among other projects, in the isolation of genes coding for membrane associated proteins which can be used as targets for antibody therapeutics against cancer. In connection with the above-identified patent application, I personally performed or directed the qualitative PCR analyses in the assay entitled "Tumor Versus Normal Differential Tissue Expression Distribution" which is described in EXAMPLE 18 in the specification that were used to identify differences in gene expression between tumor tissue and their normal counterparts.
3. My scientific Curriculum Vitae, including my list of publications, is attached to and forms part of this Declaration (Exhibit A).
4. Chromosomal aberrations, such as gene amplification, and chromosomal translocations are important markers of specific types of cancer and lead to the aberrant expression of specific genes and their encoded polypeptides. Gene amplification is a process in which specific regions of a chromosome are duplicated, thus creating multiple copies of certain genes that normally exist as a single copy. In addition, chromosomal translocations occur when

two different chromosomes break and are rejoined to each other chromosome resulting in a chimeric chromosome which displays a different expression pattern relative to the parent chromosomes. Amplification of certain genes such as Her2/Neu [Singleton *et al.*, Pathol. Annu., 27Pt1:165-190], or chromosomal translocations such as t(5;14), [Grimaldi *et al.*, Blood, 73(8):2081-2085(1989); Meeker *et al.*, Blood, 76(2):285-289(1990)] give cancer cells a growth or survival advantage relative to normal cells, and might also provide a mechanism of tumor cell resistance to chemotherapy or radiotherapy. If the chromosomal aberration results in the aberrant expression of a mRNA and the corresponding gene product (the polypeptide), as they do in the aforementioned cases, then the gene product is a promising target for cancer therapy, for example, by the therapeutic antibody approach.

5. Those who work in this field are well aware that in the vast majority of cases, when a gene is over-expressed, as evidenced by an increased production of mRNA, the gene product or polypeptide will also be over-expressed. It is unlikely that one identifies increased mRNA expression without associated increased protein expression. Stated in another way, two cell samples which have differing mRNA concentrations for a specific gene are expected to have correspondingly different concentration of protein for that gene. Techniques used to detect mRNA, such as Northern Blotting, Differential Display, *in situ* hybridization, quantitative PCR, Taqman, and more recently Microarray technology all rely on the dogma that a change in mRNA will represent a similar change in protein. If this dogma did not hold true then these techniques would have little value and not be so widely used. The use of mRNA quantitation techniques have identified a seemingly endless number of genes which are differentially expressed in various tissues and these genes have subsequently been shown to have correspondingly similar changes in their protein levels. Thus, the detection of increased mRNA expression is expected to result in increased polypeptide expression. The detection of increased polypeptide expression can be used for cancer diagnosis and treatment.

6. However, even in the rare case where the protein expression does not correlate with the mRNA expression, this still provides significant information useful for cancer diagnosis and treatment. For example, if over-expression of a gene product does not correlate with over-expression of mRNA in certain tumor types but does so in others, then identification of both gene expression and protein expression enables more accurate tumor classification and hence better determination of suitable therapy. In addition, absence of over-expression of the gene product in the presence of a particular over-expression of mRNA is crucial information for the practicing clinician. If a gene is over-expressed but the corresponding gene product is not significantly over-expressed, the clinician accordingly will decide not to treat a patient with agents that target that gene product.

7. I hereby declare that all statements made herein of my own knowledge are true and that all statements made on information or belief are believed to be true, and further that these statements were made with the knowledge that willful false statements and the like so made are punishable by fine or imprisonment, or both, under Section 1001 of Title 18 of the United States Code and that such willful statements may jeopardize the validity of the application or any patent issued thereon.

Appl. No.  
Filed

: 10/006867  
: December 6, 2001

By: \_\_\_\_\_

J. Christopher Grimaldi,

Date: \_\_\_\_\_

12/8/2003

## **J. Christopher Grimaldi**

1434-36<sup>th</sup> Ave.  
San Francisco, CA 94122  
(415) 681-1639 (Home)

### **EDUCATION**

University of California, Berkeley  
Bachelor of Arts in Molecular Biology, 1984

### **EMPLOYMENT EXPERIENCE**

#### **SRA**

Genentech Inc., South San Francisco; 1/99 to present

Previously, was responsible to direct and manage the Cloning Lab. Currently focused on isolating cancer specific genes for the Tumor Antigen (TAP), and Secreted Tumor Protein (STOP) projects for the Oncology Department as well as Immunologically relevant genes for the Immunology Department. Directed a lab of 6 scientists focused on a company-wide team effort to identify and isolate secreted proteins for potential therapeutic use (SPDI). For the SPDI project my duties were, among other things, the critically important coordination of the cloning of thousands of putative genes, by developing a smooth process of communication between the Bioinformatics, Cloning, Sequencing, and Legal teams. Collaborated with several groups to discover novel genes through the Curagen project, a unique differential display methodology. Interacted extensively with the Legal team providing essential data needed for filing patents on novel genes discovered through the SPDI, TAP and Curagen projects. My group has developed, implemented and patented high throughput cloning methodologies that have proven to be essential for the isolation of hundreds of novel genes for the SPDI, TAP and Curagen projects as well as dozens of other smaller projects.

#### **Scientist**

DNAX Research Institute, Palo Alto; 9/91 to 1/99

Involved in multiple projects aimed at understanding novel genes discovered through bioinformatics studies and functional assays. Developed and patented a method for the specific depletion of eosinophils in vivo using monoclonal antibodies. Developed and implemented essential technical methodologies and provided strategic direction in the areas of expression, cloning, protein purification, general molecular biology, and monoclonal antibody production. Trained and supervised numerous technical staff.

#### **Facilities**

##### **Manager**

Corixa, Redwood City; 5/89 - 7/91.

Directed plant-related activities, which included expansion planning, maintenance, safety, purchasing, inventory control, shipping and receiving, and laboratory management. Designed and implemented the safety program. Also served as liaison to regulatory agencies at the local, state and federal level. Was in charge of property leases, leasehold improvements, etc. Negotiated vendor contracts and directed the purchasing department. Trained and supervised personnel to carry out the above-mentioned duties.

SRA

University of California, San Francisco  
Cancer Research Institute; 2/87-4/89.

Was responsible for numerous cloning projects including: studies of somatic hypermutation, studies of AIDS-associated lymphomas, and cloning of t(5;14), t(11;14), and t(8;14) translocations. Focused on the activation of hemopoietic growth factors involved in the t(5;14) translocation in leukemia patients..

Research  
Technician

Berlex Biosciences, South San Francisco; 7/85-2/87.

Worked on a subunit porcine vaccine directed against *Mycoplasma hyopneumoniae*. Was responsible for generating genomic libraries, screening with degenerate oligonucleotides, and characterizing and expressing clones in *E. coli*. Also constructed a general purpose expression vector for use by other scientific teams.

## PUBLICATIONS

1. Hilary F. Clark, et al. "The Secreted Protein Discovery Initiative (SPDI), a Large-scale Effort to Identify Novel Human Secreted and Transmembrane Proteins: a bioinformatics assessment." *Genome Res.* Vol 13(10), 2265-2270, 2003
2. Sean H. Adams, Clarissa Chui, Sarah L. Schilbach, Xing Xian Yu, Audrey D. Goddard, J. Christopher Grimaldi, James Lee, Patrick Dowd, David A. Lewin, & Steven Colman. "BFIT, a Unique Acyl-CoA Thioesterase Induced in Thermogenic Brown Adipose Tissue: Cloning, organization of the human gene and assessment of a potential link to obesity" *Biochemical Journal*, Vol 360, 135-142, 2001
3. Szeto W, Jiang W, Tice DA, Rubinfeld B, Hollingshead PG, Fong SE, Dugger DL, Pham T, Yansura D, Wong TA, Grimaldi JC, Corpuz RT, Singh JS, Frantz GD, Devaux B, Crowley CW, Schwall RH, Eberhard DA, Rastelli L, Polakis P, and Pennica D. "Overexpression of the Retenoic Acid-Responsive Gene *Stra6* in Human Cancers and its Synergistic Activation by Wnt-1 and Retinoic Acid." *Cancer Research* Vol. 61(10), 4197-4205, 2001
4. Jeanne Kahn, Fuad Mehraban, Gláddys Ingle, Xiaohua Xin, Juliet E. Bryant, Gordon Vehar, Jill Schoenfeld, J. Christopher Grimaldi (incorrectly named as "Grimaldi, CJ"), Franklin Peale, Aparna Draksharapu, David A. Lewin, and Mary E. Gerritsen. "Gene Expression Profiling in an in Vitro Model of Angiogenesis." *American Journal of Pathology* Vol 156(6), 1887-1900, 2000.
5. Grimaldi JC, Yu NX, Grunig G, Seymour BW, Cottrez F, Robinson DS, Hosken N, Ferlin WG, Wu X, Soto H, O'Garra A, Howard MC, Coffman RL. "Depletion of eosinophils in mice through the use of antibodies specific for C-C chemokine receptor 3 (CCR3). *Journal of Leukocyte Biology*; Vol. 65(6), 846-53, 1999
6. Oliver AM, Grimaldi JC, Howard MC, Kearney JF. "Independently ligating CD38 and Fc gammaRIIB relays a dominant negative signal to B cells." *Hybridoma* Vol. 18(2), 113-9, 1999

7. Cockayne DA, Muchamuel T, Grimaldi JC, Muller-Steffner H, Randall TD, Lund FE, Murray R, Schuber F, Howard MC. "Mice deficient for the ecto-nicotinamide adenine dinucleotide glycohydrolase CD38 exhibit altered humoral immune responses." *Blood* Vol. 92(4), 1324-33, 1998
8. Frances E. Lund, Nanette W. Solvason, Michael P. Cooke, Andrew W. Heath, J. Christopher Grimaldi, Troy D. Randall, R. M. E. Parkhouse, Christopher C Goodnow and Maureen C. Howard. "Signaling through murine CD38 is impaired in antigen receptor unresponsive B cells." *European Journal of Immunology*, Vol. 25(5), 1338-1345, 1995
9. M. J. Guimaraes, J. F. Bazan, A. Zolotnik, M. V. Wiles, J. C. Grimaldi, F. Lee, T. McClanahan. "A new approach to the study of haematopoietic development in the yolk sac and embryoid body." *Development*, Vol. 121(10), 3335-3346, 1995
10. J. Christopher Grimaldi, Sriram Balasubramanian, J. Fernando Bazan, Armen Shanafelt, Gerard Zurawski and Maureen Howard. "CD38-mediated protein ribosylation." *Journal of Immunology*, Vol. 155(2), 811-817, 1995
11. Leopoldo Santos-Argumedo, Frances F. Lund, Andrew W. Heath, Nanette Solvason, Wei Wei Wu, J. Christopher Grimaldi, R. M. E. Parkhouse and Maureen Howard. "CD38 unresponsiveness of xid B cells implicates Bruton's tyrosine kinase (btk) as a regulator of CD38 induced signal transduction." *International Immunology*, Vol 7(2), 163-170, 1995
12. Frances Lund, Nanette Solvason, J. Christopher Grimaldi, R. M. E. Parkhouse and Maureen Howard. "Murine CD38: An immunoregulatory ectoenzyme." *Immunology Today*, Vol. 16(10), 469-473, 1995
13. Maureen Howard, J. Christopher Grimaldi, J. Fernando Bazan, Frances E. Lund, Leopoldo Santos-Argumedo, R. M. E. Parkhouse, Timothy F. Walseth, and Hon Cheung Lee. "Formation and Hydrolysis of Cyclic ADP-Ribose Catalyzed by Lymphocyte Antigen CD38." *Science*, Vol. 262, 1056-1059, 1993
14. Nobuyuki Harada, Leopoldo Santos-Argumedo, Ray Chang, J. Christopher Grimaldi, Frances Lund, Camilynn I. Brannan, Neal G. Copeland, Nancy A. Jenkins, Andrew Heath, R. M. E. Parkhouse and Maureen Howard. "Expression Cloning of a cDNA Encoding a Novel Murine B Cell Activation Marker: Homology to Human CD38." *The Journal of Immunology*, Vol. 151, 3111-3118, 1993
15. David J. Rawlings, Douglas C. Saffran, Satoshi Tsukada, David A. Largaespada, J. Christopher Grimaldi, Lucie Cohen Randolph N. Mohr, J. Fernando Bazan, Maureen Howard, Neal G. Copeland, Nancy A. Jenkins, Owen Witte. "Mutation of Unique Region of Bruton's Tyrosine Kinase in Immunodeficient XID Mice." *Science*, Vol. 261, 358-360, 1993
16. J. Christopher Grimaldi, Raul Torres, Christine A. Kozak, Ray Chang, Edward Clark, Maureen Howard, and Debra A. Cockayne. "Genomic Structure and Chromosomal Mapping of the Murine CD40 Gene." *The Journal of Immunology*, Vol 149, 3921-3926, 1992
17. Timothy C. Meeker, Bruce Shiramizu, Lawrence Kaplan, Brian Herndier, Henry Sanchez, J. Christopher Grimaldi, James Baumgartner, Jacob Rachlin, Ellen Feigal, Mark Rosenblum and Michael S. McGrath. "Evidence for Molecular Subtypes of HIV-Associated Lymphoma:

Division into Peripheral Monoclonal, Polyclonal and Central Nervous System Lymphoma." AIDS, Vol. 5, 669-674, 1991

18. Ann Grimaldi and Chris Grimaldi. "Small-Scale Lambda DNA Prep." Contribution to Current Protocols in Molecular Biology, Supplement 5, Winter 1989
19. J. Christopher Grimaldi, Timothy C. Meeker. "The t(5;14) Chromosomal Translocation in a Case of Acute Lymphocytic Leukemia Joins the Interleukin-3 Gene to the Immunoglobulin Heavy Chain Gene." Blood, Vol. 73, 2081-2085, 1989
20. Timothy C. Meeker, J. Christopher Grimaldi, et al. "An Additional Breakpoint Region in the BCL-1 Locus Associated with the t(11;14) (q13;q32) Translocation of B-Lymphocytic Malignancy." Blood, Vol. 74, 1801-1806, 1989
21. Timothy C. Meeker, J. Christopher Grimaldi, Robert O'Rourke, et al. "Lack of Detectable Somatic Hypermutation in the V Region of the Ig H Chain Gene of a Human Chronic B Lymphocytic Leukemia." The Journal of Immunology, Vol. 141, 3994-3998, 1988

#### MANUSCRIPTS IN PREPARATION

1. Sriram Balasubramanian, J. Christopher Grimaldi, J. Fernando Bazan, Gerard Zurawski and Maureen Howard. "Structural and functional characterization of CD38: Identification of active site residues"

#### PATENTS

1. "Methods for Eosinophil Depletion with Antibody to CCR3 Receptor" (US 6,207,155 B1).
2. "Amplification Based Cloning Method." (US 6,607,899)
3. Ashkenazi et al., "Secreted and Transmembrane Polypeptides and Nucleic Acids Encoding the Same." (this patent covers several hundred genes)
4. "IL-17 Homologous Polypeptides and Therapeutic Uses Thereof"
5. "Method of Diagnosing and Treating Cartilaginous Disorders."

#### MEMBERSHIPS AND ACTIVITIES

Editor	Frontiers in Bioscience
Member	DNAX Safety Committee 1991-1999 Biological Safety Affairs Forum (BSAF) 1990-1991 Environmental Law Foundation (ELF) 1990-1991

# The t(5;14) Chromosomal Translocation in a Case of Acute Lymphocytic Leukemia Joins the Interleukin-3 Gene to the Immunoglobulin Heavy Chain Gene

By J. Christopher Grimaldi and Timothy C. Meeker

Chromosomal translocations have proven to be important markers of the genetic abnormalities central to the pathogenesis of cancer. By cloning chromosomal breakpoints one can identify activated proto-oncogenes. We have studied a case of B-lineage acute lymphocytic leukemia (ALL) that was associated with peripheral blood eosinophilia. The chromosomal translocation t(5;14) (q31;q32) from this sample was cloned and studied at the molecular level. This

translocation joined the immunoglobulin heavy chain joining (Jh) region to the promotor region of the interleukin-3 (IL-3) gene in opposite transcriptional orientations. The data suggest that activation of the IL-3 gene by the enhancer of the immunoglobulin heavy chain gene may play a central role in the pathogenesis of this leukemia and the associated eosinophilia.

© 1989 by Grune & Stratton, Inc.

**K**ARYOTYPIC STUDIES of leukemia and lymphoma have identified frequent nonrandom chromosomal translocations. Some of these translocations juxtapose the immunoglobulin heavy chain (IgH) gene with important

protooncogenes, such as *c-myc* and *bcl-2*.<sup>1,2</sup> In this way, the IgH gene can activate proto-oncogenes, resulting in disordered gene expression and a step in the development of cancer. The investigation of additional nonrandom translocations into the IgH locus allows us to identify new genes promoting the generation of leukemia and lymphoma.

A distinct subtype of acute lymphocytic leukemia (ALL) has been characterized by B-lineage phenotype, associated eosinophilia in the peripheral blood, and a t(5;14)(q31;q32) chromosomal translocation.<sup>3,4</sup> This syndrome probably occurs in <1% of all patients with ALL. We hypothesized that the cloning of the translocation characteristic of this leukemia might allow the identification of an important gene on chromosome 5 that plays a role in the evolution of this disease. In this report we demonstrate that the interleukin-3 gene (IL-3) and the IgH gene are joined by this translocation.

## MATERIALS AND METHODS

**Sample and DNA blots.** A bone marrow aspirate from a representative patient with ALL (L1 morphology by French-American-British [FAB] criteria), peripheral eosinophilia (up to 20,000 per microliter with a normal value of <350 per microliter) and a t(5;14)(q31;q32) translocation was studied. Using published methods, genomic DNA was isolated and DNA blots were made.<sup>5</sup> Briefly, 10 µg of high molecular weight (mol wt) DNA were digested using an appropriate restriction enzyme and electrophoresed on a 0.8% agarose gel. The gel was stained with ethidium bromide, photographed, denatured, neutralized, and transferred to Hybond (Amersham, Arlington Heights, IL). After treatment of the filter with ultraviolet light, hybridization was performed. The filter was washed to a final stringency of 0.2% saturated sodium citrate (SSC) and 0.1% sodium lauryl sulfate (SDS) and exposed to film. The human Jh probe has been previously reported.<sup>6</sup>

**Genomic library.** The genomic library was made using pub-

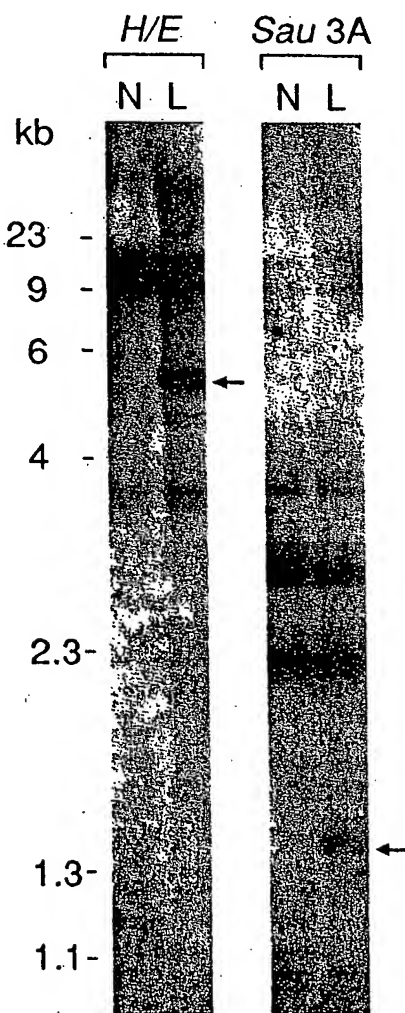


**Fig 1.** DNA blots of the leukemia sample. The restriction fragment pattern of normal human DNA (N) and the leukemia sample (L) were compared using a human Jh probe. Rearranged bands are indicated by arrows. Sample L exhibits a single rearranged band with both *Hind* III/*Eco* RI and *Sau*3A restriction digests. The rearranged bands are less intense than the other bands because the majority of cells in the sample represent normal bone marrow elements.

From the Division of Hematology/Oncology, Department of Medicine, University of California, San Francisco.

Submitted February 22, 1989; accepted March 8, 1989.

Supported by NIH Grant No. CA01102.

Address reprint requests to Timothy C. Meeker, MD, UCSF/VAMC 111H, 4150 Clement St, San Francisco, CA 94121.

Dr Grimaldi's current address is Biostan Inc, 440 Chesapeake Dr, Seaport Centre, Redwood City, CA 94063.

The publication costs of this article were defrayed in part by page charge payment. This article must therefore be hereby marked "advertisement" in accordance with 18 U.S.C. section 1734 solely to indicate this fact.

© 1989 by Grune & Stratton, Inc.

0006-4971/89/7308-0031\$3.00/0

lished methods.<sup>5</sup> Approximately 100  $\mu$ g of high mol wt genomic DNA were partially digested with the *Sau*3A restriction enzyme. Fragments from 9 to 23 kilobases (kb) in size were isolated on a sucrose gradient and ligated into phage EMBL3A (Stratagene, San Diego). Recombinant phage were packaged, plated, and screened as previously reported.<sup>5</sup>

**DNA sequencing.** Fragments for sequencing were cloned into M13 vectors and sequenced by the chain termination method using Sequenase (United States Biochemical, Cleveland).<sup>7</sup> All sequence data were derived from both strands.

### RESULTS

We studied a bone marrow sample from a patient with ALL and associated peripheral eosinophilia. Karyotypic analysis showed the characteristic t(5;14)(q31;q32) translocation. These features define a distinctive subtype of ALL.<sup>3,4</sup> The leukemic cells were analyzed for cell surface phenotype by immunofluorescence. They were positive for B1 (CD20), B4 (CD19), cALLA (CD10), HLA-DR, and terminal deoxynucleotidyl transferase (Tdt), but negative for surface immunoglobulin. This phenotypic profile describes an immature cell from the B-lymphocytic lineage.<sup>8</sup>

The leukemia DNA was analyzed by Southern blotting for rearrangements of the IgH gene. Using a human immunoglobulin Jh probe, a single rearranged band was detected by *Eco*RI, *Hind*III, *Sst*I, *Sau*3A, and *Eco*RI plus *Hind*III restriction digests, suggesting rearrangement of one allele (Fig 1). The immunoglobulin Jh region from the other allele was presumably either deleted or in the germline configuration.

We hypothesized that the t(5;14)(q31;q32) juxtaposed a

growth-promoting gene on chromosome 5 with the immunoglobulin Jh region on chromosome 14. Therefore, a genomic library was made from the leukemic sample and screened with a Jh probe. Fifteen distinct positive clones were isolated and screened for the presence of the rearranged *Sau*3A fragment that was detected by DNA blotting. By this analysis, five clones appeared to represent the rearranged allele identified by DNA blots. One of these clones (clone no. 4) was chosen for further study and a detailed restriction map was generated. The *Eco*RI, *Hind*III/*Eco*RI, and *Sst*I fragments from clone no. 4 that hybridized to the human Jh probe were also identical in size to the rearranged fragments from the leukemia sample, confirming that clone no. 4 represented the rearranged leukemic allele.

Phage clone no. 4 contained 3.7 kb of unknown origin joined to the IgH gene in the region of Jh4 (Fig 2). The IgH gene from Jh4 to the C $\mu$  region appeared to be in germline configuration. Previously, the gene encoding hematopoietic growth factor IL-3 had been mapped to chromosome 5q31 so it was suspected that clone no. 4 might contain part of this gene.<sup>9-12</sup> When the restriction map of human IL-3 and clone no. 4 were compared, they were identical for more than 3 kb (Fig 2).

We confirmed the juxtaposition of the IL-3 gene and the IgH gene by nucleic acid sequencing of the subcloned *Bst*EII/*Hpa*I fragment (Fig 2). The sequence of this fragment showed no disruption of the protein coding region or the messenger RNA of the IL-3 gene. The break in the IL-3 gene occurred in the promoter region, 452 base pairs (bp) upstream of the transcriptional start site (position 64, Fig

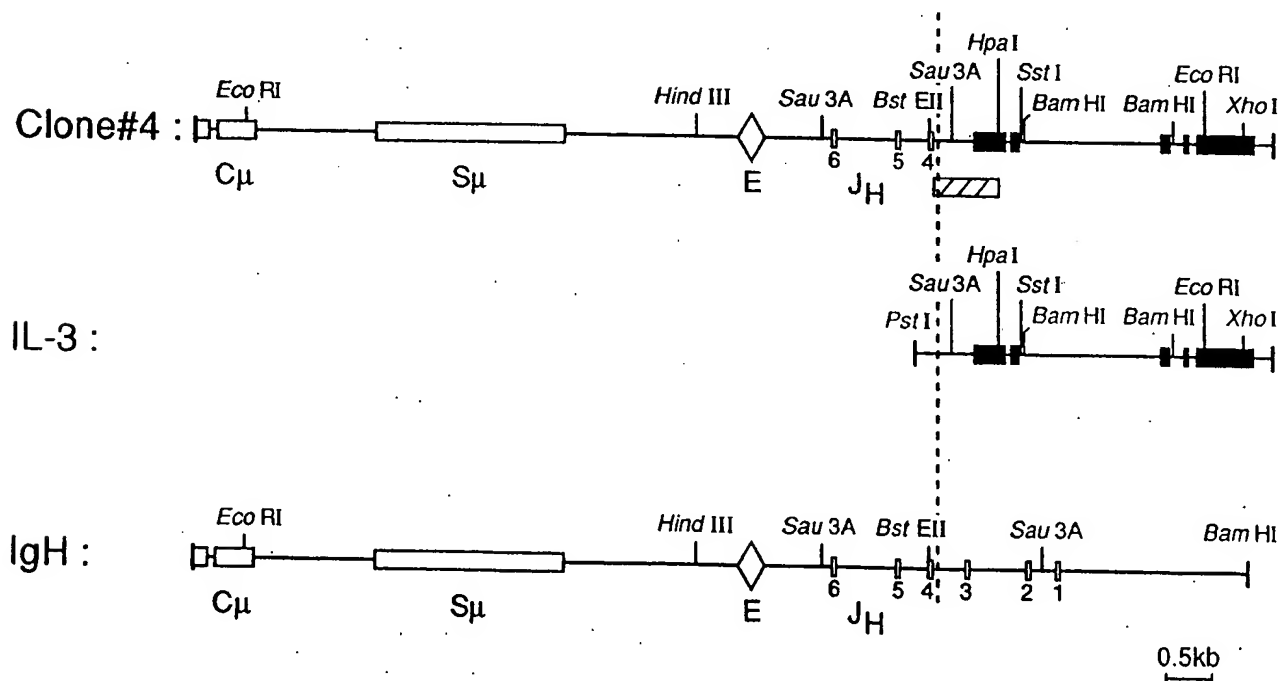


**Fig 2.** Breakpoint region: t(5;14)(q31;q32). Comparative mapping of phage clone no. 4, the germline IgH region, and the germline IL-3 gene.<sup>20,21</sup> The map of clone no. 4 is identical to that of IgH until it diverges in the region of Jh4 (at the dashed line), after which it is identical to the map of IL-3. The two genes are positioned in a head-to-head orientation. The Ig  $\mu$  chain constant region (C $\mu$ ), switch region (S $\mu$ ), enhancer (E), and Jh segments are indicated (open symbols). The five exons (dark boxes) and four introns of the IL-3 gene are shown. The hatched box indicates the sequenced region.

3A). The break in the IgH gene occurred 2 bp upstream of the Jh4 region. Between the two breaks, 25 bp of uncertain origin (putative N sequence) were inserted.<sup>13,14</sup> No sequences homologous to the immunoglobulin heptamer and nonamer could be identified in the IL-3 sequence (Fig 3B). Therefore, nucleic acid sequencing confirmed the juxtaposition of the IL-3 gene and the IgH gene. The sequence data clearly showed that the genes were positioned in opposite transcriptional orientations (head-to-head).

Available data also allowed us to determine the normal positions of the IL-3 gene and the GM-CSF gene in relation to the centromere of chromosome 5 (Fig 4). The IgH gene is known to be positioned with the variable regions toward the telomere on chromosome 14q.<sup>2,15</sup> It has also been shown that

GM-CSF maps within 9 kb of IL-3 in the same transcriptional orientation.<sup>16</sup> Using this information and assuming a simple translocation event in our sample, we can conclude that the IL-3 gene is normally more centromeric, and the GM-CSF gene more telomeric on chromosome 5q (Fig 4). Furthermore, both are transcribed with their 5' ends toward the centromere.

#### DISCUSSION

In this report we have cloned a unique chromosomal translocation that appears to be a consistent feature of a rare, yet distinct, clinical form of acute leukemia. This translocation joined the promoter of the IL-3 gene to the IgH gene. Except for the altered promoter, the IL-3 gene appeared

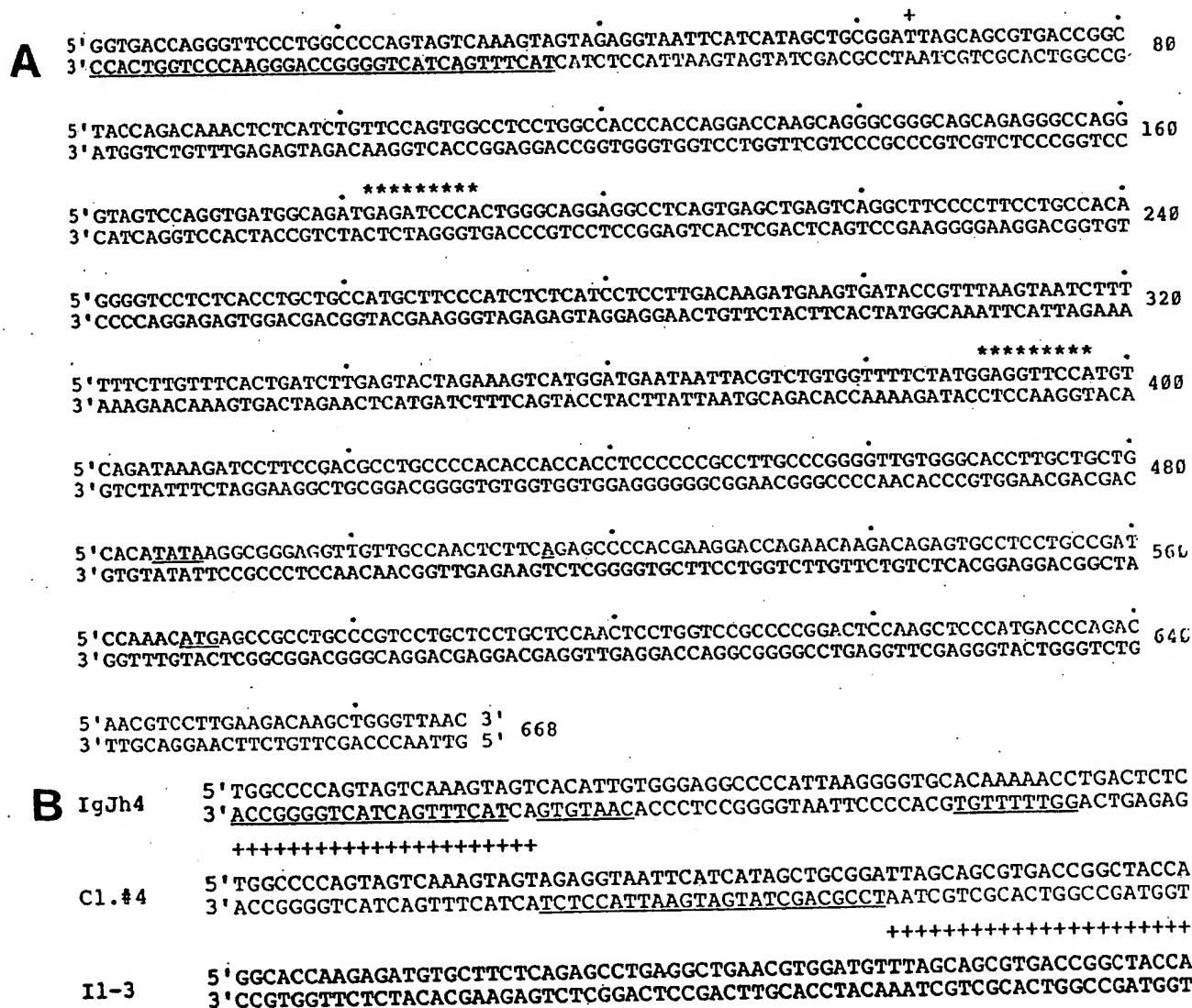


Fig 3. Sequence of t(5;14)(q31;q32) breakpoint region. (A) Nucleotide sequence of the *Bst*II/*Hpa*I fragment indicated on Fig 2. Nucleotides 1 to 36 represent the Jh4 coding region underlined on the coding strand.<sup>9</sup> Nucleotides 39 to 63 are a putative N region. The sequence from position 64 to 668 is that of the germline IL-3 gene.<sup>20</sup> The IL-3 TATA box (485), transcription start (515), and initiation methionine (567) are underlined. Two proposed regulatory sequences in the promoter are marked by asterisks (positions 182 and 389). (B) Comparative sequence of the t(5;14)(q31;q32) breakpoint region. The IgJh4 region is shown with its coding region, heptamer, and nonamer underlined. Clone no. 4 is shown with putative N region sequences underlined. The IL-3 sequence is also shown. A plus sign (+) denotes the identical nucleotide between sequences. No heptamer or nonamer is identified in the IL-3 sequence.

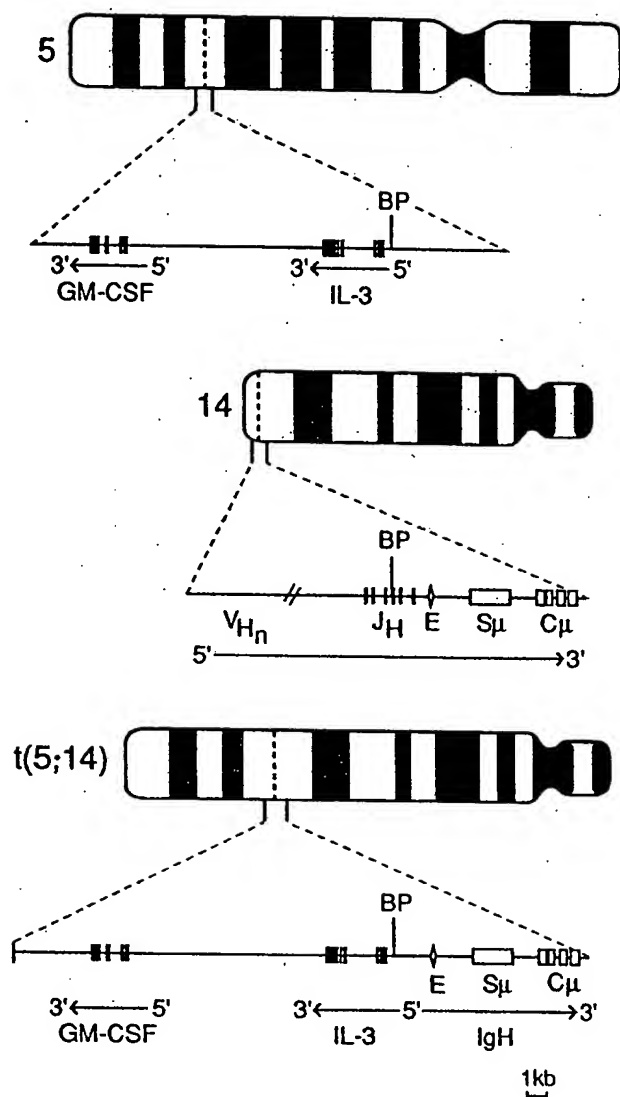


Fig 4. Diagram of the translocation. The normal chromosome 5q31 is shown with the GM-CSF gene telomeric to the IL-3 gene in the transcriptional orientation shown. On normal chromosome 14q32 the V<sub>H</sub> regions are telomeric. The t(5;14)(q31;q32) translocation results in the head-to-head orientation of these genes. Symbols are defined in Fig 2. BP, breakpoint position.

intact as no deletions, insertions, or point mutations were detected by restriction mapping of the entire gene and sequencing of part of the gene. The IgH gene has been truncated at the J<sub>H</sub>4 region, which places the immunoglobulin enhancer within 2.5 kb of the IL-3 gene.<sup>17,18</sup> This leads to the hypothesis that the enhancer is increasing transcription of a structurally normal IL-3 gene. The same mechanism is important for activation of the *c-myc* gene in some cases of Burkitt's lymphoma.<sup>19</sup> An alternate hypothesis is that the elimination of an upstream IL-3 promoter element is crucial to the activation of the IL-3 gene.

The proposed activation of the IL-3 gene suggests that an autocrine loop is important for the pathogenesis of this leukemia.<sup>20</sup> Over-expression of the IL-3 gene coupled with

the presence of the IL-3 receptor in these cells could account for a strong stimulus for proliferation. In this regard, there are data indicating that immature B-lineage lymphocytes and B-lineage leukemias may express the IL-3 receptor.<sup>21,22</sup>

An additional feature of this type of leukemia is the dramatic eosinophilia, consisting of mature forms. It has been hypothesized that the eosinophils do not arise from the malignant clone, but are stimulated by the tumor.<sup>23,24</sup> Because of the known effect of IL-3 on eosinophil differentiation, secretion of high levels of IL-3 by leukemic cells might have a role in the eosinophilia in this type of leukemia.<sup>12</sup>

The data suggest that the recombination mechanism that is active in the IgH gene during normal differentiation has a role in this translocation.<sup>13,14</sup> This is supported by the breakpoint location at the 5' end of J<sub>H</sub>4 and the presence of putative N-region sequences. On the other hand, no recombination signal sequence (heptamer and nonamer) was found in this region on chromosome 5, suggesting that additional factors also played a role. Further studies will elucidate the mechanism of this and other translocations.

In the leukemia we studied, it is possible that the immunoglobulin enhancer also activates the GM-CSF gene, since this gene is probably positioned only 14 kb away (Fig 4). This is known to be within the range of enhancer activation.<sup>25</sup> The interleukin-5 (IL-5) gene maps to chromosome 5q31.<sup>26</sup> Deregulation of the IL-5 gene by this translocation would act synergistically with IL-3 in the stimulation of eosinophil proliferation and differentiation.<sup>27</sup> These and other questions will be answered by the study of more patient samples. We plan to determine whether the t(5;14)(q31;q32) translocation is capable of activating multiple lymphokines simultaneously and whether they cooperate in the generation of this leukemia.

#### REFERENCES

1. Klein G, Klein E: Evolution of tumours and the impact of molecular oncology. *Nature* 315:190, 1985
2. Showe L, Croce C: The role of chromosomal translocations in B- and T-cell neoplasia. *Annu Rev Immunol* 5:253, 1987
3. Hogan T, Koss W, Murgo A, Amato R, Fontana J, VanScoy F: Acute lymphoblastic leukemia with chromosomal 5;14 translocation and hyper eosinophilia: Case report and literature review. *J Clin Oncol* 5:382, 1987
4. Tono-oka T, Sato Y, Matsumoto T, Ueno N, Ohkawa M, Shikano T, Takeda T: Hyper eosinophilic syndrome in acute lymphoblastic leukemia with a chromosome translocation t(5q;14q). *Med Pediatr Oncol* 12:33, 1984
5. Meeker T, Grimaldi JC, O'Rourke R, Loeb J, Juliusson G, Einhorn S: Lack of detectable somatic hypermutation in the V region of the IgH gene of a human chronic B-lymphocytic leukemia. *J Immunol* 141:3394, 1988
6. Ravetch J, Siebenlist U, Korsmeyer S, Waldmann T, Leder P: Structure of the human immunoglobulin  $\mu$  locus: Characterization of embryonic and rearranged J and D genes. *Cell* 27:583, 1981
7. Norrander U, Kempe T, Messing J: Construction of improved M13 vectors using oligodeoxynucleotide-directed mutagenesis. *Gene* 26:101, 1983
8. Foon K, Todd R: Immunologic classification of leukemia and lymphoma. *Blood* 68:1, 1986
9. LeBeau M, Epstein N, O'Brien SJ, Nienhuis AW, Yang Y-C, Clark S, Rowley J: The interleukin-3 gene is located on human

chromosome 5 and is deleted in myeloid leukemias with a deletion of 5q. *Proc Natl Acad Sci USA* 84:5913, 1987

10. LeBeau M, Chandrasekharappi S, Lemons R, Schwartz J, Larson R, Arai N, Westbrook C: Molecular and cytogenetic analysis of chromosome 5 abnormalities in myeloid disorders, in cancer cells, in *Proceedings of Molecular Diagnostics of Human Cancer*. Cold Spring Harbor Laboratory, NY, 1989 (in press)
11. Ihle J, Weinstein Y: Immunological regulation of hematopoietic/lymphoid stem cell differentiation by interleukin-3. *Adv Immunol* 39:1, 1986
12. Clark S, Kamen R: The human hematopoietic colony-stimulating factors. *Science* 236:1229, 1987
13. Bakhshi A, Wright J, Graninger W, Seto M, Owens J, Cossman J, Jensen J, Goldman P, Korsmeyer S: Mechanism of the t(14,18) chromosomal translocation: Structural analysis of both derivative 14 and 18 reciprocal partners. *Proc Natl Acad Sci USA* 84:2396, 1987
14. Tsujimoto Y, Louie E, Bashir M, Croce C: The reciprocal partners of both the t(14,18) and the t(11,14) translocations involved in B-cell neoplasms are rearranged by the same mechanism. *Oncogene* 2:347, 1988
15. Erikson J, Finan J, Nowell P, Croce C: Translocation of immunoglobulin VH genes in Burkitt lymphoma. *Proc Natl Acad Sci USA* 80:810, 1982
16. Yang Y-C, Kovacic S, Kriz R, Wolf S, Clark S, Wellems T, Nienhuis A, Epstein N: The human genes for GM-CSF and IL-3 are closely linked in tandem on chromosome 5. *Blood* 71:958, 1988
17. Gillies S, Morrison S, Oi V, Tonegawa S: A tissue-specific transcription enhancer element is located in the major intron of a rearranged immunoglobulin heavy chain gene. *Cell* 33:717, 1983
18. Banerji J, Olson L, Schaffner W: A lymphocyte-specific cellular enhancer is located downstream of the joining region in immunoglobulin heavy chain genes. *Cell* 33:729, 1983
19. Hayday A, Gillies S, Saito H, Wood C, Wiman K, Hayward

W, Tonegawa S: Activation of a translocated human *c-myc* gene by an enhancer in the immunoglobulin heavy-chain locus. *Nature* 307:334, 1984

20. Sporn M, Roberts A: Autocrine growth factors and cancer. *Nature* 313:745, 1985
21. Palacios R, Steinmetz M: IL-3-dependent mouse clones that express B-220 surface antigen, contain Ig genes in germ line configuration, and generate B lymphocytes in vivo. *Cell* 41:727, 1985
22. Uckun F, Gesner T, Song C, Myers D, Mufson A: Leukemic B-cell precursors express functional receptors for human interleukin-3. *Blood* 73:533, 1989
23. Spitzer G, Garson O: Lymphoblastic leukemia with marked eosinophilia: A report of two cases. *Blood* 42:377, 1973
24. Catovsky D, Bernasconi C, Verkonck P, Postma A, Howss J, Berg A, Rees J, Castelli G, Morra E, Galton D: The association of eosinophilia with lymphoblastic leukemia or lymphoma: A study of seven patients. *Br J Haematol* 45:523, 1980
25. Wang X-F, Calame K: The endogenous immunoglobulin heavy chain enhancer can activate tandem Vh promoters separated by a large distance. *Cell* 43:659, 1985
26. Sutherland G, Baker E, Callen D, Campbell H, Young I, Sanderson C, Garson O, Lopez A, Vadas M: Interleukin-5 is at 5q31 and is deleted in the 5q-syndrome. *Blood* 71:1150, 1988
27. Warren D, Moore M: Synergism among interleukin-1, interleukin-3, and interleukin-5 in the production of eosinophils from primitive hemopoietic stem cells. *J Immunol* 140:94, 1988
28. Yang Y-C, Clark S: Molecular cloning of a primate cDNA and the human gene for interleukin-3. *Lymphokines* 15:375, 1988
29. Yang Y-C, Ciarletta A, Temple P, Chung M, Kovacic S, Witek-Giannotti J, Leary A, Kriz R, Donahue R, Wong G, Clark S: Human IL-3 (multi-CSF): Identification by expression cloning of a novel hematopoietic growth factor related to murine IL-3. *Cell* 47:3, 1986

## RAPID COMMUNICATION

# Activation of the Interleukin-3 Gene by Chromosome Translocation in Acute Lymphocytic Leukemia With Eosinophilia

By Timothy C. Meeker, Dan Hardy, Cheryl Willman, Thomas Hogan, and John Abrams

The t(5;14)(q31;q32) translocation from B-lineage acute lymphocytic leukemia with eosinophilia has been cloned from two leukemia samples. In both cases, this translocation joined the IgH gene and the interleukin-3 (IL-3) gene. In one patient, excess IL-3 mRNA was produced by the leukemic cells. In the second patient, serum IL-3 levels were measured and shown to correlate with disease

A NUMBER OF chromosome translocations have been associated with human leukemia and lymphoma. In many cases the study of these translocations has led to the discovery or characterization of proto-oncogenes, such as *bcl-2*, *c-abl*, and *c-myc*, that are located adjacent to the translocation.<sup>1,2</sup> It is now widely understood that cancer-associated translocations disrupt nearby proto-oncogenes.

A distinct subtype of acute leukemia is characterized by the triad of B-lineage immunophenotype, eosinophilia, and the t(5;14)(q31;q32) translocation.<sup>3,4</sup> Leukemic cells from such patients have been positive for terminal deoxynucleotidyl transferase (Tdt), common acute lymphoblastic leukemia antigen (CALLA), and CD19, but negative for surface or cytoplasmic immunoglobulin. In previous work, we cloned the t(5;14) breakpoint from one leukemic sample (Case 1) and determined that the IgH and interleukin-3 (IL-3) genes were joined by this abnormality.<sup>5</sup> In this report, we extend those findings by showing that the t(5;14)(q31;q32) translocation from a second leukemia sample (Case 2) has a similar structure, and we report our study of growth factor expression in these patients.

## MATERIALS AND METHODS

**Samples and Southern blots.** Case 1 has been described.<sup>5,6</sup> Clinical features of Case 2 have been described in detail.<sup>3</sup> DNA isolation and Southern blotting was done using previously described methods.<sup>5</sup> Filters were hybridized with an immunoglobulin Jh probe, a 280 bp *Bam*HI/*Eco*RI genomic IL-3 fragment, and an IL-3 cDNA probe.<sup>7,8</sup>

**Northern blots.** RNA isolation and Northern blotting have been described.<sup>9</sup> Briefly, Northern blots were done by separating 9 µg total RNA on 1% agarose-formaldehyde gels. Equal RNA loading in each lane was confirmed by ethidium bromide staining. Blots were hybridized with an IL-3 cDNA probe extending to the *Xho* I site in exon 5, a 720 bp *Sst* I/*Kpn* I probe derived from intron 2 of the IL-3 gene, a 600 bp *Nhe* I/*Hpa* I IL-5 cDNA probe, and a 500 bp *Pst* I/*Nco* I granulocyte-macrophage colony stimulating factor (GM-CSF) cDNA probe.<sup>10-12</sup>

**Polymerase chain reaction.** Primers were designed with *Bam*HI sites for cloning. One primer hybridized to the Jh sequences from the IgH gene (Primer 144: 5'-TAGGATCCGACGGTGACCAGGGT), and the other hybridized to the region of the TATA box in the IL-3 gene (Primer 161: 5'-AACAGGATCCCGCCTTATATGTGCAG). Polymerase chain reaction (PCR) (95°C for 1 minute, 61°C for 30 seconds, and 72°C for 3 minutes) was done using 500 ng genomic DNA and 50 pmol of each primer in 100 µL containing 67 mmol/L Tris-HCl pH 8.8, 6.7 mmol/L MgCl<sub>2</sub>, 10% dimethyl sulfoxide (DMSO), 170 µg/mL bovine serum albumin (BSA) (fraction V),

activity. There was no evidence of excess granulocyte/macrophage colony stimulating factor (GM-CSF) or IL-5 expression. Our data support the formulation that this subtype of leukemia may arise in part because of a chromosome translocation that activates the IL-3 gene, resulting in autocrine and paracrine growth effects.

© 1990 by The American Society of Hematology.

16.6 mmol/L ammonium sulfate, 1.5 mmol/L each dNTP and Taq polymerase (Perkin-Elmer, Norwalk, CT).<sup>13</sup>

**Sequencing.** Sequencing was done by chain termination in M13 vectors.<sup>14</sup> As part of this study, we sequenced a subclone of a normal IL-3 promoter, covering 598 base pairs from a *Sma* I site at position -1240 (with respect to the proposed site of transcription initiation) to an *Nhe* I site at position -642. The plasmid containing this region was a gift from Naoko Arai of the DNAX Research Institute.

**Expression in Cos7 cells.** A genomic IL-3 fragment from Case 1 was cloned into the pXM expression vector.<sup>10</sup> Briefly, the *Hind*III/*Sal* I fragment containing the IL-3 gene was subcloned from the previously described phage clone 4 into pUC18.<sup>5</sup> The 2.6 kb fragment extending from the *Sma* I site 61 bp upstream of the IL-3 transcription start to the *Sma* I site in the polylinker was cloned into the blunted *Xho* I site of pXM. The negative control construct was the pXM vector without insert. Plasmids were introduced into Cos7 cells by electroporation, and supernatant was collected after 48 hours in culture.

**TF1 bioassay.** TF-1 cells were passaged in RPMI 1640 supplemented with 10% heat-inactivated fetal bovine serum, 2 mmol L-glutamine, and 1 ng/mL human GM-CSF.<sup>15</sup> Samples and antibodies were diluted in this same medium lacking GM-CSF but containing penicillin and streptomycin. A 25 µL volume of serial dilutions of patient serum was added to wells in a flat bottom 96-well microtiter plate. Rat anti-cytokine monoclonal antibody in a volume of 25 µL was added to appropriate wells and preincubated for 1 hour at 37°C. Fifty microliters of twice washed TF-1 cells were added to each well, giving a final cell concentration of  $1 \times 10^4$  cells per well (final volume, 100 µL). The plate was incubated for 48 hours. The remaining cell viability was determined metabolically by the colori-

From the Division of Hematology/Oncology 111H, Department of Medicine, University of California and the Veterans Administration Medical Center, San Francisco, CA; the Center for Molecular and Cellular Diagnostics, Department of Pathology and Cell Biology, University of New Mexico, Albuquerque, NM; the Division of Hematology/Oncology, Department of Medicine, West Virginia University, Morgantown, WV; and DNAX Research Institute, Palo Alto, CA.

Submitted March 27, 1990; accepted April 19, 1990.

Supported in part by the University of California Cancer Research Coordinating Committee and University of New Mexico Cancer Center funding from the state of New Mexico. The DNAX Research Institute is supported by Schering-Plough.

Address reprint requests to Timothy C. Meeker, MD, Division of Hematology/Oncology 111H, Department of Medicine, University of California and the Veterans Administration Medical Center, 4150 Clement St, San Francisco, CA 94121.

© 1990 by The American Society of Hematology.

0006-4971/90/7602-0022\$3.00/0



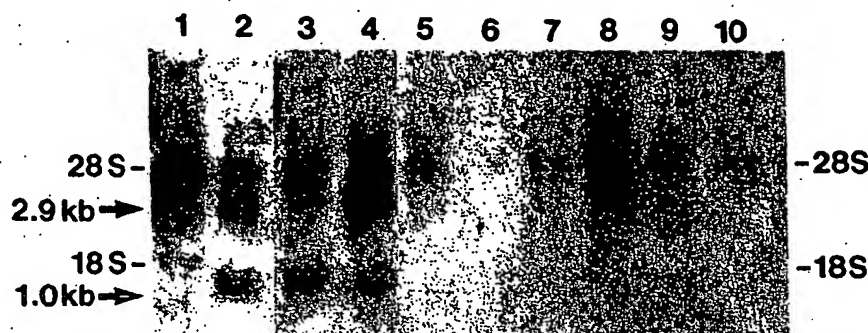


Fig 3. Documentation of IL-3 mRNA over-expression. A Northern blot was prepared and hybridized with a probe for IL-3. Lane 1 contained RNA from unstimulated peripheral blood lymphocytes (PBL) as a negative control. Lane 2 contained RNA from PBL stimulated for 4 hours with concanavalin A (ConA), and lane 3 contained RNA from PBL stimulated with ConA for 48 hours. As in the positive control lanes (2 and 3), a 1 kb band was identified in the leukemic sample from Case 1 (lane 4, lower arrow), suggesting aberrant expression of the IL-3 gene. In addition, the leukemic sample showed over-expression of an unspliced 2.9 kb IL-3 transcript (lane 4, upper arrow). We documented that this represented an unspliced precursor of the mature 1 kb transcript by showing that this band hybridized to a probe from Intron 2 of the IL-3 gene. A similar 2.9 kb band was detected in lane 2, suggesting that an IL-3 mRNA of this size is sometimes detectable in normal mitogen-stimulated cells. Lane 5 through 10 represent RNA from six samples of B-lineage acute lymphocytic leukemia without the t(5;14) translocation, indicating that only the sample with the translocation exhibited IL-3 over-expression. Case 2 could not be analyzed by Northern blot because too few cells were available for study.

the locations of the two cloned breakpoints in relation to the IL-3 gene. The two chromosome 5 breakpoints were separated by less than 500 bp.

The genomic structure in Cases 1 and 2 suggested that a normal IL-3 gene product was over-expressed as a result of the altered promoter structure. This would predict that the IL-3 gene on the translocated chromosome was capable of making IL-3 protein. This prediction was tested by expressing a genomic fragment from the translocated allele of Case 1 containing all five IL-3 exons under the control of the SV40 promoter/enhancer in the Cos7 cell line. Cell supernatants were studied in a proliferation assay using the factor dependent erythroleukemic cell line, TF-1. The supernatants derived from transfections using the vector plus insert supported TF-1 proliferation, while supernatants from transfections using the vector alone were negative in this assay (data not shown). Furthermore, the biologic activity could be blocked by an antibody to human IL-3 (BVD3-6G8). This result showed that the translocated allele retained the ability to make IL-3 mRNA and protein.

The level of expression of IL-3 mRNA in leukemic cells from Case 1 was assessed. Northern blotting showed that the mature IL-3 mRNA (approximately 1 kb) and a 2.9 kb unspliced IL-3 mRNA were excessively produced by the leukemia (Fig 3). The 2.9 kb form of the mRNA is also present at low levels in normal peripheral blood T lymphocytes after mitogen activation (Fig 3). Several B-lineage acute leukemia samples without the t(5;14) translocation had undetectable levels of IL-3 mRNA in these experiments. In addition, although genes for GM-CSF and IL-5 map close to the IL-3 gene and might have been deregulated by the translocation, no IL-5 or GM-CSF mRNA could be detected in the leukemic sample (data not shown).<sup>19,20</sup>

Three serum samples from Case 2 were assayed by immunoassay for levels of IL-3, GM-CSF, and IL-5 (Table 1). Serum IL-3 could be detected and correlated with the clinical course. When the patient's leukemic cell burden was

highest, the IL-3 level was highest. No serum GM-CSF or IL-5 could be detected.

Since the IL-3 immunoassay measured only immunoreactive factor, we confirmed that biologically active IL-3 was present by using the TF-1 bioassay. This bioassay can be rendered monospecific using appropriate neutralizing monoclonal antibodies specific for IL-3, IL-5, or GM-CSF. We observed that sera from 1-16-84 and 3-14-84 contained TF-1 stimulating activity that could be blocked with anti-IL-3 MoAb (BVD3-6G8), but not with MoAbs to IL-5 (JES1-39D10) or GM-CSF (BVD2-23B6) (Fig 4; GM-CSF data not shown). The amount of neutralizable bioactivity in these two samples correlated very well with the difference in IL-3 levels obtained by immunoassay for these samples. Furthermore, the failure to block TF-1 proliferating activity with either anti-IL-5 or anti-GM-CSF was consistent with the inability to measure these factors by immunoassay and

Table 1. Peripheral Blood Counts and Growth Factor Levels at Different Times in Case 2

	Sample Date		
	11/15/83	1/16/84	3/14/84
Peripheral blood counts (cells/ $\mu$ L)			
WBC	81,800	116,500	12,300
Lymphoblasts	0	33,785	0
Eosinophils	46,626	73,080	615
Serum growth factor levels (pg/mL)			
IL-3	<444	7,995	1,051
GM-CSF	<15	<15	<15
IL-5	<50	<50	<50

Peripheral blood counts from Case 2 at three different time points with the corresponding growth factor levels quantified by immunoassay. The patient received chemotherapy between 1/16/84 and 3/14/84 to lower his leukemic burden.<sup>3</sup> No serum samples were available for a similar analysis of Case 1.

Abbreviation: WBC, white blood cells.

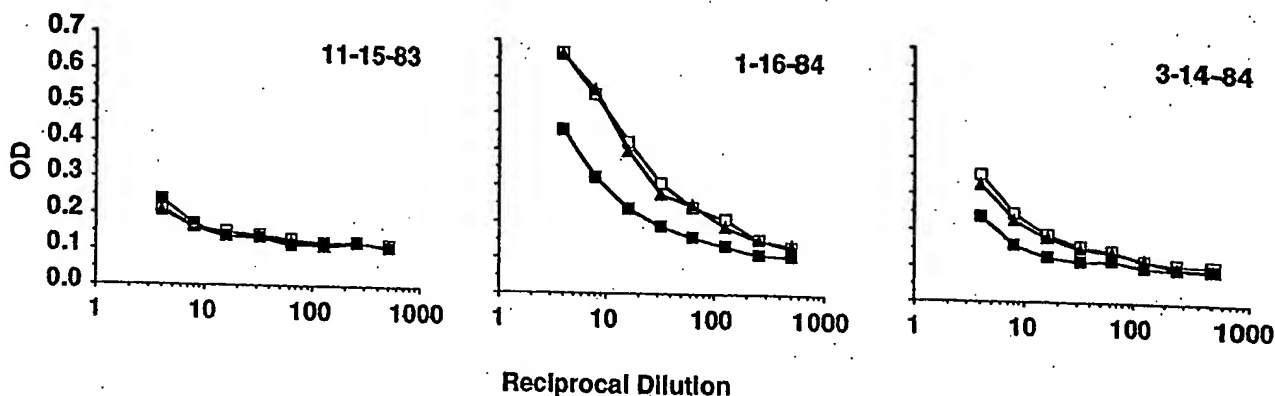


Fig 4. Bioassay of serum IL-3. Leukemic patient sera were tested for bioactive IL-3 and IL-5 in the TF-1 proliferation assay. The reciprocal of the dilution is indicated on the horizontal axis and the optical density indicating the amount of proliferation is indicated on the vertical axis. Serum from all three time points was assayed simultaneously. The assay was rendered monospecific by using a 1  $\mu$ g/mL final concentration of monoclonal rat anti-IL-3, BVD3-6G8 (■), or anti-IL-5, JES1-39D10 (▲); □ indicates no MoAb. On 1/16/84 and 3/14/84, inhibition of proliferation was evident in the presence of anti-IL-3 antibody, documenting serum levels of IL-3 on those days. Serum IL-5 was not detected in this assay, as anti-IL-5 did not alter TF-1 proliferation.

indicated that these other myeloid growth factors were not detectably circulating in the serum of this patient.

#### DISCUSSION

In this report, we have extended our analysis of acute lymphocytic leukemia and eosinophilia associated with the t(5;14) translocation. In both cases we have studied, we have documented the joining of the IL-3 gene from chromosome 5 to the IgH gene from chromosome 14. The breakpoints on chromosome 5 are within 500 bp of each other, suggesting that additional breakpoints will be clustered in a small region of the IL-3 promoter. The PCR assay we have developed will be useful in the screening of additional clinical samples for this abnormality.

The finding of a disrupted IL-3 promoter associated with an otherwise normal IL-3 gene implied that this translocation might lead to the over-expression of a normal IL-3 gene product. In this work, we have documented that this is true. In addition, neither GM-CSF nor IL-5 are over-expressed by the leukemic cells. Furthermore, in one patient, serum IL-3 could be measured and correlated with disease activity. To our knowledge, this is the first measurement of human IL-3 in serum and its association with a disease process. The measurement of serum IL-3 in this and other clinical settings may now be indicated.

The finding of the IL-3 gene adjacent to a cancer-associated translocation breakpoint suggests that its activation is important for oncogenesis. It is our thesis that an autocrine loop for IL-3 is important for the evolution of this leukemia.<sup>21</sup> The excessive IL-3 production that we have documented would be one feature of such an autocrine loop. The final proof of our thesis must await additional data. In particular, from the study of additional clinical samples, it will be necessary to document that the IL-3 receptor is present on the leukemic cells and that anti-IL-3 antibody decreases proliferation of the leukemia in vitro.

An important aspect of this work is the suggestion of a therapeutic approach for this disease. If an autocrine loop for IL-3 can be documented in this disease, attempts to lower circulating IL-3 levels or block the interaction of IL-3 with its receptor may prove useful. Because it is also possible that the eosinophilia in these patients is mediated by the paracrine effects of leukemia-derived IL-3, similar interventions may improve this aspect of the disease. Antibodies or engineered ligands to accomplish these goals may soon be available.

#### ACKNOWLEDGMENT

We thank Naoko Arai, Ken-ichi Arai, R. O'Rourke, J. Grimaldi, and T. O'Connell for technical assistance and/or helpful discussions.

#### REFERENCES

1. Klein G, Klein E: Evolution of tumours and the impact of molecular oncology. *Nature* 315:190, 1985
2. Showe L, Croce C: The role of chromosomal translocations in B- and T-cell neoplasia. *Ann Rev Immunol* 5:253, 1987
3. Hogan T, Koss W, Murgo A, Amato R, Fontana J, VanScoy F: Acute lymphoblastic leukemia with chromosomal 5;14 translocation and hypereosinophilia: Case report and literature review. *J Clin Oncol* 5:382, 1987
4. Tono-oka T, Sato Y, Matsumoto T, Ueno N, Ohkawa M, Shikano T, Takeda T: Hypereosinophilic syndrome in acute lymphoblastic leukemia with a chromosome translocation t(5q;14q). *Med Ped Oncol* 12:33, 1984
5. Grimaldi J, Meeker T: The t(5;14) chromosomal translocation in a case of acute lymphocytic leukemia joins the interleukin-3 gene to the immunoglobulin heavy chain gene. *Blood* 73:2081, 1989
6. McConnell T, Foucar K, Hardy W, Saiki J: Three-way reciprocal chromosomal translocation in an acute lymphoblastic leukemia patient with hypereosinophilia syndrome. *J Clin Oncol* 5:2042, 1987
7. Ravetch J, Siebenlist U, Korsmeyer S, Waldmann T, Leder P: Structure of the human immunoglobulin m locus: Characterization of embryonic and rearranged J and D genes. *Cell* 27:583, 1981
8. Otsuka T, Miyajima A, Brown N, Otsu K, Abrams J, Sacland S, Caux C, Malefijt R, Vries J, Meyerson P, Yokota K, Gemmel L,

- Rennick D, Lee F, Arai N, Arai K, Yokota T: Isolation and characterization of an expressible cDNA encoding human IL-3. *J Immunol* 140:2288, 1988
9. Sambrook J, Fritsch E, Maniatis T: *Molecular Cloning*. Cold Spring Harbor, NY, Cold Spring Harbor Press, 1989
10. Yang Y-C, Ciarletta A, Temple P, Chung M, Kovacic S, Witek-Giannotti J, Leary A, Kriz R, Donahue R, Wong G, Clark S: Human IL-3 (multi-CSF): Identification by expression cloning of a novel hematopoietic growth factor related to murine IL-3. *Cell* 47:3, 1986
11. Yokota T, Coffman R, Hagiwara H, Rennick D, Takebe Y, Yokota K, Gemmell L, Shrader B, Yang G, Meyerson P, Luh J, Hoy P, Pene J, Briere F, Spits H, Banchereau J, Vries J, Lee F, Arai N, Arai K: Isolation and characterization of lymphokine cDNA clones encoding mouse and human IgA-enhancing factor and eosinophil colony-stimulating factor activities: Relationship to interleukin 5. *Proc Natl Acad Sci USA* 84:7388, 1987
12. Wong G, Witek J, Temple P, Wilkens K, Leary A, Luxenberg D, Jones S, Brown E, Kay R, Orr E, Shoemaker C, Golde D, Kaufman R, Hewick R, Wang E, Clark S: Human GM-CSF: Molecular cloning of the complementary DNA and purification of the natural and recombinant proteins. *Science* 228:810, 1985
13. Saiki R, Scharf S, Faloona F, Mullis K, Horn G, Erlich H, Arnheim N: Enzymatic amplification of B-globin genomic sequences and restriction site analysis for diagnosis of sickle cell anemia. *Science* 230:1350, 1985
14. Norrander U, Kempe T, Messing J: Construction of improved M13 vectors using oligodeoxynucleotide-directed mutagenesis. *Gene* 26:101, 1983
15. Kitamura T, Tange T, Terasawa T, Chiba S, Kuwaki T, Miyagawa K, Piao Y, Miyazono K, Urabe A, Takaku F: Establishment and characterization of a unique human cell line that proliferates dependently on GM-CSF, IL-3, or erythropoietin. *J Cell Physiol* 140:323, 1989
16. Mosmann T: Rapid colorimetric assay for cellular growth and survival: Application to proliferation and cytotoxicity assays. *J Immunol Methods* 65:55, 1983
17. Bakhshi A, Wright J, Graninger W, Seto M, Owens J, Cossman J, Jensen J, Goldman P, Korsmeyer S: Mechanism of the t(14;18) chromosomal translocation: Structural analysis of both derivative 14 and 18 reciprocal partners. *Proc Natl Acad Sci USA* 84:2396, 1987
18. Tsujimoto Y, Louie E, Bashir M, Croce C: The reciprocal partners of both the t(14;18) and the t(11;14) translocations involved in B-cell neoplasms are rearranged by the same mechanism. *Oncogene* 2:347, 1988
19. Yang Y-C, Kovacic S, Kriz R, Wolf S, Clark S, Wellems T, Nienhuis A, Epstein N: The human genes for GM-CSF and IL-3 are closely linked in tandem on chromosome 5. *Blood* 71:958, 1988
20. Sutherland G, Baker E, Callen D, Campbell H, Young I, Sanderson C, Garson O, Lopez A, Vadas M: Interleukin-5 is at 5q31 and is deleted in the 5q- syndrome. *Blood* 71:1150, 1988
21. Sporn M, Roberts A: Autocrine growth factors and cancer. *Nature* 313:745, 1985

## Clinical and Pathologic Significance of the *c-erbB-2* (*HER-2/neu*) Oncogene

Timothy P. Singleton and John G. Strickler

The *c-erbB-2* oncogene was first shown to have clinical significance in 1987 by Slamon et al,<sup>79</sup> who reported that *c-erbB-2* DNA amplification in breast carcinomas correlated with decreased survival in patients with metastasis to axillary lymph nodes. Subsequent studies, however, of *c-erbB-2* activation in breast carcinoma reached conflicting conclusions about its clinical significance. This oncogene also has been reported to have clinical and pathologic implications in other neoplasms. Our review summarizes these various studies and examines the clinical relevance of *c-erbB-2* activation, which has not been emphasized in recent reviews.<sup>37,38,55</sup> The molecular biology of the *c-erbB-2* oncogene has been extensively reviewed<sup>37,38,55</sup> and will be discussed only briefly here.

### BACKGROUND

The *c-erbB-2* oncogene was discovered in the 1980s by three lines of investigation. The *neu* oncogene was detected as a mutated transforming gene in neuroblastomas induced by ethylnitrosurea treatment of fetal rats.<sup>8,73,74,76</sup> The *c-erbB-2* was a human gene discovered by its homology to the retroviral gene *v-erbB*.<sup>33,49,76</sup> *HER-2* was isolated by screening a human genomic DNA library for homology with *v-erbB*.<sup>24</sup> When the DNA sequences were determined subsequently, *c-erbB-2*, *HER-2*, and *neu* were found to represent the same gene. Recently, the *c-erbB-2* oncogene also has been referred to as *NGL*.

The *c-erbB-2* DNA is located on human chromosome 17q21<sup>24,33,66</sup> and codes for *c-erbB-2* mRNA (4.6 kb), which translates *c-erbB-2* protein (p185). This

protein is a normal component of cytoplasmic membranes. The *c-erbB-2* oncogene is homologous with, but not identical to, *c-erbB-1*, which is located on chromosome 7 and codes for the epidermal growth factor receptor.<sup>8,103</sup> The *c-erbB-2* protein is a receptor on cell membranes and has intracellular tyrosine kinase activity and an extracellular binding domain.<sup>2,105</sup> Electron microscopy with a polyclonal antibody detects *c-erbB-2* immunoreactivity on cytoplasmic membranes of neoplasms, especially on microvilli and the non-villous outer cell membrane.<sup>61</sup> In normal cells, immunohistochemical reactivity for *c-erbB-2* is frequently present at the basolateral membrane or the cytoplasmic membrane's brush border.<sup>22,62</sup>

There is experimental evidence that *c-erbB-2* protein may be involved in the pathogenesis of breast neoplasia. Overproduction of otherwise normal *c-erbB-2* protein can transform a cell line into a malignant phenotype.<sup>25</sup> Also, when the *neu* oncogene containing an activating point mutation is placed in transgenic mice with a strong promoter for increased expression, the mice develop multiple independent mammary adenocarcinomas.<sup>18,63</sup> In other experiments, monoclonal antibodies against the *neu* protein inhibit the growth (in nude mice) of a *neu*-transformed cell line,<sup>26-28</sup> and immunization of mice with *neu* protein protects them from subsequent tumor challenge with the *neu*-transformed cell line.<sup>14</sup> Some authors have speculated that the use of antagonists for the unknown ligand could be useful in future chemotherapy.<sup>85</sup> Further review of this experimental evidence is beyond the scope of this article.

The *c-erbB-2* activation most likely occurs at an early stage of neoplastic development. This hypothesis is supported by the presence of *c-erbB-2* activation in both in situ and invasive breast carcinomas. In addition, studies of metastatic breast carcinomas usually demonstrate uniform *c-erbB-2* activation at multiple sites in the same patient,<sup>11,12,39,41,52</sup> although *c-erbB-2* activation has rarely been detected in metastatic lesions but not in the primary tumor.<sup>57,60,107</sup> Even more rarely, *c-erbB-2* DNA amplification has been detected in a primary breast carcinoma but not in its lymph node metastasis.<sup>5</sup> In patients who have bilateral breast neoplasms, both lesions have similar patterns of *c-erbB-2* activation, but only a few such cases have been studied.<sup>11</sup>

## MECHANISMS OF *c-erbB-2* ACTIVATION

The most common mechanism of *c-erbB-2* activation is genomic DNA amplification, which almost always results in overproduction of *c-erbB-2* mRNA and protein.<sup>17,34,65,81</sup> The *c-erbB-2* amplification may stabilize the overproduction of mRNA or protein through unknown mechanisms. Human breast carcinomas with *c-erbB-2* amplification contain 2 to 40 times more *c-erbB-2* DNA<sup>45</sup> and 4 to 128 times more *c-erbB-2* mRNA<sup>34,60</sup> than found in normal tissue. Most human breast carcinomas with *c-erbB-2* amplification have 2 to 15 times more *c-erbB-2* DNA. Tumors with greater amplification tend to have greater overproduction.<sup>17,52,65</sup> The non-mammary neoplasms that have been studied tend to have

similar levels of *c-erbB-2* amplification or overproduction relative to the corresponding normal tissue.

The second most common mechanism of *c-erbB-2* activation is overproduction of *c-erbB-2* mRNA and protein without amplification of *c-erbB-2* DNA.<sup>81</sup> The quantities of mRNA and protein usually are less than those in amplified cases and may approach the small quantities present in normal breast or other tissues.<sup>17,60,82</sup> The *c-erbB-2* protein overproduction without mRNA overproduction or DNA amplification has been described in a few human breast carcinoma cell lines.<sup>47</sup>

Other rare mechanisms of *c-erbB-2* activation have been reported. Translocations involving the *c-erbB-2* gene have been described in a few mammary and gastric carcinomas, although some reported cases may represent restriction fragment length polymorphisms or incomplete restriction enzyme digestions that mimic translocations.<sup>31,65,75,84,90,108</sup> A single point mutation in the transmembrane portion of *neu* has been described in rat neuroblastomas induced by ethylnitrosurea.<sup>9,55</sup> The mutated *neu* protein has increased tyrosine kinase activity and aggregates at the cell membrane.<sup>10,83,98</sup> Although there has been speculation that some of the amplified *c-erbB-2* genes may contain point mutations,<sup>46</sup> none has been detected in primary human neoplasms.<sup>41,53,81</sup>

## TECHNIQUES FOR DETECTING *c-erbB-2* ACTIVATION

### Detection of *c-erbB-2* DNA Amplification

Amplification of *c-erbB-2* DNA is usually detected by DNA dot blot or Southern blot hybridization. In the dot blot method, the extracted DNA is placed directly on a nylon membrane and hybridized with a *c-erbB-2* DNA probe. In the Southern blot method, the extracted DNA is treated with a restriction enzyme, and the fragments are separated by electrophoresis, transferred to a nylon membrane, and hybridized with a *c-erbB-2* DNA probe. In both techniques, *c-erbB-2* amplification is quantified by comparing the intensity (measured by densitometry) of the hybridization bands from the sample with those from control tissue.

Several technical problems may complicate the measurement of *c-erbB-2* DNA amplification. First, the extracted tumor DNA may be excessively degraded or diluted by DNA from stromal cells.<sup>81</sup> Second, the *c-erbB-2* DNA probe must be carefully chosen and labeled. For example, oligonucleotide *c-erbB-2* probes may not be sensitive enough for measuring a low level of *c-erbB-2* amplification, because diploid copy numbers can be difficult to detect (unpublished data). Third, the total amounts of DNA in the sample and control tissue must be compensated for, often with a probe to an unamplified gene. Many studies have used control probes to genes on chromosome 17, the location of *c-erbB-2*, to correct for possible alterations in chromosome number. Identical results, however, are obtained by using control probes to genes on other chromosomes,<sup>5,65,80</sup> with rare exception.<sup>17</sup> Studies using control probes to the beta-

globin gene must be interpreted with caution, because one allele of this gene is deleted occasionally in breast carcinomas.<sup>3</sup>

Amplification of *c-erbB-2* DNA was assessed by using the polymerase chain reaction (PCR) in one recent study.<sup>32</sup> Oligoprimers for the *c-erbB-2* gene and a control gene are added to the sample's DNA, and PCR is performed. If the sample contains more copies of *c-erbB-2* DNA than of the control gene, the *c-erbB-2* DNA is replicated preferentially.

#### Detection of *c-erbB-2* mRNA Overproduction

Overproduction of *c-erbB-2* mRNA usually is measured by RNA dot blot or Northern blot hybridization. Both techniques require extraction of RNA but otherwise are analogous to DNA dot blot and Southern blot hybridization. Use of PCR for detection of *c-erbB-2* mRNA has been described in two recent abstracts.<sup>89,102</sup>

Overproduction of *c-erbB-2* mRNA can be measured by in situ hybridization. Sections are mounted on glass slides, treated with protease, hybridized with a radiolabeled probe, washed, treated with nuclease to remove unbound probe, and developed for autoradiography. Silver grains are seen only over tumor cells that overproduce *c-erbB-2* mRNA. Negative control probes are used.<sup>65,96,106</sup> Our experience indicates that these techniques are relatively insensitive for detecting *c-erbB-2* mRNA overproduction in routinely processed tissue. Although the sensitivity may be increased by modifications that allow simultaneous detection of *c-erbB-2* DNA and mRNA, in situ hybridization still is cumbersome and expensive (unpublished data).

All of the above *c-erbB-2* mRNA detection techniques have several problems that make them more difficult to perform than techniques for detecting DNA amplification. One major problem is the rapid degradation of RNA in tissue that is not immediately frozen or fixed. In addition, during the detection procedure, RNA can be degraded by RNase, a ubiquitous enzyme, which must be eliminated meticulously from laboratory solutions. Third, control probes to genes that are uniformly expressed in the tissue of interest need to be carefully selected.

#### Detection of *c-erbB-2* Protein Overproduction

The most accurate methods for detecting *c-erbB-2* protein overproduction are the Western blot method and immunoprecipitation. Both techniques can document the binding specificity of various antibodies against *c-erbB-2* protein. In Western blot studies, protein is extracted from the tissue, separated by electrophoresis (according to size), transferred to a membrane, and detected by using antibodies to *c-erbB-2*. In immunoprecipitation studies, antibodies against *c-erbB-2* are added to a tumor lysate, and the resulting protein-antibody precipitate is separated by gel electrophoresis and stained for protein. Both Western blot and immunoprecipitation are useful research tools but currently are not practical for diagnostic pathology. Two recent abstracts have described an enzyme-linked immunosorbent assay (ELISA) for detection of *c-erbB-2* protein.<sup>18,45</sup>

Overproduction of *c-erbB-2* protein is most commonly assessed by various immunohistochemical techniques. These procedures often generate conflicting results, which are explained at least partially by three factors. First, various studies have used different polyclonal and monoclonal antibodies. Because some polyclonal antibodies recognize weak bands in addition to the *c-erbB-2* protein band on Western blot or immunoprecipitation, the results of these studies should be interpreted with caution.<sup>22,36,47,61</sup> Even some monoclonal antibodies immunoprecipitate protein bands in addition to *c-erbB-2* (p185).<sup>30,59,66</sup> Second, tissue fixation contributes to variability between studies. For example, some antibodies detect *c-erbB-2* protein only in frozen tissue and do not react in fixed tissue. In general, formalin fixation diminishes the sensitivity of immunohistochemical methods and decreases the number of reactive cells.<sup>61,66</sup> When Bouin's fixative is used, there may be a higher percentage of positive cases.<sup>22</sup> Third, minimal criteria for interpreting immunohistochemical staining are generally lacking. Although there is general agreement that distinct crisp cytoplasmic membrane staining is diagnostic for *c-erbB-2* activation in breast carcinoma, the number of positive cells and the staining intensity required to diagnose *c-erbB-2* protein overproduction varies from study to study and from antibody to antibody. Degradation of *c-erbB-2* protein is not a problem because it can be detected in intact form more than 24 hours after tumor resection without fixation or freezing.<sup>64</sup>

## ACTIVATION OF *c-erbB-2* IN BREAST LESIONS

### Incidence of *c-erbB-2* Activation

Most studies of *c-erbB-2* oncogene activation do not specify histological subtypes of infiltrating breast carcinoma. Amplification of *c-erbB-2* DNA was found in 19.1 percent (519 of 2715) of invasive carcinomas in 25 studies (Table 1), and *c-erbB-2* mRNA or protein overproduction was detected in 20.9 percent (566 of 2714) of invasive carcinomas in 20 studies. Twelve studies have documented *c-erbB-2* mRNA or protein overproduction in 15 percent (88 of 604) of carcinomas that lacked *c-erbB-2* DNA amplification.

The incidence of *c-erbB-2* activation in infiltrating breast carcinoma varies with the histological subtype. Approximately 22 percent (142 of 650) of infiltrating ductal carcinomas have *c-erbB-2* activation, as expected from the above data. Other variants of breast carcinoma with frequent *c-erbB-2* activation are inflammatory carcinoma (62 percent, 54 of 87), Paget's disease (82 percent, 9 of 11), and medullary carcinoma (22 percent, 5 of 23). In contrast, *c-erbB-2* activation is infrequent in infiltrating lobular carcinoma (7 percent, 5 of 73) and tubular carcinoma (7 percent, 1 of 15).

The *c-erbB-2* protein overproduction is present in 44 percent (44 of 100) of ductal carcinomas in situ and especially comedocarcinoma in situ (68 percent, 49 of 72). The micropapillary type of ductal carcinoma in situ also tends to have *c-erbB-2* activation,<sup>40,54,68</sup> especially if larger cells are present. The greater fre-

TABLE 1. c-erbB-2 ACTIVATION IN MALIGNANT HUMAN BREAST NEOPLASMS

Histological Diagnosis	c-erbB-2 DNA Amplification <sup>a</sup>	c-erbB-2 mRNA Overproduction	c-erbB-2 Protein Overproduction <sup>b</sup>
Carcinoma, not otherwise specified	14/528, <sup>a</sup> 52/310, <sup>17</sup>	42/180, <sup>69</sup> 49/126, <sup>38</sup>	118/728, <sup>85b</sup>
	52/291, <sup>109</sup> 28/176, <sup>87</sup>	19/62, <sup>85</sup> 19/57, <sup>50</sup>	58/330, <sup>77b</sup> 47/313, <sup>85</sup>
	17/157, <sup>113</sup> 22/141, <sup>85</sup>	3/11, <sup>90</sup> 6/10, <sup>84</sup> 3/9 <sup>91</sup>	17/195, <sup>11</sup> 32/191, <sup>88</sup>
	14/136, <sup>57</sup> 12/122, <sup>4</sup>		31/185, <sup>101</sup> 34/102, <sup>42</sup>
	19/103, <sup>79</sup> 15/95, <sup>90</sup>		24/53, <sup>82b</sup> 23/47, <sup>13</sup>
	15/86, <sup>111</sup> 17/73, <sup>77</sup>		22/45, <sup>9</sup> 11/36, <sup>94</sup>
	16/66, <sup>42</sup> 8/61, <sup>50</sup>		7/24, <sup>81</sup> 1/10 <sup>81</sup>
	11/57, <sup>82</sup> 10/57, <sup>85</sup>		
	13/51, <sup>13</sup> 8/49, <sup>81</sup>		
	10/38, <sup>82</sup> 12/38, <sup>94</sup>		
	1/25, <sup>15</sup> 7/24, <sup>81</sup>		
	7/15, <sup>31</sup> 7/10, <sup>88</sup>		
	2/10 <sup>87</sup>		
	—	18/136, <sup>81</sup> 14/73, <sup>34</sup>	16/231, <sup>77b</sup> 18/136, <sup>81</sup>
Carcinoma, type not specified but lacking c-erbB-2 DNA amplification		8/16, <sup>83</sup> 0/8, <sup>90</sup> 1/4, <sup>81</sup>	13/35, <sup>13</sup> 14/29, <sup>82b</sup>
		0/3 <sup>88</sup>	1/28, <sup>82</sup> 3/24, <sup>94</sup>
Infiltrating ductal carcinoma	21/118, <sup>82</sup> 23/107, <sup>34</sup>	35/95 <sup>34</sup>	0/17 <sup>81</sup>
	17/50, <sup>44</sup> 7/37 <sup>9</sup>		22/137, <sup>80</sup> 14/93, <sup>88</sup>
	14/53 (comedo-carcinoma) <sup>18</sup>		9/34 <sup>88</sup>
	3/33 (tubuloductal carcinoma) <sup>18</sup>		

Inflammatory carcinoma	33/80, <sup>35</sup> 3/6 <sup>32</sup>	46/75 <sup>35</sup>	5/6 <sup>32a</sup>
Page's disease	—	—	5/6, <sup>40</sup> 2/3, <sup>54</sup> 2/2 <sup>52</sup>
Tubular carcinoma	0/5, <sup>16</sup> 0/1 <sup>53</sup>	—	1/9 <sup>40</sup>
Medullary carcinoma	2/4, <sup>16</sup> 0/1 <sup>34</sup>	0/1 <sup>34</sup>	1/12, <sup>40</sup> 1/3, <sup>53</sup> 1/2, <sup>52</sup>
			0/1 <sup>39</sup>
Mucinous carcinoma	0/1, <sup>16</sup> 0/1 <sup>53</sup>	—	1/2 <sup>53</sup>
Invasive papillary carcinoma	0/2 <sup>53</sup>	—	—
Infiltrating lobular carcinoma	1/15, <sup>16</sup> 0/6 <sup>34</sup>	1/5 <sup>34</sup>	2/27, <sup>52</sup> 0/12, <sup>40</sup> 0/9, <sup>39</sup>
			1/5 <sup>53</sup>
Mammary fibrosarcoma	0/1 <sup>53</sup>	—	—
"Benign cystosarcoma"	—	—	0/1 <sup>53</sup>
Ductal CIS <sup>a</sup> with minimal invasion	3/5 <sup>52</sup>	—	—
Ductal CIS	0/2 <sup>34</sup>	1/2 <sup>34</sup>	33/74, <sup>40</sup> 10/24 <sup>53</sup>
Ductal CIS, solid or comedo type	—	—	20/33, <sup>53</sup> 19/29, <sup>52</sup>
			10/10 <sup>54</sup>
Ductal CIS, micropapillary type	—	—	10/10 <sup>53</sup>
Ductal CIS, micropapillary or cribriform type	—	—	1(focal)/1 <sup>54</sup>
Ductal CIS, papillary or cribriform type	—	—	0/16, <sup>52</sup> 1/9, <sup>53</sup> 0/3 <sup>40</sup>
Lobular CIS	—	—	0/16 <sup>40</sup>

<sup>a</sup>Shown as number of cases with activation/number of cases studied; reference is given as a superscript.

<sup>b</sup>These protein studies used Western blots; the rest used immunohistochemical methods.

<sup>c</sup>CIS = carcinoma in situ.

quency of *c-erbB-2* protein overproduction in comedocarcinoma in situ, compared with infiltrating ductal carcinoma, could be explained by the fact that many infiltrating ductal carcinomas arise from other types of intraductal carcinoma, which show *c-erbB-2* activation infrequently. Others have speculated that carcinoma in situ with *c-erbB-2* activation tends to regress or to lose *c-erbB-2* activation during progression to invasion.<sup>40,68,92</sup> Infiltrating and in situ components of ductal carcinoma, however, usually are similar with respect to *c-erbB-2* activation,<sup>11,39</sup> although some authors have noted more heterogeneity of the immunohistochemical staining pattern in invasive than in in situ carcinoma.<sup>40,43,68</sup> Activation of *c-erbB-2* is infrequent in lobular carcinoma in situ. If lesions contain more than one histological pattern of carcinoma in situ, the *c-erbB-2* protein overproduction tends to occur in the comedocarcinoma in situ but may include other areas of carcinoma in situ.<sup>42,54,68</sup> Overproduction of *c-erbB-2* protein in ductal carcinoma in situ correlates with larger cell size and a periductal lymphoid infiltrate.<sup>68</sup>

Activation of *c-erbB-2* has not been identified in benign breast lesions, including fibrocystic disease, fibroadenomas, and radial scars (Table 2). Strong membrane immunohistochemical reactivity for *c-erbB-2* has not been described in atypical ductal hyperplasia, although weak accentuation of membrane staining has been noted infrequently.<sup>39,42,54</sup> In normal breast tissue, *c-erbB-2* DNA is diploid, and *c-erbB-2* is expressed at lower levels than in activated tumors.<sup>34,35,65,88</sup>

These preliminary data suggest that *c-erbB-2* activation may not be useful for resolving many of the common problems in diagnostic surgical pathology. For example, *c-erbB-2* activation is infrequent in tubular carcinoma and radial scars. In addition, because *c-erbB-2* activation is unusual in atypical ductal hyperplasia, cribriform carcinoma in situ, and papillary carcinoma in situ, detection of *c-erbB-2* activation in these lesions may not be helpful in their differential diagnosis. The histological features of comedocarcinoma in situ, which commonly overproduces *c-erbB-2*, are unlikely to be mistaken for those of benign lesions. Activation of

TABLE 2. *c-erbB-2* ACTIVATION IN BENIGN HUMAN BREAST LESIONS

Histological Diagnosis	<i>c-erbB-2</i> DNA Amplification <sup>a</sup>	<i>c-erbB-2</i> mRNA Overproduction	<i>c-erbB-2</i> Protein Overproduction
Fibrocystic disease	0/10 <sup>93</sup>	—	0/32, <sup>39</sup> 0/9, <sup>88</sup> 0/8 <sup>66</sup>
Atypical ductal hyperplasia	—	—	2(weak)/21, <sup>54</sup> 1(cytoplasmic)/13 <sup>39</sup>
Benign ductal hyperplasia	—	—	0/12 <sup>39</sup>
Sclerosing adenosis	—	—	0/4 <sup>39</sup>
Fibroadenomas	0/16, <sup>34</sup> 0/6, <sup>93</sup> 0/2, <sup>21</sup> 0/1 <sup>91</sup>	0/6, <sup>35</sup> 0/3 <sup>34</sup>	0/21, <sup>88</sup> 0/10, <sup>66</sup> 0/8, <sup>88</sup> 0/3 <sup>42</sup>
Radial scars	—	—	0/22 <sup>39</sup>
Blunt duct adenosis	—	—	0/14 <sup>38</sup>
"Breast mastosis"	—	0/3 <sup>35</sup>	—

<sup>a</sup>Shown as number of cases with activation/number of cases studied; reference is given as a superscript.

c-erbB-2, however, does favor infiltrating ductal carcinoma over infiltrating lobular carcinoma. Further studies of these issues would be useful.

#### **Correlation of c-erbB-2 Activation With Pathologic Prognostic Factors**

Multiple studies have attempted to correlate c-erbB-2 activation with various pathologic prognostic factors (Table 3). Activation of c-erbB-2 was correlated with lymph node metastasis in 8 of 28 series, with higher histological grade in 6 of 17 series, and with higher stage in 4 of 14 series. Large tumor size was not associated with c-erbB-2 activation in most studies (11 of 14). Tetraploid DNA content and low proliferation, measured by Ki-67, have been suggested as prognostic factors and may correlate with c-erbB-2 activation.<sup>6,7</sup>

#### **Correlation of c-erbB-2 Activation With Clinical Prognostic Factors**

Various studies have attempted also to correlate c-erbB-2 activation with clinical features that may predict a poor outcome (Table 4). Activation of c-erbB-2 correlated with absence of estrogen receptors in 10 of 28 series and with absence of progesterone receptors in 6 of 18 series. In most studies, patient age did not correlate with c-erbB-2 activation, and, in the rest of the reports, c-erbB-2 activation was associated with either younger or older ages.

#### **Correlation of c-erbB-2 Activation With Patient Outcome**

Slamon et al<sup>79,81</sup> first showed that amplification of the c-erbB-2 oncogene independently predicts decreased survival of patients with breast carcinoma. The correlation of c-erbB-2 amplification with poor outcome was nearly as strong as the correlation of number of involved lymph nodes with poor outcome. Slamon et al also reported that c-erbB-2 amplification is an important prognostic indicator only in patients with lymph node metastasis.<sup>79,81</sup>

A large number of subsequent studies also attempted to correlate c-erbB-2 activation with prognosis (Table 5). In 12 series, there was a correlation between c-erbB-2 activation and tumor recurrence or decreased survival. In five of these series, the predictive value of c-erbB-2 activation was reported to be independent of other prognostic factors. In contrast, 18 series did not confirm the correlation of c-erbB-2 activation with recurrence or survival. Four possible explanations for this controversy are discussed below.

One problem is that c-erbB-2 amplification correlates with prognosis mainly in patients with lymph node metastasis. As summarized in Table 5, most studies of patients with axillary lymph node metastasis showed a correlation of c-erbB-2 activation with poor outcome. In contrast, most studies of patients without axillary metastasis have not demonstrated a correlation with patient outcome. Table 6 summarizes the studies in which all patients (with and without axillary metastasis) were considered as one group. There is a trend for studies with a higher percentage of metastatic cases to show an association between c-erbB-2 activation and poor outcome. Thus, most of the current evidence suggests that c-erbB-2 activation has prognostic value only in patients with metastasis to lymph nodes.

TABLE 3. CORRELATION OF c-erbB-2 ACTIVATION WITH PATHOLOGIC PROGNOSTIC FACTORS IN BREAST CARCINOMA

Prognostic Factor	P <sup>a</sup>	c-erbB-2 DNA Amplification <sup>b</sup>	c-erbB-2 mRNA Overproduction	c-erbB-2 Protein Overproduction <sup>c</sup>
Metastasis to axillary lymph nodes	<0.05 0.05-0.15 >0.15	(118) <sup>35</sup> (105) <sup>34</sup> (49) <sup>21</sup> (103) <sup>79</sup> (86) <sup>79</sup> (58) <sup>111</sup> (279) <sup>17</sup> (176) <sup>87</sup> (157) <sup>113</sup> (122) <sup>4</sup> (85) <sup>90</sup> (50) <sup>92</sup> (50) <sup>44</sup> (47) <sup>13</sup> (41) <sup>93</sup>	(104) <sup>35</sup> (92) <sup>34</sup> (9) <sup>31</sup> — (50) <sup>50</sup> — —	(350) <sup>350</sup> (36) <sup>113</sup> (189) <sup>32</sup> (329) <sup>176</sup> (261) <sup>36</sup> (195) <sup>11</sup> (185) <sup>101</sup> (102) <sup>39</sup> (50) <sup>220</sup> (330) <sup>176</sup> (189) <sup>32</sup> (350) <sup>350</sup> (185) <sup>101</sup> (34) <sup>32</sup> (349) <sup>176</sup> (102) <sup>39</sup> (56) <sup>220</sup>
Larger size	<0.05 0.05-0.15 >0.15	(280) <sup>17</sup> (86) <sup>79</sup> (178) <sup>87</sup> (157) <sup>113</sup> (103) <sup>79</sup> (64) <sup>77</sup> (58) <sup>111</sup> (45) <sup>21</sup> (300) <sup>17</sup> (64) <sup>77</sup> (58) <sup>111</sup> (56) <sup>92</sup>	— — (51) <sup>90</sup> — —	— — (350) <sup>350</sup> (185) <sup>101</sup> (34) <sup>32</sup> (349) <sup>176</sup> (102) <sup>39</sup> (56) <sup>220</sup>
Higher stage	<0.05 0.05-0.15 >0.15	(176) <sup>87</sup> (157) <sup>113</sup> (84) <sup>90</sup> (61) <sup>90</sup> (53) <sup>21</sup> (52) <sup>87</sup> (41) <sup>93</sup> (47) <sup>13</sup> (15) <sup>31</sup>	— — — (63) <sup>95</sup>	— — — (176) <sup>101</sup> (168) <sup>11</sup> (38) <sup>13</sup>
Higher histological grade	<0.05 0.05-0.15 >0.15	(122) <sup>4</sup> (113) <sup>34</sup> (95) <sup>90</sup> (58) <sup>111</sup> (50) <sup>44</sup> (41) <sup>93</sup>	— (86) <sup>35</sup> (65) <sup>35</sup>	— (290) <sup>36</sup> (189) <sup>32</sup> (102) <sup>39</sup>

<sup>a</sup>A correlation is statistically significant at <0.05, equivocal at best between 0.05 and 0.15, and not statistically significant at >0.15.<sup>b</sup>Numbers inside parentheses are the number of patients in an individual study; superscript is the reference. Some studies analyzed more than one group of patients.<sup>c</sup>By Western blot method; all other protein studies used immunohistochemical methods.

TABLE 4. CORRELATION OF c-erbB-2 ACTIVATION WITH CLINICAL PROGNOSTIC FACTORS IN BREAST CARCINOMA

Prognostic Factor	P <sup>a</sup>	c-erbB-2 DNA Amplification <sup>b</sup>	c-erbB-2 mRNA Overproduction	c-erbB-2 Protein Overproduction <sup>c</sup>
Absence of estrogen receptors	<0.05	(253) <sup>109</sup> (141) <sup>35</sup> (109) <sup>34</sup> (86) <sup>79</sup> (50) <sup>44</sup> (47) <sup>13</sup>	(104) <sup>35</sup>	(350) <sup>85c</sup> (330) <sup>17c</sup> (185) <sup>101</sup>
	0.05-0.15	(157) <sup>113</sup> (122) <sup>4</sup> (103) <sup>79</sup> (95) <sup>100</sup> (64) <sup>77</sup> (61) <sup>50</sup>	(180) <sup>85</sup> (62) <sup>65</sup> (62) <sup>35</sup> (57) <sup>50</sup>	(290) <sup>85</sup> (172) <sup>11</sup> (51) <sup>52c</sup> (38) <sup>13</sup>
	>0.15	(58) <sup>111</sup> (53) <sup>21</sup> (51) <sup>52</sup> (41) <sup>35</sup>		
Absence of progesterone receptors	<0.05	(253) <sup>109</sup> (141) <sup>35</sup> (109) <sup>34</sup> (50) <sup>44</sup>	—	(350) <sup>85c</sup> (306) <sup>17c</sup>
	0.05-0.15	(86) <sup>79</sup> (49) <sup>52</sup>	—	—
	>0.15	(157) <sup>113</sup> (122) <sup>4</sup> (103) <sup>79</sup> (84) <sup>77</sup>	(180) <sup>85</sup> (103) <sup>35</sup> (82) <sup>35</sup> (58) <sup>35</sup>	(90) <sup>11</sup> (49) <sup>52c</sup>
Age (menopausal status)	<0.05	—	—	(younger: 330) <sup>17c</sup> (older: 58) <sup>52c</sup>
	0.05-0.15	(younger: 86) <sup>79</sup> (230) <sup>17</sup> (178) <sup>87</sup> (157) <sup>113</sup>	—	—
	>0.15	(122) <sup>4</sup> (116) <sup>34</sup> (103) <sup>79</sup> (95) <sup>100</sup> (64) <sup>77</sup> (58) <sup>111</sup> (56) <sup>52</sup> (53) <sup>21</sup> (49) <sup>13</sup> (41) <sup>35</sup> (15) <sup>31</sup>	(62) <sup>35</sup>	(350) <sup>85c</sup> (290) <sup>85</sup> (189) <sup>52</sup> (162) <sup>11</sup> (45) <sup>52</sup>

<sup>a</sup>A correlation is statistically significant at <0.05, equivocal at best between 0.05 and 0.15, and not statistically significant at >0.15<sup>b</sup>Numbers inside parentheses are the number of patients in an individual study; superscript is the reference. Some studies analyzed more than one group of patients.<sup>c</sup>By Western blot method; all other protein studies used immunohistochemical methods.

176

T.P. SINGLETON AND J.G. STRICKLER

**TABLE 5. CORRELATION OF c-erbB-2 ACTIVATION WITH OUTCOME IN PATIENTS WITH BREAST CARCINOMA**

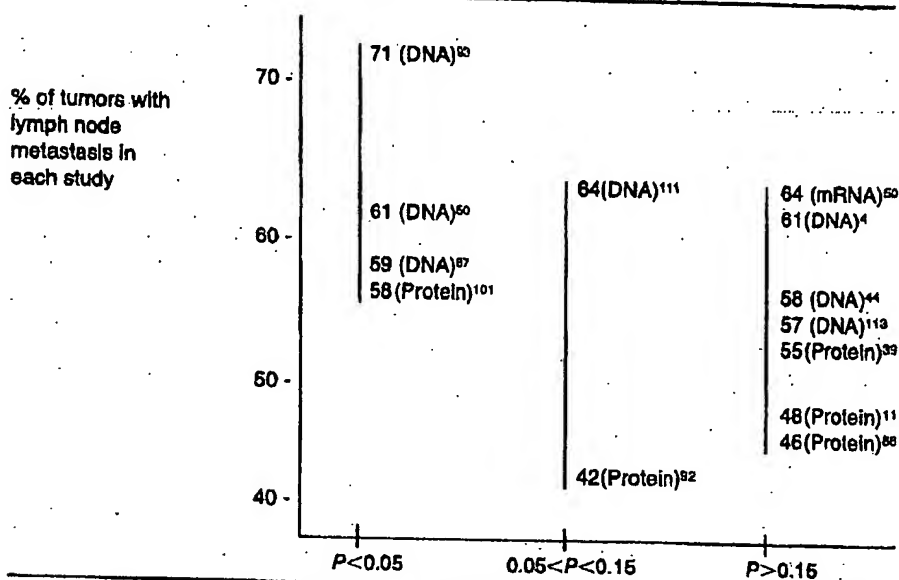
P <sup>a</sup>	Type of c-erbB-2 Activation <sup>b</sup>	Number of Patients		Statistical Analysis <sup>c</sup>	Reference
		Total	With Metastasis to Axillary Lymph Nodes		
<0.05	DNA	176		M	87
<0.05	DNA	61		U	60
<0.05	DNA	57		U	65
<0.05	DNA	41		U	93
<0.05	mRNA	62		U	65
<0.05	Protein	102		M	101
<0.05	DNA		345	M	81
<0.05	DNA		120	U	17
<0.05	DNA		91	U	87
<0.05	DNA		86	M	79
<0.05	Protein-WB		350	M	85
<0.05	Protein		62	U	101
0.05-0.15	DNA	67		U	111
0.05-0.15	Protein	189		M	92
0.05-0.15	Protein		120	U	86
>0.15	DNA	130		U	113
>0.15	DNA	122		M	4
>0.15	DNA	50		U	44
>0.15	mRNA	57		U	50
>0.15	Protein	290		M	86
>0.15	Protein	195		U	11
>0.15	Protein	102		U	39
>0.15	Protein		137	U	17
>0.15	DNA			M	81
>0.15	DNA			U	17
>0.15	DNA			U	87
>0.15	Protein-WB			U	85
>0.15	Protein-WB			U	17
>0.15	Protein			U	86
>0.15	Protein			U	40

<sup>a</sup>The endpoints of these studies were tumor recurrence or decreased survival or both. Correlation between c-erbB-2 activation and a poorer patient outcome is statistically significant at <0.05, is of equivocal significance at 0.05 to 0.15, and is not significant at >0.15.

<sup>b</sup>Shown as variable measured. Letters "WB" indicate assay by Western blot; the other protein studies used immunohistochemical methods.

<sup>c</sup>M = multivariate statistical analysis; U = univariate statistical analysis.

**TABLE 6. PERCENTAGE OF BREAST CARCINOMAS WITH METASTASIS COMPARED WITH PROGNOSTIC SIGNIFICANCE OF c-erbB-2 ACTIVATION**



*P* for correlation of c-erbB-2 activation with patient outcome.

Each study's percentage of breast carcinomas with metastasis is compared with the correlation between c-erbB-2 activation and outcome. These data include only those studies that considered, as one group, all breast cancer patients, whether or not they had axillary metastasis. Superscripts are the references. In parentheses are the types of c-erbB-2 activation. *P* values are interpreted as in Table 3.

A second problem is that various types of breast carcinoma are grouped together in many survival studies. Because the current literature suggests that c-erbB-2 activation is infrequent in lobular carcinoma, studies that combine infiltrating ductal and lobular carcinomas may dilute the prognostic effect of c-erbB-2 activation in ductal tumors. In addition, most studies do not analyze inflammatory breast carcinoma separately. This condition frequently shows c-erbB-2 activation and has a worse prognosis than the usual mammary carcinoma, but it is an uncommon lesion.

A third potential problem is the paucity of studies that attempt to correlate c-erbB-2 activation with clinical outcome in subsets of breast carcinoma without metastasis. Two recent abstracts reported that in patients without lymph node metastasis who had various risk factors for recurrence (such as large tumor size and absence of estrogen receptors), c-erbB-2 overexpression predicted early recurrence.<sup>23,67</sup> In patients with ductal carcinoma in situ, one small study found no association between tumor recurrence and c-erbB-2 activation.<sup>40</sup>

A fourth problem is the lack of data regarding whether the prognosis correlates better with c-erbB-2 DNA amplification or with mRNA or protein overproduction. Most studies that find a correlation between c-erbB-2 activa-

tion and poor patient outcome measure *c-erbB-2* DNA amplification (Table 5), and breast carcinoma patients with greater amplification of *c-erbB-2* may have poorer survival.<sup>79,81</sup> Recent studies suggest that amplification has more prognostic power than overproduction,<sup>17,34,35</sup> but the clinical significance of *c-erbB-2* overproduction without DNA amplification deserves further research.<sup>17,52</sup> Few studies have attempted to correlate patient outcome with *c-erbB-2* mRNA overproduction, and many studies of *c-erbB-2* protein overproduction use relatively less reliable methods such as immunohistochemical studies with polyclonal antibodies.

### Comparison of *c-erbB-2* Activation With Other Oncogenes in Breast Carcinoma

Other oncogenes that may have prognostic implications in human breast cancer are reviewed elsewhere.<sup>71,106</sup> This section will be restricted to a comparison between the clinical relevance of *c-erbB-2* and these other oncogenes.

The *c-myc* gene is often activated in breast carcinomas, but *c-myc* activation generally has less prognostic importance than *c-erbB-2* activation.<sup>21,34,77,87,93</sup> One study found a correlation between increased mRNAs of *c-erbB-2* and *c-myc*, although other reports have not confirmed this.<sup>34,106</sup> Subsequent research, however, could demonstrate a subset of breast carcinomas in which *c-myc* has more prognostic importance than *c-erbB-2*.

The gene *c-erbB-1* for the epidermal growth factor receptor (EGFR) is homologous with *c-erbB-2* but is infrequently amplified in breast carcinomas.<sup>79</sup> Overproduction of EGFR, however, occurs more frequently than amplification and may correlate with a poor prognosis. In studies that have examined both *c-erbB-2* and EGFR in the same tumor, *c-erbB-2* has a stronger correlation with poor prognostic factors.<sup>35,52</sup> Studies have tended to show no correlation between amplification of *c-erbB-2* and *c-erbB-1* or overproduction of *c-erbB-2* and EGFR, although at the molecular level EGFR mediates phosphorylation of *c-erbB-2* protein.<sup>51,52,61,88,100</sup> Recent reviews describe EGFR in breast carcinoma.<sup>43,100</sup>

The genes *c-erbA* and *ear-1* are homologous to the thyroid hormone receptor, and they are located adjacent to *c-erbB-2* on chromosome 17. These genes are frequently coamplified with *c-erbB-2* in breast carcinomas. The absence of *c-erbA* expression in breast carcinomas, however, is evidence against an important role for this gene in breast neoplasia.<sup>90</sup> Amplification of *c-erbB-2* can occur without *ear-1* amplification, and these tumors have a decreased survival that is similar to tumors with both *c-erbB-2* and *ear-1* amplification.<sup>67</sup> Consequently, *c-erbB-2* amplification seems to be more important than amplification of *c-erbA* or *ear-1*.

Other genes also have been compared with *c-erbB-2* activation in breast carcinomas. One study found a significant correlation between increased *c-erbB-2* mRNA and increased mRNAs of *fos*, platelet-derived growth factor chain A, and *Ki-ras*.<sup>106</sup> Allelic deletion of *c-Ha-ras* may indicate a poorer prognosis in breast carcinoma,<sup>21</sup> but it has not been compared with *c-erbB-2* activation. Some studies have suggested a correlation between advanced stage or recurrence of breast carcinoma and activation of any one of several oncogenes.<sup>21,113</sup>

## ACTIVATION OF c-erbB-2 IN NON-MAMMARY TISSUES

### Incidence of c-erbB-2 Activation in Non-Mammary Tissues

Table 7 summarizes the normal tissues in which c-erbB-2 expression has been detected, usually with immunohistochemical methods using polyclonal anti-

**TABLE 7. PRESENCE OR ABSENCE OF c-erbB-2 mRNA OR c-erbB-2 PROTEIN IN NORMAL HUMAN TISSUES**

Tissues With c-erbB-2 mRNA	Tissues Producing c-erbB-2 Protein <sup>a</sup>	Tissues Lacking c-erbB-2 mRNA	Tissues Lacking c-erbB-2 Protein
Skin <sup>24</sup>	Epidermis <sup>56</sup> External root sheath <sup>56</sup> Eccrine sweat gland <sup>56</sup>		
	Fetal oral mucosa <sup>62</sup> Fetal esophagus <sup>62</sup>		Postnatal oral mucosa <sup>62</sup> Postnatal esophagus <sup>62</sup>
Stomach <sup>24</sup>	Stomach <sup>22,62</sup> Fetal intestine <sup>62a</sup>		
Jejunum <sup>24</sup>	Small intestine <sup>22,62</sup>		
Colon <sup>24</sup>	Colon <sup>22,62</sup>		
Kidney <sup>24</sup>	Fetal kidney <sup>62a</sup>	Kidneys <sup>104</sup>	Glomerulus <sup>62</sup> Postnatal Bowman's capsule <sup>62</sup> Postnatal proximal tubule <sup>62</sup>
	Fetal proximal tubule <sup>62</sup> Distal tubule <sup>62</sup> Fetal collecting duct <sup>62</sup> Fetal renal pelvis <sup>62</sup> Fetal ureter <sup>62</sup>		Postnatal collecting duct <sup>62</sup> Postnatal renal pelvis <sup>62</sup> Postnatal fetal ureter <sup>62</sup>
Liver <sup>24</sup>	Hepatocytes <sup>22</sup> Pancreatic acini <sup>22</sup> Pancreatic ducts <sup>22,62</sup> Endocrine cells of islets of Langerhans <sup>22</sup>		Liver <sup>62,65</sup>  Pancreatic islets <sup>62</sup>
Lung <sup>24</sup>	Fetal trachea <sup>62</sup> Fetal bronchioles <sup>62</sup> Bronchioles <sup>62</sup>		Postnatal trachea <sup>62</sup> Postnatal bronchioles <sup>62</sup>  Postnatal alveoli <sup>62,69</sup>
Fetal brain <sup>24</sup>	Fetal ganglion cells <sup>62</sup>		Postnatal brain <sup>62</sup> Postnatal ganglion cells <sup>62</sup>
Thyroid <sup>1</sup>			
Uterus <sup>24</sup>	Ovary <sup>12</sup> Blood vessels <sup>42</sup>		Endothelium <sup>62</sup>
Placenta <sup>24</sup>			Adrenocortical cells <sup>62</sup> Postnatal thymus <sup>62</sup> Fibroblasts <sup>62</sup> Smooth muscle cells <sup>62</sup> Cardiac muscle cells <sup>62</sup>

<sup>a</sup>This protein study used Western blots; the rest used immunohistochemical methods.

bodies. Only a few studies have been performed, and some of these do not demonstrate convincing cell membrane reactivity in the published photographs. The interpretations in these studies, however, are listed, with the caveat that these findings should be confirmed by immunoprecipitation or Western or RNA blots. Production of *c-erbB-2* has been identified in normal epithelium of the gastrointestinal tract and skin. Discrepancies regarding *c-erbB-2* protein in other tissues could be due, at least in part, to differences in techniques.

The data on *c-erbB-2* activation in various non-mammary neoplasms should be interpreted with caution, because only small numbers of tumors have been studied, usually by immunohistochemical methods using polyclonal antibodies. Studies using cell lines have been excluded, because cell culture can induce amplification and overexpression of other genes, although this has not been documented for *c-erbB-2*.

Activation of *c-erbB-2* has been identified in 32 percent (64 of 203) of ovarian carcinomas in eight studies (Table 8). One abstract<sup>45</sup> stated that ovarian carcinomas contained significantly more *c-erbB-2* protein than ovarian non-epithelial malignancies. Another report<sup>41</sup> showed that 12 percent of ovarian carcinomas had *c-erbB-2* overproduction without amplification.

Activation of *c-erbB-2* has been identified in 20 percent (40 of 198) of gastric adenocarcinomas in seven studies, including 33 percent (21 of 64) of

TABLE 8. *c-erbB-2* ACTIVATION IN HUMAN GYNECOLOGIC TUMORS\*

Tumor Type	<i>c-erbB-2</i> DNA Amplification	<i>c-erbB-2</i> mRNA Over-production	<i>c-erbB-2</i> Protein Over-production
Ovary—carcinoma, not otherwise specified	31/120, <sup>81</sup> 1/11, <sup>57</sup> 0/5, <sup>107</sup> 0/5, <sup>84</sup> 0/3, <sup>112</sup> 0/2, <sup>72</sup> 0/1 <sup>110</sup>	23/67 <sup>81</sup>	23/73, <sup>12</sup> 36/72 <sup>81</sup>
Ovary—serous (papillary) carcinoma	2/7, <sup>110</sup> 1/7, <sup>112</sup> 0/5 <sup>72</sup>	—	—
Ovary—endometrioid carcinoma	0/3 <sup>110</sup>	—	—
Ovary—mucinous carcinoma	1/2, <sup>110</sup> 0/1 <sup>72</sup>	—	—
Ovary—clear cell carcinoma	0/2, <sup>112</sup> 0/1 <sup>72</sup>	—	—
Ovary—mixed epithelial carcinoma	0/2 <sup>72</sup>	—	—
Ovary—endometrioid borderline tumor	0/1 <sup>72</sup>	—	—
Ovary—mucinous borderline tumor	0/3 <sup>72</sup>	—	—
Ovary—serous cystadenoma	0/4 <sup>72</sup>	—	—
Ovary—mucinous cystadenoma	0/2 <sup>72</sup>	—	—
Ovary—sclerosing stromal tumor	0/1 <sup>72</sup>	—	—
Ovary—fibrothecoma	0/1 <sup>72</sup>	—	—
Uterus—endometrial adenocarcinoma	0/4, <sup>84</sup> 0/1 <sup>110</sup>	—	—

\*Shown as number of cases with amplification (or overproduction)/total number of cases studied; reference is given as superscript. All protein studies used immunohistochemical methods.

intestinal or tubular subtypes and 9 percent (4 of 47) of diffuse or signet ring cell subtypes (Table 9). Activation of c-erbB-2 has been detected in 2 percent (6 of 281) of colorectal carcinomas, although an additional immunohistochemical study detected c-erbB-2 protein in seven of eight tissues fixed in Bouin's solution. One study found greater immunohistochemical reactivity for c-erbB-2 protein in colonic adenomatous polyps than in the adjacent normal epithelium, using Bouin's fixative. Lesions with anaplastic features and progression to invasive carcinoma tended to show decreased immunohistochemical reactivity for c-erbB-2 protein.<sup>22</sup> Hepatocellular carcinomas (12 of 14 cases) and cholangiocarcinomas (46 of 63 cases) reacted with antibodies against c-erbB-2 in one study, but some of these "positive" cases showed only diffuse cytoplasmic staining, which

TABLE 9. c-erbB-2 ACTIVATION IN HUMAN GASTROINTESTINAL TUMORS\*

Tumor Type	c-erbB-2 DNA Amplification	c-erbB-2 Protein Overproduction
Esophagus—squamous cell carcinoma	0/1 <sup>107</sup>	0/1 <sup>81</sup>
Stomach—carcinoma, poorly differentiated	0/22 <sup>108</sup>	—
Stomach—adenocarcinoma	2/24, <sup>84</sup> 2/8, <sup>107</sup> 2/8, <sup>111</sup> 2/8, <sup>87</sup> 0/1 <sup>108</sup>	4/27, <sup>20</sup> 3/10 <sup>81</sup>
Stomach—carcinoma, intestinal or tubular type	5/10 <sup>108</sup>	16/54 <sup>20</sup>
Stomach—carcinoma, diffuse or signet ring cell type	0/2 <sup>108</sup>	4/45 <sup>20</sup>
Colorectum—carcinoma	2/49, <sup>84</sup> 1/45, <sup>111</sup> 1/45, <sup>87</sup> 1/45, <sup>80</sup> 0/40, <sup>81</sup> 0/32, <sup>107</sup> 0/3 <sup>82</sup>	1/22, <sup>58</sup> 7/8 <sup>22b</sup>
Colon—villous adenoma	0/1 <sup>80</sup>	—
Colon—tubulovillous adenoma	0/5 <sup>80</sup>	—
Colon—tubular adenoma	0/7 <sup>80</sup>	19/19 <sup>22b</sup>
Colon—hyperplastic polyp	0/1 <sup>80</sup>	—
Intestine—leiomyosarcoma	—	0/1 <sup>61</sup>
Hepatocellular carcinoma	0/12 <sup>111</sup>	12/14, <sup>85</sup> 0/2 <sup>61</sup>
Hepatoblastoma	0/1 <sup>57</sup>	—
Cholangiocarcinoma	—	46/63 <sup>85</sup>
Pancreas—adenocarcinoma	—	2/80, <sup>41c</sup> 0/2 <sup>61</sup>
Pancreas—acinar carcinoma	—	0/1 <sup>41</sup>
Pancreas—clear cell carcinoma	—	0/2 <sup>41</sup>
Pancreas—large cell carcinoma	—	0/3 <sup>41</sup>
Pancreas—signet ring carcinoma	—	0/1 <sup>41</sup>
Pancreas—chronic inflammation	—	0/14 <sup>41c</sup>

\*Shown as number of cases with amplification (or overproduction)/total number of cases studied; reference is given as superscript. All protein studies used immunohistochemical methods. No studies analyzed for c-erbB-2 mRNA.

<sup>b</sup>Tissues fixed in Bouin's solution.

<sup>c</sup>Only cases with distinct membrane staining are interpreted as showing c-erbB-2 overproduction.

TABLE 10. *c-erbB-2* ACTIVATION IN HUMAN PULMONARY TUMORS<sup>a</sup>

Tumor Type	<i>c-erbB-2</i> DNA Amplification	<i>c-erbB-2</i> Protein Overproduction
Non-small cell carcinoma	2/60, <sup>75</sup> 0/60 <sup>81</sup>	1/84 <sup>58</sup>
Epidermoid carcinoma	0/13, <sup>82</sup> 0/10, <sup>57</sup> 0/6 <sup>20</sup>	3/5 <sup>88</sup>
Adenocarcinoma	0/21, <sup>82</sup> 1/13, <sup>80</sup> 0/7, <sup>111</sup> 0/7, <sup>57</sup> 0/3 <sup>107</sup>	4/12 <sup>88</sup>
Large cell carcinoma	0/9, <sup>82</sup> 0/6 <sup>20</sup>	—
Small cell carcinoma	—	0/26, <sup>58</sup> 0/3 <sup>89</sup>
Carcinoid tumor	0/1 <sup>82</sup>	0/3 <sup>89</sup>

<sup>a</sup>Shown as number of cases with amplification (or overproduction)/total number of cases studied; reference is given as superscript. All protein studies used immunohistochemical methods. No studies analyzed for *c-erbB-2* mRNA.

does not indicate *c-erbB-2* activation in breast neoplasms.<sup>85</sup> Also, some pancreatic carcinomas and chronic pancreatitis tissue had cytoplasmic immunohistochemical reactivity for *c-erbB-2* protein, in addition to the rare case of pancreatic adenocarcinoma with distinct cell membrane staining.<sup>41</sup>

Tables 10 through 14 summarize the studies of *c-erbB-2* activation in other neoplasms. The *c-erbB-2* oncogene is not activated in most of these tumors. Activation of *c-erbB-2* has been detected in 1 percent (4 of 299) of pulmonary non-small cell carcinomas in nine studies, although one additional report<sup>89</sup> found *c-erbB-2* protein overproduction in 41 percent (7 of 17). Renal cell carcinoma had *c-erbB-2* activation in 7 percent (2 of 30) in four studies. Overproduction of *c-erbB-2* protein was described in one transitional cell carcinoma of the urinary bladder, a grade 2 papillary lesion.<sup>88</sup> Squamous cell carcinoma and basal cell carcinoma of the skin may contain *c-erbB-2* protein, but it is not clear

TABLE 11. *c-erbB-2* ACTIVATION IN HUMAN HEMATOLOGIC PROLIFERATIONS<sup>a</sup>

Tumor Type	<i>c-erbB-2</i> DNA Amplification	<i>c-erbB-2</i> mRNA Overproduction	<i>c-erbB-2</i> Protein Overproduction
Hematologic malignancies	0/23 <sup>111</sup>	—	—
Malignant lymphoma	0/9, <sup>57</sup> 0/3 <sup>107</sup>	0/1 <sup>1</sup>	0/15 <sup>81</sup>
Acute leukemia	0/14 <sup>57</sup>	—	—
Acute lymphoblastic leukemia	0/1 <sup>107</sup>	—	—
Acute myeloblastic leukemia	0/3 <sup>107</sup>	—	—
Chronic leukemia	0/19 <sup>57</sup>	—	—
Chronic lymphocytic leukemia	0/6 <sup>107</sup>	—	—
Chronic myelogenous leukemia	0/8 <sup>107</sup>	—	—
Myeloproliferative disorder	0/1 <sup>57</sup>	—	—

<sup>a</sup>Shown as number of cases with amplification (or overproduction)/total number of cases studied; reference is given as superscript. All protein studies used immunohistochemical methods.

TABLE 12. c-erbB-2 ACTIVATION IN HUMAN TUMORS OF SOFT TISSUE AND BONE\*

Tumor Type	c-erbB-2 DNA Amplification
Sarcoma	0/10, <sup>111</sup> 0/8 <sup>57</sup>
Malignant fibrous histiocytoma	0/1 <sup>107</sup>
Liposarcoma	0/3 <sup>107</sup>
Pleomorphic sarcoma	0/1 <sup>107</sup>
Rhabdomyosarcoma	0/1 <sup>107</sup>
Osteogenic sarcoma	0/2, <sup>107</sup> 0/2 <sup>57</sup>
Chondrosarcoma	0/1 <sup>107</sup>
Ewing's sarcoma	0/1 <sup>57</sup>
Schwannoma	0/1 <sup>57</sup>

\*Shown as number of cases with amplification (or overproduction)/total number of cases studied; reference is given as superscript. No studies analyzed for c-erbB-2 mRNA or c-erbB-2 protein.

whether the protein level is increased over that of normal skin.<sup>58</sup> Thyroid carcinomas and adenomas can have low levels of increased c-erbB-2 mRNA. One abstract described low-level c-erbB-2 DNA amplification in one of ten salivary gland pleomorphic adenomas.<sup>48</sup>

#### Correlation of c-erbB-2 Activation With Patient Outcome

Very few studies have attempted to correlate c-erbB-2 activation in non-mammary tumors with outcome. Slamon et al<sup>61</sup> showed that c-erbB-2 amplification or overexpression in ovarian carcinomas correlates with decreased survival, especially when marked activation is present. However, they did not report the stage, histological grade, or histological subtype of these neoplasms. Another study of stages III and IV ovarian carcinomas found a correlation between decreased survival and c-erbB-2 protein overproduction, but not between survival and histological grade.<sup>18</sup> One abstract stated that c-erbB-2 protein overproduction in 10 of 16 pulmonary adenocarcinomas correlated with decreased disease-free interval.<sup>70</sup> Another abstract described a tendency for immunohisto-

TABLE 13. c-erbB-2 ACTIVATION IN HUMAN TUMORS OF THE URINARY TRACT\*

Tumor Type	c-erbB-2 DNA Amplification	c-erbB-2 mRNA Overproduction	c-erbB-2 Protein Overproduction
Kidney—renal cell carcinoma	1/5, <sup>57</sup> 1/4, <sup>107</sup> 0/5 <sup>54</sup>	0/16 <sup>104</sup>	—
Wilms' tumor	0/4 <sup>57</sup>	—	—
Prostate—adenocarcinoma	—	—	0/23 <sup>58</sup>
Urinary bladder—carcinoma	—	—	1/46 <sup>58</sup>

\*Shown as number of cases with amplification (or overproduction)/total number of cases studied; reference is given as superscript. All protein studies used immunohistochemical methods.

184 T.P. SINGLETON AND J.G. STRICKLER

TABLE 14. *c-erbB-2* ACTIVATION IN MISCELLANEOUS HUMAN TUMORS\*

Tumor Type	<i>c-erbB-2</i> DNA Amplification	<i>c-erbB-2</i> mRNA Overproduction	<i>c-erbB-2</i> Protein Over- production
Skin—malignant melanoma	—	—	0/10 <sup>58</sup>
Skin, head and neck—squamous cell carcinoma	0/7 <sup>107</sup>	—	—
Site not stated—squamous cell carcinoma	0/8, <sup>57</sup> 0/2 <sup>78</sup>	—	—
Salivary gland—adenocarcinoma	1/1 <sup>76</sup>	—	—
Parotid gland—adenoid cystic carcinoma	—	—	0/1 <sup>61</sup>
Thyroid—anaplastic carcinoma	0/1 <sup>1</sup>	0/1 <sup>1</sup>	—
Thyroid—papillary carcinoma	0/5 <sup>1</sup>	3(low levels)/5 <sup>1</sup>	—
Thyroid—adenocarcinoma	0/1 <sup>64</sup>	—	—
Thyroid—adenoma	0/2 <sup>1</sup>	1(low levels)/2 <sup>1</sup>	—
Neuroblastoma	0/35, <sup>61</sup> 0/9, <sup>57</sup> 0/1 <sup>76</sup>	—	—
Meningioma	0/2 <sup>57</sup>	—	—

\*Shown as number of cases with amplification (or overproduction)/total number of cases studied; reference is given as superscript. All protein studies used immunohistochemical methods.

chemical reactivity for *c-erbB-2* protein to correlate with higher grades of prostatic adenocarcinoma.<sup>97</sup> Additional prognostic studies of ovarian carcinomas and other neoplasms are needed.

## SUMMARY

Activation of the *c-erbB-2* oncogene can occur by amplification of *c-erbB-2* DNA and by overproduction of *c-erbB-2* mRNA and *c-erbB-2* protein. Approximately 20 percent of breast carcinomas show evidence of *c-erbB-2* activation, which correlates with a poor prognosis primarily in patients with metastasis to axillary lymph nodes. Studies that have attempted to correlate *c-erbB-2* activation with other prognostic factors in breast carcinoma have reported conflicting conclusions. The pathologic and clinical significance of *c-erbB-2* activation in other neoplasms is unclear and should be assessed by additional studies.

## REFERENCES

1. Aasland R, Lillehaug JR, Male R, et al. Expression of oncogenes in thyroid tumors: Coexpression of *c-erbB2/neu* and *c-erbB*. *Br J Cancer*. 57:358, 1988
2. Akiyama T, Sudo C, Ogawara H, et al. The product of the human *c-erbB-2* gene: A 185-kilodalton glycoprotein with tyrosine kinase activity. *Science*. 232:1644, 1986

3. Ali IU, Lidereau R, Theillet C, Callahan R. Reduction to homozygosity of genes on chromosome 11 in human breast neoplasia. *Science*. 238:185, 1987
4. Ali IU, Campbell G, Lidereau R, Callahan R. Amplification of c-erbB-2 and aggressive human breast tumors. *Science*. 240:1795, 1988
5. Ali IU, Campbell G, Lidereau R, Callahan R. Lack of evidence for the prognostic significance of c-erbB-2 amplification in human breast carcinoma. *Oncogene Res*. 3:139, 1988
6. Bacus SS, Bacus JW, Slamon DJ, Press MF. HER-2/neu oncogene expression and DNA ploidy analysis in breast cancer. *Arch Pathol Lab Med*. 114:164, 1990
7. Bacus SS, Ruby SG, Weinberg DS, et al. HER-2/neu oncogene expression and proliferation in breast cancers. *Am J Pathol*. 137:103, 1990
8. Bargmann CI, Hung MC, Weinberg RA. The neu oncogene encodes an epidermal growth factor receptor-related protein. *Nature*. 319:226, 1986
9. Bargmann CI, Hung MC, Weinberg RA. Multiple independent activations of the neu oncogene by a point mutation altering the transmembrane domain of p185. *Cell*. 45:649, 1986
10. Bargmann CI, Weinberg RA. Oncogenic activation of the neu-encoded receptor protein by point mutation and deletion. *EMBO J*. 7:2043, 1988
11. Barnes DM, Lammie GA, Millis RR, et al. An immunohistochemical evaluation of c-erbB-2 expression in human breast carcinoma. *Br J Cancer*. 58:448, 1988
12. Berchuck A, Kamel A, Whitaker R, et al. Overexpression of HER-2/neu is associated with poor survival in advanced epithelial ovarian cancer. *Cancer Res*. 50:4087, 1990
13. Berger MS, Locher GW, Saurer S, et al. Correlation of c-erbB-2 gene amplification and protein expression in human breast carcinoma with nodal status and nuclear grading. *Cancer Res*. 48:1238, 1988
14. Bernards R, Destree A, McKenzie S, et al. Effective tumor immunotherapy directed against an oncogene-encoded product using a vaccinia virus vector. *Proc Natl Acad Sci USA*. 84:6854, 1987
15. Blunno I, Pozzi MR, Pierotti MA, et al. Structure and expression of oncogenes in surgical specimens of human breast carcinomas. *Br J Cancer*. 57:464, 1988
16. Borg A, Linell F, Idvall I, et al. Her2/neu amplification and comedo type breast carcinoma. *Lancet*. 1:1268, 1989
17. Borg A, Tandon AK, Sigurdsson H, et al. HER-2/neu amplification predicts poor survival in node-positive breast cancer. *Cancer Res*. 50:4332, 1990
18. Bouchard L, Lamarre L, Tremblay PJ, Jolicoeur P. Stochastic appearance of mammary tumors in transgenic mice carrying the MMTV/c-neu oncogene. *Cell*. 57:931, 1989
19. Carney WP, Retos C, Petit D, et al. Quantitation of the neu oncogene protein using a monoclonal antibody based immunoassay (abstract). *Mod Pathol*. 3:15A, 1990
20. Cline MJ, Battifora H. Abnormalities of protooncogenes in non-small cell lung cancer: Correlations with tumor type and clinical characteristics. *Cancer*. 60:2669, 1987
21. Cline MJ, Battifora H, Yokota J. Proto-oncogene abnormalities in human breast cancer: Correlations with anatomic features and clinical course of disease. *J Clin Oncol*. 5:999, 1987
22. Cohen JA, Weiner DB, More KF, et al. Expression pattern of the neu (NGL) gene-encoded growth factor receptor protein (p185<sup>neu</sup>) in normal and transformed epithelial tissues of the digestive tract. *Oncogene*. 4:81, 1989
23. Colnaghi MI, Miotti S, Andreola S, et al. New prognostic factors in breast cancer (abstract). *Am Assoc Cancer Res Ann Meeting*. 30:230A, 1989

24. Coussens L, Yang-Feng TL, Liao YC, et al. Tyrosine kinase receptor with extensive homology to EGF receptor shares chromosomal location with *neu* oncogene. *Science*. 230:1132, 1985
25. Di Fiore PP, Pierce JH, Kraus MH, et al. *erbB-2* is a potent oncogene when overexpressed in NIH/3T3 cells. *Science*. 237:178, 1987
26. Drebin JA, Link VC, Weinberg RA, Greene MI. Inhibition of tumor growth by a monoclonal antibody reactive with an oncogene-encoded tumor antigen. *Proc Natl Acad Sci USA*. 83:9129, 1986
27. Drebin JA, Link VC, Greene MI. Monoclonal antibodies reactive with distinct domains of the *neu* oncogene-encoded p185 molecule exert synergistic anti-tumor effects in vivo. *Oncogene*. 2:273, 1988
28. Drebin JA, Link VC, Greene MI. Monoclonal antibodies specific for the *neu* oncogene product directly mediate anti-tumor effects in vivo. *Oncogene*. 2:387, 1988
29. Falck VG, Gullick WJ. *c-erbB-2* oncogene product staining in gastric adenocarcinoma. An immunohistochemical study. *J Pathol*. 159:107, 1989
30. Fendly BM, Winget M, Hudziak RM, et al. Characterization of murine monoclonal antibodies reactive to either the human epidermal growth factor receptor or *HER2/neu* gene product. *Cancer Res*. 50:1550, 1990
31. Fontaine J, Tesseraux M, Klein V, et al. Gene amplification and expression of the *neu* (*c-erbB-2*) sequence in human mammary carcinoma. *Oncology*. 45:360, 1988
32. Frye RA, Benz CC, Liu E. Detection of amplified oncogenes by differential polymerase chain reaction. *Oncogene*. 4:1153, 1989
33. Fukushige SI, Matsubara KI, Yoshida M, et al. Localization of a novel *v-erbB*-related gene, *c-erbB-2*, on human chromosome 17 and its amplification in a gastric cancer cell line. *Mol Cell Biol*. 6:955, 1986
34. Guerin M, Barrois M, Terrier MJ, et al. Overexpression of either *c-myc* or *c-erbB-2/neu* proto-oncogenes in human breast carcinomas: Correlation with poor prognosis. *Oncogene Res*. 3:21, 1988
35. Guerin M, Gabillot M, Mathieu MC, et al. Structure and expression of *c-erbB-2* and EGF receptor genes in inflammatory and non-inflammatory breast cancer: Prognostic significance. *Int J Cancer*. 43:201, 1989
36. Gullick WJ, Berger MS, Bennett PLP, et al. Expression of the *c-erbB-2* protein in normal and transformed cells. *Int J Cancer*. 40:246, 1987
37. Gullick WJ, Venter DJ. The *c-erbB2* gene and its expression in human cancers. In: Waxman J, Sikora K, eds. *The Molecular Biology of Cancer*. Boston, Blackwell Sci Publ; 1989: 38-53
38. Gullick WJ. Expression of the *c-erbB-2* proto-oncogene protein in human breast cancer. *Recent Results Cancer Res*. 113:51, 1989
39. Gusterson BA, Machin LG, Gullick WJ, et al. *c-erbB-2* expression in benign and malignant breast disease. *Br J Cancer*. 58:453, 1988
40. Gusterson BA, Machin LG, Gullick WJ, et al. Immunohistochemical distribution of *c-erbB-2* in infiltrating and in situ breast cancer. *Int J Cancer*. 42:842, 1988
41. Hall PA, Hughes CM, Staddon SL, et al. The *c-erbB-2* proto-oncogene in human pancreatic cancer. *J Pathol*. 161:195, 1990
42. Hanna W, Kahn HJ, Andrulis I, Pawson T. Distribution and patterns of staining of *neu* oncogene product in benign and malignant breast diseases. *Mod Pathol*. 3:455, 1990
43. Harris AL, Nicholson S. Epidermal growth factor receptors in human breast cancer.

- In: Lippman ME, Dickson RB, eds. *Breast Cancer: Cellular and Molecular Biology*. Boston, Kluwer Academic Publ; 1988: 93-118
44. Heintz NH, Leslie KO, Rogers LA, Howard PL. Amplification of the c-erbB-2 oncogene and prognosis of breast adenocarcinoma. *Arch Pathol Lab Med*. 114:160, 1990
  45. Huettnner P, Carney W, Delellis R, et al. Quantification of the neu oncogene product in ovarian neoplasms (abstract). *Mod Pathol*. 3:46A, 1990
  46. Hung MC, Yan DH, Zhao X. Amplification of the proto-neu oncogene facilitates oncogenic activation by a single point mutation. *Proc Natl Acad Sci USA*. 86:2545, 1989
  47. Hynes NE, Gerber HA, Saurer S, Groner B. Overexpression of the c-erbB-2 protein in human breast tumor cell lines. *J Cell Biochem*. 39:167, 1989
  48. Kahn HJ, Hanna W, Auger M, Andreulis I. Expression and amplification of neu oncogene in pleomorphic adenoma of salivary glands (abstract). *Mod Pathol*. 3:50A, 1990
  49. King CR, Kraus MH, Aaronson SA. Amplification of a novel v-erbB-related gene in a human mammary carcinoma. *Science*. 229:974, 1985
  50. King CR, Swain SM, Porter L, et al. Heterogeneous expression of erbB-2 messenger RNA in human breast cancer. *Cancer Res*. 49:4185, 1989
  51. Kokai Y, Dobashi K, Weiner DB, et al. Phosphorylation process induced by epidermal growth factor receptor alters the oncogenic and cellular neu (NGL) gene products. *Proc Natl Acad Sci USA*. 85:5389, 1988
  52. Lacroix H, Iglehart JD, Skinner MA, Kraus MH. Overexpression of erbB-2 or EGF receptor proteins present in early stage mammary carcinoma is detected simultaneously in matched primary tumors and regional metastases. *Oncogene*. 4:145, 1989
  53. Lemoine NR, Staddon S, Dickson C, et al. Absence of activating transmembrane mutations in the c-erbB-2 proto-oncogene in human breast cancer. *Oncogene*. 5:237, 1990
  54. Lodato RF, Maguire HC, Greene MJ, et al. Immunohistochemical evaluation of c-erbB-2 oncogene expression in ductal carcinoma in situ and atypical ductal hyperplasia of the breast. *Mod Pathol*. 3:449, 1990
  55. Maguire HC, Greene MI. The neu (c-erbB-2) oncogene. *Semin Oncol*. 16:148, 1989
  56. Maguire HC, Jaworsky C, Cohen JA, et al. Distribution of neu (c-erbB-2) protein in human skin. *J Invest Dermatol*. 89:786, 1989
  57. Masuda H, Battifora H, Yokota J, et al. Specificity of proto-oncogene amplification in human malignant diseases. *Mol Biol Med*. 4:213, 1987
  58. McCann A, Dervan PA, Johnston PA, et al. c-erbB-2 oncoprotein expression in primary human tumors. *Cancer*. 65:88, 1990
  59. McKenzie SJ, Marks PJ, Lam T, et al. Generation and characterization of monoclonal antibodies specific for the human neu oncogene product, p185. *Oncogene*. 4:543, 1989
  60. Meltzer SJ, Ahnen DJ, Battifora H, et al. Protooncogene abnormalities in colon cancers and adenomatous polyps. *Gastroenterology*. 92:1174, 1987
  61. Mori S, Akiyama T, Morishita Y, et al. Light and electron microscopical demonstration of c-erbB-2 gene product-like immunoreactivity in human malignant tumors. *Virchows Arch [B]*. 54:8, 1987
  62. Mori S, Akiyama T, Yamada Y, et al. C-erbB-2 gene product, a membrane protein commonly expressed in human fetal epithelial cells. *Lab Invest*. 61:93, 1989
  63. Muller WJ, Sinn E, Pattengale PK, et al. Single-step induction of mammary

- adenocarcinoma in transgenic mice bearing the activated *c-neu* oncogene. *Cell*. 54:105, 1988
64. Ong G, Gullick W, Sikora K. Oncoprotein stability after tumor resection. *Br J Cancer*. 61:538, 1990
65. Parks HC, Lillycrop K, Howell A, Craig RK. *C-erbB2* mRNA expression in human breast tumors: Comparison with *c-erbB2* DNA amplification and correlation with prognosis. *Br J Cancer*. 61:39, 1990
66. Popescu NC, King CR, Kraus MH. Localization of the *erbB-2* gene on normal and rearranged chromosomes 17 to bands q12-21.32. *Genomics*. 4:362, 1989
67. Press MF, Pike MC, Paterson MC, et al. Overexpression of *HER-2/neu* proto-oncogene in node negative breast cancer: Correlation with increased risk of early recurrent disease (abstract). *Mod Pathol*. 3:80A, 1990
68. Ramachandra S, Machin L, Ashley S, et al. Immunohistochemical distribution of *c-erbB-2* in situ breast carcinoma: A detailed morphological analysis. *J Pathol*. 161:7, 1990
69. Rio MC, Bellocq JP, Gairard B, et al. Specific expression of the pS2 gene in subclasses of breast cancers in comparison with expression of the estrogen and progesterone receptors and the oncogene *ERBB2*. *Proc Natl Acad Sci USA*. 84:9243, 1987
70. Robinson R, Kern J, Weiner D, et al. p185<sup>neu</sup> expression in human lung non-small cell carcinomas: An immunohistochemical study with clinicopathologic correlation (abstract). *Mod Pathol*. 3:85A, 1990
71. Rochlitz CF, Benz CC. Oncogenes in human solid tumors. In: Benz C, Liu E, eds. *Oncogenes*. Boston, Kluwer Academic Publ; 1989: 199-240
72. Sasano H, Garret CT, Wilkinson DS, et al. Protooncogene amplification and tumor ploidy in human ovarian neoplasms. *Hum Pathol*. 21:382, 1990
73. Schechter AL, Stern DF, Vaidyanathan L, et al. The *neu* oncogene: An *erbB*-related gene encoding a 185,000-M<sub>r</sub> tumor antigen. *Nature*. 312:513, 1984
74. Schechter AL, Hung MC, Vaidyanathan L, et al. The *neu* gene: An *erbB*-homologous gene distinct from and unlinked to the gene encoding the EGF receptor. *Science*. 229:976, 1985
75. Schneider PM, Hung MC, Chiocca SM, et al. Differential expression of the *c-erbB-2* gene in human small cell and non-small cell lung cancer. *Cancer Res*. 49:4968, 1989
76. Semba K, Kamata N, Toyoshima K, Yamamoto T. A *v-erbB*-related protooncogene, *c-erbB-2*, is distinct from the *c-erbB-1*/epidermal growth factor-receptor gene and is amplified in a human salivary gland adenocarcinoma. *Proc Natl Acad Sci USA*. 82:6497, 1985
77. Seshadri R, Matthews C, Dobrovic A, Horsfall DJ. The significance of oncogene amplification in primary breast cancer. *Int J Cancer*. 43:270, 1989
78. Shih C, Padhy LC, Murray M, Weinberg RA. Transforming genes of carcinomas and neuroblastomas introduced into mouse fibroblasts. *Nature*. 290:261, 1981
79. Slamon DJ, Clark GM, Wong SG, et al. Human breast cancer: Correlation of relapse and survival with amplification of the *HER-2/neu* oncogene. *Science*. 235:177, 1987
80. Slamon DJ, Clark GM. Amplification of *c-erbB-2* and aggressive human breast tumors. *Science*. 240:1795, 1988
81. Slamon DJ, Godolphin W, Jones LA, et al. Studies of the *HER-2/neu* proto-oncogene in human breast and ovarian cancer. *Science*. 244:707, 1989

82. Slebos RJC, Evers SG, Wagenaar SS, Rodenhuis S: Cellular protooncogenes are infrequently amplified in untreated non-small cell lung cancer. *Br J Cancer*. 59:76, 1989
83. Stern DF, Kamps MP, Cao H: Oncogenic activation of p185<sup>neu</sup> stimulates tyrosine phosphorylation in vivo. *Mol Cell Biol*. 8:3969, 1988
84. Tal M, Wetzler M, Josefberg Z, et al: Sporadic amplification of the *HER2/neu* protooncogene in adenocarcinomas of various tissues. *Cancer Res*. 48:1517, 1988
85. Tandon AK, Clark GM, Chamness GC, et al: *HER-2/neu* oncogene protein and prognosis in breast cancer. *J Clin Oncol*. 7:1120, 1989
86. Thor AD, Schwartz LH, Koerner FC, et al: Analysis of *c-erbB-2* expression in breast carcinomas with clinical follow-up. *Cancer Res*. 49:7147, 1989
87. Tsuda H, Hirohashi S, Shimamoto Y, et al: Correlation between long-term survival in breast cancer patients and amplification of two putative oncogene-coamplification units: *hst-1/int-2* and *c-erbB-2/ear-1*. *Cancer Res*. 49:3104, 1989
88. Tsutsumi Y, Naber SP, DeLellis RA, et al: *Neu* oncogene protein and epidermal growth factor receptor are independently expressed in benign and malignant breast tissues. *Hum Pathol*. 21:750, 1990
89. Tsutsumi Y, Stork PJ, Wolfe HJ: Detection of DNA amplification and mRNA overexpression of the *neu* oncogene in breast carcinomas by polymerase chain reaction (abstract). *Mod Pathol*. 3:101A, 1990
90. Van de Vijver M, van de Bersselaar R, Devilee P, et al: Amplification of the *neu* (*c-erbB-2*) oncogene in human mammary tumors is relatively frequent and is often accompanied by amplification of the linked *c-erbA* oncogene. *Mol Cell Biol*. 7:2019, 1987
91. Van de Vijver MJ, Mooi WJ, Wisman P, et al: Immunohistochemical detection of the *neu* protein in tissue sections of human breast tumors with amplified *neu* DNA. *Oncogene*. 2:175, 1988
92. Van de Vijver MJ, Peterse JL, Mooi WJ, et al: *Neu*-protein overexpression in breast cancer: Association with comedo-type ductal carcinoma in situ and limited prognostic value in stage II breast cancer. *N Engl J Med*. 319:1239, 1988
93. Varley JM, Swallow JE, Brammar WJ, et al: Alterations to either *c-erbB-2* (*neu*) or *c-myc* proto-oncogenes in breast carcinomas correlate with poor short-term prognosis. *Oncogene*. 1:423, 1987
94. Venter DJ, Tuzi NL, Kumar S, Gullick WJ: Overexpression of the *c-erbB-2* oncoprotein in human breast carcinomas: Immunohistological assessment correlates with gene amplification. *Lancet*. 2:69, 1987
95. Voravud N, Foster CS, Gilbertson JA, et al: Oncogene expression in cholangiocarcinoma and in normal hepatic development. *Hum Pathol*. 20:1163, 1989
96. Walker RA, Senior PV, Jones JL, et al: An immunohistochemical and in situ hybridization study of *c-myc* and *c-erbB-2* expression in primary human breast carcinomas. *J Pathol*. 158:97, 1989
97. Ware JL, Maygarden SJ, Koontz WW, Strom SC: Differential reactivity with anti-*c-erbB-2* antiserum among human malignant and benign prostatic tissue (abstract). *Am Assoc Cancer Res Ann Meeting*. 30:437A, 1989
98. Weiner DB, Liu J, Cohen JA, et al: A point mutation in the *neu* oncogene mimics ligand induction of receptor aggregation. *Nature*. 339:230, 1989
99. Weiner DB, Nordberg J, Robinson R, et al: Expression of the *neu* gene-encoded protein (p185<sup>neu</sup>) in human non-small cell carcinomas of the lung. *Cancer Res*. 50:421, 1990

190 T.P. SINGLETON AND J.G. STRICKLER

100. Wells A. The epidermal growth factor receptor and its ligand. In: Benz C, Liu E, eds. *Oncogenes*. Boston, Kluwer Academic Pub; 1989: 143-168
101. Wright C, Angus B, Nicholson S, et al. Expression of c-erbB-2 oncoprotein: A prognostic indicator in human breast cancer. *Cancer Res.* 49:2087, 1989
102. Wu A, Colombero A, Low J, et al. Analysis of expression and mutation of the erbB-2 gene in breast carcinoma by the polymerase chain reaction (abstract). *Mod Pathol.* 3:108A, 1990
103. Yamamoto T, Ikawa S, Akiyama T, et al. Similarity of protein encoded by the human c-erbB-2 gene to epidermal growth factor receptor. *Nature.* 319:230, 1986
104. Yao M, Shuin T, Misiaki H, Kubota Y. Enhanced expression of c-myc and epidermal growth factor receptor (C-erbB-1) genes in primary human renal cancer. *Cancer Res.* 48:6753, 1988
105. Yarden Y, Weinberg RA. Experimental approaches to hypothetical hormones: Detection of a candidate ligand of the neu protooncogene. *Proc Natl Acad Sci USA.* 86:3179, 1989
106. Yee LD, Kacinski BM, Carter D. Oncogene structure, function and expression in breast cancer. *Semin Diagn Pathol.* 6:110, 1989
107. Yokota J, Yamamoto T, Toyoshima K, et al. Amplification of c-erbB-2 oncogene in human adenocarcinomas in vivo. *Lancet.* 1:765, 1986
108. Yokota J, Yamamoto T, Miyajima N, et al. Genetic alterations of the c-erbB-2 oncogene occur frequently in tubular adenocarcinoma of the stomach and are often accompanied by amplification of the v-erbA homologue. *Oncogene.* 2:283, 1988
109. Zeillinger R, Kury F, Czerwenka K, et al. HER-2 amplification, steroid receptors and epidermal growth factor receptor in primary breast cancer. *Oncogene.* 4:109, 1989
110. Zhang X, Silva E, Gershenson D, Hung MC. Amplification and rearrangement of c-erbB proto-oncogenes in cancer of human female genital tract. *Oncogene.* 4:985, 1989
111. Zhou D, Battifora H, Yokota J, et al. Association of multiple copies of the c-erbB-2 oncogene with spread of breast cancer. *Cancer Res.* 47:6123, 1987
112. Zhou D, Gonzalez-Cadavid N, Ahuja H, et al. A unique pattern of proto-oncogene abnormalities in ovarian adenocarcinomas. *Cancer.* 62:1573, 1988
113. Zhou D, Ahuja H, Cline MJ. Proto-oncogene abnormalities in human breast cancer: c-erbB-2 amplification does not correlate with recurrence of disease. *Oncogene.* 4:105, 1989

PATENT

IN THE UNITED STATES PATENT AND TRADEMARK OFFICE

In re Application of: Ashkenazi et al.	Group Art Unit: 1647
Serial No.: 09/903,925	Examiner: Fozia Hamid
Filed: July 11, 2001	<b>CERTIFICATE OF MAILING</b> I hereby certify that this correspondence is being deposited with the United States Postal Service with sufficient postage as first class mail in an envelope addressed to: Assistant Commissioner of Patents, Washington, D.C. 20231 on
For: SECRETED AND TRANSMEMBRANE POLYPEPTIDES AND NUCLEIC ACIDS	Date

DECLARATION OF AUDREY D. GODDARD, Ph.D UNDER 37 C.F.R. § 1.132

Assistant Commissioner of Patents  
Washington, D.C. 20231

Sir:

I, Audrey D. Goddard, Ph.D. do hereby declare and say as follows:

1. I am a Senior Clinical Scientist at the Experimental Medicine/BioOncology, Medical Affairs Department of Genentech, Inc., South San Francisco, California 94080.
2. Between 1993 and 2001, I headed the DNA Sequencing Laboratory at the Molecular Biology Department of Genentech, Inc. During this time, my responsibilities included the identification and characterization of genes contributing to the oncogenic process, and determination of the chromosomal localization of novel genes.
3. My scientific Curriculum Vitae, including my list of publications, is attached to and forms part of this Declaration (Exhibit A).

Serial No.: \*

Filed: \*

4. I am familiar with a variety of techniques known in the art for detecting and quantifying the amplification of oncogenes in cancer, including the quantitative TaqMan PCR (i.e., "gene amplification") assay described in the above captioned patent application.

5. The TaqMan PCR assay is described, for example, in the following scientific publications: Higuchi *et al.*, Biotechnology 10:413-417 (1992) (Exhibit B); Livak *et al.*, PCR Methods Appl. 4:357-362 (1995) (Exhibit C) and Heid *et al.*, Genome Res. 6:986-994 (1996) (Exhibit D). Briefly, the assay is based on the principle that successful PCR yields a fluorescent signal due to Taq DNA polymerase-mediated exonuclease digestion of a fluorescently labeled oligonucleotide that is homologous to a sequence between two PCR primers. The extent of digestion depends directly on the amount of PCR, and can be quantified accurately by measuring the increment in fluorescence that results from decreased energy transfer. This is an extremely sensitive technique, which allows detection in the exponential phase of the PCR reaction and, as a result, leads to accurate determination of gene copy number.

6. The quantitative fluorescent TaqMan PCR assay has been extensively and successfully used to characterize genes involved in cancer development and progression. Amplification of protooncogenes has been studied in a variety of human tumors, and is widely considered as having etiological, diagnostic and prognostic significance. This use of the quantitative TaqMan PCR assay is exemplified by the following scientific publications: Pennica *et al.*, Proc. Natl. Acad. Sci. USA 95(25):14717-14722 (1998) (Exhibit E); Pitti *et al.*, Nature 396(6712):699-703 (1998) (Exhibit F) and Bieche *et al.*, Int. J. Cancer 78:661-666 (1998) (Exhibit G), the first two of which I am co-author. In particular, Pennica *et al.* have used the quantitative TaqMan PCR assay to study relative gene amplification of WISP and c-myc in various cell lines, colorectal tumors and normal mucosa. Pitti *et al.* studied the genomic amplification of a decoy receptor for Fas ligand in lung and colon cancer, using the quantitative TaqMan PCR assay. Bieche *et al.* used the assay to study gene amplification in breast cancer.

Serial No.: \*

Filed: \*

7. It is my personal experience that the quantitative TaqMan PCR technique is technically sensitive enough to detect at least a 2-fold increase in gene copy number relative to control. It is further my considered scientific opinion that an at least 2-fold increase in gene copy number in a tumor tissue sample relative to a normal (i.e., non-tumor) sample is significant and useful in that the detected increase in gene copy number in the tumor sample relative to the normal sample serves as a basis for using relative gene copy number as quantitated by the TaqMan PCR technique as a diagnostic marker for the presence or absence of tumor in a tissue sample of unknown pathology. Accordingly, a gene identified as being amplified at least 2-fold by the quantitative TaqMan PCR assay in a tumor sample relative to a normal sample is useful as a marker for the diagnosis of cancer, for monitoring cancer development and/or for measuring the efficacy of cancer therapy.

8. I declare further that all statements made herein of my own knowledge are true and that all statements made on information and belief are believed to be true. I declare that these statements were made with the knowledge that willful false statements and the like so made are punishable by fine or imprisonment, or both, under Section 1001 of Title 18 of the United States Code, and that such willful false statements may jeopardize the validity of the application or any patent issuing thereon.

Jan. 16, 2003

Date

Audrey D. Goddard

Audrey D. Goddard, Ph.D.

**AUDREY D. GODDARD, Ph.D.**

Genentech, Inc.  
1 DNA Way  
South San Francisco, CA, 94080  
650.225.6429  
goddarda@gene.com

110 Congo St.  
San Francisco, CA, 94131  
415.841.9154  
415.819.2247 (mobile)  
agoddard@pacbell.net

**PROFESSIONAL EXPERIENCE**

**Genentech, Inc.**  
**South San Francisco, CA**

**1993-present**

**2001 - present      Senior Clinical Scientist**  
Experimental Medicine / BioOncology, Medical Affairs

**Responsibilities:**

- *Companion diagnostic oncology products*
- *Acquisition of clinical samples from Genentech's clinical trials for translational research*
- *Translational research using clinical specimen and data for drug development and diagnostics*
- *Member of Development Science Review Committee, Diagnostic Oversight Team, 21 CFR Part 11 Subteam*

**Interests:**

- *Ethical and legal implications of experiments with clinical specimens and data*
- *Application of pharmacogenomics in clinical trials*

**1998 - 2001      Senior Scientist**  
Head of the DNA Sequencing Laboratory, Molecular Biology Department, Research

**Responsibilities:**

- *Management of a laboratory of up to nineteen—including postdoctoral fellow, associate scientist, senior research associate and research assistants/associate levels*
- *Management of a \$750K budget*
- *DNA sequencing core facility supporting a 350+ person research facility*
- *DNA sequencing for high throughput gene discovery, - ESTs, cDNAs, and constructs*
- *Genomic sequence analysis and gene identification*
- *DNA sequence and primary protein analysis*

**Research:**

- *Chromosomal localization of novel genes*
- *Identification and characterization of genes contributing to the oncogenic process*
- *Identification and characterization of genes contributing to inflammatory diseases*
- *Design and development of schemes for high throughput genomic DNA sequence analysis*
- *Candidate gene prediction and evaluation*

**1993 - 1998      Scientist**

Head of the DNA Sequencing Laboratory, Molecular Biology Department, Research

**Responsibilities**

- *DNA sequencing core facility supporting a 350+ person research facility*
- *Assumed responsibility for a pre-existing team of five technicians and expanded the group into fifteen, introducing a level of middle management and additional areas of research*
- *Participated in the development of the basic plan for high throughput secreted protein discovery program – sequencing strategies, data analysis and tracking, database design*
- *High throughput EST and cDNA sequencing for new gene identification.*
- *Design and implementation of analysis tools required for high throughput gene identification.*
- *Chromosomal localization of genes encoding novel secreted proteins.*

**Research:**

- *Genomic sequence scanning for new gene discovery.*
- *Development of signal peptide selection methods.*
- *Evaluation of candidate disease genes.*
- *Growth hormone receptor gene SNPs in children with Idiopathic short stature*

**Imperial Cancer Research Fund  
London, UK with Dr. Ellen Solomon**

**1989-1992**

**6/89 – 12/92: Postdoctoral Fellow**

- *Cloning and characterization of the genes fused at the acute promyelocytic leukemia translocation breakpoints on chromosomes 17 and 15.*
- *Prepared a successfully funded European Union multi-center grant application*

**McMaster University  
Hamilton, Ontario, Canada with Dr. G. D. Sweeney**

**1983**

**5/83 – 8/83: NSERC Summer Student**

- *In vitro metabolism of  $\beta$ -naphthoflavone in C57Bl/6J and DBA mice*

**EDUCATION**

**Ph.D.**

"Phenotypic and genotypic effects of mutations in the human retinoblastoma gene."

**Supervisor:** Dr. R. A. Phillips

University of Toronto  
Toronto, Ontario, Canada.  
Department of Medical  
Biophysics.

**1989**

**Honours B.Sc**

"The *in vitro* metabolism of the cytochrome P-448 inducer  $\beta$ -naphthoflavone in C57BL/6J mice."

**Supervisor:** Dr. G. D. Sweeney

McMaster University,  
Hamilton, Ontario, Canada.  
Department of Biochemistry

**1983**

## ACADEMIC AWARDS

Imperial Cancer Research Fund Postdoctoral Fellowship	1989-1992
Medical Research Council Studentship	1983-1988
NSERC Undergraduate Summer Research Award	1983
Society of Chemical Industry Merit Award (Hons. Biochem.)	1983
Dr. Harry Lyman Hooker Scholarship	1981-1983
J.L.W. Gill Scholarship	1981-1982
Business and Professional Women's Club Scholarship	1980-1981
Wyerhauser Foundation Scholarship	1979-1980

## INVITED PRESENTATIONS

Genentech's gene discovery pipeline: High throughput identification, cloning and characterization of novel genes. Functional Genomics: From Genome to Function, Litchfield Park, AZ, USA. October 2000

High throughput identification, cloning and characterization of novel genes. G2K: Back to Science, Advances in Genome Biology and Technology I. Marco Island, FL, USA. February 2000

Quality control in DNA Sequencing: The use of Phred and Phrap. Bay Area Sequencing Users Meeting, Berkeley, CA, USA. April 1999

High throughput secreted protein identification and cloning. Tenth International Genome Sequencing and Analysis Conference, Miami, FL, USA. September 1998

The evolution of DNA sequencing: The Genentech perspective. Bay Area Sequencing Users Meeting, Berkeley, CA, USA. May 1998

Partial Growth Hormone Insensitivity: The role of GH-receptor mutations in Idiopathic Short Stature. Tenth Annual National Cooperative Growth Study Investigators Meeting, San Francisco, CA, USA. October, 1996

Growth hormone (GH) receptor defects are present in selected children with non-GH-deficient short stature: A molecular basis for partial GH-insensitivity. 76<sup>th</sup> Annual Meeting of The Endocrine Society, Anaheim, CA, USA. June 1994

A previously uncharacterized gene, myl, is fused to the retinoic acid receptor alpha gene in acute promyelocytic leukemia. XV International Association for Comparative Research on Leukemia and Related Disease, Padua, Italy. October 1991

## PATENTS

Goddard A, Godowski PJ, Gurney AL. NL2 Tie ligand homologue polypeptide. Patent Number: 6,455,496. Date of Patent: Sept. 24, 2002.

Goddard A, Godowski PJ and Gurney AL. NL3 Tie ligand homologue nucleic acids. Patent Number: 6,426,218. Date of Patent: July 30, 2002.

Godowski P, Gurney A, Hillan KJ, Botstein D, Goddard A, Roy M, Ferrara N, Tumas D, Schwall R. NL4 Tie ligand homologue nucleic acid. Patent Number: 6,4137,770. Date of Patent: July 2, 2002.

Ashkenazi A, Fong S, Goddard A, Gurney AL, Napier MA, Tumas D, Wood WI. Nucleic acid encoding A-33 related antigen poly peptides. Patent Number: 6,410,708. Date of Patent: Jun. 25, 2002.

Botstein DA, Cohen RL, Goddard AD, Gurney AL, Hillan KJ, Lawrence DA, Levine AJ, Pennica D, Roy MA and Wood WI. WISP polypeptides and nucleic acids encoding same. Patent Number: 6,387,657. Date of Patent: May 14, 2002.

Goddard A, Godowski PJ and Gurney AL. Tie ligands. Patent Number: 6,372,491. Date of Patent: April 16, 2002.

Godowski PJ, Gurney AL, Goddard A and Hillan K. TIE ligand homologue antibody. Patent Number: 6,350,450. Date of Patent: Feb. 26, 2002.

Fong S, Ferrara N, Goddard A, Godowski PJ, Gurney AL, Hillan K and Williams PM. Tie receptor tyrosine kinase ligand homologues. Patent Number: 6,348,351. Date of Patent: Feb. 19, 2002.

Goddard A, Godowski PJ and Gurney AL. Ligand homologues. Patent Number: 6,348,350. Date of Patent: Feb. 19, 2002.

Attie KM, Carlsson LMS, Gesundheit N and Goddard A. Treatment of partial growth hormone insensitivity syndrome. Patent Number: 6,207,640. Date of Patent: March 27, 2001.

Fong S, Ferrara N, Goddard A, Godowski PJ, Gurney AL, Hillan K and Williams PM. Nucleic acids encoding NL-3. Patent Number: 6,074,873. Date of Patent: June 13, 2000

Attie K, Carlsson LMS, Gesundheit N and Goddard A. Treatment of partial growth hormone insensitivity syndrome. Patent Number: 5,824,642. Date of Patent: October 20, 1998

Attie K, Carlsson LMS, Gesundheit N and Goddard A. Treatment of partial growth hormone insensitivity syndrome. Patent Number: 5,646,113. Date of Patent: July 8, 1997

Multiple additional provisional applications filed

## PUBLICATIONS

- Seshasayee D, Dowd P, Gu Q, Erickson S, Goddard AD: Comparative sequence analysis of the *HER2* locus in mouse and man. Manuscript in preparation.
- Abuzzahab MJ, Goddard A, Grigorescu F, Lautier C, Smith RJ and Chernausek SD. Human IGF-1 receptor mutations resulting in pre- and post-natal growth retardation. Manuscript in preparation.
- Aggarwal S, Xie, M-H, Foster J, Frantz G, Stinson J, Corpuz RT, Simmons L, Hillan K, Yansura DG, Vandlen RL, Goddard AD and Gurney AL. FHFR, a novel receptor for the fibroblast growth factors. Manuscript submitted.
- Adams SH, Chui C, Schilbach SL, Yu XX, Goddard AD, Grimaldi JC, Lee J, Dowd P, Colman S., Lewin DA. (2001) BFIT, a unique acyl-CoA thioesterase induced in thermogenic brown adipose tissue: Cloning, organization of the human gene, and assessment of a potential link to obesity. *Biochemical Journal* **360**: 135-142.
- Lee J, Ho WH, Maruoka M, Corpuz RT, Baldwin DT, Foster JS, Goddard AD, Yansura DG, Vandlen RL, Wood WI, Gurney AL. (2001) IL-17E, a novel proinflammatory ligand for the IL-17 receptor homolog IL-17Rh1. *Journal of Biological Chemistry* **276**(2): 1660-1664.
- Xie M-H, Aggarwal S, Ho W-H, Foster J, Zhang Z, Stinson J, Wood WI, Goddard AD and Gurney AL. (2000) Interleukin (IL)-22, a novel human cytokine that signals through the interferon-receptor related proteins CRF2-4 and IL-22R. *Journal of Biological Chemistry* **275**: 31335-31339.
- Weiss GA, Watanabe CK, Zhong A, Goddard A and Sidhu SS. (2000) Rapid mapping of protein functional epitopes by combinatorial alanine scanning. *Proc. Natl. Acad. Sci. USA* **97**: 8950-8954.
- Guo S, Yamaguchi Y, Schilbach S, Wada T, Lee J, Goddard A, French D, Handa H, Rosenthal A. (2000) A regulator of transcriptional elongation controls vertebrate neuronal development. *Nature* **408**: 366-369.
- Yan M, Wang L-C, Hymowitz SG, Schilbach S, Lee J, Goddard A, de Vos AM, Gao WQ, Dixit VM. (2000) Two-amino acid molecular switch in an epithelial morphogen that regulates binding to two distinct receptors. *Science* **290**: 523-527.
- Sehl PD, Tai JTN, Hillan KJ, Brown LA, Goddard A, Yang R, Jin H and Lowe DG. (2000) Application of cDNA microarrays in determining molecular phenotype in cardiac growth, development, and response to injury. *Circulation* **101**: 1990-1999.
- Guo S, Brush J, Teraoka H, Goddard A, Wilson SW, Mullins MC and Rosenthal A. (1999) Development of noradrenergic neurons in the zebrafish hindbrain requires BMP, FGF8, and the homeodomain protein soulless/Phox2A. *Neuron* **24**: 555-566.
- Stone D, Murone, M, Luoh, S, Ye W, Armanini P, Gurney A, Phillips HS, Brush, J, Goddard A, de Sauvage FJ and Rosenthal A. (1999) Characterization of the human suppressor of fused, a negative regulator of the zinc-finger transcription factor Gli. *J. Cell Sci.* **112**: 4437-4448.
- Xie M-H, Holcomb I, Deuel B, Dowd P, Huang A, Vagts A, Foster J, Liang J, Brush J, Gu Q, Hillan K, Goddard A and Gurney, A.L. (1999) FGF-19, a novel fibroblast growth factor with unique specificity for FGFR4. *Cytokine* **11**: 729-735.

Yan M, Lee J, Schilbach S, Goddard A and Dixit V. (1999) mE10, a novel caspase recruitment domain-containing proapoptotic molecule. *J. Biol. Chem.* **274**(15): 10287-10292.

Gurney AL, Marsters SA, Huang RM, Pitti RM, Mark DT, Baldwin DT, Gray AM, Dowd P, Brush J, Heldens S, Schow P, Goddard AD, Wood WI, Baker KP, Godowski PJ and Ashkenazi A. (1999) Identification of a new member of the tumor necrosis factor family and its receptor, a human ortholog of mouse GITR. *Current Biology* **9**(4): 215-218.

Ridgway JBB, Ng E, Kern JA, Lee J, Brush J, Goddard A and Carter P. (1999) Identification of a human anti-CD55 single-chain Fv by subtractive panning of a phage library using tumor and nontumor cell lines. *Cancer Research* **59**: 2718-2723.

Pitti RM, Marsters SA, Lawrence DA, Roy M, Kischkel FC, Dowd P, Huang A, Donahue CJ, Sherwood SW, Baldwin DT, Godowski PJ, Wood WI, Gurney AL, Hillan KJ, Cohen RL, Goddard AD, Botstein D and Ashkenazi A. (1998) Genomic amplification of a decoy receptor for Fas ligand in lung and colon cancer. *Nature* **396**(6712): 699-703.

Pennica D, Swanson TA, Welsh JW, Roy MA, Lawrence DA, Lee J, Brush J, Taneyhill LA, Deuel B, Lew M, Watanabe C, Cohen RL, Melhem MF, Finley GG, Quirke P, Goddard AD, Hillan KJ, Gurney AL, Botstein D and Levine AJ. (1998) WISP genes are members of the connective tissue growth factor family that are up-regulated in wnt-1-transformed cells and aberrantly expressed in human colon tumors. *Proc. Natl. Acad. Sci. USA*. **95**(25): 14717-14722.

Yang RB, Mark MR, Gray A, Huang A, Xie MH, Zhang M, Goddard A, Wood WI, Gurney AL and Godowski PJ. (1998) Toll-like receptor-2 mediates lipopolysaccharide-induced cellular signalling. *Nature* **395**(6699): 284-288.

Merchant AM, Zhu Z, Yuan JQ, Goddard A, Adams CW, Presta LG and Carter P. (1998) An efficient route to human bispecific IgG. *Nature Biotechnology* **16**(7): 677-681.

Marsters SA, Sheridan JP, Pitti RM, Brush J, Goddard A and Ashkenazi A. (1998) Identification of a ligand for the death-domain-containing receptor Apo3. *Current Biology* **8**(9): 525-528.

Xie J, Murone M, Luoh SM, Ryan A, Gu Q, Zhang C, Bonifas JM, Lam CW, Hynes M, Goddard A, Rosenthal A, Epstein EH Jr. and de Sauvage FJ. (1998) Activating Smoothed mutations in sporadic basal-cell carcinoma. *Nature*. **391**(6662): 90-92.

Marsters SA, Sheridan JP, Pitti RM, Huang A, Skubatch M, Baldwin D, Yuan J, Gurney A, Goddard AD, Godowski P and Ashkenazi A. (1997) A novel receptor for Apo2L/TRAIL contains a truncated death domain. *Current Biology*. **7**(12): 1003-1006.

Hynes M, Stone DM, Dowd M, Pitts-Meek S, Goddard A, Gurney A and Rosenthal A. (1997) Control of cell pattern in the neural tube by the zinc finger transcription factor *Gli-1*. *Neuron* **19**: 15-26.

Sheridan JP, Marsters SA, Pitti RM, Gurney A, Skubatch M, Baldwin D, Ramakrishnan L, Gray CL, Baker K, Wood WI, Goddard AD, Godowski P, and Ashkenazi A. (1997) Control of TRAIL-Induced Apoptosis by a Family of Signaling and Decoy Receptors. *Science* **277** (5327): 818-821.

- Goddard AD, Dowd P, Chernausek S, Geffner M, Gertner J, Hintz R, Hopwood N, Kaplan S, Plotnick L, Rogol A, Rosenfield R, Saenger P, Mauras N, Hershkopf R, Angulo M and Attie, K. (1997) Partial growth hormone insensitivity: The role of growth hormone receptor mutations in idiopathic short stature. *J. Pediatr.* **131**: S51-55.
- Klein RD, Sherman D, Ho WH, Stone D, Bennett GL, Moffat B, Vandlen R, Simmons L, Gu Q, Hongo JA, Devaux B, Poulsen K, Armanini M, Nozaki C, Asai N, Goddard A, Phillips H, Henderson CE, Takahashi M and Rosenthal A. (1997) A GPI-linked protein that interacts with Ret to form a candidate neurturin receptor. *Nature*. **387**(6634): 717-21.
- Stone DM, Hynes M, Armanini M, Swanson TA, Gu Q, Johnson RL, Scott MP, Pennica D, Goddard A, Phillips H, Noll M, Hooper JE, de Sauvage F and Rosenthal A. (1996) The tumour-suppressor gene patched encodes a candidate receptor for Sonic hedgehog. *Nature* **384**(6605): 129-34.
- Marsters SA, Sheridan JP, Donahue CJ, Pitti RM, Gray CL, Goddard AD, Bauer KD and Ashkenazi A. (1996) Apo-3, a new member of the tumor necrosis factor receptor family, contains a death domain and activates apoptosis and NF-kappa  $\beta$ . *Current Biology* **6**(12): 1669-76.
- Rothe M, Xiong J, Shu HB, Williamson K, Goddard A and Goeddel DV. (1996) I-TRAF is a novel TRAF-interacting protein that regulates TRAF-mediated signal transduction. *Proc. Natl. Acad. Sci. USA* **93**: 8241-8246.
- Yang M, Luoh SM, Goddard A, Reilly D, Henzel W and Bass S. (1996) The bglX gene located at 47.8 min on the Escherichia coli chromosome encodes a periplasmic beta-glucosidase. *Microbiology* **142**: 1659-65.
- Goddard AD and Black DM. (1996) Familial Cancer in Molecular Endocrinology of Cancer. Waxman, J. Ed. Cambridge University Press, Cambridge UK, pp.187-215.
- Treanor JJS, Goodman L, de Sauvage F, Stone DM, Poulsen KT, Beck CD, Gray C, Armanini MP, Pollocks RA, Hefti F, Phillips HS, Goddard A, Moore MW, Buj-Bello A, Davis AM, Asai N, Takahashi M, Vandlen R, Henderson CE and Rosenthal A. (1996) Characterization of a receptor for GDNF. *Nature* **382**: 80-83.
- Klein RD, Gu Q, Goddard A and Rosenthal A. (1996) Selection for genes encoding secreted proteins and receptors. *Proc. Natl. Acad. Sci. USA* **93**: 7108-7113.
- Winslow JW, Moran P, Valverde J, Shih A, Yuan JQ, Wong SC, Tsai SP, Goddard A, Henzel WJ, Hefti F and Caras I. (1995) Cloning of AL-1, a ligand for an Eph-related tyrosine kinase receptor involved in axon bundle formation. *Neuron* **14**: 973-981.
- Bennett BD, Zeigler FC, Gu Q, Fendly B, Goddard AD, Gillett N and Matthews W. (1995) Molecular cloning of a ligand for the EPH-related receptor protein-tyrosine kinase Htk. *Proc. Natl. Acad. Sci. USA* **92**: 1866-1870.
- Huang X, Yuang J, Goddard A, Foulis A, James RF, Lernmark A, Pujol-Borrell R, Rabinovitch A, Somoza N and Stewart TA. (1995) Interferon expression in the pancreases of patients with type I diabetes. *Diabetes* **44**: 658-664.
- Goddard AD, Yuan JQ, Fairbairn L, Dexter M, Borrow J, Kozak C and Solomon E. (1995) Cloning of the murine homolog of the leukemia-associated PML gene. *Mammalian Genome* **6**: 732-737.

Goddard AD, Covello R, Luoh SM, Clackson T, Attie KM, Gesundheit N, Rundle AC, Wells JA, Carlsson LMTI and The Growth Hormone Insensitivity Study Group. (1995) Mutations of the growth hormone receptor in children with idiopathic short stature. *N. Engl. J. Med.* 333: 1093-1098.

Kuo SS, Moran P, Gripp J, Armanini M, Phillips HS, Goddard A and Caras IW. (1994) Identification and characterization of Batk, a predominantly brain-specific non-receptor protein tyrosine kinase related to Csk. *J. Neurosci. Res.* 38: 705-715.

Mark MR, Scadden DT, Wang Z, Gu Q, Goddard A and Godowski PJ. (1994) Rse, a novel receptor-type tyrosine kinase with homology to Axl/Ufo, is expressed at high levels in the brain. *Journal of Biological Chemistry* 269: 10720-10728.

Borrow J, Shipley J, Howe K, Kiely F, Goddard A, Sheer D, Srivastava A, Antony AC, Fioretos T, Mitelman F and Solomon E. (1994) Molecular analysis of simple variant translocations in acute promyelocytic leukemia. *Genes Chromosomes Cancer* 9: 234-243.

Goddard AD and Solomon E. (1993) Genetics of Cancer. *Adv. Hum. Genet.* 21: 321-376.

Borrow J, Goddard AD, Gibbons B, Katz F, Swirsky D, Fioretos T, Dube I, Winfield DA, Kingston J, Hagemeijer A, Rees JKH, Lister AT and Solomon E. (1992) Diagnosis of acute promyelocytic leukemia by RT-PCR: Detection of PML-RARA and RARA-PML fusion transcripts. *Br. J. Haematol.* 82: 529-540.

Goddard AD, Borrow J and Solomon E. (1992) A previously uncharacterized gene, PML, is fused to the retinoic acid receptor alpha gene in acute promyelocytic leukemia. *Leukemia* 6 Suppl 3: 117S-119S.

Zhu X, Dunn JM, Goddard AD, Squire JA, Becker A, Phillips RA and Gallie BL. (1992) Mechanisms of loss of heterozygosity in retinoblastoma. *Cytogenet. Cell. Genet.* 59: 248-252.

Foulkes W, Goddard A and Patel K. (1991) Retinoblastoma linked with Seascale. [letter]. *British Med. J.* 302: 409.

Goddard AD, Borrow J, Freemont PS and Solomon E. (1991) Characterization of a novel zinc finger gene disrupted by the t(15;17) in acute promyelocytic leukemia. *Science* 254: 1371-1374.

Solomon E, Borrow J and Goddard AD. (1991) Chromosomal aberrations in cancer. *Science* 254: 1153-1160.

Pajunen L, Jones TA, Goddard A, Sheer D, Solomon E, Pihlajaniemi T and Kivirikko KI. (1991) Regional assignment of the human gene coding for a multifunctional peptide (P4HB) acting as the  $\beta$ -subunit of prolyl-4-hydroxylase and the enzyme protein disulfide isomerase to 17q25. *Cytogenet. Cell. Genet.* 56: 165-168.

Borrow J, Black DM, Goddard AD, Yagle MK, Frischauf A.-M and Solomon E. (1991) Construction and regional localization of a NotI linking library from human chromosome 17q. *Genomics* 10: 477-480.

Borrow J, Goddard AD, Sheer D and Solomon E. (1990) Molecular analysis of acute promyelocytic leukemia breakpoint cluster region on chromosome 17. *Science* 249: 1577-1580.

Myers JC, Jones TA, Pohjolainen E-R, Kadri AS, Goddard AD, Sheer D, Solomon E and Pihlajaniemi T. (1990) Molecular cloning of 5(IV) collagen and assignment of the gene to the region of the region of the X-chromosome containing the Alport Syndrome locus. *Am. J. Hum. Genet.* 46: 1024-1033.

Gallie BL, Squire JA, Goddard A, Dunn JM, Canton M, Hinton D, Zhu X and Phillips RA. (1990) Mechanisms of oncogenesis in retinoblastoma. *Lab. Invest.* 62: 394-408.

Goddard AD, Phillips RA, Gröger V, Passarge E, Hopping W, Gallie BL and Horsthemke B. (1990) Use of the RB1 cDNA as a diagnostic probe in retinoblastoma families. *Clinical Genetics* 37: 117-126.

Zhu XP, Dunn JM, Phillips RA, Goddard AD, Paton KE, Becker A and Gallie BL. (1989) Germine, but not somatic, mutations of the RB1 gene preferentially involve the paternal allele. *Nature* 340: 312-314.

Gallie BL, Dunn JM, Goddard A, Becker A and Phillips RA. (1988) Identification of mutations in the putative retinoblastoma gene. In Molecular Biology of The Eye: Genes, Vision and Ocular Disease. UCLA Symposia on Molecular and Cellular Biology, New Series, Volume 88. J. Piatigorsky, T. Shinohara and P.S. Zelenka, Eds. Alan R. Liss, Inc., New York, 1988, pp. 427-436.

Goddard AD, Balakier H, Canton M, Dunn J, Squire J, Reyes E, Becker A, Phillips RA and Gallie BL. (1988) Infrequent genomic rearrangement and normal expression of the putative RB1 gene in retinoblastoma tumors. *Mol. Cell. Biol.* 8: 2082-2088.

Squire J, Dunn J, Goddard A, Hoffman T, Musarella M, Willard HF, Becker AJ, Gallie BL and Phillips RA. (1986) Cloning of the esterase D gene: A polymorphic gene probe closely linked to the retinoblastoma locus on chromosome 13. *Proc. Natl. Acad. Sci. USA* 83: 6573-6577.

Squire J, Goddard AD, Canton M, Becker A, Phillips RA and Gallie BL (1986) Tumour induction by the retinoblastoma mutation is independent of N-myc expression. *Nature* 322: 555-557.

Goddard AD, Heddle JA, Gallie BL and Phillips RA. (1985) Radiation sensitivity of fibroblasts of bilateral retinoblastoma patients as determined by micronucleus induction *in vitro*. *Mutation Research* 152: 31-38.

# RESEARCH/

## SIMULTANEOUS AMPLIFICATION AND DETECTION OF SPECIFIC DNA SEQUENCES

Russell Higuchi\*, Gavin Dollinger, P. Sean Walsh and Robert Griffith

Roche Molecular Systems, Inc., 1400 53rd St., Emeryville, CA 94608; Chiron Corporation, 1400 53rd St., Emeryville, CA 94608; \*Corresponding author.

We have enhanced the polymerase chain reaction (PCR) such that specific DNA sequences can be detected without opening the reaction tube. This enhancement requires the addition of ethidium bromide (EtBr) to a PCR. Since the fluorescence of EtBr increases in the presence of double-stranded (ds) DNA an increase in fluorescence in such a PCR indicates a positive amplification, which can be easily monitored externally. In fact, amplification can be continuously monitored in order to follow its progress. The ability to simultaneously amplify specific DNA sequences and detect the product of the amplification both simplifies and improves PCR and may facilitate its automation and more widespread use in the clinic or in other situations requiring high sample throughput.

Although the potential benefits of PCR<sup>1</sup> to clinical diagnostics are well known<sup>2-5</sup>, it is still not widely used in this setting, even though it is four years since thermostable DNA polymerases<sup>6</sup> made PCR practical. Some of the reasons for its slow acceptance are high cost, lack of automation of pre- and post-PCR processing steps, and false positive results from carryover contamination. The first two points are related in that labor is the largest contributor to cost at the present stage of PCR development. Most current assays require some form of "downstream" processing once thermocycling is done in order to determine whether the target DNA sequence was present and has amplified. These include DNA hybridization<sup>7,8</sup>, gel electrophoresis with or without use of restriction digestion<sup>9</sup>, HPLC<sup>10</sup>, or capillary electrophoresis<sup>11</sup>. These methods are labor-intensive, have low throughput, and are difficult to automate. The third point is also closely related to downstream processing. The handling of the PCR product in these downstream processes increases the chances that amplified DNA will spread through the typing lab, resulting in a risk of

"carryover" false positives in subsequent testing.

These downstream processing steps would be eliminated if specific amplification and detection of amplified DNA took place simultaneously within an unopened reaction vessel. Assays in which such different processes take place without the need to separate reaction components have been termed "homogeneous". No truly homogeneous PCR assay has been demonstrated to date, although progress towards this end has been reported. Chehab et al.<sup>12</sup> developed a PCR-product detection scheme using fluorescent primers that resulted in a fluorescent PCR product. Allele specific primers, each with different fluorescent tags, were used to indicate the genotype of the DNA. However, the unincorporated primers must still be removed in a downstream process in order to visualize the result. Recently, Holland et al.<sup>13</sup> developed an assay in which the endogenous 5' exonuclease assay of *Taq* DNA polymerase was exploited to cleave a labeled oligonucleotide probe. The probe would only cleave if PCR amplification had produced its complementary sequence. In order to detect the cleavage products, however, a subsequent process is again needed.

We have developed a truly homogeneous assay for PCR and PCR product detection based upon the greatly increased fluorescence that ethidium bromide and other DNA binding dyes exhibit when they are bound to ds-DNA.<sup>14-16</sup> As outlined in Figure 1, a prototype PCR

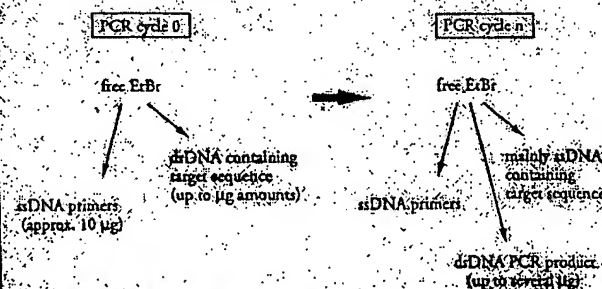


**FIGURE 1** Principle of simultaneous amplification and detection of PCR product. The components of a PCR containing EtBr that are fluorescent are listed—EtBr itself, EtBr bound to either ssDNA or dsDNA. There is a large fluorescence enhancement when EtBr is bound to DNA and binding is greatly enhanced when DNA is double stranded. After sufficient (n) cycles of PCR, the net increase in dsDNA results in additional EtBr binding, and a net increase in total fluorescence.

0 1/16 1/8 1/4 1/2 1 2 4 8  $\mu\text{g/ml}$  EtBr



**FIGURE 1** Gel electrophoresis of PCR amplification products of the human nuclear gene, HLA-DQ $\alpha$ , made in the presence of increasing amounts of EtBr (up to 8  $\mu\text{g/ml}$ ). The presence of EtBr has no obvious effect on the yield or specificity of amplification.

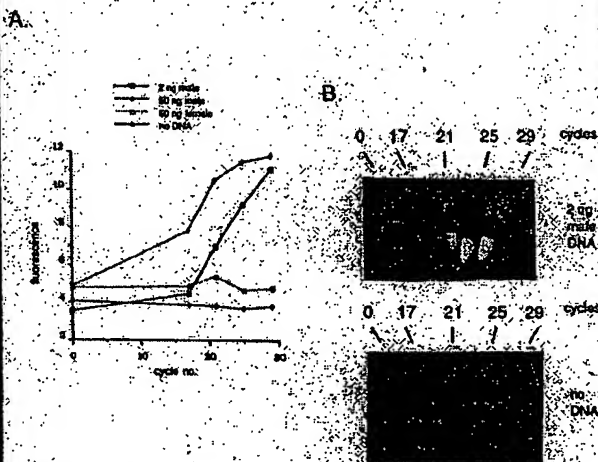


**FIGURE 3** (A) Fluorescence measurements from PCR tubes that contain 0.5  $\mu\text{g/ml}$  EtBr and that are specific for Y-chromosome repeat sequences. Five replicate PCRs were begun containing each of the DNAs specified. At each indicated cycle, one of the five replicate PCRs for each DNA was removed from thermocycling and its fluorescence measured. Units of fluorescence are arbitrary. (B) UV photograph of PCR tubes (0.5 ml Eppendorf-style, polypropylene micro-centrifuge tubes) containing reactions, those starting from 2 ng male DNA and control reactions without any DNA, from (A).

begins with primers that are single-stranded DNA (ss-DNA), dNTPs, and DNA polymerase. An amount of dsDNA containing the target sequence (target DNA) is also typically present. This amount can vary, depending on the application, from single-cell amounts of DNA<sup>17</sup> to micrograms per-PCR<sup>18</sup>. If EtBr is present, the reagents that will fluoresce, in order of increasing fluorescence, are free EtBr itself, and EtBr bound to the single-stranded DNA primers and to the double-stranded target DNA (by its intercalation between the stacked bases of the DNA double-helix). After the first denaturation cycle, target DNA will be largely single-stranded. After a PCR is completed, the most significant change is the increase in the amount of dsDNA (the PCR product itself) of up to several micrograms. Formerly free EtBr is bound to the additional dsDNA, resulting in an increase in fluorescence. There is also some decrease in the amount of ssDNA primer, but because the binding of EtBr to ssDNA is much less than to dsDNA, the effect of this change on the total fluorescence of the sample is small. The fluorescence increase can be measured by directing excitation illumination through the walls of the amplification vessel

before and after, or even continuously during, thermocycling.

## RESULTS

**PCR in the presence of EtBr.** In order to assess the effect of EtBr in PCR, amplifications of the human HLA-DQ $\alpha$  gene<sup>19</sup> were performed with the dye present at concentrations from 0.06 to 8.0  $\mu\text{g/ml}$  (a typical concentration of EtBr used in staining of nucleic acids following gel electrophoresis is 0.5  $\mu\text{g/ml}$ ). As shown in Figure 2, gel electrophoresis revealed little or no difference in the yield or quality of the amplification product whether EtBr was absent or present at any of these concentrations, indicating that EtBr does not inhibit PCR.

**Detection of human Y-chromosome specific sequences.** Sequence-specific fluorescence enhancement of EtBr as a result of PCR was demonstrated in a series of amplifications containing 0.5  $\mu\text{g/ml}$  EtBr and primers specific to repeat DNA sequences found on the human Y-chromosome<sup>20</sup>. These PCRs initially contained either 60 ng male, 60 ng female, 2 ng male human or no DNA. Five replicate PCRs were begun for each DNA. After 0, 17, 21, 24 and 29 cycles of thermocycling, a PCR for each DNA was removed from the thermocycler, and its fluorescence measured in a spectrofluorometer and plotted vs. amplification cycle number (Fig. 3A). The shape of this curve reflects the fact that by the time an increase in fluorescence can be detected, the increase in DNA is becoming linear and not exponential with cycle number. As shown, the fluorescence increased about three-fold over the background fluorescence for the PCRs containing human male DNA, but did not significantly increase for negative control PCRs, which contained either no DNA or human female DNA. The more male DNA present to begin with—60 ng versus 2 ng—the fewer cycles were needed to give a detectable increase in fluorescence. Gel electrophoresis on the products of these amplifications showed that DNA fragments of the expected size were made in the male DNA containing reactions and that little DNA synthesis took place in the control samples.

In addition, the increase in fluorescence was visualized by simply laying the completed, unopened PCR tubes on a UV transilluminator and photographing them through a red filter. This is shown in figure 3B for the reactions that began with 2 ng male DNA and those with no DNA.

**Detection of specific alleles of the human  $\beta$ -globin gene.** In order to demonstrate that this approach has adequate specificity to allow genetic screening, a detection of the sickle-cell anemia mutation was performed. Figure 4 shows the fluorescence from completed amplifications containing EtBr (0.5  $\mu\text{g/ml}$ ) as detected by photography of the reaction tubes on a UV transilluminator. These reactions were performed using primers specific for either the wild-type or sickle-cell mutation of the human  $\beta$ -globin gene<sup>21</sup>. The specificity for each allele is imparted by placing the sickle-mutation site at the terminal 3' nucleotide of one primer. By using an appropriate primer annealing temperature, primer extension—and thus amplification—can take place only if the 3' nucleotide of the primer is complementary to the  $\beta$ -globin allele present.<sup>21,22</sup>

Each pair of amplifications shown in Figure 4 consists of a reaction with either the wild-type allele specific (left tube) or sickle-allele specific (right tube) primers. Three different DNAs were typed: DNA from a homozygous wild-type  $\beta$ -globin individual (AA), from a heterozygous sickle  $\beta$ -globin individual (AS), and from a homozygous sickle  $\beta$ -globin individual (SS). Each DNA (50 ng genomic DNA to start each PCR) was analyzed in triplicate (3 pairs

of reactions each). The DNA type was reflected in the relative fluorescence intensities in each pair of completed amplifications. There was a significant increase in fluorescence only where a  $\beta$ -globin allele DNA matched the primer set. When measured on a spectrofluorometer (data not shown), this fluorescence was about three times that present in a PCR where both  $\beta$ -globin alleles were mismatched to the primer set. Gel electrophoresis (not shown) established that this increase in fluorescence was due to the synthesis of nearly a microgram of a DNA fragment of the expected size for  $\beta$ -globin. There was little synthesis of dsDNA in reactions in which the allele-specific primer was mismatched to both alleles.

**Continuous monitoring of a PCR.** Using a fiber optic device, it is possible to direct excitation illumination from a spectrofluorometer to a PCR undergoing thermocycling and to return its fluorescence to the spectrofluorometer. The fluorescence readout of such an arrangement, directed at an EtBr-containing amplification of Y-chromosome specific sequences from 25 ng of human male DNA, is shown in Figure 5. The readout from a control PCR with no target DNA is also shown. Thirty cycles of PCR were monitored for each.

The fluorescence trace as a function of time clearly shows the effect of the thermocycling. Fluorescence intensity rises and falls inversely with temperature. The fluorescence intensity is minimum at the denaturation temperature (94°C) and maximum at the annealing/extension temperature (50°C). In the negative-control PCR, these fluorescence maxima and minima do not change significantly over the thirty thermocycles, indicating that there is little dsDNA synthesis without the appropriate target DNA, and there is little if any bleaching of EtBr during the continuous illumination of the sample.

In the PCR containing male DNA, the fluorescence maxima at the annealing/extension temperature begin to increase at about 4000 seconds of thermocycling, and continue to increase with time, indicating that dsDNA is being produced at a detectable level. Note that the fluorescence minima at the denaturation temperature do not significantly increase, presumably because at this temperature there is no dsDNA for EtBr to bind. Thus the course of the amplification is followed by tracking the fluorescence increase at the annealing temperature. Analysis of the products of these two amplifications by gel electrophoresis showed a DNA fragment of the expected size for the male DNA-containing sample and no detectable DNA synthesis for the control sample.

## DISCUSSION

Downstream processes such as hybridization to a sequence-specific probe can enhance the specificity of DNA detection by PCR. The elimination of these processes means that the specificity of this homogeneous assay depends solely on that of PCR. In the case of sickle-cell disease, we have shown that PCR alone has sufficient DNA sequence specificity to permit genetic screening. Using appropriate amplification conditions, there is little non-specific production of dsDNA in the absence of the appropriate target allele.

The specificity required to detect pathogens can be more or less than that required to do genetic screening, depending on the number of pathogens in the sample and the amount of other DNA that must be taken with the sample. A difficult target is HIV, which requires detection of a viral genome that can be at the level of a few copies per thousands of host cells<sup>6</sup>. Compared with genetic screening, which is performed on cells containing at least one copy of the target sequence, HIV detection requires both more specificity and the input of more total

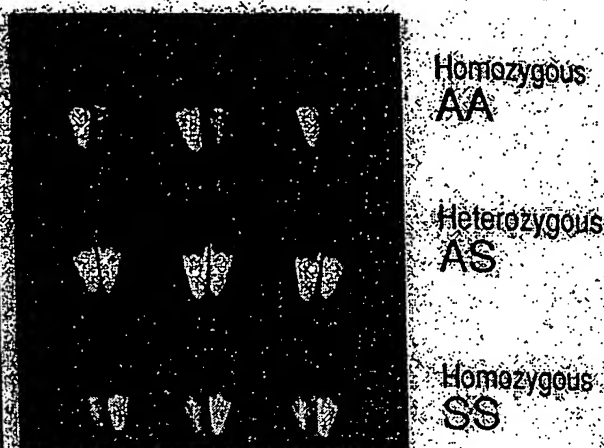


**FIGURE 4** UV photograph of PCR tubes containing amplifications using EtBr that are specific to wild-type (A) or sickle (S) alleles of the human  $\beta$ -globin gene. The left of each pair of tubes contains allele-specific primers to the wild-type alleles, the right tube primers to the sickle allele. The photograph was taken after 30 cycles of PCR, and the input DNAs and the alleles they contain are indicated. Fifty ng of DNA was used to begin PCR. Typing was done in triplicate (3 pairs of PCR) for each input DNA.

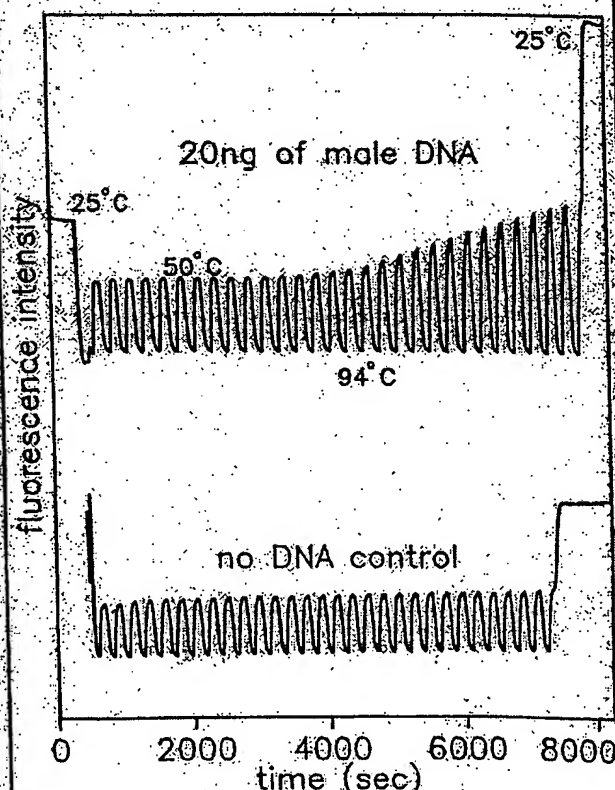


**FIGURE 5** Continuous real-time monitoring of a PCR. A fiber optic was used to carry excitation light to a PCR in progress and also emitted light back to a fluorometer (see Experimental Protocol). Amplification using human male DNA specific primers in a PCR starting with 20 ng of human male DNA (top), or in a control PCR without DNA (bottom), were monitored. Thirty cycles of PCR were followed for each. The temperature cycled between 94°C (denaturation) and 50°C (annealing and extension). Note in the male DNA PCR, the cycle (time) dependent increase in fluorescence at the annealing/extension temperature.

DNA—up to microgram amounts—in order to have sufficient numbers of target sequences. This large amount of starting DNA in an amplification significantly increases the background fluorescence over which any additional fluorescence produced by PCR must be detected. An additional complication that occurs with targets in low copy number is the formation of the "primer-dimer" artifact. This is the result of the extension of one primer using the other primer as a template. Although this occurs infrequently, once it occurs the extension product is a substrate for PCR amplification, and can compete with true PCR targets if those targets are rare. The primer-dimer product is of course dsDNA and thus is a potential source of false signal in this homogeneous assay.

To increase PCR specificity and reduce the effect of primer-dimer amplification, we are investigating a number of approaches, including the use of nested primer amplifications that take place in a single tube<sup>22</sup>, and the "hot-start", in which nonspecific amplification is reduced by raising the temperature of the reaction before DNA synthesis begins<sup>23</sup>. Preliminary results using these approaches suggest that primer-dimer is effectively reduced and it is possible to detect the increase in EtBr fluorescence in a PCR instigated by a single HIV genome in a background of  $10^6$  cells. With larger numbers of cells, the background fluorescence contributed by genomic DNA becomes problematic. To reduce this background, it may be possible to use sequence-specific DNA-binding dyes that can be made to preferentially bind PCR product over genomic DNA by incorporating the dye-binding DNA sequence into the PCR product through a 5' "add-on" to the oligonucleotide primer<sup>24</sup>.

We have shown that the detection of fluorescence generated by an EtBr-containing PCR is straightforward, both once PCR is completed and continuously during thermocycling. The ease with which automation of specific DNA detection can be accomplished is the most promising aspect of this assay. The fluorescence analysis of completed PCRs is already possible with existing instrumentation in 96-well format<sup>25</sup>. In this format, the fluorescence in each PCR can be quantitated before, after, and even at selected points during thermocycling by moving the rack of PCRs to a 96-microwell plate fluorescence reader<sup>26</sup>.

The instrumentation necessary to continuously monitor multiple PCRs simultaneously is also simple in principle. A direct extension of the apparatus used here is to have multiple fiberoptics transmit the excitation light and fluorescent emissions to and from multiple PCRs. The ability to monitor multiple PCRs continuously may allow quantitation of target DNA copy number. Figure 3 shows that the larger the amount of starting target DNA, the sooner during PCR a fluorescence increase is detected. Preliminary experiments (Higuchi and Dollinger, manuscript in preparation) with continuous monitoring have shown a sensitivity to two-fold differences in initial target DNA concentration.

Conversely, if the number of target molecules is known—as it can be in genetic screening—continuous monitoring may provide a means of detecting false positive and false negative results. With a known number of target molecules, a true positive would exhibit detectable fluorescence by a predictable number of cycles of PCR. Increases in fluorescence detected before or after that cycle would indicate potential artifacts. False negative results due to, for example, inhibition of DNA polymerase, may be detected by including within each PCR an inefficiently amplifying marker. This marker results in a fluorescence increase only after a large number of cycles—many more than are necessary to detect a true

positive. If a sample fails to have a fluorescence increase after this many cycles, inhibition may be suspected. Since, in this assay, conclusions are drawn based on the presence or absence of fluorescence signal alone, such controls may be important. In any event, before any test based on this principle is ready for the clinic, an assessment of its false positive/false negative rates will need to be obtained using a large number of known samples.

In summary, the inclusion in PCR of dyes whose fluorescence is enhanced upon binding dsDNA makes it possible to detect specific DNA amplification from outside the PCR tube. In the future, instruments based upon this principle may facilitate the more widespread use of PCR in applications that demand the high throughput of samples.

#### EXPERIMENTAL PROTOCOL

**Human HLA-DQ $\alpha$  gene amplifications containing EtBr.** PCRs were set up in 100  $\mu$ l volumes containing 10 mM Tris-HCl, pH 8.3; 50 mM KCl; 4 mM MgCl<sub>2</sub>; 2.5 units of *Taq* DNA polymerase (Perkin-Elmer Cetus, Norwalk, CT); 20 pmole each of human HLA-DQ $\alpha$  gene specific oligonucleotide primers GH26 and GH27<sup>19</sup>, and approximately  $10^3$  copies of DQ $\alpha$  PCR product diluted from a previous reaction. Ethidium bromide (EtBr; Sigma) was used at the concentrations indicated in Figure 2. Thermocycling proceeded for 20 cycles in a model 480 thermocycler (Perkin-Elmer Cetus, Norwalk, CT) using a "step-cycle" program of 94°C for 1 min, denaturation and 60°C for 30 sec, annealing and 72°C for 30 sec, extension.

**Y-chromosome specific PCR.** PCRs (100  $\mu$ l total reaction volume) containing 0.5  $\mu$ g/ml EtBr were prepared as described for HLA-DQ $\alpha$ , except with different primers and target DNAs. These PCRs contained 15 pmole each male DNA-specific primers Y1.1 and Y1.2<sup>20</sup>, and either 60 ng male, 60 ng female, 2 ng male, or no human DNA. Thermocycling was 94°C for 1 min and 60°C for 1 min using a "step-cycle" program. The number of cycles for a sample were as indicated in Figure 3. Fluorescence measurement is described below.

**Allele-specific, human  $\beta$ -globin gene PCR.** Amplifications of 100  $\mu$ l volume using 0.5  $\mu$ g/ml of EtBr were prepared as described for HLA-DQ $\alpha$  above except with different primers and target DNAs. These PCRs contained either primer pair HGP2/HB14A (wild-type globin specific primers) or HGP2/HB14S (sickle-globin specific primers) at 10 pmole each primer per PCR. These primers were developed by Wu et al.<sup>21</sup>. Three different target DNAs were used in separate amplifications—50 ng each of human DNA that was homozygous for the sickle trait (SS), DNA that was heterozygous for the sickle trait (AS), or DNA that was homozygous for the w.t. globin (AA). Thermocycling was for 30 cycles at 94°C for 1 min, and 55°C for 1 min, using a "step-cycle" program. An annealing temperature of 55°C had been shown by Wu et al.<sup>21</sup> to provide allele-specific amplification. Completed PCRs were photographed through a red filter (Wratten 23A) after placing the reaction tubes atop a model TM-36 transilluminator (UV products, San Gabriel, CA).

**Fluorescence measurement.** Fluorescence measurements were made on PCRs containing EtBr in a Fluorolog-2 fluorometer (SPEX, Edison, NJ). Excitation was at the 500 nm band with about 2 nm bandwidth with a CG 435 nm cut-off filter (Melles Griest, Inc., Irvine, CA) to exclude second-order light. Emitted light was detected at 570 nm with a bandwidth of about 7 nm. An OG 550 nm cut-off filter was used to remove the excitation light.

**Continuous fluorescence monitoring of PCR.** Continuous monitoring of a PCR in progress was accomplished using the spectrofluorometer and settings described above as well as a fiberoptic accessory (SPEX cat. no. 1950) to both send excitation light to, and receive emitted light from, a PCR placed in a well of a model 480 thermocycler (Perkin-Elmer Cetus). The probe end of the fiberoptic cable was attached with "5 minute epoxy" to the open top of a PCR tube (a 0.5 ml polypropylene centrifuge tube with its cap removed) effectively sealing it. The exposed top of the PCR tube and the end of the fiberoptic cable were shielded from room light and the room lights were kept dimmed during each run. The monitored PCR was an amplification of Y-chromosome specific repeat sequences as described above, except using an annealing/extension temperature of 60°C. The reaction was covered with mineral oil (2 drops) to prevent evaporation. Thermocycling and fluorescence measurement were started simultaneously. A time base scan with a 10 second integration time

was used and the emission signal was ratioed to the excitation signal to control for changes in light source intensity. Data were collected using the dm3000f, version 2.5 (SPEX) data system.

#### Acknowledgments

We thank Bob Jones for help with the spectrofluorometric measurements and Heatherbell Tong for editing this manuscript.

#### References

- Mullis, K. A., Faloona, F., Scharf, S., Horn, G. and Erlich, H. 1986. Specific enzymatic amplification of DNA *in vitro*: The polymerase chain reaction. *CSHSQB* 51:263-273.
- White, T. J., Arnheim, N. and Erlich, H. A. 1989. The polymerase chain reaction. *Trends Genet.* 5:185-189.
- Erlich, H. A., Gelfand, D. and Smitsky, J. J. 1991. Recent advances in the polymerase chain reaction. *Science* 252:1643-1651.
- Saiki, R. K., Gelfand, D. H., Stoffel, S., Scharf, S. J., Higuchi, R., Horn, G. T., Mullis, K. B. and Erlich, H. A. 1988. Primer-directed enzymatic amplification of DNA with a thermostable DNA polymerase. *Science* 239:487-491.
- Saiki, R. K., Walsh, P. S., Levenson, C. H. and Erlich, H. A. 1989. Genetic analysis of amplified DNA with immobilized sequence-specific oligonucleotide probes. *Proc. Natl. Acad. Sci. USA* 86:6230-6234.
- Kwok, S. Y., Mack, D. H., Mullis, K. B., Folz, B. J., Ehrlich, G. D., Blair, D. and Friedman-Kien, A. S. 1987. Identification of human immunodeficiency virus sequences by using *in vitro* enzymatic amplification and oligonucleotide cleavage detection. *J. Virol.* 61:1690-1694.
- Chehab, F. F., Doherty, M., Cai, S. P., Kan, Y. W., Cooper, S. and Rubin, E. M. 1987. Detection of sickle cell anemia and thalassemias. *Nature* 329:293-294.
- Horn, G. T., Richards, B. and Klinger, K. W. 1989. Amplification of a highly polymorphic VNTR segment by the polymerase chain reaction. *Nuc. Acids Res.* 16:2140.
- Karl, E. D. and Dong, M. W. 1990. Rapid analysis and purification of polymerase chain reaction products by high-performance liquid chromatography. *Biotechniques* 8:546-555.
- Heiger, D. N., Cohen, A. S. and Karger, B. L. 1990. Separation of DNA restriction fragments by high performance capillary electrophoresis with low and zero crosslinked polyacrylamide using continuous and pulsed electric fields. *J. Chromatogr.* 516:33-48.
- Kwok, S. Y. and Higuchi, R. G. 1989. Avoiding false positives with PCR. *Nature* 339:237-238.
- Chehab, F. F. and Kan, Y. W. 1989. Detection of specific DNA sequences by fluorescence amplification: a color complementation assay. *Proc. Natl. Acad. Sci. USA* 86:9178-9182.
- Holland, P. M., Abramson, R. D., Watson, R. and Gelfand, D. H. 1991. Detection of specific polymerase chain reaction product by utilizing the 5' to 3' exonuclease activity of *Thermus aquaticus* DNA polymerase. *Proc. Natl. Acad. Sci. USA* 88:7276-7280.
- Markovits, J., Roques, B. P. and Le Pecq, J. B. 1979. Ethidium dimer: a new reagent for the fluorimetric determination of nucleic acids. *Anal. Biochem.* 94:259-264.
- Kapuscinski, J. and Szel, W. 1979. Interactions of 4,6-diamidino-2-phenylindole with synthetic polynucleotides. *Nuc. Acids Res.* 6:3519-3534.
- Searle, M. S. and Emptrey, K. J. 1990. Sequence-specific interaction of Hoechst 33258 with the minor groove of an adenine-rich DNA duplex studied in solution by <sup>1</sup>H NMR spectroscopy. *Nuc. Acids Res.* 18:3763-3767.
- Li, H. H., Gyllenstein, U. B., Cui, X. F., Saiki, R. K., Erlich, H. A. and Arnheim, N. 1988. Amplification and analysis of DNA sequences in single human sperm and diploid cells. *Nature* 335:414-417.
- Abbott, M. A., Folz, B. J., Byrne, B. C., Kwok, S. Y., Smitsky, J. J. and Erlich, H. A. 1988. Enzymatic amplification: qualitative and quantitative methods for detecting proviral DNA amplified *in vitro*. *J. Infect. Dis.* 158:1158.
- Saiki, R. K., Bugawan, T. L., Horn, G. T., Mullis, K. B. and Erlich, H. A. 1986. Analysis of enzymatically amplified  $\beta$ -globin and HLA-D $\alpha$  DNA with allele-specific oligonucleotide probes. *Nature* 324:163-166.
- Kogan, S. G., Doherty, M. and Gitschier, J. 1987. An improved method for prenatal diagnosis of genetic diseases by analysis of amplified DNA sequences. *N. Engl. J. Med.* 317:985-990.
- Wu, D. Y., Uguzzo, L., Fal, B. E. and Wallace, R. B. 1989. Allele-specific enzymatic amplification of  $\beta$ -globin genomic DNA for diagnosis of sickle cell anemia. *Proc. Natl. Acad. Sci. USA* 86:2757-2760.
- Kwok, S., Kellogg, D. E., McKinney, N., Spasic, D., Goda, L., Levenson, C. and Smitsky, J. J. 1990. Effects of primer-template mismatches on the polymerase chain reaction: Human immunodeficiency virus type 1 model studies. *Nuc. Acids Res.* 18:999-1005.
- Chou, Q., Russell, M., Birch, D., Raymond, J. and Bloch, W. 1992. Prevention of pre-PCR mis-priming and primer dimerization improves low-copy-number amplifications. Submitted.
- Higuchi, R. 1989. Using PCR to engineer DNA. p. 61-70. *In*: PCR Technology, H. A. Erlich (Ed.), Stockton Press, New York, NY.
- Hall, L., Atwood, J. G., DiCesare, J., Katz, E., Fieritz, E., Williams, J. F. and Woudenberg, T. 1991. A high-performance system for automation of the polymerase chain reaction. *Biotechniques* 10:102-103, 108-112.
- Tumosa, N. and Kahan, L. 1989. Fluorescent EIA screening of monoclonal antibodies to cell surface antigens. *J. Immun. Meth.* 116:59-63.

# IBL

IMMUNO-BIOLOGICAL LABORATORIES

## sCD-14 ELISA

### Trauma, Shock and Sepsis

The CD-14 molecule is expressed on the surface of monocytes and some macrophages. Membrane-bound CD-14 is a receptor for lipopolysaccharide (LPS) complexed to LPS-Binding-Protein (LBP). The concentration of its soluble form is altered under certain pathological conditions. There is evidence for an important role of sCD-14 with polytrauma, sepsis, burnings and inflammations. During septic conditions and acute infections it seems to be a prognostic marker and is therefore of value in monitoring these patients.

IBL offers an ELISA for quantitative determination of soluble CD-14 in human serum, plasma, cell-culture supernatants and other biological fluids.

Assay features:

- 12x8 determinations (microtiter strips),
- precoated with a specific monoclonal antibody,
- 2x1 hour incubation,
- standard range: 3 - 96 ng/ml
- detection limit: 1 ng/ml
- CV: intra- and interassay <8%

For more information call or fax

GESELLSCHAFT FÜR IMMUNOCHEMIE UND BIOLOGIE MBH  
OSTERSTRASSE 86 · D-2000 HAMBURG 20 · GERMANY TEL +49/491 00 61 64 · FAX +40/40 11 08

BIOTECHNOLOGY VOL 10 APRIL 1992

# Oligonucleotides with Fluorescent Dyes at Opposite Ends Provide a Quenched Probe System Useful for Detecting PCR Product and Nucleic Acid Hybridization

Kenneth J. Livak, Susan J.A. Flood, Jeffrey Marmaro, William Giusti, and Karl Deetz

Perkin-Elmer, Applied Biosystems Division, Foster City, California 94404

The 5' nuclease PCR assay detects the accumulation of specific PCR product by hybridization and cleavage of a double-labeled fluorogenic probe during the amplification reaction. The probe is an oligonucleotide with both a reporter fluorescent dye and a quencher dye attached. An increase in reporter fluorescence intensity indicates that the probe has hybridized to the target PCR product and has been cleaved by the 5'  $\rightarrow$  3' nucleolytic activity of *Taq* DNA polymerase. In this study, probes with the quencher dye attached to an internal nucleotide were compared with probes with the quencher dye attached to the 3' end nucleotide. In all cases, the reporter dye was attached to the 5' end. All intact probes showed quenching of the reporter fluorescence. In general, probes with the quencher dye attached to the 3' end nucleotide exhibited a larger signal in the 5' nuclease PCR assay than the internally labeled probes. It is proposed that the larger signal is caused by increased likelihood of cleavage by *Taq* DNA polymerase when the probe is hybridized to a template strand during PCR. Probes with the quencher dye attached to the 3' end nucleotide also exhibited an increase in reporter fluorescence intensity when hybridized to a complementary strand. Thus, oligonucleotides with reporter and quencher dyes attached at opposite ends can be used as homogeneous hybridization probes.

A homogeneous assay for detecting the accumulation of specific PCR product that uses a double-labeled fluorogenic probe was described by Lee et al.<sup>(1)</sup> The assay exploits the 5'  $\rightarrow$  3' nucleolytic activity of *Taq* DNA polymerase<sup>(2,3)</sup> and is diagrammed in Figure 1. The fluorogenic probe consists of an oligonucleotide with a reporter fluorescent dye, such as a fluorescein, attached to the 5' end and a quencher dye, such as a rhodamine, attached internally. When the fluorescein is excited by irradiation, its fluorescent emission will be quenched if the rhodamine is close enough to be excited through the process of fluorescence energy transfer (FET).<sup>(4,5)</sup> During PCR, if the probe is hybridized to a template strand, *Taq* DNA polymerase will cleave the probe because of its inherent 5'  $\rightarrow$  3' nucleolytic activity. If the cleavage occurs between the fluorescein and rhodamine dyes, it causes an increase in fluorescein fluorescence intensity because the fluorescein is no longer quenched. The increase in fluorescein fluorescence intensity indicates that the probe-specific PCR product has been generated. Thus, FET between a reporter dye and a quencher dye is critical to the performance of the probe in the 5' nuclease PCR assay.

Quenching is completely dependent on the physical proximity of the two dyes.<sup>(6)</sup> Because of this, it has been assumed that the quencher dye must be attached near the 5' end. Surprisingly, we have found that attaching a rhodamine dye at the 3' end of a probe still provides adequate quenching for the probe to perform in the 5' nuclease

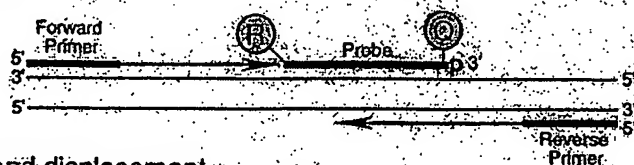
PCR assay. Furthermore, cleavage of this type of probe is not required to achieve some reduction in quenching. Oligonucleotides with a reporter dye on the 5' end and a quencher dye on the 3' end exhibit a much higher reporter fluorescence when double-stranded as compared with single-stranded. This should make it possible to use this type of double-labeled probe for homogeneous detection of nucleic acid hybridization.

## MATERIALS AND METHODS

### Oligonucleotides

Table 1 shows the nucleotide sequence of the oligonucleotides used in this study. Linker arm nucleotide (LAN) phosphoramidite was obtained from Glen Research. The standard DNA phosphoramidites, 6-carboxyfluorescein (6-FAM) phosphoramidite, 6-carboxytetramethylrhodamine succinimidyl ester (TAMRA NHS ester), and Phosphalink for attaching a 3'-blocking phosphate, were obtained from Perkin-Elmer, Applied Biosystems Division. Oligonucleotide synthesis was performed using an ABI model 394 DNA synthesizer (Applied Biosystems). Primer and complement oligonucleotides were purified using Oligo Purification Cartridges (Applied Biosystems). Double-labeled probes were synthesized with 6-FAM-labeled phosphoramidite at the 5' end, LAN replacing one of the T's in the sequence, and Phosphalink at the 3' end. Following deprotection and ethanol precipitation, TAMRA NHS ester was coupled to the LAN-containing oligonucleotide in 250

## Polymerization



## Strand displacement



## Cleavage



## Polymerization completed



FIGURE 3. Diagram of 5' nuclease assay. Stepwise representation of the 5' → 3' nucleolytic activity of Taq DNA polymerase acting on a fluorogenic probe during one extension phase of PCR.

mm Na-bicarbonate buffer (pH 9.0) at room temperature. Unreacted dye was removed by passage over a PD-10 Sephadex column. Finally, the double-labeled probe was purified by preparative high-performance liquid chromatography (HPLC) using an Aquapore C<sub>8</sub> 220×4.6-mm column with 7-μm particle size. The column was developed with a 24-min linear gradient of 8–20% acetonitrile in 0.1 M TEAA (triethylamine acetate). Probes are named by designating the sequence from Table 1 and the position of the LAN-TAMRA moiety. For example, probe A1-7 has sequence A1 with LAN-TAMRA at nucleotide position 7 from the 5' end.

## PCR Systems

All PCR amplifications were performed in the Perkin-Elmer GeneAmp-PCR System 9600 using 50-μl reactions that contained 10 mM Tris-HCl (pH 8.3), 50 mM KCl, 200 μM dATP, 200 μM dCTP, 200 μM dGTP, 400 μM dUTP, 0.5 unit of AmpliTaq DNA polymerase (Perkin-Elmer). A 295-bp segment from exon 3 of the human β-actin

gene (nucleotides 2141–2435 in the sequence of Nakajima-Iijima et al.<sup>(9)</sup>) was amplified using primers AFP and ARP (Table 1), which are modified slightly from those of du Breuil et al.<sup>(9)</sup> Actin amplification reactions contained 4 mM MgCl<sub>2</sub>, 20 ng of human genomic DNA, 50 nM A1 or A3 probe, and 300 nM each

primer. The thermal regimen was 50°C (2 min), 95°C (10 min), 40 cycles of 95°C (20 sec), 60°C (1 min), and hold at 72°C. A 515-bp segment was amplified from a plasmid that consists of a segment of λ DNA (nucleotides 32,220–32,747) inserted in the *Sma*I site of vector pUC119. These reactions contained 3.5 mM MgCl<sub>2</sub>, 1 ng of plasmid DNA, 50 nM P2 or P5 probe, 200 nM primer F119, and 200 nM primer R119. The thermal regimen was 50°C (2 min), 95°C (10 min), 25 cycles of 95°C (20 sec), 57°C (1 min), and hold at 72°C.

## Fluorescence Detection

For each amplification reaction, a 40-μl aliquot of a sample was transferred to an individual well of a white, 96-well microtiter plate (Perkin-Elmer). Fluorescence was measured on the Perkin-Elmer TaqMan LS-50B System, which consists of a luminescence spectrometer with plate reader assembly, a 485-nm excitation filter, and a 515-nm emission filter. Excitation was at 488 nm using a 5-nm slit width. Emission was measured at 518 nm for 6-FAM (the reporter or R value) and 582 nm for TAMRA (the quencher or Q value) using a 10-nm slit width. To determine the increase in reporter emission that is caused by cleavage of the probe during PCR, three normalizations are applied to the raw emission data. First, emission intensity of a buffer blank is subtracted for each wavelength. Second, emission intensity of the reporter is

TABLE 1. Sequences of Oligonucleotides

Name	Type	Sequence
F119	primer	ACCCACAGGAAGTGATCACCCTC
R119	primer	ATGTGGCGTTCCGGGTGACGTTGTC
P2	probe	TGGCATCTACTGATCGTTGCCAACCAGT <sub>p</sub>
P2C	complement	GTACTGGTTGGCAACGATCAGTAATGCGATG
P5	probe	CGGATTGTCTGGTATCTATGACAAGGAT <sub>p</sub>
P5C	complement	TTCATCCTTGTCATAGATACCAGCAATCCG
AFP	primer	TCACCCAGACTGTGCCATCTACGA
ARP	primer	CAGCGGAACCGCTCATTGCCAATGG
A1	probe	ATGGCTCCGCCATGGCATCCTGGCT <sub>p</sub>
A1C	complement	AGACCGAGGATGGCATGGGGCAAGGCCATAC
A3	probe	CGCCGTGGACTTCGAGCAAGAGAT <sub>p</sub>
A3C	complement	CCATCTCTTGCTGGAGTCCAGGGCGAC

For each oligonucleotide used in this study, the nucleic acid sequence is given, written in the 5' → 3' direction. There are three types of oligonucleotides: PCR primer, fluorogenic probe used in the 5' nuclease assay, and complement used to hybridize to the corresponding probe. For the probes, the underlined base indicates a position where LAN with TAMRA attached was substituted for a T (p). The presence of a 3' phosphate on each probe.

A1-2	RAQGGCCCTCCCGCATGCCATCCTGGGp
A1-7	RATGCCCCQCCCCATGCCATCCTGGGp
A1-14	RATGCCCCQCCCCAQQCCATCCTGGGp
A1-19	RATGCCCCQCCCCATGCCAQCTGGGp
A1-22	RATGCCCCQCCCCATGCCATCCQGGGp
A1-26	RATGCCCCQCCCCATGCCATCCTGGGp

Probe	518 nm		582 nm		RQ <sup>-</sup>	RQ <sup>+</sup>	$\Delta$ RQ
	no temp.	+ temp.	no temp.	+ temp.			
A1-2	25.5 $\pm$ 2.1	32.7 $\pm$ 1.9	38.2 $\pm$ 3.0	38.2 $\pm$ 2.0	0.67 $\pm$ 0.01	0.66 $\pm$ 0.06	0.19 $\pm$ 0.06
A1-7	53.5 $\pm$ 4.3	395.1 $\pm$ 21.4	108.5 $\pm$ 6.3	110.3 $\pm$ 6.3	0.49 $\pm$ 0.03	3.58 $\pm$ 0.17	3.09 $\pm$ 0.18
A1-14	127.0 $\pm$ 4.9	403.5 $\pm$ 19.1	109.7 $\pm$ 5.3	93.1 $\pm$ 6.3	1.16 $\pm$ 0.02	4.34 $\pm$ 0.15	3.18 $\pm$ 0.15
A1-19	187.5 $\pm$ 17.9	422.7 $\pm$ 7.7	70.3 $\pm$ 7.4	73.0 $\pm$ 2.8	2.67 $\pm$ 0.05	5.80 $\pm$ 0.15	3.13 $\pm$ 0.16
A1-22	224.6 $\pm$ 9.4	482.2 $\pm$ 43.6	100.0 $\pm$ 4.0	96.2 $\pm$ 9.6	2.25 $\pm$ 0.03	5.02 $\pm$ 0.11	2.77 $\pm$ 0.12
A1-26	160.2 $\pm$ 8.9	454.1 $\pm$ 18.4	93.1 $\pm$ 5.4	80.7 $\pm$ 3.2	1.72 $\pm$ 0.02	5.01 $\pm$ 0.08	3.29 $\pm$ 0.08

**FIGURE 2** Results of 5' nuclease assay comparing  $\beta$ -actin probes with TAMRA at different nucleotide positions. As described in Materials and Methods, PCR amplifications containing the indicated probes were performed, and the fluorescence emission was measured at 518 and 582 nm. Reported values are the average  $\pm$  1 s.d. for six reactions run without added template (no temp.) and six reactions run with template (+ temp.). The RQ ratio was calculated for each individual reaction and averaged to give the reported RQ<sup>-</sup> and RQ<sup>+</sup> values.

divided by the emission intensity of the quencher to give an RQ ratio for each reaction tube. This normalizes for well-to-well variations in probe concentration and fluorescence measurement. Finally,  $\Delta$ RQ is calculated by subtracting the RQ value of the no-template control (RQ<sup>-</sup>) from the RQ value for the complete reaction including template (RQ<sup>+</sup>).

## RESULTS

A series of probes with increasing distances between the fluorescein reporter and rhodamine quencher were tested to investigate the minimum and maximum spacing that would give an acceptable performance in the 5' nuclease PCR assay. These probes hybridize to a target

sequence in the human  $\beta$ -actin gene. Figure 2 shows the results of an experiment in which these probes were included in PCR that amplified a segment of the  $\beta$ -actin gene containing the target sequence. Performance in the 5' nuclease PCR assay is monitored by the magnitude of  $\Delta$ RQ, which is a measure of the increase in reporter fluorescence caused by PCR amplification of the probe target. Probe A1-2 has a  $\Delta$ RQ value that is close to zero, indicating that the probe was not cleaved appreciably during the amplification reaction. This suggests that with the quencher dye on the second nucleotide from the 5' end, there is insufficient room for *Taq* polymerase to cleave efficiently between the reporter and quencher. The other five probes exhibited comparable  $\Delta$ RQ values that are

clearly different from zero. Thus, all five probes are being cleaved during PCR amplification resulting in a similar increase in reporter fluorescence. It should be noted that complete digestion of a probe produces a much larger increase in reporter fluorescence than that observed in Figure 2 (data not shown). Thus, even in reactions where amplification occurs, the majority of probe molecules remain uncleaved. It is mainly for this reason that the fluorescence intensity of the quencher dye TAMRA changes little with amplification of the target. This is what allows us to use the 582 nm fluorescence reading as a normalization factor.

The magnitude of RQ<sup>-</sup> depends mainly on the quenching efficiency inherent in the specific structure of the probe and the purity of the oligonucleotide. Thus, the larger RQ<sup>-</sup> values indicate that probes A1-14, A1-19, A1-22, and A1-26 probably have reduced quenching as compared with A1-7. Still, the degree of quenching is sufficient to detect a highly significant increase in reporter fluorescence when each of these probes is cleaved during PCR.

To further investigate the ability of TAMRA on the 3' end to quench 6-FAM on the 5' end, three additional pairs of probes were tested in the 5' nuclease PCR assay. For each pair, one probe has TAMRA attached to an internal nucleotide and the other has TAMRA attached to the 3' end nucleotide. The results are shown in Table 2. For all three sets, the probe with the 3' quencher exhibits a  $\Delta$ RQ value that is considerably higher than for the probe with the internal quencher. The RQ<sup>-</sup> values suggest that differences in quenching are not as great as those observed with some of the A1 probes. These results demonstrate that a quencher dye on the 3' end of an oligonucleotide can quench efficiently the

**TABLE 2** Results of 5' Nuclease Assay Comparing Probes with TAMRA Attached to an Internal or 3'-terminal Nucleotide

Probe	518 nm		582 nm		RQ <sup>-</sup>	RQ <sup>+</sup>	$\Delta$ RQ
	no temp.	+ temp.	no temp.	+ temp.			
A3-6	54.6 $\pm$ 3.2	84.8 $\pm$ 3.7	116.2 $\pm$ 6.4	115.6 $\pm$ 2.5	0.47 $\pm$ 0.02	0.73 $\pm$ 0.03	0.26 $\pm$ 0.04
A3-24	72.1 $\pm$ 2.9	236.5 $\pm$ 11.1	84.2 $\pm$ 4.0	90.2 $\pm$ 3.8	0.86 $\pm$ 0.02	2.62 $\pm$ 0.05	1.76 $\pm$ 0.05
P2-7	82.8 $\pm$ 4.4	384.0 $\pm$ 34.1	105.1 $\pm$ 5.4	120.4 $\pm$ 10.2	0.79 $\pm$ 0.02	3.19 $\pm$ 0.16	2.40 $\pm$ 0.16
P2-27	113.4 $\pm$ 6.6	555.4 $\pm$ 14.1	140.7 $\pm$ 8.5	118.7 $\pm$ 4.8	0.81 $\pm$ 0.01	4.68 $\pm$ 0.10	3.88 $\pm$ 0.10
P5-10	77.5 $\pm$ 6.5	244.4 $\pm$ 15.9	86.7 $\pm$ 4.3	95.8 $\pm$ 6.7	0.89 $\pm$ 0.05	2.55 $\pm$ 0.06	1.66 $\pm$ 0.08
P5-28	64.0 $\pm$ 5.2	333.6 $\pm$ 12.0	100.6 $\pm$ 6.1	94.7 $\pm$ 6.3	0.64 $\pm$ 0.02	3.53 $\pm$ 0.12	2.89 $\pm$ 0.13

Reactions containing the indicated probes and calculations were performed as described in Materials and Methods and in the legend to Fig. 2.

fluorescence of a reporter dye on the 5' end. The degree of quenching is sufficient for this type of oligonucleotide to be used as a probe in the 5' nuclease PCR assay.

To test the hypothesis that quenching by a 3' TAMRA depends on the flexibility of the oligonucleotide, fluorescence was measured for probes in the single-stranded and double-stranded states. Table 3 reports the fluorescence observed at 518 and 582 nm. The relative degree of quenching is assessed by calculating the RQ ratio. For probes with TAMRA 6–10 nucleotides from the 5' end, there is little difference in the RQ values when comparing single-stranded with double-stranded oligonucleotides. The results for probes with TAMRA at the 3' end are much different. For these probes, hybridization to a complementary strand causes a dramatic increase in RQ. We propose that this loss of quenching is caused by the rigid structure of double-stranded DNA, which prevents the 5' and 3' ends from being in proximity.

When TAMRA is placed toward the 3' end, there is a marked  $Mg^{2+}$  effect on quenching. Figure 3 shows a plot of observed RQ values for the A1 series of probes as a function of  $Mg^{2+}$  concentration. With TAMRA attached near the 5' end (probe A1-2 or A1-7), the RQ value at 0 mM  $Mg^{2+}$  is only slightly higher than RQ at 10 mM  $Mg^{2+}$ . For probes A1-19, A1-22, and A1-26, the RQ values at 0 mM  $Mg^{2+}$  are very high, indicating a much

reduced quenching efficiency. For each of these probes, there is a marked decrease in RQ at 1 mM  $Mg^{2+}$  followed by a gradual decline as the  $Mg^{2+}$  concentration increases to 10 mM. Probe A1-14 shows an intermediate RQ value at 0 mM  $Mg^{2+}$  with a gradual decline at higher  $Mg^{2+}$  concentrations. In a low-salt environment with no  $Mg^{2+}$  present, a single-stranded oligonucleotide would be expected to adopt an extended conformation because of electrostatic repulsion. The binding of  $Mg^{2+}$  ions acts to shield the negative charge of the phosphate backbone so that the oligonucleotide can adopt conformations where the 3' end is close to the 5' end. Therefore, the observed  $Mg^{2+}$  effects support the notion that quenching of a 5' reporter dye by TAMRA at or near the 3' end depends on the flexibility of the oligonucleotide.

#### DISCUSSION

The striking finding of this study is that it seems the rhodamine dye TAMRA, placed at any position in an oligonucleotide, can quench the fluorescent emission of a fluorescein (6-FAM) placed at the 5' end. This implies that a single-stranded, double-labeled oligonucleotide must be able to adopt conformations where the TAMRA is close to the 5' end. It should be noted that the decay of 6-FAM in the excited state requires a certain amount of time. Therefore, what

matters for quenching is not the average distance between 6-FAM and TAMRA but, rather, how close TAMRA can get to 6-FAM during the lifetime of the 6-FAM excited state. As long as the decay time of the excited state is relatively long compared with the molecular motions of the oligonucleotide, quenching can occur. Thus, we propose that TAMRA at the 3' end, or any other position, can quench 6-FAM at the 5' end because TAMRA is in proximity to 6-FAM often enough to be able to accept energy transfer from an excited 6-FAM.

Details of the fluorescence measurements remain puzzling. For example, Table 3 shows that hybridization of probes A1-26, A3-24, and P5-28 to their complementary strands not only causes a large increase in 6-FAM fluorescence at 518 nm but also causes a modest increase in TAMRA fluorescence at 582 nm. If TAMRA is being excited by energy transfer from quenched 6-FAM, then loss of quenching attributable to hybridization should cause a decrease in the fluorescence emission of TAMRA. The fact that the fluorescence emission of TAMRA increases indicates that the situation is more complex. For example, we have anecdotal evidence that the bases of the oligonucleotide, especially G, quench the fluorescence of both 6-FAM and TAMRA to some degree. When double-stranded, base-pairing may reduce the ability of the bases to quench. The primary factor causing the quenching of 6-FAM in an intact probe is the TAMRA dye. Evidence for the importance of TAMRA is that 6-FAM fluorescence remains relatively unchanged when probes labeled only with 6-FAM are used in the 5' nuclease PCR assay (data not shown). Secondary effectors of fluorescence, both before and after cleavage of the probe, need to be explored further.

Regardless of the physical mechanism, the relative independence of position and quenching greatly simplifies the design of probes for the 5' nuclease PCR assay. There are three main factors that determine the performance of a double-labeled fluorescent probe in the 5' nuclease PCR assay. The first factor is the degree of quenching observed in the intact probe. This is characterized by the value of RQ, which is the ratio of reporter to quencher fluorescent emissions for a no-template control PCR. Influences on the value of RQ include the particular reporter and quencher

TABLE 3 Comparison of Fluorescence Emissions of Single-stranded and Double-stranded Fluorogenic Probes

Probe	518 nm		582 nm		RQ	
	ss	ds	ss	ds	ss	ds
A1-7	27.75	68.53	61.08	138.18	0.45	0.50
A1-26	43.31	509.38	53.50	93.86	0.81	5.43
A3-6	16.75	62.88	39.33	165.57	0.43	0.38
A3-24	30.05	578.64	67.72	140.25	0.45	3.21
P2-7	35.02	70.13	54.63	121.09	0.64	0.58
P2-27	39.89	320.47	65.10	61.13	0.61	5.25
P5-10	27.34	144.85	61.95	165.54	0.44	0.87
P5-28	33.65	462.29	72.39	104.61	0.46	4.43

(ss) Single-stranded: The fluorescence emissions at 518 or 582 nm for solutions containing a final concentration of 50 nM indicated probe, 10 mM Tris-HCl (pH 8.3), 50 mM KCl, and 10 mM  $MgCl_2$ . (ds) Double-stranded: The solutions contained, in addition, 100 nM A1C for probes A1-7 and A1-26, 100 nM A3C for probes A3-6 and A3-24, 100 nM P2C for probes P2-7 and P2-27, or 100 nM P5C for probes P5-10 and P5-28. Before the addition of  $MgCl_2$ , 120  $\mu$ l of each sample was heated at 95°C for 5 min. Following the addition of 80  $\mu$ l of 25 mM  $MgCl_2$ , each sample was allowed to cool to room temperature and the fluorescence emissions were measured. Reported values are the average of three determinations.

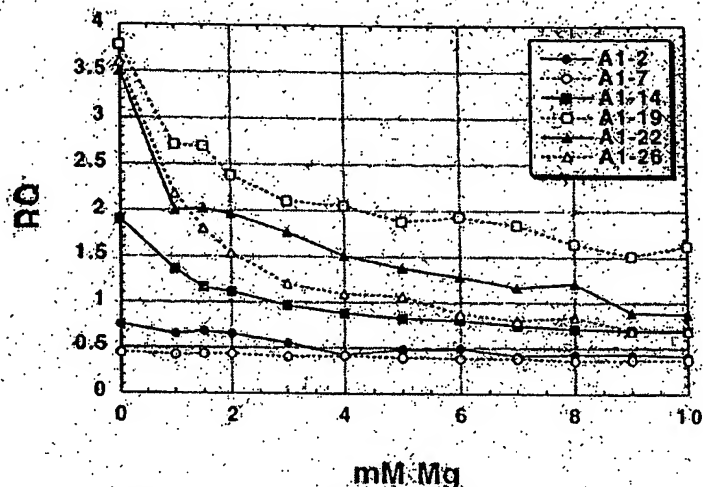


FIGURE 3 Effect of  $Mg^{2+}$  concentration on RQ ratio for the A1 series of probes. The fluorescence emission intensity at 518 and 582 nm was measured for solutions containing 50 nM probe, 10 mM Tris-HCl (pH 8.3), 50 mM KCl, and varying amounts (0–10 mM) of  $MgCl_2$ . The calculated RQ ratios (518 nm intensity divided by 582 nm intensity) are plotted vs.  $MgCl_2$  concentration (mM Mg). The key (upper right) shows the probes examined.

dyes used, spacing between reporter and quencher dyes, nucleotide sequence context effects, presence of structure or other factors that reduce flexibility of the oligonucleotide, and purity of the probe. The second factor is the efficiency of hybridization, which depends on probe  $T_m$ , presence of secondary structure in probe or template, annealing temperature, and other reaction conditions. The third factor is the efficiency at which *Taq* DNA polymerase cleaves the bound probe between the reporter and quencher dyes. This cleavage is dependent on sequence complementarity between probe and template as shown by the observation that mismatches in the segment between reporter and quencher dyes drastically reduce the cleavage of probe.<sup>(1)</sup>

The rise in RQ<sup>-</sup> values for the A1 series of probes seems to indicate that the degree of quenching is reduced somewhat as the quencher is placed toward the 3' end. The lowest apparent quenching is observed for probe A1-19 (see Fig. 3) rather than for the probe where the TAMRA is at the 3' end (A1-26). This is understandable, as the conformation of the 3' end position would be expected to be less restricted than the conformation of an internal position. In effect, a quencher at the 3' end is freer to adopt conformations close to the 5' reporter dye than is an internally placed quencher. For the other three sets of

probes, the interpretation of RQ<sup>-</sup> values is less clear-cut. The A3 probes show the same trend as A1, with the 3' TAMRA probe having a larger RQ<sup>-</sup> than the internal TAMRA probe. For the P2 pair, both probes have about the same RQ<sup>-</sup> value. For the P5 probes, the RQ<sup>-</sup> for the 3' probe is less than for the internally labeled probe. Another factor that may explain some of the observed variation is that purity affects the RQ<sup>-</sup> value. Although all probes are HPLC purified, a small amount of contamination with unquenched reporter can have a large effect on RQ<sup>-</sup>.

Although there may be a modest effect on degree of quenching, the position of the quencher apparently can have a large effect on the efficiency of probe cleavage. The most drastic effect is observed with probe A1-2, where placement of the TAMRA on the second nucleotide reduces the efficiency of cleavage to almost zero. For the A3, P2, and P5 probes,  $\Delta RQ$  is much greater for the 3' TAMRA probes as compared with the internal TAMRA probes. This is explained most easily by assuming that probes with TAMRA at the 3' end are more likely to be cleaved between reporter and quencher than are probes with TAMRA attached internally. For the A1 probes, the cleavage efficiency of probe A1-7 must already be quite high, as  $\Delta RQ$  does not increase when the quencher is placed closer to the 3' end. This illus-

trates the importance of being able to use probes with a quencher on the 3' end in the 5' nuclease PCR assay. In this assay, an increase in the intensity of reporter fluorescence is observed only when the probe is cleaved between the reporter and quencher dyes. By placing the reporter and quencher dyes on the opposite ends of an oligonucleotide probe, any cleavage that occurs will be detected. When the quencher is attached to an internal nucleotide, sometimes the probe works well (A1-7) and other times not so well (A3-6). The relatively poor performance of probe A3-6 presumably means the probe is being cleaved 3' to the quencher rather than between the reporter and quencher. Therefore, the best chance of having a probe that reliably detects accumulation of PCR product in the 5' nuclease PCR assay is to use a probe with the reporter and quencher dyes on opposite ends.

Placing the quencher dye on the 3' end may also provide a slight benefit in terms of hybridization efficiency. The presence of a quencher attached to an internal nucleotide might be expected to disrupt base pairing and reduce the  $T_m$  of a probe. In fact, a 2°C–3°C reduction in  $T_m$  has been observed for two probes with internally attached TAMRAs.<sup>(9)</sup> This disruptive effect would be minimized by placing the quencher at the 3' end. Thus, probes with 3' quenchers might exhibit slightly higher hybridization efficiencies than probes with internal quenchers.

The combination of increased cleavage and hybridization efficiencies means that probes with 3' quenchers probably will be more tolerant of mismatches between probe and target as compared with internally labeled probes. This tolerance of mismatches can be advantageous, as when trying to use a single probe to detect PCR-amplified products from samples of different species. Also, it means that cleavage of probe during PCR is less sensitive to alterations in annealing temperature or other reaction conditions. The one application where tolerance of mismatches may be a disadvantage is for allelic discrimination. Lee et al.<sup>(10)</sup> demonstrated that allele-specific probes were cleaved between reporter and quencher only when hybridized to a perfectly complementary target. This allowed them to distinguish the normal human cystic fibrosis allele from the  $\Delta F508$  mutant. Their probes had TAMRA attached to the seventh nucleotide from

the 5' end and were designed so that any mismatches were between the reporter and quencher. Increasing the distance between reporter and quencher would lessen the disruptive effect of mismatches and allow cleavage of the probe on the incorrect target. Thus, probes with a quencher attached to an internal nucleotide may still be useful for allelic discrimination.

In this study loss of quenching upon hybridization was used to show that quenching by a 3' TAMRA is dependent on the flexibility of a single-stranded oligonucleotide. The increase in reporter fluorescence intensity, though, could also be used to determine whether hybridization has occurred or not. Thus, oligonucleotides with reporter and quencher dyes attached at opposite ends should also be useful as hybridization probes. The ability to detect hybridization in real time means that these probes could be used to measure hybridization kinetics. Also, this type of probe could be used to develop homogeneous hybridization assays for diagnostics or other applications. Bagwell et al.<sup>(10)</sup> describe just this type of homogeneous assay where hybridization of a probe causes an increase in fluorescence caused by a loss of quenching. However, they utilized a complex probe design that requires adding nucleotides to both ends of the probe sequence to form two imperfect hairpins. The results presented here demonstrate that the simple addition of a reporter dye to one end of an oligonucleotide and a quencher dye to the other end generates a fluorogenic probe that can detect hybridization or PCR amplification.

#### ACKNOWLEDGMENTS

We acknowledge Lincoln McBride of Perkin-Elmer for his support and encouragement on this project and Mitch Winnik of the University of Toronto for helpful discussions on time-resolved fluorescence.

#### REFERENCES

1. Lee, L.G., C.R. Connell, and W. Bloch. 1993. Allelic discrimination by nick-translation PCR with fluorogenic probes. *Nucleic Acids Res.* 21: 3761-3766.
2. Holland, J.M., R.D. Abramson, R. Watson, and D.H. Gelfand. 1991. Detection of specific polymerase chain reaction products by utilizing the 5' to 3' exonuclease activity of *Thermus aquaticus* DNA polymerase. *Proc. Natl. Acad. Sci.* 88: 7276-7280.
3. Lyamichev, V., M.A.D. Brow, and J.E. Dahlberg. 1993. Structure-specific endonucleolytic cleavage of nucleic acids by eubacterial DNA polymerases. *Science* 260: 778-783.
4. Förster, V.Th. 1948. Zwischenmolekulare Energiewanderung und Fluoreszenz. *Ann. Phys. (Leipzig)* 2: 55-75.
5. Lakowicz, J.R. 1983. Energy transfer. In *Principles of fluorescent spectroscopy*, pp. 303-339. Plenum Press, New York, NY.
6. Stryer, L. and R.P. Haugland. 1967. Energy transfer: A spectroscopic ruler. *Proc. Natl. Acad. Sci.* 58: 719-726.
7. Nakajima-Iijima, S., H. Hamada, P. Reddy, and T. Kakunaga. 1985. Molecular structure of the human cytoplasmic beta-actin gene: Inter-species homology of sequences in the introns. *Proc. Natl. Acad. Sci.* 82: 6133-6137.
8. du Breuil, R.M., J.M. Patel, and B.V. Mendelow. 1993. Quantitation of  $\beta$ -actin-specific mRNA transcripts using xeno-competitive PCR. *PCR Methods Applic.* 3: 57-59.
9. Uyak, K.J. (unpubl.).
10. Bagwell, C.B., M.E. Munson, R.L. Christensen, and E.J. Lovett. 1994. A new homogeneous assay system for specific nucleic acid sequences: Poly-dA and poly-A detection. *Nucleic Acids Res.* 22: 2424-2425.

Received December 20, 1994; accepted in revised form March 6, 1995.

# Real Time Quantitative PCR

Christian A. Heid,<sup>1</sup> Junko Stevens,<sup>2</sup> Kenneth J. Livak,<sup>2</sup> and  
P. Mickey Williams<sup>1,3</sup>

<sup>1</sup>BioAnalytical Technology Department, Genentech, Inc., South San Francisco, California 94080;

<sup>2</sup>Applied BioSystems Division of Perkin Elmer Corp., Foster City, California 94404

We have developed a novel "real time" quantitative PCR method. The method measures PCR product accumulation through a dual-labeled fluorogenic probe (i.e., TaqMan Probe). This method provides very accurate and reproducible quantitation of gene copies. Unlike other quantitative PCR methods, real-time PCR does not require post-PCR sample handling, preventing potential PCR product carry-over contamination and resulting in much faster and higher throughput assays. The real-time PCR method has a very large dynamic range of starting target molecule determination (at least five orders of magnitude). Real-time quantitative PCR is extremely accurate and less labor-intensive than current quantitative PCR methods.

Quantitative nucleic acid sequence analysis has had an important role in many fields of biological research. Measurement of gene expression (RNA) has been used extensively in monitoring biological responses to various stimuli (Tan et al. 1994; Huang et al. 1995a,b; Prud'homme et al. 1995). Quantitative gene analysis (DNA) has been used to determine the genome quantity of a particular gene, as in the case of the human *HER2* gene, which is amplified in ~36% of breast tumors (Slamon et al. 1987). Gene and genome quantitation (DNA and RNA) also have been used for analysis of human immunodeficiency virus (HIV) burden demonstrating changes in the levels of virus throughout the different phases of the disease (Connor et al. 1993; Piatak et al. 1993b; Furtado et al. 1995).

Many methods have been described for the quantitative analysis of nucleic acid sequences (both for RNA and DNA; Southern 1975; Sharp et al. 1980; Thomas 1980). Recently, PCR has proven to be a powerful tool for quantitative nucleic acid analysis. PCR and reverse transcriptase (RT)-PCR have permitted the analysis of minimal starting quantities of nucleic acid (as little as one cell equivalent). This has made possible many experiments that could not have been performed with traditional methods. Although PCR has provided a powerful tool, it is imperative

that it be used properly for quantitation (Raeymaekers 1995). Many early reports of quantitative PCR and RT-PCR described quantitation of the PCR product but did not measure the initial target sequence quantity. It is essential to design proper controls for the quantitation of the initial target sequences (Pere 1992; Clementi et al. 1993).

Researchers have developed several methods of quantitative PCR and RT-PCR. One approach measures PCR product quantity in the log phase of the reaction before the plateau (Kelllogg et al. 1990; Pang et al. 1990). This method requires that each sample has equal input amounts of nucleic acid and that each sample under analysis amplifies with identical efficiency up to the point of quantitative analysis. A gene sequence (contained in all samples at relatively constant quantities, such as  $\beta$ -actin) can be used for sample amplification efficiency normalization. Using conventional methods of PCR detection and quantitation (gel electrophoresis or plate-capture hybridization), it is extremely laborious to assure that all samples are analyzed during the log phase of the reaction (for both the target gene and the normalization gene). Another method, quantitative competitive (QC)-PCR, has been developed and is used widely for PCR quantitation. QC-PCR relies on the inclusion of an internal control competitor in each reaction (Becker-Andre 1991; Piatak et al. 1993a,b). The efficiency of each reaction is normalized to the internal competitor. A known amount of internal competitor can be

<sup>3</sup>Corresponding author.

E-MAIL: mickey@gene.com; FAX (415) 225-1411.

added to each sample. To obtain relative quantitation, the unknown target PCR product is compared with the known competitor PCR product. Success of a quantitative competitive PCR assay relies on developing an internal control that amplifies with the same efficiency as the target molecule. The design of the competitor and the validation of amplification efficiencies require a dedicated effort. However, because QC-PCR does not require that PCR products be analyzed during the log phase of the amplification, it is the easier of the two methods to use.

Several detection systems are used for quantitative PCR and RT-PCR analysis: (1) agarose gels, (2) fluorescent labeling of PCR products and detection with laser-induced fluorescence using capillary electrophoresis (Fasco et al. 1995; Williams et al. 1996) or acrylamide gels, and (3) plate capture and sandwich probe hybridization (Mulder et al. 1994). Although these methods proved successful, each method requires post-PCR manipulations that add time to the analysis and may lead to laboratory contamination. The sample throughput of these methods is limited (with the exception of the plate capture approach), and, therefore, these methods are not well suited for uses demanding high sample throughput (i.e., screening of large numbers of biomolecules or analyzing samples for diagnostics or clinical trials).

Here we report the development of a novel assay for quantitative DNA analysis. The assay is based on the use of the 5' nuclease assay, first described by Holland et al. (1991). The method uses the 5' nuclease activity of *Taq* polymerase to cleave a nonextendible hybridization probe during the extension phase of PCR. The approach uses dual-labeled fluorogenic hybridization probes (Lee et al. 1993; Bassler et al. 1995; Livak et al. 1995a,b). One fluorescent dye serves as a reporter [FAM (i.e., 6-carboxyfluorescein)] and its emission spectra is quenched by the second fluorescent dye, TAMRA (i.e., 6-carboxy-tetramethylrhodamine). The nuclease degradation of the hybridization probe releases the quenching of the FAM fluorescent emission, resulting in an increase in peak fluorescent emission at 518 nm. The use of a sequence detector (ABI Prism) allows measurement of fluorescent spectra of all 96 wells of the thermal cycler continuously during the PCR amplification. Therefore, the reactions are monitored in real time. The output data is described and quantitative analysis of input target DNA sequences is discussed below.

## RESULTS

### PCR Product Detection in Real Time

The goal was to develop a high-throughput, sensitive, and accurate gene quantitation assay for use in monitoring lipid-mediated therapeutic gene delivery. A plasmid encoding human factor VIII gene sequence, pF8TM (see Methods), was used as a model therapeutic gene. The assay uses fluorescent Taqman methodology and an instrument capable of measuring fluorescence in real time (ABI Prism 7700 Sequence Detector). The Taqman reaction requires a hybridization probe labeled with two different fluorescent dyes. One dye is a reporter dye (FAM), the other is a quenching dye (TAMRA). When the probe is intact, fluorescent energy transfer occurs and the reporter dye fluorescent emission is absorbed by the quenching dye (TAMRA). During the extension phase of the PCR cycle, the fluorescent hybridization probe is cleaved by the 5'-3' nucleolytic activity of the DNA polymerase. On cleavage of the probe, the reporter dye emission is no longer transferred efficiently to the quenching dye, resulting in an increase of the reporter dye fluorescent emission spectra. PCR primers and probes were designed for the human factor VIII sequence and human  $\beta$ -actin gene (as described in Methods). Optimization reactions were performed to choose the appropriate probe and magnesium concentrations yielding the highest intensity of reporter fluorescent signal without sacrificing specificity. The instrument uses a charge-coupled device (i.e., CCD camera) for measuring the fluorescent emission spectra from 500 to 650 nm. Each PCR tube was monitored sequentially for 25 msec with continuous monitoring throughout the amplification. Each tube was re-examined every 8.5 sec. Computer software was designed to examine the fluorescent intensity of both the reporter dye (FAM) and the quenching dye (TAMRA). The fluorescent intensity of the quenching dye, TAMRA, changes very little over the course of the PCR amplification (data not shown). Therefore, the intensity of TAMRA dye emission serves as an internal standard with which to normalize the reporter dye (FAM) emission variations. The software calculates a value termed  $\Delta R_n$  (or  $\Delta RQ$ ) using the following equation:  $\Delta R_n = (R_n^+) - (R_n^-)$ , where  $R_n^+$  = emission intensity of reporter/emission intensity of quencher at any given time in a reaction tube, and  $R_n^-$  = emission intensity of re-

porter/emission intensity of quencher measured prior to PCR amplification in that same reaction tube. For the purpose of quantitation, the last three data points ( $\Delta R_n$ ) collected during the extension step for each PCR cycle were analyzed. The nucleolytic degradation of the hybridization probe occurs during the extension phase of PCR, and, therefore, reporter fluorescent emission increases during this time. The three data points were averaged for each PCR cycle and the mean value for each was plotted in an "amplification plot" shown in Figure 1A. The  $\Delta R_n$  mean value is plotted on the y-axis, and time, represented by cycle number, is plotted on the x-axis. During the early cycles of the PCR amplification, the  $\Delta R_n$

value remains at base line. When sufficient hybridization probe has been cleaved by the Taq polymerase nuclease activity, the intensity of reporter fluorescent emission increases. Most PCR amplifications reach a plateau phase of reporter fluorescent emission if the reaction is carried out to high cycle numbers. The amplification plot is examined early in the reaction, at a point that represents the log phase of product accumulation. This is done by assigning an arbitrary threshold that is based on the variability of the base-line data. In Figure 1A, the threshold was set at 10 standard deviations above the mean of base-line emission calculated from cycles 1 to 15. Once the threshold is chosen, the point at which

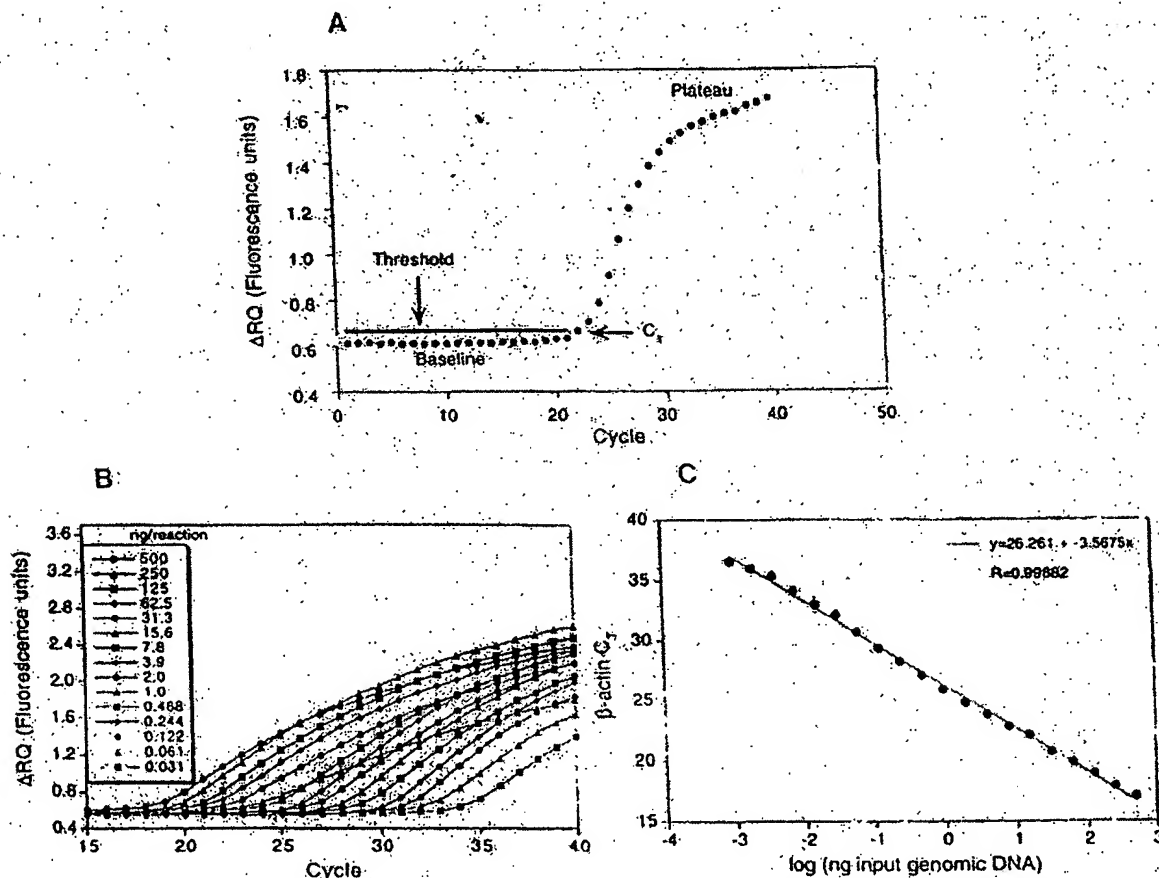


**Figure 1** PCR product detection in real time. (A) The Model 7700 software will construct amplification plots from the extension-phase fluorescent emission data collected during the PCR amplification. The standard deviation is determined from the data points collected from the base line of the amplification plot.  $C_T$  values are calculated by determining the point at which the fluorescence exceeds a threshold limit (usually 10 times the standard deviation of the base line). (B) Overlay of amplification plots of serially (1:2) diluted human genomic DNA samples amplified with  $\beta$ -actin primers. (C) Input DNA concentration of the samples plotted versus  $C_T$ . All points represent the mean of triplicate PCR amplifications, and error bars are shown (but not always visible).

the amplification plot crosses the threshold is defined as  $C_T$ .  $C_T$  is reported as the cycle number at this point. As will be demonstrated, the  $C_T$  value is predictive of the quantity of input target.

#### $C_T$ Values Provide a Quantitative Measurement of Input Target Sequences

Figure 1B shows amplification plots of 15 different PCR amplifications overlaid. The amplifications were performed on a 1:2 serial dilution of human genomic DNA. The amplified target was human  $\beta$ -actin. The amplification plots shift to the right (to higher threshold cycles) as the input target quantity is reduced. This is expected because reactions with fewer starting copies of the target molecule require greater amplification to degrade enough probe to attain the threshold fluorescence. An arbitrary threshold of 10 standard deviations above the base line was used to determine the  $C_T$  values. Figure 1C represents the  $C_T$  values plotted versus the sample dilution value. Each dilution was amplified in triplicate PCR amplifications and plotted as mean values with error bars representing one standard deviation. The  $C_T$  values decrease linearly with increasing target quantity. Thus,  $C_T$  values can be used as a quantitative measurement of the input target number. It should be noted that the amplification plot for the 15.6-ng sample shown in Figure 1B does not reflect the same fluorescent rate of increase exhibited by most of the other samples. The 15.6-ng sample also achieves endpoint plateau at a lower fluorescent value than would be expected based on the input DNA. This phenomenon has been observed occasionally with other samples (data not shown) and may be attributable to late-cycle inhibition; this hypothesis is still under investigation. It is important to note that the flattened slope and early plateau do not impact significantly the calculated  $C_T$  value as demonstrated by the fit on the line shown in Figure 1C. All triplicate amplifications resulted in very similar  $C_T$  values—the standard deviation did not exceed 0.5 for any dilution. This experiment contains a >100,000-fold range of input target molecules. Using  $C_T$  values for quantitation permits a much larger assay range than directly using total fluorescent emission intensity for quantitation. The linear range of fluorescent intensity measurement of the ABI Prism 7700 Sequence Detector only spans three logs, resulting in only a 1000-fold dynamic range of input molecules. Thus,  $C_T$  values provide accurate measure-

ments over a very large range of relative starting target quantities.

#### Sample Preparation Validation

Several parameters influence the efficiency of PCR amplification: magnesium and salt concentrations, reaction conditions (i.e., time and temperature), PCR target size and composition, primer sequences, and sample purity. All of the above factors are common to a single PCR assay, except sample to sample purity. In an effort to validate the method of sample preparation for the factor VIII assay, PCR amplification reproducibility and efficiency of 10 replicate sample preparations were examined. After genomic DNA was prepared from the 10 replicate samples, the DNA was quantitated by ultraviolet spectroscopy. Amplifications were performed analyzing  $\beta$ -actin gene content in 100 and 25 ng of total genomic DNA. Each PCR amplification was performed in triplicate. Comparison of  $C_T$  values for each triplicate sample show minimal variation based on standard deviation and coefficient of variance (Table 1). Therefore, each of the triplicate PCR amplifications was highly reproducible, demonstrating that real time PCR using this instrumentation introduces minimal variation into the quantitative PCR analysis. Comparison of the mean  $C_T$  values of the 10 replicate sample preparations also showed minimal variability, indicating that each sample preparation yielded similar results for  $\beta$ -actin gene quantity. The highest  $C_T$  difference between any of the samples was 0.85 and 0.71 for the 100 and 25 ng samples, respectively. Additionally, the amplification of each sample exhibited an equivalent rate of fluorescent emission intensity change per amount of DNA target analyzed as indicated by similar slopes derived from the sample dilutions (Fig. 2). Any sample containing an excess of a PCR inhibitor would exhibit a greater measured  $\beta$ -actin  $C_T$  value for a given quantity of DNA. In addition, the inhibitor would be diluted along with the sample in the dilution analysis (Fig. 2), altering the expected  $C_T$  value change. Each sample amplification yielded a similar result in the analysis, demonstrating that this method of sample preparation is highly reproducible with regard to sample purity.

#### Quantitative Analysis of a Plasmid After Transient Transfection

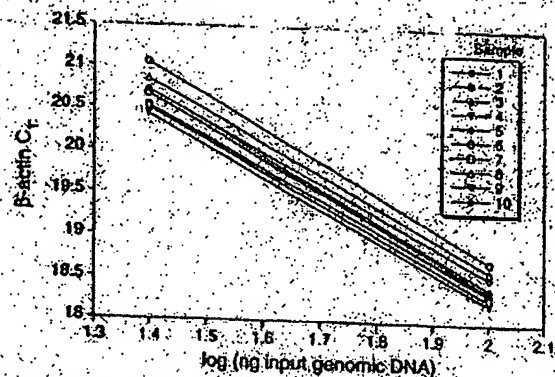
293 cells were transiently transfected with a vec-

Table 1. Reproducibility of Sample Preparation Method

Sample no.	100 ng				25 ng			
	$C_T$	mean	standard deviation	CV	$C_T$	mean	standard deviation	CV
1	18.24	18.27	0.06	0.32	20.48	20.51	0.03	0.17
	18.23				20.55			
	18.33				20.5			
2	18.33	18.37	0.06	0.32	20.61	20.54	0.11	0.54
	18.35				20.59			
	18.44				20.41			
3	18.3	18.34	0.07	0.36	20.54	20.54	0.06	0.28
	18.3				20.6			
	18.42				20.49			
4	18.15	18.23	0.08	0.46	20.48	20.43	0.05	0.26
	18.23				20.44			
	18.32				20.38			
5	18.4	18.42	0.04	0.23	20.68	20.73	0.13	0.61
	18.38				20.87			
	18.46				20.63			
6	18.54	18.74	0.24	1.26	21.09	21.06	0.03	0.15
	18.67				21.04			
	19				21.04			
7	18.28	18.39	0.12	0.66	20.67	20.68	0.04	0.2
	18.36				20.73			
	18.52				20.65			
8	18.45	18.63	0.16	0.83	20.98	20.86	0.12	0.57
	18.7				20.84			
	18.73				20.75			
9	18.18	18.29	0.1	0.55	20.46	20.51	0.07	0.32
	18.34				20.54			
	18.36				20.48			
10	18.42	18.55	0.12	0.65	20.79	20.73	0.1	0.46
	18.57				20.78			
	18.66				20.62			
Mean	(1-10)	18.42	0.17	0.90		20.66	0.19	0.94

for containing a partial cDNA for human factor VIII, pF8TM. A series of transfections was set up using a decreasing amount of the plasmid (40, 4, 0.5, and 0.1  $\mu$ g). Twenty-four hours post-transfection, total DNA was purified from each flask of cells.  $\beta$ -Actin gene quantity was chosen as a value for normalization of genomic DNA concentration from each sample. In this experiment,  $\beta$ -actin gene content should remain constant relative to total genomic DNA. Figure 3 shows the result of the  $\beta$ -actin DNA measurement (100 ng total DNA determined by ultraviolet spectroscopy) of each sample. Each sample was analyzed in triplicate and the mean  $\beta$ -actin  $C_T$  values of the triplicates were plotted (error bars represent one standard deviation). The highest difference

between any two sample means was 0.95  $C_T$ . Ten nanograms of total DNA of each sample were also examined for  $\beta$ -actin. The results again showed that very similar amounts of genomic DNA were present; the maximum mean  $\beta$ -actin  $C_T$  value difference was 1.0. As Figure 3 shows, the rate of  $\beta$ -actin  $C_T$  change between the 100- and 10-ng samples was similar (slope values range between -3.56 and -3.45). This verifies again that the method of sample preparation yields samples of identical PCR integrity (i.e., no sample contained an excessive amount of a PCR inhibitor). However, these results indicate that each sample contained slight differences in the actual amount of genomic DNA analyzed. Determination of actual genomic DNA concentration was accomplished



**Figure 2** Sample preparation purity. The replicate samples shown in Table 1 were also amplified in triplicate using 25 ng of each DNA sample. The figure shows the input DNA concentration (100 and 25 ng) vs.  $C_T$ . In the figure, the 100 and 25 ng points for each sample are connected by a line.

by plotting the mean  $\beta$ -actin  $C_T$  value obtained for each 100-ng sample on a  $\beta$ -actin standard curve (shown in Fig. 4C). The actual genomic DNA concentration of each sample,  $a$ , was obtained by extrapolation to the x-axis.

Figure 4A shows the measured (i.e., non-normalized) quantities of factor VIII plasmid DNA (pF8TM) from each of the four transient cell transfections. Each reaction contained 100-ng of total sample DNA (as determined by UV spectroscopy). Each sample was analyzed in triplicate.

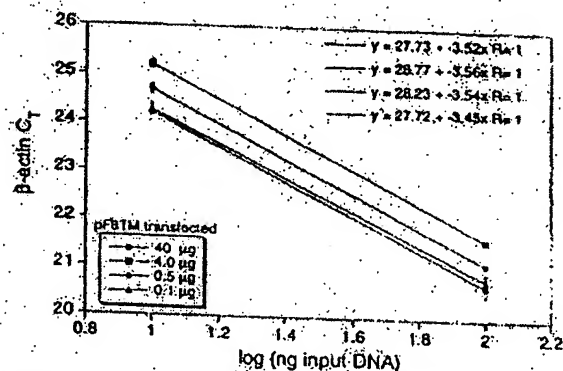


**Figure 3** Analysis of transfected cell DNA quantity and purity. The DNA preparations of the four 293 cell transfections (40, 4, 0.5, and 0.1  $\mu$ g of pF8TM) were analyzed for the  $\beta$ -actin gene. 100 and 10 ng (determined by ultraviolet spectroscopy) of each sample were amplified in triplicate. For each amount of pF8TM that was transfected, the  $\beta$ -actin  $C_T$  values are plotted versus the total input DNA concentration.

## REAL TIME QUANTITATIVE PCR

PCR amplifications. As shown, pF8TM purified from the 293 cells decreases (mean  $C_T$  values increase) with decreasing amounts of plasmid transfected. The mean  $C_T$  values obtained for pF8TM in Figure 4A were plotted on a standard curve comprised of serially diluted pF8TM, shown in Figure 4B. The quantity of pF8TM,  $b$ , found in each of the four transfections was determined by extrapolation to the x-axis of the standard curve in Figure 4B. These uncorrected values,  $b$ , for pF8TM were normalized to determine the actual amount of pF8TM found per 100 ng of genomic DNA by using the equation:

$$\frac{b \times 100 \text{ ng}}{a} = \text{actual pF8TM copies per 100 ng of genomic DNA}$$

where  $a$  = actual genomic DNA in a sample and  $b$  = pF8TM copies from the standard curve. The normalized quantity of pF8TM per 100 ng of genomic DNA for each of the four transfections is shown in Figure 4D. These results show that the quantity of factor VIII plasmid associated with the 293 cells, 24 hr after transfection, decreases with decreasing plasmid concentration used in the transfection. The quantity of pF8TM associated with 293 cells, after transfection with 40  $\mu$ g of plasmid, was 35 pg per 100 ng genomic DNA. This results in ~520 plasmid copies per cell.

## DISCUSSION

We have described a new method for quantitating gene copy numbers using real-time analysis of PCR amplifications. Real-time PCR is compatible with either of the two PCR (RT-PCR) approaches: (1) quantitative competitive where an internal competitor for each target sequence is used for normalization (data not shown) or (2) quantitative comparative PCR using a normalization gene contained within the sample (i.e.,  $\beta$ -actin) or a "housekeeping" gene for RT-PCR. If equal amounts of nucleic acid are analyzed for each sample and if the amplification efficiency before quantitative analysis is identical for each sample, the internal control (normalization gene or competitor) should give equal signals for all samples.

The real-time PCR method offers several advantages over the other two methods currently employed (see the introduction). First, the real-time PCR method is performed in a closed-tube system and requires no post-PCR manipulation.

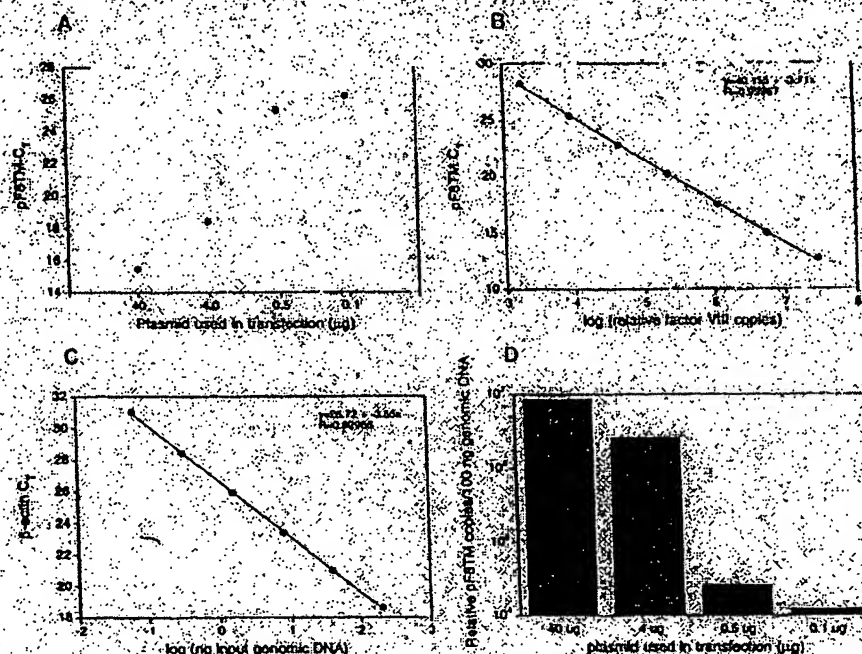


**Figure 4.** Quantitative analysis of pF8TM in transfected cells. (A) Amount of plasmid DNA used for the transfection plotted against the mean  $C_T$  value determined for pF8TM remaining 24 hr after transfection. (B, C) Standard curves of pF8TM and  $\beta$ -actin, respectively. pF8TM DNA (B) and genomic DNA (C) were diluted serially 1:5 before amplification with the appropriate primers. The  $\beta$ -actin standard curve was used to normalize the results of A to 100 ng of genomic DNA. (D) The amount of pF8TM present per 100 ng of genomic DNA.

of sample. Therefore, the potential for PCR contamination in the laboratory is reduced because amplified products can be analyzed and disposed of without opening the reaction tubes. Second, this method supports the use of a normalization gene (i.e.,  $\beta$ -actin) for quantitative PCR or house-keeping genes for quantitative RT-PCR controls. Analysis is performed in real time during the log phase of product accumulation. Analysis during log phase permits many different genes (over a wide input target range) to be analyzed simultaneously, without concern of reaching reaction plateau at different cycles. This will make multi-gene analysis assays much easier to develop, because individual internal competitors will not be needed for each gene under analysis. Third, sample throughput will increase dramatically with the new method because there is no post-PCR processing time. Additionally, working in a 96-well format is highly compatible with automation technology.

The real-time PCR method is highly reproducible. Replicate amplifications can be analyzed

for each sample minimizing potential error. The system allows for a very large assay dynamic range (approaching 1,000,000-fold starting target). Using a standard curve for the target of interest, relative copy number values can be determined for any unknown sample. Fluorescent threshold values,  $C_T$ , correlate linearly with relative DNA copy numbers. Real time quantitative RT-PCR methodology (Gibson et al., this issue) has also been developed. Finally, real time quantitative PCR methodology can be used to develop high-throughput screening assays for a variety of applications [quantitative gene expression (RT-PCR), gene copy assays (Her2, HIV, etc.), genotyping (knockout mouse analysis), and immuno-PCR].

Real-time PCR may also be performed using intercalating dyes (Higuchi et al., 1992) such as ethidium bromide. The fluorogenic probe method offers a major advantage over intercalating dyes—greater specificity (i.e., primer dimers and nonspecific PCR products are not detected).

## METHODS

### Generation of a Plasmid Containing a Partial cDNA for Human Factor VIII

Total RNA was harvested (RNAzol B from Tel-Test, Inc., Friendswood, TX) from cells transfected with a factor VIII expression vector, pCIS2.8c25D (Eaton et al., 1986; Gorman et al., 1990). A factor VIII partial cDNA sequence was generated by RT-PCR (GeneAmp EZ 11th RNA PCR Kit (part N808-0179, PE Applied Biosystems, Foster City, CA)) using the PCR primers F8for and F8rev (primer sequences are shown below). The amplicon was reamplified using modified F8for and F8rev primers (appended with BamHI and HindIII restriction site sequences at the 5' end) and cloned into pGEM-3Z (Promega Corp., Madison, WI). The resulting clone, pF8TM, was used for transient transfection of 293 cells.

### Amplification of Target DNA and Detection of Amplicon Factor VIII Plasmid DNA

(pF8TM) was amplified with the primers F8for 5'-CCG-GTCCCAAGACTGACGTGTC-3' and F8rev 5'-AAACCT-CAGCCTGGATGGTAGG-3'. The reaction produced a 422-bp PCR product. The forward primer was designed to recognize a unique sequence found in the 5' untranslated region of the parent pCIS2.8c25D plasmid and therefore does not recognize and amplify the human factor VIII gene. Primers were chosen with the assistance of the computer program Oligo 4.0 (National Biosciences, Inc., Plymouth, MN). The human  $\beta$ -actin gene was amplified with the primers  $\beta$ -actin forward primer 5'-TCACCCAGACTGT-GCCCATCTACGA-3' and  $\beta$ -actin reverse primer 5'-CAG-CGGAACCGCTCATTGCCAATGG-3'. The reaction produced a 295-bp PCR product.

Amplification reactions (50  $\mu$ l) contained a DNA sample, 10 $\times$  PCR Buffer II (5  $\mu$ l), 200  $\mu$ M dATP, dCTP, dGTP, and 400  $\mu$ M dUTP, 4 mM MgCl<sub>2</sub>, 1.25 Units AmpliTaq DNA polymerase, 0.5 unit AmpErase uracil N-glycosylase (UNG), 50 pmole of each factor VIII primer, and 15 pmole of each  $\beta$ -actin primer. The reactions also contained one of the following detection probes (100 nM each): F8probe 5'-(FAM)AGCTCTCCACCTGCTTCTCTGT-GCCTT(TAMRA)-p-3' and  $\beta$ -actin probe 5'-(FAM)ATGCC-X(TAMRA)CCCCATGCCATCp-3' where p indicates phosphorylation and X indicates a linker arm nucleotide. Reaction tubes were MicroAmp Optical Tubes (part number N801-0933, Perkin Elmer) that were frosted (at Perkin Elmer) to prevent light from reflecting. Tube caps were similar to MicroAmp caps but specially designed to prevent light scattering. All of the PCR consumables were supplied by PE Applied Biosystems (Foster City, CA) except the factor VIII primers, which were synthesized at Genentech, Inc. (South San Francisco, CA). Probes were designed using the Oligo 4.0 software, following guidelines suggested in the Model 7700 Sequence Detector Instrument manual. Briefly, probe T<sub>m</sub> should be at least 5°C higher than the annealing temperature used during thermal cycling; primers should not form stable duplexes with the probe.

The thermal cycling conditions included 2 min at 50°C and 10 min at 95°C. Thermal cycling proceeded with 40 cycles of 95°C for 0.5 min and 60°C for 2 min. All

## REAL TIME QUANTITATIVE PCR

reactions were performed in the Model 7700 Sequence Detector (PE Applied Biosystems), which contains a GeneAmp PCR System 9600. Reaction conditions were programmed on a Power Macintosh 7100 (Apple Computer, Santa Clara, CA) linked directly to the Model 7700 Sequence Detector. Analysis of data was also performed on the Macintosh computer. Collection and analysis software was developed at PE Applied Biosystems.

### Transfection of Cells with Factor VIII Construct

Four T175 flasks of 293 cells (ATCC CRL 1573), a human fetal kidney suspension cell line, were grown to 80% confluency and transfected pF8TM. Cells were grown in the following media: 50% HAM'S F12 without GHT, 50% low glucose Dulbecco's modified Eagle medium (DMEM) without glycine with sodium bicarbonate, 10% fetal bovine serum, 2 mM L-glutamine, and 1% penicillin-streptomycin. The media was changed 30 min before the transfection. pF8TM DNA amounts of 40, 4.05, and 0.1  $\mu$ g were added to 1.5 ml of a solution containing 0.125 M CaCl<sub>2</sub> and 1 $\times$  HEPES. The four mixtures were left at room temperature for 10 min and then added dropwise to the cells. The flasks were incubated at 37°C and 5% CO<sub>2</sub> for 24 hr, washed with PBS, and resuspended in PBS. The resuspended cells were divided into aliquots and DNA was extracted immediately using the QIAamp Blood Kit (Qiagen, Chatsworth, CA). DNA was eluted into 200  $\mu$ l of 20 mM Tris-HCl at pH 8.0.

## ACKNOWLEDGMENTS

We thank Genentech's DNA Synthesis Group for primer synthesis and Genentech's Graphics Group for assistance with the figures.

The publication costs of this article were defrayed in part by payment of page charges. This article must therefore be hereby marked "advertisement" in accordance with 18 USC section 1734 solely to indicate this fact.

## REFERENCES

- Bässler, H.A., S.J. Flood, K.J. Livak, J. Marmaro, R. Knorr, and C.A. Batt. 1995. Use of a fluorogenic probe in a PCR-based assay for the detection of *Listeria* monocytogenes. *App. Environ. Microbiol.* 61: 3724-3728.
- Becker-Andre, M. 1991. Quantitative evaluation of mRNA levels. *Meth. Mol. Cell. Biol.* 2: 189-201.
- Clementi, M., S. Menzo, P. Bagharello, A. Manzin, A. Valenza, and P.E. Varaldo. 1993. Quantitative PCR and RT-PCR in virology. [Review]. *PCR Methods Applic.* 2: 191-196.
- Connor, R.I., H. Mohri, Y. Gao, and D.D. Ho. 1993. Increased viral burden and cytopathicity correlate temporally with CD4<sup>+</sup> T-lymphocyte decline and clinical progression in human immunodeficiency virus type 1-infected individuals. *J. Virol.* 67: 1772-1777.
- Eaton, D.L., W.I. Wood, D. Eaton, P.E. Hass, P. Hollingshead, K. Wion, J. Mather, R.M. Lawn, G.A.

# HEID ET AL.

- Vehar, and C. Gorman. 1986. Construction and characterization of an active factor VIII variant lacking the central one-third of the molecule. *Biochemistry* 25: 8343-8347.
- Fasco, M.J., C.P. Treanor, S. Spiayak, H.L. Figge, and L.S. Kaminsky. 1995. Quantitative RNA-polymerase chain reaction-DNA analysis by capillary electrophoresis and laser-induced fluorescence. *Anal. Biochem.* 224: 140-147.
- Ferre, F. 1992. Quantitative or semi-quantitative PCR: Reality versus myth. *PCR Methods Applic.* 2: 1-9.
- Furtado, M.R., L.A. Kingsley, and S.M. Wolinsky. 1995. Changes in the viral mRNA expression pattern correlate with a rapid rate of CD4+ T-cell number decline in human immunodeficiency virus type 1-infected individuals. *J. Virol.* 69: 2092-2100.
- Gibson, U.E.M., C.A. Held, and P.M. Williams. 1996. A novel method for real time-quantitative competitive RT-PCR. *Genome Res.* (this issue).
- Gorman, C.M., D.R. Gies, and G. McCray. 1990. Transient production of proteins using an adenovirus transformed cell line. *DNA Prot. Engin. Tech.* 2: 3-10.
- Higuchi, R., G. Dollinger, P.S. Walsh, and R. Griffith. 1992. Simultaneous amplification and detection of specific DNA sequences. *Biotechnology* 10: 413-417.
- Holland, P.M., R.D. Abramson, R. Watson, and D.H. Gelfand. 1991. Detection of specific polymerase chain reaction product by utilizing the 5' to 3' exonuclease activity of *Thermus aquaticus* DNA polymerase. *Proc. Natl. Acad. Sci.* 88: 7276-7280.
- Huang, S.K., H.Q. Xiao, T.J. Klein, G. Paciotti, D.G. Marsh, L.M. Lichtenstein, and M.C. Liu. 1995a. IL-13 expression at the sites of allergen challenge in patients with asthma. *J. Immun.* 155: 2688-2694.
- Huang, S.K., M. Yi, E. Palmer, and D.G. Marsh. 1995b. A dominant T cell receptor beta-chain in response to a short ragweed allergen, Amb a 5. *J. Immun.* 154: 6157-6162.
- Kellogg, D.E., J.J. Sninsky, and S. Kowk. 1990. Quantitation of HIV-1 proviral DNA relative to cellular DNA by the polymerase chain reaction. *Anal. Biochem.* 189: 202-208.
- Lee, L.G., C.R. Connell, and W. Bloch. 1993. Allelic discrimination by nick-translation PCR with fluorogenic probes. *Nucleic Acids Res.* 21: 3761-3766.
- Livak, K.J., S.J. Flood, J. Marmaro, W. Giusti, and K. Deetz. 1995a. Oligonucleotides with fluorescent dyes at opposite ends provide a quenched probe system useful for detecting PCR product and nucleic acid hybridization. *PCR Methods Applic.* 4: 357-362.
- Livak, K.J., J. Marmaro, and J.A. Todd. 1995b. Towards fully automated genome-wide polymorphism screening [Letter]. *Nature Genet.* 9: 341-342.
- Mulder, J., N. McKinney, C. Christopherson, J. Sninsky, L. Greenfield, and S. Kwok. 1994. Rapid and simple PCR assay for quantitation of human immunodeficiency virus type 1 RNA in plasma: Application to acute retroviral infection. *J. Clin. Microbiol.* 32: 292-300.
- Pang, S., Y. Koyanagi, S. Miles, C. Wiley, H.V. Vinters, and L.S. Chen. 1990. High levels of unintegrated HIV-1 DNA in brain tissue of AIDS dementia patients. *Nature* 343: 85-89.
- Platak, M.J., K.C. Luk, B. Williams, and J.D. Lifson. 1993a. Quantitative competitive polymerase chain reaction for accurate quantitation of HIV DNA and RNA species. *Biotechniques* 14: 70-81.
- Platak, M.J., M.S. Saag, L.C. Yang, S.J. Clark, J.C. Kappes, K.C. Luk, B.H. Hahn, G.M. Shaw, and J.D. Lifson. 1993b. High levels of HIV-1 in plasma during all stages of infection determined by competitive PCR [see Comments]. *Science* 259: 1749-1754.
- Prud'homme, G.J., D.H. Kono, and A.N. Theofilopoulos. 1995. Quantitative polymerase chain reaction analysis reveals marked overexpression of interleukin-1 beta, interleukin-1 and interferon-gamma mRNA in the lymph nodes of lupus-prone mice. *Mol. Immunol.* 32: 495-503.
- Raeymaekers, L. 1995. A commentary on the practical applications of competitive PCR. *Genome Res.* 5: 91-94.
- Sharp, P.A., A.J. Berk, and S.M. Berget. 1980. Transcription maps of adenovirus. *Methods Enzymol.* 65: 750-768.
- Slamon, D.J., G.M. Clark, S.G. Wong, W.J. Levin, A. Ellrich, and W.L. McGuire. 1987. Human breast cancer: Correlation of relapse and survival with amplification of the HER-2/neu oncogene. *Science* 235: 177-182.
- Southern, E.M. 1975. Detection of specific sequences among DNA fragments separated by gel electrophoresis. *J. Mol. Biol.* 98: 503-517.
- Tan, X., X. Sun, C.F. Gonzalez, and W. Hsueh. 1994. PAF and TNF increase the precursor of NF-kappa B-p50 mRNA in mouse intestine: Quantitative analysis by competitive PCR. *Biochim. Biophys. Acta* 1215: 157-162.
- Thomas, P.S. 1980. Hybridization of denatured RNA and small DNA fragments transferred to nitrocellulose. *Proc. Natl. Acad. Sci.* 77: 5201-5205.
- Williams, S., C. Schwer, A. Krishnarao, C. Heid, B. Karger, and P.M. Williams. 1996. Quantitative competitive PCR: Analysis of amplified products of the HIV-1 gag gene by capillary electrophoresis with laser induced fluorescence detection. *Anal. Biochem.* (in press).

Received June 3, 1996; accepted in revised form July 29, 1996.

## WISP genes are members of the connective tissue growth factor family that are up-regulated in Wnt-1-transformed cells and aberrantly expressed in human colon tumors

DIANE PENNICA<sup>1</sup>\*, TODD A. SWANSON<sup>2</sup>, JAMES W. WELSH<sup>3</sup>, MARGARET A. ROY<sup>4</sup>, DAVID A. LAWRENCE<sup>2</sup>, JAMES LEE<sup>1</sup>, JENNIFER BRUSH<sup>1</sup>, LISA A. PANEVILLI<sup>1</sup>, BETHANNE DEVELL<sup>1</sup>, MICHAEL LEW<sup>1</sup>, COLIN WATANABE<sup>1</sup>, ROBERT L. COHEN<sup>1</sup>, MONA F. MCELHEN<sup>1</sup>, GENE C. FINLEY<sup>1</sup>, PHIL CURRIE<sup>1</sup>, AUDREY D. GODDARD<sup>1</sup>, KENNETH J. HILLAN<sup>1</sup>, AUSTIN L. GURNEY<sup>1</sup>, DAVID BOJSTEIN<sup>1</sup>†, AND ARNOLD J. LEVINE<sup>1</sup>‡

<sup>1</sup>Department of Molecular Oncology, Molecular Biology, Scientific Computing, and Pathology, Genentech Inc., 460 Point San Francisco, CA 94060; <sup>2</sup>University of Pittsburgh School of Medicine, Veterans Administration Medical Center, Pittsburgh, PA 15240; <sup>3</sup>University of Leeds, Leeds, LS2 9JT, United Kingdom; <sup>4</sup>Department of Genetics, Stanford University, Palo Alto, CA 94305; and <sup>5</sup>Department of Molecular Biology, Princeton University, Princeton, NJ 08540

Contributed by David Bojstein and Arnold J. Levine, October 21, 1998

**ABSTRACT** Wnt family members are critical to many developmental processes, and components of the Wnt signaling pathway have been linked to tumorigenesis in familial and sporadic colon carcinomas. Here we report the identification of two genes, *WISP-1* and *WISP-2*, that are up-regulated in the mouse mammary epithelial cell line C57MG transformed by Wnt-1, but not by Wnt-3. Together with a third related gene, *WISP-3*, these proteins define a subfamily of the connective tissue growth factor family. Two distinct systems demonstrated *WISP* induction to be associated with the expression of Wnt-1. These included (i) C57MG cells infected with a Wnt-1 retroviral vector or expressing Wnt-1 under the control of a tetracycline-repressible promoter, and (ii) Wnt-1 transgenic mice. The *WISP-1* gene was localized to human chromosome 6q24.1-6q24.3. *WISP-1* genomic DNA was amplified in colon cancer cell lines and in human colon tumors and its RNA overexpressed (2- to >30-fold) in 84% of the tumors examined compared with patient-matched normal mucosa. *WISP-1* mapped to chromosome 6q22-6q23 and also was overexpressed (4- to >40-fold) in 63% of the colon tumors analyzed. In contrast, *WISP-2*, mapped to human chromosome 20q12-20q13 and its DNA was amplified, but RNA expression was reduced (2- to >30-fold) in 79% of the tumors. These results suggest that the *WISP* genes may be downstream of Wnt-1 signaling and that aberrant levels of *WISP* expression in colon cancer may play a role in colon tumorigenesis.

Wnt-1 is a member of an expanding family of cysteine-rich glycosylated signaling proteins that mediate diverse developmental processes such as the control of cell proliferation, adhesion, cell polarity, and the establishment of cell fates (1, 2). Wnt-1 originally was identified as an oncogene activated by the insertion of mouse mammary tumor virus in virus-induced mammary adenocarcinomas (3, 4). Although Wnt-1 is not expressed in the normal mammary gland, expression of Wnt-1 in transgenic mice causes mammary tumors (5).

In mammalian cells, Wnt family members initiate signaling by binding to the seven transmembrane-spanning Frizzled receptors and recruiting the cytoplasmic protein Dishevelled (Dsh) to the cell membrane (1, 2, 6). Dsh then inhibits the kinase activity of the normally constitutively active glycogen synthase kinase-3 $\beta$  (GSK-3 $\beta$ ), resulting in an increase in  $\beta$ -catenin levels. Stabilized  $\beta$ -catenin interacts with the transcription factor TCF/Leff, forming a complex that appears in

the nucleus and binds TCF/Leff target DNA elements to activate transcription (7, 8). Other experiments suggest that the adenomatous polyposis coli (APC) tumor suppressor gene also plays an important role in Wnt signaling by regulating  $\beta$ -catenin levels (9). APC is phosphorylated by GSK-3 $\beta$ , binds to  $\beta$ -catenin, and facilitates its degradation. Mutations in either APC or  $\beta$ -catenin have been associated with colon carcinomas and melanomas, suggesting these mutations contribute to the development of these types of cancer, implicating the Wnt pathway in tumorigenesis (1).

Although much has been learned about the Wnt signaling pathway over the past several years, only a few of the transcriptionally activated downstream components activated by Wnt have been characterized. Those that have been described cannot account for all of the diverse functions attributed to Wnt signaling. Among the candidate Wnt target genes are those encoding the nodal-related ligands, *Xfr2*, a member of the transforming growth factor (TGF- $\beta$ ) superfamily and the homeobox genes, *engrailed*, *soosecold*, *wingless*, and *slimsh* (2). A recent report also identifies *c-myc* as a target gene of the Wnt signaling pathway (10).

To identify additional downstream genes in the Wnt signaling pathway that are relevant to the transformed cell phenotype, we used a PCR-based cDNA subtraction strategy, suppression subtractive hybridization (SSH) (11), using RNA isolated from C57MG mouse mammary epithelial cells and C57MG cells stably transformed by a Wnt-1 retrovirus. Overexpression of Wnt-1 in this cell line is sufficient to induce a partially transformed phenotype characterized by elongated and refractile cells that lose contact inhibition and form a multilayered array (12, 13). We reasoned that genes differentially expressed between these two cell lines might contribute to the transformed phenotype.

In this paper, we describe the cloning and characterization of two genes up-regulated in Wnt-1-transformed cells, *WISP-1* and *WISP-2*, and a third related gene, *WISP-3*. The *WISP* genes are members of the CCN family of growth factors, which includes connective tissue growth factor (CTGF), Cyr61, and nov, a family not previously linked to Wnt signaling.

### MATERIALS AND METHODS

**SSH.** SSH was performed by using the PCR Selective cDNA Subtraction Kit (CLONTECH). Tester double-stranded

**Abbreviations:** TGF, transforming growth factor; C57MG, collagenase-resistant mouse; SSH, suppression subtractive hybridization; Wnt, wingless; and Leff, type C module.

Data deposition: The sequences reported in this paper have been deposited in the Genbank database (accession nos. AF100777, AF100778, AF100779, AF100780, and AF100781).

To whom reprint requests should be addressed: e-mail: diane@gene.com.

The publication costs of this article were defrayed in part by page charge payment. This article must therefore be hereby marked "advertisement" in accordance with 18 U.S.C. 1734 solely to indicate this fact.

© 1998 by The National Academy of Sciences 0735-0918/98/9514711-02\$05.00/0  
PNAS is available online at www.pnas.org.

cDNA was synthesized from 2  $\mu$ g of poly(A)<sup>+</sup> RNA isolated from the C57MG/Wnt-1 cell line and driver cDNA from 2  $\mu$ g of poly(A)<sup>+</sup> RNA from the parent C57MG cells. The subtracted cDNA library was subcloned into a pSMT-1 vector for further analysis.

**cDNA Library Screening.** Clones encoding full-length mouse *WISP-1* were isolated by screening a  $\lambda$ gt10 mouse embryo cDNA library (CLONTECH) with a 70-bp probe from the original partial clone 568 sequence corresponding to amino acids 123–169. Clones encoding full-length human *WISP-1* were isolated by screening  $\lambda$ gt10 lung and fetal kidney cDNA libraries with the same probe at low stringency. Clones encoding full-length mouse and human *WISP-2* were isolated by screening a C57MG/Wnt1 or human fetal lung cDNA library with a probe corresponding to nucleotides 1463–1512. Full-length cDNAs encoding *WISP-3* were cloned from human bone marrow and fetal kidney libraries.

**Expression of Human *WISP* RNA.** PCR amplification of first-strand cDNA was performed with human Multiple Tissue cDNA panels (CLONTECH) and 300  $\mu$ M of each dNTP at 94°C for 1 sec, 62°C for 30 sec, 72°C for 1 min, for 22–32 cycles. *WISP* and glyceraldehyde 3-phosphate dehydrogenase primer sequences are available on request.

**In Situ Hybridization.** <sup>32</sup>P-labeled sense and antisense riboprobes were transcribed from an 892-bp PCR product corresponding to nucleotides 601–1440 of mouse *WISP-1* or a 294-bp PCR product corresponding to nucleotides 82–375 of mouse *WISP-2*. All tissues were processed as described (40).

**Radiation Hybrid Mapping.** Genomic DNA from each hybrid in the Stanford G3 and GeneBridge4 Radiation Hybrid Panels (Research Genetics, Huntsville, AL) and human and hamster control DNAs were PCR amplified, and the results were submitted to the Stanford or Massachusetts Institute of Technology Web servers.

**Cell Lines, Tumors, and Mucosa Specimens.** Tissue specimens were obtained from the Department of Pathology (University of Pittsburgh) for patients undergoing colon resection and from the University of Leeds (United Kingdom). Genomic DNA was isolated (Qiagen) from the pooled blood of 10 normal human donors, surgical specimens, and the following ATCC human cell lines: SW480 (COLO 320DM; HT 29; WIDr) and SW403 (colon adenocarcinoma), SW620 (lymph node metastasis, colon adenocarcinoma), HCT 116 (colon carcinoma), SK-CO-1 (colon adenocarcinoma, ascites), and HM7 (a variant of ATCC colon adenocarcinoma cell line LS 174T). DNA concentration was determined by using Hoechst dye 33258 intercalation fluorimetry. Total RNA was prepared by homogenization in Trizol reagent followed by centrifugation over CsCl cushions or prepared by using RNeasy.

**Gene Amplification and RNA Expression Analysis.** Relative gene amplification and RNA expression of *WISP*s and *c-myc* in the cell lines, colorectal tumors, and normal mucosa were determined by quantitative PCR. Gene-specific primers and fluorescent probes (sequences available on request) were designed and used to amplify and quantitate the genes. The relative gene copy number was derived by using the formula  $2^{-\Delta\Delta C_T}$ , where  $\Delta C_T$  represents the difference in amplification cycles required to detect the *WISP* genes in peripheral blood lymphocyte DNA compared with colon tumor DNA or colon tumor RNA compared with normal mucosal RNA. The  $\Delta$  method was used for calculation of the SE of the gene copy number or RNA expression level. The *WISP*-specific signal was normalized to that of the glyceraldehyde 3-phosphate dehydrogenase housekeeping gene. All TaqMan assay reagents were obtained from Berkin-Tier Applied Biosystems.

## RESULTS

**Isolation of *WISP-1* and *WISP-2* by SSH.** To identify Wnt-1-inducible genes, we used the technique of SSH using the

mouse mammary epithelial cell line C57MG and C57MG cells that stably express Wnt-1 (11). Candidate differentially expressed cDNAs (1,384 total) were sequenced. Thirty-nine percent of the sequences matched known genes or homologues, 32% matched expressed sequence tags, and 29% had no match. To confirm that the transcript was differentially expressed, semiquantitative reverse transcription-PCR and Northern analysis were performed by using mRNA from the C57MG and C57MG/Wnt-1 cells.

Two of the cDNAs, *WISP-1* and *WISP-2*, were differentially expressed, being induced in the C57MG/Wnt-1 cell line but not in the parent C57MG cells or C57MG cells overexpressing Wnt-1c (Fig. 1A and B). Wnt-1, unlike Wnt-1c, does not induce the morphological transformation of C57MG cells and has no effect on  $\beta$ -catenin levels (13, 14). Expression of *WISP-1* was up-regulated approximately 3-fold in the C57MG/Wnt-1 cell line and *WISP-2* by approximately 5-fold by both Northern analysis and reverse transcription-PCR.

An independent but similar system was used to examine *WISP* expression after Wnt-1 induction. C57MG cells expressing the *Wnt-1* gene under the control of a tetracycline-repressible promoter produce low amounts of Wnt-1 in the repressed state but show a strong induction of *Wnt-1* mRNA and protein within 24 hr after tetracycline removal (8). The levels of Wnt-1 and *WISP* RNA isolated from these cells at various times after tetracycline removal were assessed by quantitative PCR. Strong induction of Wnt-1 mRNA was seen as early as 10 hr after tetracycline removal. Induction of *WISP* mRNA (2- to 6-fold) was seen at 48 and 72 hr (data not shown). These data support our previous observations that show that *WISP* induction is correlated with Wnt-1 expression. Because the induction is slow, occurring after approximately 48 hr, the induction of *WISP*s may be an indirect response to Wnt-1 signaling.

cDNA clones of human *WISP-1* were isolated and the sequence compared with mouse *WISP-1*. The cDNA sequences of mouse and human *WISP-1* were 1,766 and 1,830 bp in length, respectively, and encode proteins of 567 aa, with predicted relative molecular masses of  $\sim$ 40,000 ( $M_r$  40 k). Both have hydrophobic N-terminal signal sequences, 38 conserved cysteine residues, and four potential N-linked glycosylation sites and are 84% identical (Fig. 2A).

Full-length cDNA clones of mouse and human *WISP-2* were 1,734 and 1,293 bp in length, respectively, and encode proteins of 251 and 250 aa, respectively, with predicted relative molecular masses of  $\sim$ 27,000 ( $M_r$  27 k) (Fig. 2B). Mouse and human *WISP-2* are 83% identical. Human *WISP-2* has no potential N-linked glycosylation sites, and mouse *WISP-2* has one at

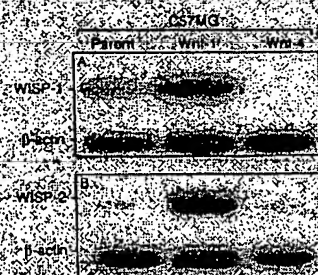


**Fig. 1.** *WISP-1* and *WISP-2* are induced by Wnt-1, but not Wnt-1c, expression in C57MG cells. Northern analysis of *WISP-1* (A) and *WISP-2* (B) expression in C57MG, C57MG/Wnt-1, and C57MG/Wnt-1c cells. Poly(A)<sup>+</sup> RNA (2  $\mu$ g) was subjected to Northern blot analysis and hybridized with a 70-bp mouse *WISP-1*-specific probe (amino acids 238–300) or a 194-bp mouse *WISP-2*-specific probe (nucleotides 1438–1627) in the 3' untranslated region. Blots were rehybridized with human  $\beta$ -actin probe.

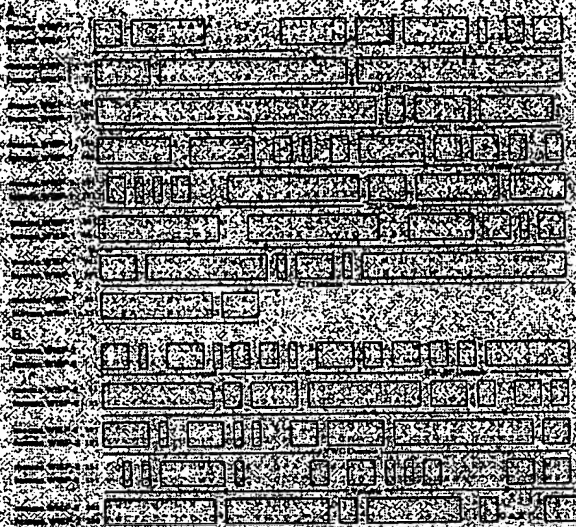


Fig. 2. Encoded amino acid sequence alignment of mouse and human WISP-1 (A) and mouse and human WISP-2 (B). The potential signal sequence, insulin-like growth factor-binding protein (IGF-BP), VWC, thrombospondin (TSP), and C-terminal (CT) domains are underlined.

position 197. WISP-2 has 28 cysteine residues that are conserved among the 38 cysteines found in WISP-1.

**Identification of WISP-3.** To search for related proteins, we screened expressed sequence tag (EST) databases with the WISP-1 protein sequence and identified several ESTs as potentially related sequences. We identified a homologous protein that we have called WISP-3. A full-length human WISP-3 cDNA of 1,374 bp was isolated corresponding to those ESTs that encode a 354-aa protein with a predicted molecular mass of 39,293. WISP-3 has two potential N-linked glycosylation sites and 36 cysteine residues. An alignment of the three human WISP proteins shows that WISP-1 and WISP-3 are the most similar (42% identity), whereas WISP-2 has 37% identity with WISP-1 and 32% identity with WISP-3 (Fig. 3A).

**WISPs Are Homologues to the CCN Family of Proteins.** Human WISP-1, WISP-2, and WISP-3 are novel sequences; however, mouse WISP-1 is the same as the recently identified *Elm1* gene. *Elm1* is expressed in low, but not high, grade mouse melanoma cells and suppresses the *in vivo* growth and metastatic potential of K-1735 mouse melanoma cells (15). Human and mouse WISP-2 are homologous to the recently described rat gene, *rCp-1*, (16). Significant homology (30–44%) was seen to the CCN family of growth factors. This family includes three members, CTGF, Cyr1, and the protooncogene *nov*. CTGF is a chemotactic and mitogenic factor for fibroblasts that is implicated in wound healing and fibrotic disorders and is induced by TGF- $\beta$  (17). Cyr1 is an extracellular matrix signaling molecule that promotes cell adhesion, proliferation, migration, angiogenesis, and tumor growth (18–19). *nov* (neuroblastoma overexpressed) is an immediate early gene associated with quiescence and found altered in Wilms tumors (20). The proteins of the CCN family share functional, but not sequence, similarity to Wnt-1. All are secreted, cysteine-rich heparin-binding glycoproteins that associate with the cell surface and extracellular matrix.

WISP proteins exhibit the modular architecture of the CCN family characterized by four conserved cysteine-rich domains (Fig. 3B) (21). The N-terminal domain, which includes the first 12 cysteine residues, contains a consensus sequence (CGCCGXXC) conserved in mouse insulin-like growth factor (IGF)



Fig. 3. (A) Encoded amino acid sequence alignment of human WISPs. The cysteine residues of WISP-1 and WISP-2 that are not present in WISP-3 are indicated with a dot. (B) Schematic representation of the WISP proteins showing the domain structure and cysteine residues (vertical lines). The four cysteine residues in the VWC domain that are absent in WISP-3 are indicated with a dot. (C) Expression of WISP mRNA in human tissues. PCR was performed on human multiple tissue cDNA panels (CLONTECH) from the indicated adult and fetal tissues.

binding proteins (BP). This sequence is conserved in WISP-2 and WISP-3, whereas WISP-1 has a glutamine in the third position instead of a glycine. CTGF recently has been shown to specifically bind IGF (22) and a truncated *nov* protein lacking the IGF-BP domain is oncogenic (23). The von Willebrand factor type C module (VWC) also found in certain collagens and mucins, covers the next 10 cysteine residues and is thought to participate in protein complex formation and oligomerization (24). The VWC domain of WISP-3 differs from all CCN family members described previously. It contains only six of the 10 cysteine residues (Fig. 3A and B). A short variable region follows the VWC domain. The third module, the thrombospondin (TSP) domain, is involved in binding to sulfated glycoconjugates and contains six cysteine residues and a conserved WSXSCG motif first identified in thrombospondin (25). The C-terminal (CT) module containing the remaining 10 cysteines is thought to be involved in dimerization and receptor binding (26). The CT domain is present in all CCN family members described to date but is absent in WISP-2 (Fig. 3A and B). The existence of a putative signal sequence and the absence of a transmembrane domain suggest that WISPs are secreted proteins, an observation supported by an analysis of their expression and secretion from mammalian cell and baculovirus cultures (data not shown).

**Expression of WISP mRNA in Human Tissues.** Tissue-specific expression of human WISP was characterized by PCR

analysis of adult and fetal multiple tissue cDNA panels, *WISP-1* expression was seen in the adult heart, kidney, lung, pancreas, placenta, ovary, small intestine, and spleen (Fig. 3C). Little or no expression was detected in the brain, liver, skeletal muscle, colon, peripheral blood leukocytes, prostate, testis, or thymus. *WISP-2* had a more restricted tissue expression and was detected in adult skeletal muscle, colon, ovary, and fetal lung. Predominant expression of *WISP-3* was seen in adult kidney and testis and fetal kidney. Lower levels of *WISP-3* expression were detected in placenta, ovary, prostate, and small intestine.

**In Situ Localization of *WISP-1* and *WISP-2*.** Expression of *WISP-1* and *WISP-2* was assessed by *in situ* hybridization in mammary tumors from Wnt-1 transgenic mice. Strong expression of *WISP-1* was observed in stromal fibroblasts lying within the fibrovascular tumor stroma (Fig. 4A–D). However, low-level *WISP-1* expression also was observed locally within tumor cells (data not shown). No expression was observed in normal breast-like *WISP-1*. *WISP-2* expression also was seen in the tumor stroma in breast tumors from Wnt-1 transgenic animals (Fig. 4E–H). However, *WISP-2* expression in the stroma was in spindle-shaped cells adjacent to capillary vessels, whereas



**Fig. 4.** (A, C, E, and G) Representative hematoxylin/eosin stained images from breast tumors in Wnt-1 transgenic mice. The corresponding dark-field images showing *WISP-1* expression are shown in B and D. The tumor is a moderately well-differentiated adenocarcinoma showing evidence of adenoid cystic change. At low power (A and B), expression of *WISP-1* is seen in the delicate branching fibrovascular tumor stroma (arrowhead). At higher magnification, expression is seen in the stromal fibroblasts (C and D), and tumor cells are negative. Focal expression of *WISP-1* however was observed in tumor cells in some areas. Images of *WISP-2* expression are shown in E–H. At low power (E and F), expression of *WISP-2* is seen in cells lying within the fibrovascular tumor stroma. At higher magnification, these cells appeared to be adjacent to capillary vessels, whereas tumor cells are negative (G and H).

the predominant cell type expressing *WISP-1* was the stromal fibroblast.

**Chromosome Localization of the *WISP* Genes.** The chromosomal location of the human *WISP* genes was determined by radiation hybrid mapping panels. *WISP-1* is approximately 1.45 cR from the meiotic marker AFM259c5 (logarithm of odds [od] score 36.31) on chromosome 8q24.1 (Fig. 4A) in the same region as the human locus of the *myb* family member (27) and roughly 4 Mbs distal to *c-myc* (28). Preliminary fine mapping indicates that *WISP-1* is located linearly between 6.15–6.18 Mb. *WISP-2* is linked to the marker SHGC 33922 (od = 1,000) on chromosome 20p12–20p13.1. Human *WISP-3* mapped to chromosome 6q22–6q23 and is linked to the marker AFM2112c2 (od = 1,000). *WISP-3* is approximately 180 kbs proximal to CTGF and 23 Mbs proximal to the human collagen oncogene *MTB* (27, 29).

**Amplification and Aberrant Expression of *WISP* in Human Colon Tumors.** Amplification of protooncogenes is seen in many human tumors and has etiological and prognostic significance. For example, in a variety of tumor types, *c-myc* amplification has been associated with malignant progression and poor prognosis (30). Because *WISP-1* resides in the same general chromosomal location (8q24) as *c-myc*, we asked whether it was a target of gene amplification, and if so, whether this amplification was independent of the *c-myc* locus. Genomic DNA from human colon cancer cell lines was assessed by quantitative PCR and Southern blot analysis (Fig. 5A and B). Both methods detected similar degrees of *WISP-1* amplification. Most cell lines showed significant (2- to 4-fold) amplification, with the HT-29 and WDR cell lines demonstrating an 8-fold increase. Significantly, the pattern of amplification observed did not correlate with that observed for *c-myc*, indicating that the *c-myc* gene is not part of the amplification that involves the *WISP-1* locus.

We next examined whether the *WISP* genes were amplified in a panel of 25 primary human colon adenocarcinomas. The relative *WISP* gene copy number in each colon tumor DNA was compared with pooled normal DNA from 10 donors by quantitative PCR (Fig. 6). The copy number of *WISP-1* and *WISP-2* was significantly greater than one, approximately 2-fold for *WISP-1* in about 60% of the tumors and 2- to 4-fold for *WISP-2* in 32% of the tumors ( $P < 0.001$  for each). The copy number for *WISP-3* was indistinguishable from one ( $P = 0.166$ ). In addition, the copy number of *WISP-2* was significantly higher than that of *WISP-1* ( $P < 0.001$ ).

The levels of *WISP* transcripts in RNA isolated from 19 adenocarcinomas and their matched normal mucosa were

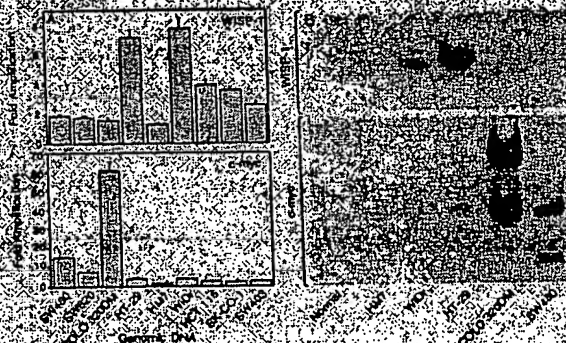


**Fig. 5.** Amplification of *WISP-1* genomic DNA in colon cancer cell lines. (A) Amplification in cell line DNA was determined by quantitative PCR. (B) Southern blot containing genomic DNA (10 µg) digested with *EcoRI* (*WISP-1*) or *XbaI* (*c-myc*) were hybridized with a 180 bp human *WISP-1* probe (nucleotides 186–219) or a human *c-myc* probe (located at bp 12015–12019). The *WISP* and *c-myc* genes are detected in normal human genomic DNA after a longer run exposure.

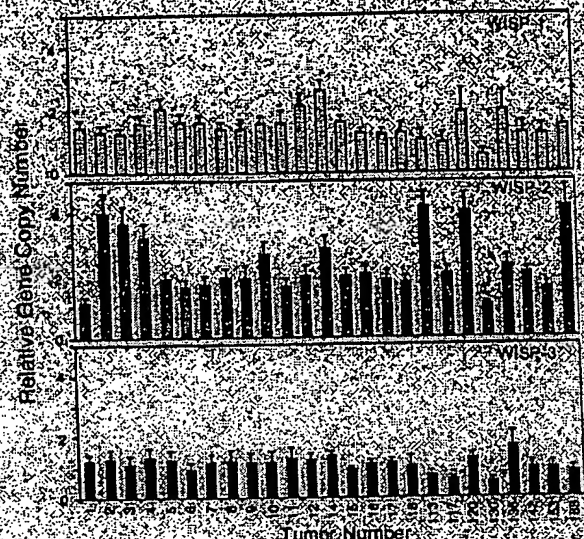


**Fig. 6.** Genomic amplification of *WISP* genes in human colon tumors. The relative gene copy numbers of the *WISP* genes in 25 adenocarcinomas was assayed by quantitative PCR by comparing DNA from primary human tumors with pooled DNA from 40 healthy donors. The data are means  $\pm$  SEM from one experiment done in triplicate. The experiment was repeated at least three times.

assessed by quantitative PCR (Fig. 7). The level of *WISP-1* RNA present in tumor tissue varied but was significantly increased (2- to  $>25$ -fold) in 84% (26/31) of the human colon tumors examined compared with normal adjacent mucosa. Four of 19 tumors showed greater than 10-fold overexpression. In contrast, in 79% (15/19) of the tumors examined *WISP-2* RNA expression was significantly lower in the tumor than the mucosa. Similar to *WISP-1*, *WISP-3* RNA was overexpressed in 63% (12/19) of the colon tumors compared with the normal

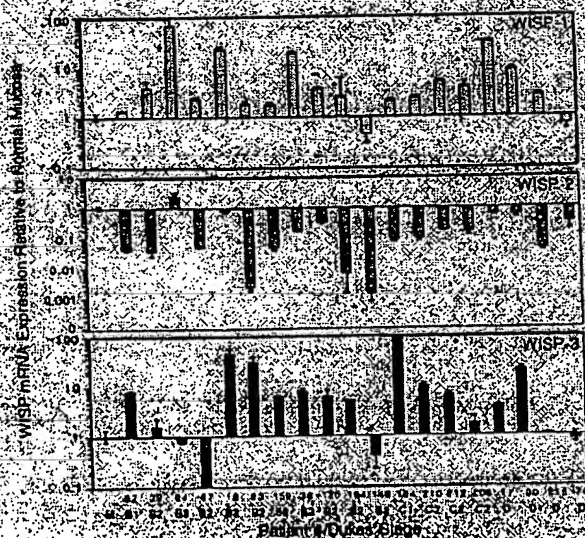


**Fig. 7.** *WISP* RNA expression in primary human colon tumors relative to expression in normal mucosa from the same patient. Expression of *WISP* mRNA in 19 adenocarcinomas was assayed by quantitative PCR. The Duke stage of the tumor is listed under the sample number. The data are means  $\pm$  SEM from one experiment done in triplicate. Three experiments were performed in duplicate.

mucosa. The amount of overexpression of *WISP-3* ranged from 4- to 340-fold.

## DISCUSSION

One approach to understanding the molecular basis of cancer is to identify differences in gene expression between cancer cells and normal cells. Strategies based on assumptions that steady-state mRNA levels will differ between normal and malignant cells have been used to clone differentially expressed genes (31). We have used a PCR-based selection strategy (SSH) to identify genes selectively expressed in C57MG mouse mammary epithelial cells transformed by Wnt-1.

Three of the genes isolated, *WISP-1*, *WISP-2*, and *WISP-3*, are members of the CCN family of growth factors, which includes CTGF, Cyr61, and *nov*, a family not previously linked to Wnt signaling.

Two independent experimental systems demonstrated that *WISP* induction was associated with the expression of Wnt-1. The first was C57MG cells infected with a Wnt-1 retroviral vector or C57MG cells expressing Wnt-1 under the control of a tetracycline-repressible promoter, and the second was in Wnt-1 transgenic mice, where breast tissue expresses Wnt-1, whereas normal breast tissue does not. No *WISP* RNA expression was detected in mammary tumors induced by polyoma virus middle T antigen (data not shown). These data suggest a link between Wnt-1 and *WISP* in that in these two situations *WISP* induction was correlated with Wnt-1 expression.

It is not clear whether the *WISPs* are directly or indirectly induced by the downstream components of the Wnt-1 signaling pathway (i.e.,  $\beta$ -catenin, TCF-1, Lef-1). The increased levels of *WISP* RNA were measured in Wnt-1-transformed cells hours or days after Wnt-1 transformation. Thus, *WISP* expression could result from Wnt-1 signaling directly through  $\beta$ -catenin transcription factor regulation or alternatively through Wnt-1 signaling turning on a transcription factor, which in turn regulates *WISPs*.

The *WISPs* define an additional subfamily of the CCN family of growth factors. One striking difference observed in the protein sequence of *WISP-1* is the absence of a CT domain, which is present in CTGF, Cyr61, *nov*, *WISP-2*, and *WISP-3*. This domain is thought to be involved in receptor binding and dimerization. Growth factors, such as TGF- $\beta$ , platelet-derived growth factor, and nerve growth factor, which contain a cysteine knot motif exist as dimers (32). It is tempting to speculate that *WISP-1* and *WISP-3* may exist as dimers, whereas *WISP-2* exists as a monomer. If the CT domain is also important for receptor binding, *WISP-2* may bind to receptor through a different region of the molecule than the other CCN family members. No specific receptors have been identified for CTGF or *nov*. A recent report has shown that integrin  $\alpha_5\beta_1$  serves as an adhesion receptor for Cyr61 (33).

The strong expression of *WISP-1* and *WISP-2* in cells lying within the fibrovascular tumor stroma in breast tumors from Wnt-1 transgenic animals is consistent with previous observations that transcripts for the related CTGF gene are primarily expressed in the fibrous stroma of mammary tumors (34). Epithelial cells are thought to control the proliferation of connective tissue stroma in mammary tumors by a cascade of growth factor signals similar to that controlling connective tissue formation during wound repair. It has been proposed that mammary tumor cells or inflammatory cells at the tumor interstitium secrete TGF- $\beta$ , which is the stimulus for stromal proliferation (34). TGF- $\beta$  is secreted by a large percentage of malignant breast tumors and may be one of the growth factors that stimulates the production of CTGF and *WISP* in the stroma.

It was of interest that *WISP-1* and *WISP-2* expression was observed in the stromal cells that surrounded the tumor cells



Robert M. Piro, Scott A. Margsters††, David A. Lawrence,†  
Margaret Roy, Frank C. Kischkel, Patrick Dowd,  
Arthur Huang, Christopher Donahue,  
Steven W. Sherwood, Daryl J. Baldwin, Paul J. Godowski,  
William L. Wood, Austin L. Gurney, Kenneth J. Hulan,  
Robert C. Cohen, Andrew D. Goddard, David Boistein,  
A. Avi Ashkenazi

Fas ligand (FasL) is produced by activated T cells and natural killer cells and it induces apoptosis (programmed cell death) in target cells through the death receptor Fas/CD95 (ref. 1). One important role of FasL and Fas is to mediate immune-cytotoxic killing of cells that are potentially harmful to the organism, such as virus-infected or tumour cells. Here we report the discovery of a soluble decoy receptor, termed decoy receptor 3 (DcR3), that binds to FasL and inhibits FasL-induced apoptosis. The DcR3 gene was amplified in about half of 35 primary lung and colon tumours studied, and DcR3 messenger RNA was expressed in malignant tissue. Thus, certain tumours may escape FasL-dependent immune-cytotoxic attack by expressing a decoy receptor that blocks FasL.

By searching expressed sequence tag (EST) databases, we identified a set of related ESTs that showed homology to the tumour necrosis factor (TNF) receptor (TNFR) gene superfamily. Using the overlapping sequence, we isolated a previously unknown full-length complementary DNA from human fetal lung. We named the protein encoded by this cDNA decoy receptor 3 (DcR3). The cDNA encodes a 300-amino acid polypeptide that resembles members of the TNFR family (Fig. 1a); the amino terminus contains a leader sequence, which is followed by four tandem cysteine-rich domains (CRDs). Like one other TNFR homologue, osteoprotegerin (OPG), DcR3 lacks an apparent transmembrane sequence, which indicates that it may be a secreted, rather than a membrane-associated, molecule. We expressed a recombinant histidine-tagged form of DcR3 in mammalian cells. DcR3 was secreted into the cell culture medium, and migrated on polyacrylamide gels as a protein of relative molecular mass 35,000 (data not shown). DcR3 shares sequence identity in particular with OPG (31%) and TNFR2 (29%), and has relatively less homology with Fas (17%). All of the cysteines in the four CRDs of DcR3 and OPG are conserved; however, the carboxy-terminal portion of DcR3 is 301 residues shorter.

WE analysed expression of *DeR3* mRNA in human tissues by northern blotting (Fig. 1b). We detected a predominant 2 kilobase transcript in fetal lung, brain and liver and in adult spleen, colon and lung. In addition, we observed relatively high *DeR3* mRNA expression in the human colon carcinoma cell line SW480.

To investigate potential ligand interactions of DCR3, we generated a recombinant, His-tagged DCR3 protein. We tested binding of DCR3 to human 293 cells transfected with individual GPCR-family ligands, which are expressed as type 7 transmembrane proteins (these transmembrane proteins have their N-termini in the cytosol). DCR3 showed a significant increase in binding to cells transfected with *hGIR1* (Fig. 2a) but not to cells transfected with *hGIR2*, *hGIR3*, *hGIR4*, *hGIR5*, *hGIR6*, *hGIR7*, *hGIR8*, *hGIR9*, *hGIR10*, *hGIR11*, *hGIR12*, *hGIR13*, *hGIR14*, *hGIR15*, *hGIR16*, *hGIR17*, *hGIR18*, *hGIR19*, *hGIR20*, *hGIR21*, *hGIR22*, *hGIR23*, *hGIR24*, *hGIR25*, *hGIR26*, *hGIR27*, *hGIR28*, *hGIR29*, *hGIR30*, *hGIR31*, *hGIR32*, *hGIR33*, *hGIR34*, *hGIR35*, *hGIR36*, *hGIR37*, *hGIR38*, *hGIR39*, *hGIR40*, *hGIR41*, *hGIR42*, *hGIR43*, *hGIR44*, *hGIR45*, *hGIR46*, *hGIR47*, *hGIR48*, *hGIR49*, *hGIR50*, *hGIR51*, *hGIR52*, *hGIR53*, *hGIR54*, *hGIR55*, *hGIR56*, *hGIR57*, *hGIR58*, *hGIR59*, *hGIR60*, *hGIR61*, *hGIR62*, *hGIR63*, *hGIR64*, *hGIR65*, *hGIR66*, *hGIR67*, *hGIR68*, *hGIR69*, *hGIR70*, *hGIR71*, *hGIR72*, *hGIR73*, *hGIR74*, *hGIR75*, *hGIR76*, *hGIR77*, *hGIR78*, *hGIR79*, *hGIR80*, *hGIR81*, *hGIR82*, *hGIR83*, *hGIR84*, *hGIR85*, *hGIR86*, *hGIR87*, *hGIR88*, *hGIR89*, *hGIR90*, *hGIR91*, *hGIR92*, *hGIR93*, *hGIR94*, *hGIR95*, *hGIR96*, *hGIR97*, *hGIR98*, *hGIR99*, *hGIR100*, *hGIR101*, *hGIR102*, *hGIR103*, *hGIR104*, *hGIR105*, *hGIR106*, *hGIR107*, *hGIR108*, *hGIR109*, *hGIR110*, *hGIR111*, *hGIR112*, *hGIR113*, *hGIR114*, *hGIR115*, *hGIR116*, *hGIR117*, *hGIR118*, *hGIR119*, *hGIR120*, *hGIR121*, *hGIR122*, *hGIR123*, *hGIR124*, *hGIR125*, *hGIR126*, *hGIR127*, *hGIR128*, *hGIR129*, *hGIR130*, *hGIR131*, *hGIR132*, *hGIR133*, *hGIR134*, *hGIR135*, *hGIR136*, *hGIR137*, *hGIR138*, *hGIR139*, *hGIR140*, *hGIR141*, *hGIR142*, *hGIR143*, *hGIR144*, *hGIR145*, *hGIR146*, *hGIR147*, *hGIR148*, *hGIR149*, *hGIR150*, *hGIR151*, *hGIR152*, *hGIR153*, *hGIR154*, *hGIR155*, *hGIR156*, *hGIR157*, *hGIR158*, *hGIR159*, *hGIR160*, *hGIR161*, *hGIR162*, *hGIR163*, *hGIR164*, *hGIR165*, *hGIR166*, *hGIR167*, *hGIR168*, *hGIR169*, *hGIR170*, *hGIR171*, *hGIR172*, *hGIR173*, *hGIR174*, *hGIR175*, *hGIR176*, *hGIR177*, *hGIR178*, *hGIR179*, *hGIR180*, *hGIR181*, *hGIR182*, *hGIR183*, *hGIR184*, *hGIR185*, *hGIR186*, *hGIR187*, *hGIR188*, *hGIR189*, *hGIR190*, *hGIR191*, *hGIR192*, *hGIR193*, *hGIR194*, *hGIR195*, *hGIR196*, *hGIR197*, *hGIR198*, *hGIR199*, *hGIR200*, *hGIR201*, *hGIR202*, *hGIR203*, *hGIR204*, *hGIR205*, *hGIR206*, *hGIR207*, *hGIR208*, *hGIR209*, *hGIR210*, *hGIR211*, *hGIR212*, *hGIR213*, *hGIR214*, *hGIR215*, *hGIR216*, *hGIR217*, *hGIR218*, *hGIR219*, *hGIR220*, *hGIR221*, *hGIR222*, *hGIR223*, *hGIR224*, *hGIR225*, *hGIR226*, *hGIR227*, *hGIR228*, *hGIR229*, *hGIR230*, *hGIR231*, *hGIR232*, *hGIR233*, *hGIR234*, *hGIR235*, *hGIR236*, *hGIR237*, *hGIR238*, *hGIR239*, *hGIR240*, *hGIR241*, *hGIR242*, *hGIR243*, *hGIR244*, *hGIR245*, *hGIR246*, *hGIR247*, *hGIR248*, *hGIR249*, *hGIR250*, *hGIR251*, *hGIR252*, *hGIR253*, *hGIR254*, *hGIR255*, *hGIR256*, *hGIR257*, *hGIR258*, *hGIR259*, *hGIR260*, *hGIR261*, *hGIR262*, *hGIR263*, *hGIR264*, *hGIR265*, *hGIR266*, *hGIR267*, *hGIR268*, *hGIR269*, *hGIR270*, *hGIR271*, *hGIR272*, *hGIR273*, *hGIR274*, *hGIR275*, *hGIR276*, *hGIR277*, *hGIR278*, *hGIR279*, *hGIR280*, *hGIR281*, *hGIR282*, *hGIR283*, *hGIR284*, *hGIR285*, *hGIR286*, *hGIR287*, *hGIR288*, *hGIR289*, *hGIR290*, *hGIR291*, *hGIR292*, *hGIR293*, *hGIR294*, *hGIR295*, *hGIR296*, *hGIR297*, *hGIR298*, *hGIR299*, *hGIR300*, *hGIR301*, *hGIR302*, *hGIR303*, *hGIR304*, *hGIR305*, *hGIR306*, *hGIR307*, *hGIR308*, *hGIR309*, *hGIR310*, *hGIR311*, *hGIR312*, *hGIR313*, *hGIR314*, *hGIR315*, *hGIR316*, *hGIR317*, *hGIR318*, *hGIR319*, *hGIR320*, *hGIR321*, *hGIR322*, *hGIR323*, *hGIR324*, *hGIR325*, *hGIR326*, *hGIR327*, *hGIR328*, *hGIR329*, *hGIR330*, *hGIR331*, *hGIR332*, *hGIR333*, *hGIR334*, *hGIR335*, *hGIR336*, *hGIR337*, *hGIR338*, *hGIR339*, *hGIR340*, *hGIR341*, *h*

methods. Peptides KENK or AEQK were dissolved in water, made isotonic with NaCl and added into RPMI growth medium. T-cell proliferation assays were done essentially as described [14]. Briefly, after antigen pulsing (50 µg/ml TGFβ) with tetrapeptides (1.1 µg/ml), PEMCs or EBV-B cells were washed in PBS and fixed for 45 s in 0.05% glutaraldehyde. Glycine was added to a final concentration of 0.1 M and the cells were washed five times in RPMI 1640 medium containing 1% FCS before co-culture with T cells done in round-bottom 96 well microtitre plates. After 48 h the cultures were pulsed with 1 µCi of <sup>3</sup>H-thymidine and harvested for scintillation counting (10 h later). Digestion of native TGFβ was done by incubating 200 µg TGFβ with 0.25 µg pig kidney legumain in 500 µl 50 mM citrate buffer, pH 5.5, for 2 h at 37°C. Glycopeptide digestions. The peptides HIDEED1, HIDEIN (glucosamine) EDE1 and HIDEED1, which are based on the TGFβ sequence, and QQQHILGSGNVTDGSGNEGLER (KTK), which is based on human transferrin, were obtained by custom synthesis. The three C-terminal acidic residues were added to the natural sequence to aid solubility. The transferrin glycopeptide QQQHILGSGNVTDGSGNEGLER was prepared by tryptic (Promega) digestion of 5-mg reduced, carboxy-methylated human transferrin followed by concanavalin A chromatography. Glycopeptides corresponding to residues 632–642 and 421–452 were isolated by reverse-phase HPLC and identified by mass spectrometry and N-terminal sequencing. The lyophilized transferrin-derived peptides were redissolved in 50 mM sodium acetate, pH 5.5, 10 mM dithiothreitol, 20% methanol. Digestions were performed for 5 h at 37°C with 4–20 µl/ml 100 µg pig kidney legumain or 6 µl TCEP. Products were analysed by HPLC or MALDI-TOF mass spectrometry using a matrix of 0.1% DHB in 0.1% cyanidric acid in 50% acetonitrile/0.1% TFA and a Perceptive Biosystems Elite STR mass spectrometer set to linear or reflector mode. Internal standard division was obtained with a variation of 56–13 mass units.

1. Oishi, J.M. & A. Oishi. Sedation and Characterization of mammalian leguminan an anaparting.  
Biochem. Biophys. Res. Commun. 172: 8050-8093 (1997)

1. Kohnson, A. G. and B. A. Cohen. 1991. The two primary mechanisms of antigen presentation and the contribution by use of the invariant chain. *Arch. Biochem. Biophys.* 283: 208-211 (1991).
2. Haimly, F., F. Haimly, J. A. Briller, P. J. Aparicio, and J. P. DiCorleone. 1991. Antigen presentation and peptide activity in adult *Schistosoma mansoni*. *Parasitology* 111: 875-880 (1991).
3. Keweler, K. C. Antigen processing for presentation by class II major histocompatibility complex. *Respects derived by cathepsin D.* *Eur. J. Immunol.* 21: 1519-1524 (1992).
4. Hesse, B. J. An essential role for cathepsin D in class II-associated invariant chain processing and peptide loading. *Immunity* 4: 357-366 (1996).
5. Rodriguez, G. M., A. Drenth, and S. Selvakumaran. D in antigen presentation of ovalbumin. *J. Immunol.* 149: 1074-1078 (1992).
6. Hewlett, N. A. of Natural processing sites for human cathepsin E and cathepsin D in tissue main implications for T-cell epitope generation. *J. Immunol.* 157: 4693-4699 (1997).
7. Wirth, G. Capable and processing of endogenous antigen for presentation on MHC molecules. *Annu. Rev. Immunol.* 15: 413-430 (1997).
8. Chapman, R. A. Endosomal proteases and MHC class II function. *Curr. Opin. Immunol.* 10: 95-103 (1998).
9. Henshel, G. and Miller, J. Endosomal proteases and antigen processing. *Trends Biochem. Sci.* 22: 377-382 (1997).
10. Li, F. and Halbrook, J. Cathepsin D and -Osteonectin immunoreactivity in T-cells and dendritic cells of lymphoid tissue within transgenic *Canine*. *Cell* 62: 253-271 (1990).
11. Pearlin, D. T., A. Lockley, R. M. The instructive role of innate immunity in the acquired immune response. *Science* 272: 9-14 (1996).
12. Alexander, C. and Janeway, C. A. Innate immunity: the virtuous or vicious cycle of recognition. *Cell* 51: 291-293 (1997).
13. Wyatt, R. et al. The antigenic structure of the HIV gp120 envelope glycoprotein. *Nature* 393: 705-711 (1998).
14. Reynolds, P. et al. N-glycosylation of HIV gp120 may control recognition by T lymphocytes. *J. Immunol.* 147: 3122-3132 (1991).
15. Davidson, H., W. Wei, M. C. A. Wang, C. Endocytosis, intracellular trafficking, and processing of membrane IgG and monovalent antigen/membrane IgG complexes in B lymphocytes. *J. Immunol.* 164: 4101-4102 (1990).
16. Burton, A. J. and Kinsch, H. Cathepsin B, cathepsin H and cathepsin L. *Methods Enzymol.* 60: 515-559 (1981).
17. Mason, A. J., Ballantine, S. P., Smallwood, A. E., and Fairweather, N. P. Expression of retinal wash fragment C in *Escherichia coli* purification and potential use as a vaccine. *Biochemistry* 37: 1043-1046 (1998).
18. Lane, D. P. and Harlow, E. *Antibodies: A Laboratory Manual* (Gold Spring Harbor Laboratory Press, 1988).
19. Janeway, C. A. Antigen presentation: interaction between I and B cells. *Nature* 314: 517-519 (1985).
20. Smith, L. A. and C. Chakravarti. Effect of transport of newly synthesized T cell and B cell surface molecules from MHC class II compartments to the cell surface. *Development* 129: 645-651 (1997).

**Acknowledgements:** We thank M. Kervison for helpful discussions and advice, S. Sanyal and M. Grady for editorial and technical assistance, J. Spruce, A. Kinnison and the BTHS Nursing Unit Hospital for help during the study. Good monocyte preparations and our colleagues for healthy blood controls and for manufacturing T.H.M. were kindly supported by the Wellcome Trust and by an EMBO Long Term Fellowship to R.Y.

markedly (data not shown). DcR3-Fc immunoprecipitated shed Fas from FasL-transfected 293 cells (Fig. 2b) and purified soluble Fas (Fig. 2c) as did the Fc-tagged ectodomain of Fas but not TNFR1. Gel filtration chromatography showed that DcR3-Fc and soluble FasL formed a stable complex (Fig. 2d). Equilibrium analysis indicated that DcR3-Fc and Fas-Fc bound to soluble FasL with a comparable affinity ( $K_d = 0.8 \pm 0.2$  and  $1.1 \pm 0.1$  nM, respectively, Fig. 2e), and that DcR3-Fc could block nearly all of the binding of soluble FasL to Fas-Fc (Fig. 2e, inset). Thus, DcR3 competes with Fas for binding to FasL.

To determine whether binding of DcR3 inhibits FasL activity, we tested the effect of DcR3-Fc on apoptosis induction by soluble FasL in Jurkat T leukaemia cells, which express Fas (Fig. 3a). DcR3-Fc and Fas-Fc blocked soluble FasL-induced apoptosis in a similar dose-dependent manner, with half-maximal inhibition at  $\sim 0.1 \mu\text{g ml}^{-1}$ . Time course analysis showed that the inhibition did not merely delay cell death but rather persisted for at least 24 hours (Fig. 3b). We also tested the effect of DcR3-Fc on activation-induced cell death (AICD) of mature T lymphocytes, a FasL-dependent process. Consistent with previous results, activation of interleukin-2-stimulated CD4-positive T cells with anti-CD3 antibody increased the level of apoptosis twofold, and Fas-Fc blocked this effect substantially (Fig. 3c). DcR3-Fc blocked the

induction of apoptosis to a similar extent. Thus, DcR3 binding blocks apoptosis induction by FasL.

FasL-induced apoptosis is important in elimination of virus-infected cells and cancer cells by natural killer cells and cytotoxic lymphocytes; an alternative mechanism involves perforin and granzymes<sup>10</sup>. Peripheral blood natural killer cells triggered marked cell death in Jurkat T leukaemia cells (Fig. 3d). DcR3-Fc and Fas-Fc each reduced killing of target cells from  $\sim 65\%$  to  $\sim 30\%$ , with half-maximal inhibition at  $\sim 10$  ng ml<sup>-1</sup>; the residual killing was probably mediated by the perforin/granzyme pathway. Thus, DcR3 binding blocks FasL-dependent natural killer cell activity. Higher DcR3-Fc and Fas-Fc concentrations were required to block natural killer cell activity compared with those required to block soluble FasL activity, which is consistent with the greater potency of membrane-associated FasL compared with soluble FasL.

Given the role of immune cytotoxic cells in elimination of tumour cells and the fact that DcR3 can act as an inhibitor of FasL, we proposed that DcR3 expression might contribute to the ability of some tumours to escape immune cytotoxic attack. As genomic amplification frequently contributes to tumorigenesis, we investigated whether the DcR3 gene is amplified in cancer. We analysed DcR3 gene copy number by quantitative polymerase chain



**Figure 1** Primary structure and expression of human DcR3. **a**, Alignment of the amino acid sequences of DcR3 and of its orthologues (OPG). The C-terminal 10 residues of OPG are not shown. The putative signal cleavage site (arrow) and cysteine-rich domains (CD1-4) and the TNF-linked glycosylation site (asterisk) are shown. **b**, Expression of DcR3 mRNA. Northern hybridization analysis was done using the DcR3 cDNA as a probe and blots of poly(A)<sup>+</sup> RNA (400 ng) from human fetal and adult tissues, or cancer cell lines (PBL, peripheral blood lymphocytes).

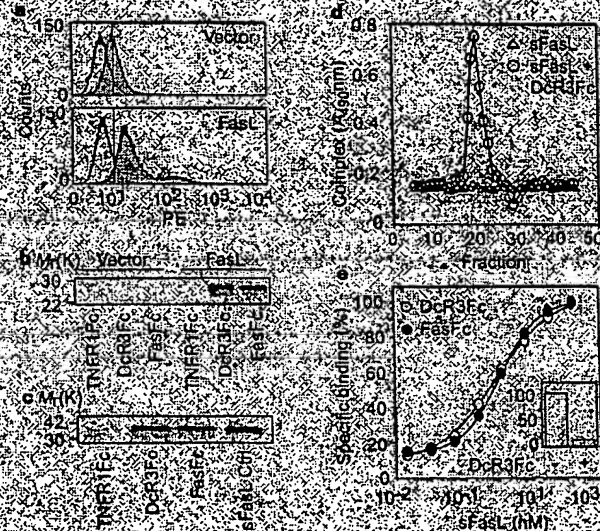


**Figure 2** Interaction of DcR3 with FasL. **a**, 293 cells were transfected with pRK5-vector (top) or with pRK5 encoding full-length FasL (bottom), incubated with DcR3-Fc (solid line, shaded area), TNFR1-Fc (dotted line) or buffer control (dashed line) (the dashed and dotted lines overlap), and analysed for binding by FACS. Statistical analysis showed a significant difference ( $P < 0.001$ ) between the binding of DcR3-Fc to cells transfected with FasL or pRK5. PE, phycoerythrin; labelled cells. **b**, 293 cells were transfected with FasL and metabolically labelled, and supernatants were immunoprecipitated with Fc-tagged TNFR1, DcR3 or Fas-Fc. Purified soluble FasL (or Fas) was immunoprecipitated with TNFR1-Fc, DcR3-Fc or Fas-Fc and visualized by immunoblot with anti-Fas antibody. Spots were loaded directly for comparison in the right-hand lane. **c**, Flag-tagged FasL was incubated with DcR3-Fc or with buffer and resolved by gel filtration column. Fractions were analysed in an assay that detects complexes containing DcR3-Fc and FasL. **d**, **e**, Equilibrium binding of DcR3-Fc from vector or FasL-Fc transfected cells to DcR3-Fc was analysed by immunoblotting with anti-Fas antibody. **f**, Equilibrium binding of DcR3-Fc to FasL was analysed by immunoblotting with anti-Fas antibody.

reaction (PCR) in genomic DNA from 35 primary lung and colon tumours relative to pooled genomic DNA from peripheral blood leukocytes (PBLs) of 10 healthy donors. Eight of 18 lung tumours and 9 of 17 colon tumours showed DcR3 gene amplification, ranging from 2- to 18-fold (Fig. 4a, b). To confirm this result, we analyzed the colon tumour DNAs with three more independent sets of DcR3-based PCR primers and probes. We observed nearly the same amplification (data not shown).

We then analysed DcR3 mRNA expression in primary tumour tissue sections by *in situ* hybridization. We detected DcR3 expression and out of 15 lung tumours, 2 out of 2 colon tumours, 1 out of 3 breast tumours and 1 out of 1 gastric tumour (data not shown). A section through a squamous cell carcinoma of the lung is shown in Fig. 4c. DcR3 mRNA was localized to infiltrating malignant epithelium, but was essentially absent from adjacent stroma, indicating tumour-specific expression. Although the individual tumour specimens that we analysed for mRNA expression and gene amplification were different, the *in situ* hybridization results are consistent with the finding that the DcR3 gene is amplified frequently in tumours. SW480 colon carcinoma cells, which showed abundant DcR3 mRNA expression (Fig. 4b), also had marked DcR3 gene amplification, as shown by quantitative PCR (fourfold) and by Southern blot hybridization (fivefold) (data not shown).

If DcR3 amplification in cancer is functionally relevant, then DcR3 should be amplified more than neighbouring genomic regions that are not important for tumour survival. To test this,

we mapped the human DcR3 gene by radiation hybrid analysis. DcR3 showed linkage to marker AFB2 (6x27 cM), which maps to chromosomal position 20q12. Next, we isolated from a bacterial artificial chromosome (BAC) library a human genomic clone that carries DcR3, and sequenced the ends of the clone insert. We then determined, from the nine colon tumours that showed two-fold or greater amplification of DcR3, the copy number of the DcR3 flanking sequences (reverse and forward) from the BAC, and of seven genomic markers that span chromosome 20 (Fig. 4b). The DcR3-linked reverse marker showed an average amplification of roughly threefold, slightly less than the approximately fourfold amplification of DcR3; the other markers showed little or no amplification. These data indicate that DcR3 may be at the centromere of a distal chromosome 20 region that is amplified in colon cancer, consistent with the possibility that DcR3 amplification promotes tumour survival.

Our results show that DcR3 binds specifically to FasL and inhibits FasL activity. We did not detect DcR3 binding to several other TNF ligand-family members; however, this does not rule out the possibility that DcR3 interacts with other ligands, as do some other TNFR family members, including OPG<sup>21</sup>.

FasL is important in regulating the immune response; however, little is known about how FasL function is controlled. One mechanism involves the molecule of FLIP, which modulates apoptosis signaling downstream of Fas<sup>22</sup>. A second mechanism involves proteolytic shedding of FasL from the cell surface<sup>23</sup>. DcR3 competes with FasL for

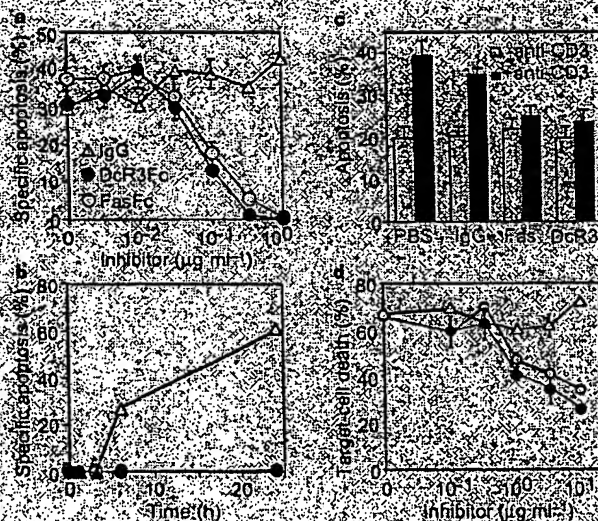


**Figure 3** Inhibition of FasL activity by DcR3. **a**, Human Jurkat leukemia cells were incubated with Flag-tagged soluble FasL (FasL; 5 ng/ml), oligomerized DcR3-Fc, Fas-Fc or human IgG1 and assayed for apoptosis (mean  $\pm$  s.e.m. of triplicates). **b**, Jurkat cells were incubated with FasL-Flag plus anti-Flag antibody (anti-Flag) in presence of 1  $\mu$ g/ml DcR3-Fc (filled circles), Fas-Fc (open circles) or human IgG1 (triangles), and apoptosis was determined at the indicated time points. **c**, Peripheral blood T cells were stimulated with PHA and interleukin-2 followed by anti-CD3 (anti-CD3) and anti-CD28 antibody (filled bars) together with phosphatidylserine (PS) (human IgG1, Fas-Fc or DcR3-Fc; 10  $\mu$ g/ml). After 16 h, apoptosis of CD4<sup>+</sup> cells was determined (mean  $\pm$  s.e.m. of results from five donors). **d**, Peripheral blood natural killer cells were incubated with <sup>51</sup>C-labelled target cells in the presence of DcR3-Fc (filled circles), Fas-Fc (open circles) or human IgG1 (triangles), and target cell death was determined by release of <sup>51</sup>C (mean  $\pm$  s.e.m. of five donors; each triplicate).

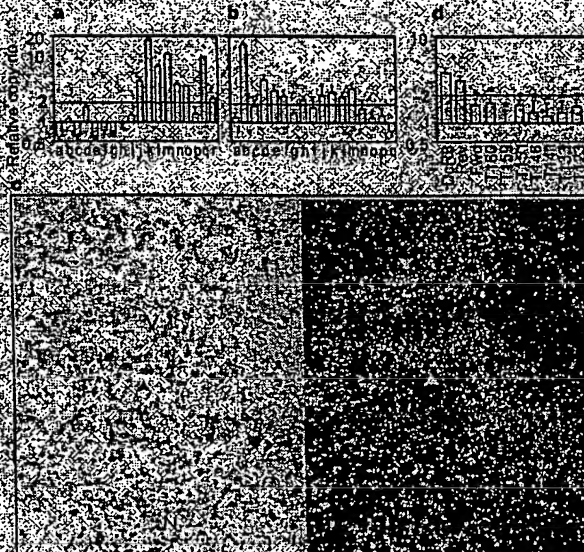


**Figure 4** Genomic amplification of DcR3 in tumours. **a**, Lung cancers comprising eight adenocarcinomas (a, c, e, g, i, k, m, o, q, s, u, w, y) and seven squamous cell carcinomas (a, c, e, g, i, k, m, o, q, s, u, w, y). **b**, Colon tumours comprising 17 adenocarcinomas (a, c, e, g, i, k, m, o, q, s, u, w, y) and one bronchial adenocarcinoma (a, c, e, g, i, k, m, o, q, s, u, w, y). The data are means  $\pm$  s.e.m. of 2 experiments, done in duplicate. **c**, Colon tumours comprising 17 adenocarcinomas (a, c, e, g, i, k, m, o, q, s, u, w, y) and one bronchial adenocarcinoma (a, c, e, g, i, k, m, o, q, s, u, w, y). The data are means  $\pm$  s.e.m. of five experiments done in duplicate. **d**, *In situ* hybridization analysis of DcR3 mRNA expression in a squamous cell carcinoma of the lung. **e**, A representative bright-field image (left) and the corresponding dark-field image (right) show DcR3 mRNA overexpressing malignant epithelium (arrowhead). **f**, A representative bright-field image (left) and the corresponding dark-field image (right) show DcR3 mRNA overexpressing malignant epithelium (arrowhead). **g**, A representative bright-field image (left) and the corresponding dark-field image (right) show DcR3 mRNA overexpressing malignant epithelium (arrowhead). **h**, A representative bright-field image (left) and the corresponding dark-field image (right) show DcR3 mRNA overexpressing malignant epithelium (arrowhead). **i**, A representative bright-field image (left) and the corresponding dark-field image (right) show DcR3 mRNA overexpressing malignant epithelium (arrowhead). **j**, A representative bright-field image (left) and the corresponding dark-field image (right) show DcR3 mRNA overexpressing malignant epithelium (arrowhead). **k**, A representative bright-field image (left) and the corresponding dark-field image (right) show DcR3 mRNA overexpressing malignant epithelium (arrowhead). **l**, A representative bright-field image (left) and the corresponding dark-field image (right) show DcR3 mRNA overexpressing malignant epithelium (arrowhead). **m**, A representative bright-field image (left) and the corresponding dark-field image (right) show DcR3 mRNA overexpressing malignant epithelium (arrowhead). **n**, A representative bright-field image (left) and the corresponding dark-field image (right) show DcR3 mRNA overexpressing malignant epithelium (arrowhead). **o**, A representative bright-field image (left) and the corresponding dark-field image (right) show DcR3 mRNA overexpressing malignant epithelium (arrowhead). **p**, A representative bright-field image (left) and the corresponding dark-field image (right) show DcR3 mRNA overexpressing malignant epithelium (arrowhead). **q**, A representative bright-field image (left) and the corresponding dark-field image (right) show DcR3 mRNA overexpressing malignant epithelium (arrowhead). **r**, A representative bright-field image (left) and the corresponding dark-field image (right) show DcR3 mRNA overexpressing malignant epithelium (arrowhead). **s**, A representative bright-field image (left) and the corresponding dark-field image (right) show DcR3 mRNA overexpressing malignant epithelium (arrowhead). **t**, A representative bright-field image (left) and the corresponding dark-field image (right) show DcR3 mRNA overexpressing malignant epithelium (arrowhead). **u**, A representative bright-field image (left) and the corresponding dark-field image (right) show DcR3 mRNA overexpressing malignant epithelium (arrowhead). **v**, A representative bright-field image (left) and the corresponding dark-field image (right) show DcR3 mRNA overexpressing malignant epithelium (arrowhead). **w**, A representative bright-field image (left) and the corresponding dark-field image (right) show DcR3 mRNA overexpressing malignant epithelium (arrowhead). **x**, A representative bright-field image (left) and the corresponding dark-field image (right) show DcR3 mRNA overexpressing malignant epithelium (arrowhead). **y**, A representative bright-field image (left) and the corresponding dark-field image (right) show DcR3 mRNA overexpressing malignant epithelium (arrowhead). **z**, A representative bright-field image (left) and the corresponding dark-field image (right) show DcR3 mRNA overexpressing malignant epithelium (arrowhead).

Fast binding, hence, it may represent a third mechanism of intracellular regulation of FasL activity. A decoy receptor that modulates the function of the cytokine interleukin-1 has been described<sup>1</sup>. In addition, two decoy receptors that belong to the TNFR family, DcR1 and DcR2, regulate the FasL-related apoptosis-inducing molecule Apo2L<sup>2,3</sup>. Unlike DcR1 and DcR2, which are membrane-associated proteins, DcR3 is directly secreted into the extracellular space. One other secreted TNFR family member is OPG, which shares greater sequence homology with DcR3 (34%) than do DcR1 (17%) or DcR2 (19%). OPG functions as a third decoy for Apo2L<sup>4</sup>. Thus, DcR3 and OPG define a new subset of TNFR family members that function as secreted decoys to modulate ligands that induce apoptosis. Fox viruses produce soluble TNFR homologues that neutralize specific TNF family ligands, thereby modulating the antiviral immune response<sup>5</sup>. Our results indicate that a similar mechanism, namely production of a soluble decoy receptor for FasL, may contribute to immune evasion by certain tumours.

# Methods

**Isolation of DcR3 cDNA.** Several overlapping ESTs in GenBank (accession numbers AA025672, AA025673, and W61500) and the human cDNA library (Pharmaceuticals, accession numbers 1539258, 1539259, 1539260, 1542861, 1789372 and 207027) showed similarity to members of the TNFR family. We screened human cDNA libraries by PCR with primers based on the region of EST consensus. Total lung was positive for a product of the expected size. By hybridization to a PCR-generated probe based on the EST, one positive clone (DNA30932) was identified. When searching for potential alternatively spliced forms of DcR3 that might encode a transmembrane protein, we isolated 30 more clones; the coding regions of these clones were identical in size to that of the initial clone (data not shown).

**Fc fusion proteins (immunoadhesins).** The entire DcR3 sequence, or the ectodomain or part of TNFR1, was fused to the hinge and Fc region of human IgG1 expressed in insect Sf9 cells or in human 293 cells and purified as described.

**Fluorescence-activated cell sorting (FACS) analysis.** We transfected 293 cells using calcium phosphate of Efficient (Qiagen) with pRK5 vector of pRK5 encoding full-length human FasL (2 µg) (together with pRK5 encoding CrmA (2 µg) to prevent cell death). After 48 h, the cells were incubated with biotinylated DcR3-Fc or TNFR1-Fc and then with phycoerythrin-conjugated streptavidin (Cytochrome). Cells were assayed by FACS. The data were analyzed by Kolmogorov-Smirnov statistical analysis. There was some detectable staining of control transfected cells by DcR3-Fc as these cells express endogenous FasL (data not shown). It is possible that DcR3 recognized some other factor that is expressed constitutively on 293 cells.

**Immunoprecipitation.** Human 293 cells were transfected as above and metabolically labelled with [<sup>35</sup>S]methionine and [<sup>35</sup>S]cysteine (100 mCi, Amersham). After 16 h of culture in the presence of 2 mM DTT (10 µM) the medium was immunoprecipitated with DcR3-Fc, Fas-Fc or TNFR1-Fc (5 µg), followed by protein A-Sepharose (Repligen). The precipitates were resolved by SDS-PAGE and visualized on a phosphorimager (Fuji BAS2000). Alternatively, purified, Flag-tagged soluble FasL (1 µg) (Alexis) was incubated with each Fc fusion protein (1 µg), precipitated with protein A-Sepharose, resolved by SDS-PAGE and visualized by immunoblotting with rabbit anti-FasL antibody (Oncogene Research).

**Analysis of complex formation.** Flag-tagged soluble FasL (25 µg) was incubated with buffer or with DcR3-Fc (40 µg) for 15 min at 25 °C. The reaction was loaded onto a Superdex 200 HR 10/30 column (Pharmacia) and developed with PBS/P8 dilutions. Fractions were collected. The presence of DcR3-Fc-FasL complex in each fraction was analysed by placing aliquots into microtitre wells pre-coated with anti-human IgG (Boehringer). After capture, DcR3-Fc followed by detection with biotinylated anti-Flag antibody Bio 672 (Kodak) and streptavidin horseradish peroxidase (Amersham). Calibration of the column indicated an apparent relative molecular mass of the complex of 220 kDa (data not shown), which is consistent with a stoichiometry of two DcR3-Fc trimers and one soluble FasL homotrimer.

**Equilibrium binding analysis.** Microtitre wells were coated with anti-human

IgG blocked with PBSA. In PBS, DcR3-Fc (0.1 µg/ml) was added followed by serially diluted Flag-tagged soluble FasL. Bound ligand was detected with anti-Flag antibody as above. In the competition assay, FasL was immunoprecipitated above and the wells were blocked with excess IgG1 before addition of Flag-tagged soluble FasL plus DcR3-Fc.

**Fc cell AICD.** CD3<sup>+</sup> lymphocytes were isolated from peripheral blood of individual donors using anti-CD3 magnetic beads (Mileny Biotech), stimulated with phytohemagglutinin (PHA) 2 µg/ml for 24 h and cultured in the presence of interleukin-2 (100 U/ml). For AICD, the cells were placed in wells coated with anti-CD3 antibody (Pharmingen) and analysed for apoptosis 18 h later by FACS analysis of Annexin-V binding of CD3<sup>+</sup> cells.

**Natural killer cell activity.** Natural killer cells were isolated from peripheral blood of individual donors using anti-CD56 magnetic beads (Mileny Biotech) and incubated for 16 h with [<sup>51</sup>Cr]-labelled Jurkat cells at an effector to target ratio of 1:1 in the presence of DcR3-Fc. Fas-Fc or human IgG1. Target cell death was determined by release of [<sup>51</sup>Cr] in effector target co-cultures relative to release of [<sup>51</sup>Cr] by detergent lysis of equal numbers of Jurkat cells.

**Gene amplification analysis.** Surgical specimens were provided by J. Kerr (lung tumours) and P. Quirke (colon tumours). Genomic DNA was extracted (Qiagen) and the concentration was determined using a Roche dye 53238 intercalation fluorometry. Amplification was determined by quantitative PCR using a LightCycler instrument (AB). The method was validated by comparison of PCR and Southern hybridization data for the Myc and HER-2 oncogenes (data not shown). Gene-specific primers and fluorescent probes were designed on the basis of the sequence of DcR3 or of nearby regions identified on a BAC carrying the human DcR3 gene. Alternatively, primers and probes were based on Stanford Human Genome Center marker AFM218x7 (F1360), which is linked to DcR3 (likelihood score = 5.4). SHCC-36268 (T159), the nearest available marker which maps to a 500 kbp apart from T160 and by a centromere that spans chromosome 20. The DcR3-specific primer sequences were 5'-GTTTTCGCGCAGCGG-3' and 5'-ATGACGCGCGAGCAG-3' and the fluorescent probe sequence was 5'-TAM-ATGACGCGCGAGCAGCAGCAG-3' (TAM is 5'-fluorescein-phosphoramidite). Relative gene copy numbers were derived using the formula  $2^{-(C_T - C_T^{\text{ref}})}$ , where  $C_T$  is the difference in amplification cycles required to detect DcR3 in peripheral blood lymphocyte DNA compared to test DNA.

Received 24 September; accepted 4 November 1998

1. Nagata, S. Apoptosis by death factor. *Cell* **68**, 281-286 (1992).
2. Smith, C. A., Farrah, T. & Goodwin, G. D. The TNF receptor superfamily: of cellular and viral proteins, activation, signalling and death. *Cell* **74**, 291-301 (1993).
3. Simpson, W. J. & Smith, C. A. DcR3 encodes a novel secreted protein involved in the regulation of bone density. *EMBO J.* **16**, 297-311 (1997).
4. Smith, T., Kishimoto, T., Collier, A. C., Nagata, S. Molecular cloning and expression of Fas ligand, a novel member of the TNF family. *Cell* **75**, 1167-1174 (1993).
5. Fournier, C. et al. Human gamma herpesvirus encodes a unique, secreted, and homologous to human FasL. *Nature* **371**, 723-726 (1994).
6. Smith, C. A. et al. Isolation of a novel member of the TNF receptor superfamily, a novel member of the TNF family. *J. Biol. Chem.* **271**, 12637-12640 (1996).
7. Weller, S. J. et al. Identification and characterization of a new member of the TNF family that induces apoptosis. *Immunity* **5**, 571-582 (1997).
8. Marsters, S. A. et al. Identification of a ligand for the death domain-containing receptor Apo2. *Cell* **88**, 513-518 (1992).
9. Ghichopoulos, Y. et al. TWEAK, a new secreted ligand in the TNF family, that weakly induces apoptosis. *J. Biol. Chem.* **272**, 32400-32410 (1997).
10. Wong, B. K. et al. TRANCE is a novel ligand of the TNF family that activates c-Jun N-terminal kinase in T cells. *J. Biol. Chem.* **272**, 25190-25194 (1997).
11. Anderson, D. M. et al. A member of the TNF family that induces FasL-induced apoptosis and inhibits FasL-induced apoptosis. *Nature* **380**, 77-81 (1997).
12. Lacey, D. L. et al. Osteopontin is a cytokine that regulates osteoclast differentiation and activation. *Cell* **88**, 163-173 (1992).
13. Doherty, J. W., Walczak, H., Baumhueter, C., Doherty, C., Krammer, P. H. Autoactive T cell surface molecules by Apo2L (FasL). *Nature* **375**, 694-697 (1995).
14. Arase, H., Arase, N. & Saito, T. Fas-mediated cytotoxicity by freshly isolated natural killer cells. *J. Exp. Med.* **181**, 105-113 (1995).
15. Medema, J. P. et al. Regulation of Fas and FasL expression by NK cells by cytokines and the involvement of FasL in NK cell-induced cytotoxicity. *Exp. Cell Res.* **179**, 404-411 (1997).
16. Moller, S. Mechanisms of FasL-induced cytotoxicity. *Cell* **71**, 1-10 (1997).
17. Smith, C. A. et al. A novel member of the TNF family that induces FasL-induced apoptosis. *Nature* **380**, 77-81 (1997).
18. Ghichopoulos, Y. et al. Osteopontin is a cytokine that regulates osteoclast differentiation and activation. *Cell* **88**, 163-173 (1992).
19. Ghichopoulos, Y. et al. Osteopontin is a cytokine that regulates osteoclast differentiation and activation. *Cell* **88**, 163-173 (1992).
20. Ghichopoulos, Y. et al. Osteopontin is a cytokine that regulates osteoclast differentiation and activation. *Cell* **88**, 163-173 (1992).
21. Ghichopoulos, Y. et al. Osteopontin is a cytokine that regulates osteoclast differentiation and activation. *Cell* **88**, 163-173 (1992).
22. Ghichopoulos, Y. et al. Osteopontin is a cytokine that regulates osteoclast differentiation and activation. *Cell* **88**, 163-173 (1992).

10. Ashworth, A. & Durr, V. M. Death receptor signalling and modulation. *Cell* **74**, 1305-1306 (1993).
11. Ashworth, A. & Durr, V. M. Immunomodulation in relation to the death receptor. *Cell* **74**, 1305-1306 (1993).
12. Ashworth, A. & Durr, V. M. Activation of apoptosis by Apo-1 binds to independent of FADD has been shown by *Crk*. *Cell* **74**, 1305-1306 (1993).

Authors' disclosures of potential conflicts of interest and author contributions are found in the article. Correspondence and requests for materials should be addressed to J.A. (E-mail: jay@ucla.edu). The copyright for this article is held by the copyright owner.

Correspondence and requests for materials should be addressed to J.A. (E-mail: jay@ucla.edu). The copyright for this article is held by the copyright owner.

## Crystal structure of the ATP-binding subunit of an ABC transporter

Li Wei Hung<sup>1</sup>, Jits Xiaoyan Wang<sup>1</sup>, Kishiko Nikaido<sup>1</sup>, Pei-Qi Li<sup>2</sup>, Giovanna Ferro-Luzzi Ames<sup>1</sup> & Sung-Hou Kim<sup>1</sup>

<sup>1</sup>E. O. Lawrence Berkeley National Laboratory, <sup>2</sup>Department of Molecular and Cell Biology, and <sup>3</sup>Department of Chemistry, University of California at Berkeley, Berkeley, California 94720, USA

ABC transporters (also known as traffic ATPases) form a large family of proteins responsible for the translocation of a variety of compounds across membranes of both prokaryotes and eukaryotes. The recently completed *Escherichia coli* genome sequence revealed that the largest family of paralogous *E. coli* proteins is composed of ABC transporters. Many eukaryotic proteins of medical significance belong to this family, such as the cystic fibrosis transmembrane conductance regulator (CFTR), the P-glycoprotein (or multidrug resistance protein) and the heterodimeric transporter associated with antigen processing (TAP1-TAP2). Here we report the crystal structure at 2.5 Å resolution of HisP, the ATP-binding subunit of the histidine permease, which is an ABC transporter from *Salmonella typhimurium*. We correlate the details of this structure with the biochemical, genetic and biophysical properties of the wild-type and several mutant HisP proteins. The structure provides a basis for understanding properties of ABC transporters and of defective CFTR proteins.

ABC transporters contain four structural domains: two nucleotide-binding domains (NBDs), which are highly conserved throughout the family, and two transmembrane domains. In prokaryotes, these domains are often separate subunits which are assembled into a membrane-bound complex; in eukaryotes, the domains are generally fused into a single polypeptide chain. The periplasmic histidine permease of *S. typhimurium* and *E. coli* is a well-characterized ABC transporter that is a good model for this superfamily. It consists of a membrane-bound complex, HisOMP, which comprises integral membrane subunits HisQ and HisM, and two copies of HisP, the ATP-binding subunit. HisP, which has properties intermediate between those of integral and peripheral membrane proteins, is accessible from both sides of the membrane, presumably by its interaction with HisQ and HisM. The two HisP subunits form a dimer, as shown by their cooperativity in ATP hydrolysis, the requirement for both subunits to be present for activity, and the formation of a HisP dimer upon chemical cross-linking. Soluble HisP also forms a dimer. HisP has been purified and characterized in an active, soluble form, which can be reconstituted into a fully active membrane-bound complex.

The overall shape of the crystal structure of the HisP monomer is that of an 'L' with two thick arms (arm I and arm II). The ATP-binding pocket is near the end of arm I (Fig. 1). A six-stranded  $\beta$ -sheet ( $\beta 1$  and  $\beta 2$ - $\beta 12$ ) spans both arms of the 'L' with a domain of  $\alpha$ -helices ( $\alpha 1$ - $\alpha 5$ ) and a domain of mostly  $\alpha$ -helices ( $\alpha 6$ - $\alpha 9$ ) on the



Figure 1 Crystal structure of HisP. **a**, View of the dimer along an axis perpendicular to its two-fold axis. The top and bottom of the dimer are suggested to face towards the periplasmic and cytoplasmic sides, respectively (see text). The thickness of arm II is about 25 Å, comparable to that of membrane. **b**, Helices are shown in orange and  $\beta$ -sheets in green. **c**, View along the two-fold axis of the dimer showing the relative displacement of the monomers and apparent in **a**. The  $\beta$ -sheets of the dimer interface are labelled. **d**, View of one monomer from the bottom of arm I as shown in **a**, towards arm II, showing the ATP-binding pocket. **e**, The protein and the bound ATP are in ribbon and ball-and-stick representations, respectively. Key residues discussed in the text are indicated in **c**. These figures were prepared with MOLSCRIPT (Cambridge University).

## NOVEL APPROACH TO QUANTITATIVE POLYMERASE CHAIN REACTION USING REAL-TIME DETECTION: APPLICATION TO THE DETECTION OF GENE AMPLIFICATION IN BREAST CANCER

Yvan Bleche<sup>1</sup>, Marine Ouilvi<sup>1</sup>, Marie-Hélène Châmpredaz<sup>1</sup>, Dominique Vignat<sup>2</sup>, Rosine Libereau<sup>1</sup> and Michel Vignat<sup>1</sup>

<sup>1</sup>Laboratoire de Génétique Moléculaire, Faculté des Sciences Pharmaceutiques et Biologiques de Paris, Paris, France

<sup>2</sup>Laboratoire d'Oncogénétique, Centre René Huguenin, St-Cloud, France

Gene amplification is a common event in the progression of human cancers and amplified oncogenes have been shown to have diagnostic, prognostic and therapeutic relevance. A kinetic quantitative polymerase chain reaction (PCR) method based on fluorescent TaqMan methodology and a new instrument (ABI Prism 7700 Sequence Detection System) capable of measuring fluorescence in real time, was used to quantify gene amplification in tumor DNA. Reactions are characterized by the point during cycling when PCR amplification is still in the exponential phase, rather than the amount of PCR product accumulated after a fixed number of cycles. None of the reaction components is limited during the exponential phase, meaning that values are highly reproducible in reactions starting with the same copy number. This greatly improves the precision of DNA quantification. Moreover, real-time PCR does not require post-PCR sample handling, thereby preventing potential PCR product carryover contamination; it possesses a wide dynamic range of quantification and results in much faster and higher sample throughput. The real-time PCR method was used to develop and validate a simple and rapid assay for the detection and quantification of the 3 most frequently amplified genes (*myc*, *c-myc* and *erbB2*) in breast tumors. Extra copies of *myc*, *c-myc* and *erbB2* were observed in 40, 23 and 35%, respectively of 108 breast tumor DNA; the largest observed number of gene copies were 45, 18 and 15, respectively. These results correlated well with those of Southern blotting. The use of this new semi-automated technique will make molecular analysis of human cancers simpler and more reliable and should find broad applications in clinical and research settings. *Int. J. Cancer* 78:661-666, 1998.

© 1998 Wiley-Liss, Inc.

Gene amplification plays an important role in the pathogenesis of various solid tumors, including breast cancer, probably because overexpression of the amplified target genes confers a selective advantage. The first technique used to detect genomic amplification was cytogenetic analysis. Amplification of several chromosome regions, visualized either as extrachromosomal double minutes (dmins) or as integrated homogeneously staining regions (HSRs), are among the main visible cytogenetic abnormalities in breast tumors. Other techniques such as comparative genomic hybridization (CGH) (Kallioniemi *et al.*, 1994) have also been used in broad searches for regions of increased DNA copy numbers in tumor cells and have revealed some 20 amplified chromosomal regions in breast tumors. Positional cloning efforts are underway to identify the critical gene(s) in each amplified region. To date, genes known to be amplified frequently in breast cancers include *myc* (8/24), *trkA* (1/3), and *erbB2* (17/24) (for review, see Bleche and Libereau, 1995).

Amplification of the *myc*, *c-myc* and *erbB2* proto-oncogenes should have clinical relevance in breast cancer, since independent studies have shown that these alterations can be used to identify subpopulations with a worse prognosis (Berns *et al.*, 1992; Schuurman *et al.*, 1992; Slamon *et al.*, 1987; Moss *et al.*, 1994) suggested that these gene alterations may also be useful for the prediction and assessment of the efficacy of adjuvant chemotherapy and hormone therapy.

However, published results diverge both in terms of the frequency of these alterations and their clinical value. For instance, over 500 studies in 40 years have failed to resolve the controversy

surrounding the link suggested by Slamon *et al.* (1987) between *erbB2* amplification and disease progression. These discrepancies are partly due to the clinical, histological and ethnic heterogeneity of breast cancer, but technical considerations are also probably involved.

Specific genes (DNAs) were initially quantified in tumor cells by means of blotting procedures such as Southern and dot blotting. These batch techniques require large amounts of DNA (5-10  $\mu$ g/reaction) to yield reliable quantitative results. Furthermore, meticulous care is required at all stages of the procedures to generate blots of sufficient quality for reliable dosage analysis. Recently, PCR has proven to be a powerful tool for quantitative DNA analysis, especially with minimal starting quantities of tumor samples (small early stage tumors and formalin-fixed, paraffin-embedded tissues).

Quantitative PCR can be performed by evaluating the amount of product either after a given number of cycles (end-point quantitative PCR) or after a varying number of cycles during the exponential phase (kinetic quantitative PCR). In the first case, an internal standard distinct from the target molecule is required to ascertain PCR efficiency. The method is relatively easy but implies generating, quantifying and storing an internal standard for each gene studied. Nevertheless, it is the most frequently applied method to date.

One of the major advantages of the kinetic method is its rapidity in quantifying a new gene: since no internal standard is required (an external standard curve is sufficient), moreover, the kinetic method has a wide dynamic range (at least 3 orders of magnitude), giving an accurate value for samples differing in their copy number. Unfortunately, the method is cumbersome and has therefore been rarely used. It involves aliquot sampling of each assay mix at regular intervals and quantifying, for each aliquot, the amplification product. Interest in the kinetic method has been stimulated by a novel approach using fluorescent TaqMan methodology and a new instrument (ABI Prism 7700 Sequence Detection System) capable of measuring fluorescence in real time (Ginsberg *et al.*, 1996; Heid *et al.*, 1996). The TaqMan reaction is based on the 5' nuclease assay first described by Holland *et al.* (1991). The latter uses the 5' nuclease activity of Taq polymerase to cleave a specific fluorogenic oligonucleotide probe during the extension phase of PCR. The approach uses dual-labeled fluorogenic hybridization probes (Lee *et al.*, 1993). One fluorescent dye, covalently linked to the 5' end of the oligonucleotide, serves as a reporter (FAM (i.e., 6-carboxy-fluorescein)) and its emission spectrum is quenched by a second fluorescent dye (TAMRA (i.e., 6-carboxy-tetramethyl rhodamine)) attached to the 3' end. During the extension phase of the PCR

Grant sponsors: Association Pour la Recherche sur le Cancer and Ministère de l'Enseignement Supérieur et de la Recherche.

Correspondence to: Laboratoire de Génétique Moléculaire, Faculté des Sciences Pharmaceutiques et Biologiques de Paris, 4 Avenue de l'Observatoire, F-75006 Paris, France. Tel: (33) 1 40 70 1954. E-mail: yvbleche@easnet.fr

Received 2 May 1998; Revised 30 June 1998

of extensive degradation) are both difficult to assess. We therefore also quantified a control gene (*gHb*) mapping to chromosome region 10p11-q13, in which no genetic alterations have been found in breast tumor DNA by means of CGH [Kallioniemi *et al.*, 1994].

Thus, the ratio of the copy number of the target gene to the copy number of the *alb* gene normalizes the amount and quality of genomic DNA. The ratio defining the level of amplification is termed 'N', and is determined as follows:

$$N = \frac{\text{copy number of target gene (app. myc. cent.) (ethB)}}{\text{copy number of reference gene (d/b)}}$$

**Primer, probes, reference human genomic DNA and PCR consumables.** Primers and probes were chosen with the assistance of the computer programs Oligo 4.0 (National Biosciences, Plymouth, MN), EuGene (Dambien Systems, Cincinnati, OH) and Primer Express (Perkin-Elmer Applied Biosystems, Foster City, CA).

Here, we applied this semi-automated procedure to determine the copy number of the 3 most frequently amplified genes in breast tumours (*myc*, *erbB1* and *erbB2*), as well as 2 genes (*alb* and *apf*) located in a chromosome region in which no genetic changes have been observed in breast tumours. The results for 108 breast tumours were compared with previous Southern blot data for the same samples.

Samples were obtained from 108 primary breast tumors removed surgically from patients at the Centre René Haddad in 1996. Of the 108 patients, 44 had undergone radiotherapy or chemotherapy immediately after surgery; the tumor samples were placed in liquid nitrogen and extraction of high-molecular-weight DNA. Patients were included in this study if the tumor sample used for DNA preparation contained more than 50% of tumor cells (histological analysis). A blood sample was also taken from 18 of the same patients.

**Theoretical basis.** Reactions are characterized by the point during cycling when amplification of the PCR product is first detected, rather than by the amount of PCR product accumulated after a fixed number of cycles. The higher the starting copy number of the genomic DNA target, the earlier a significant increase in fluorescence is observed. The parameter  $C_t$  (threshold cycle) is defined as the fractional cycle number at which the fluorescence generated by cleavage of the probe passes a fixed threshold above baseline. The target gene copy number in unknown samples is quantified by measuring  $C_t$  and by using a standard curve to determine the starting copy number. The precise amount of genomic DNA (based on optical density and usually 1.25  $\mu$ l) is

**Standard curve construction.** The kinetic method requires a standard curve. The latter was constructed with serial dilutions of specific PCR products, according to Ptáček *et al.* (1993). In practice, each specific PCR product was obtained by amplifying 10 ng of a standard human genomic DNA (Boehringer, Mannheim, Germany) with the same primer pairs as those used later for real-time quantitative PCR. These PCR products were purified using MicroSpin S-400 HR columns (Pharmacia, Uppsala, Sweden), electrophoresed through an acrylamide gel, and stained with ethidium bromide to check their quality. The PCR products were then quantified spectrophotometrically and pooled and serially diluted 10-fold in mouse genomic DNA (Clontech, Palo Alto, CA) at a constant concentration of 2 ng/μl. The standard curve used for real-time quantitative PCR was based on serial dilutions of the pool of PCR products ranging from  $10^2$  (0.03 copies of each gene) to  $10^7$  (10<sup>3</sup> copies). This series of diluted PCR products was aliquoted and stored at -80°C until use.

**PCR amplification.** Amplification mixes (30 µl) contained the sample DNA (around 20 ng, around 6600 copies of genomic genes), 10× TaqMan buffer (5 µl), 200 µM dATP, dCTP, dGTP, and 400 µM dUTP, 5 mM MgCl<sub>2</sub>, 1.25 units of AmpliTaq Gold, 4.5 units of Amperase Uracil-N-glycosylase (UNG), 200 nM each primer, and 100 nM probe. The thermal cycling conditions comprised 2 min at 90°C and 10 min at 95°C. Thermal cycling consisted of 40 cycles at 95°C for 15 s and 65°C for 1 min. Each assay included a standard curve (from 10<sup>1</sup> to 10<sup>6</sup> copies) in duplicate, a no-template control, 20 ng and 50 ng of calibrator human genomic DNA (Boehringer) in triplicate, and about 20 ng of unknown genomic DNA in triplicate (26 samples can thus be analyzed on a 96-well microplate). All samples with a coefficient of variation (CV) higher than 10% were rejected.

**Equipment for real-time detection.** The 7400 system has a built-in thermal cyclers and a laser directed via fiber-optical cables to each of the 96 sample wells. A charge-coupled device (CCD) camera collects the emission from each sample and the data are analyzed automatically. The software accompanying the 9200 system calculates  $C_{50}$  and determines the starting copy number in the samples.

**Determination of gene amplification.** Gene amplification was calculated as described above. Only samples with an  $N$  value higher than 2 were considered to be amplified.

### RESULTS

To validate the method, real-time PCR was performed on genomic DNA extracted from 108 primary breast tumors and 18 normal leukocyte DNA samples from some of the same patients. The target genes were the *myc*, *cond1*, and *erbB2* proto-oncogenes and the B-amyloid precursor protein gene (*app*), which maps to a chromosome region (21q21.2) in which no genomic alterations have been found in breast tumors (Kallioniemi *et al.*, 1994). The reference disomic gene was the albumin gene (*alb*) (chromosome 4q11-q13).

### Validation of the standard curve and dynamic range of real-time PCR

The standard curve was constructed from PCR products serially diluted in genomic mouse DNA at a constant concentration of 2 ng/ $\mu$ l. It should be noted that the 3 primer pairs chosen to analyze the 3 target genes do not amplify genomic mouse DNA (data not shown). Figure 1 shows the real-time PCR standard curve for the *alb* gene. The dynamic range was wide (at least 4 orders of magnitude), with samples containing as few as  $10^1$  copies or as many as  $10^5$  copies.

### Copy number ratio of the 2 reference genes (*app* and *alb*)

The *app* to *alb* copy number ratio was determined on 18 normal leukocyte DNA samples and all 108 primary breast tumor DNA

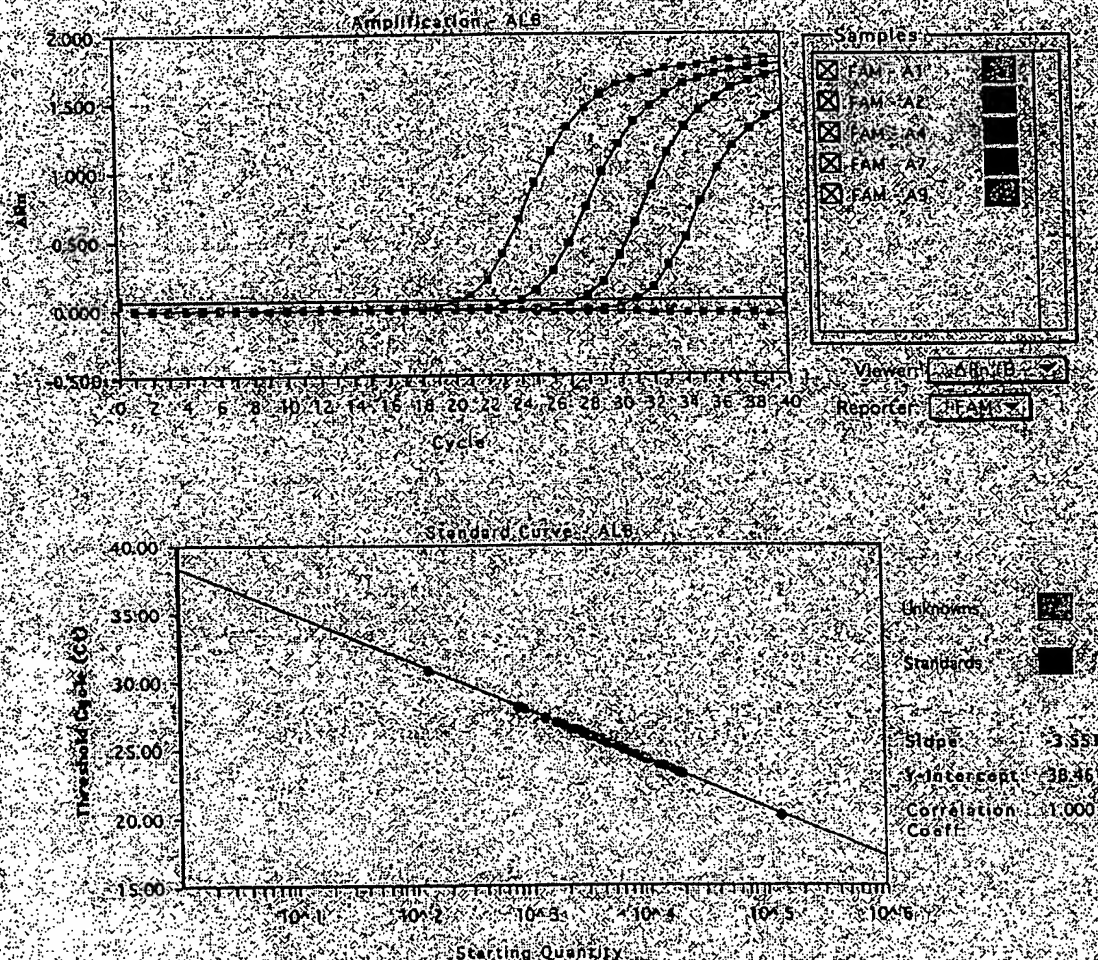


**FIGURE 1.** Albumin (*alb*) gene dosage by real-time PCR. Top: Amplification plots for reactions with starting *alb* gene copy number ranging from  $10^5$  (A9) to  $10^1$  (A2) and no template control (A1). Cycle number is plotted as change in normalized reporter signal ( $\Delta Rn$ ). For each reaction tube, the fluorescence signal of the reporter dye (FAM) is divided by the fluorescence signal of the passive reference dye (ROX) to obtain  $Rn$ , defined as the normalized reporter signal.  $\Delta Rn$  represents the normalized reporter signal ( $Rn$ ) minus the baseline signal established in the first 4 PCR cycles. This increase during PCR as *alb* PCR product copy number increases until the reaction reaches a plateau.  $C_t$  (threshold cycle) represents the fractional cycle number at which a significant increase in  $Rn$  above a baseline signal (horizontal black line) can first be detected. Two replicate plots were performed for each standard sample, but the data for only one are shown here. Bottom: Standard curve plotting log starting copy number ( $C_t$  threshold cycle). The black dots represent the data for standard samples plotted in duplicate and the red dots the data for unknown genomic DNA samples plotted in triplicate. The standard curve shows 4 orders of linear dynamic range.

**IN THE UNITED STATES PATENT AND TRADEMARK OFFICE**

Applicant : Ashkenazi et al.  
 App. No. : 09/903,925  
 Filed : July 11, 2001  
 For : SECRETED AND  
 TRANSMEMBRANE  
 POLYPEPTIDES AND NUCLEIC  
 ACIDS ENCODING THE SAME  
 Examiner : Hamud, Fozia M

Group Art Unit 1647

**CERTIFICATE OF EXPRESS MAILING**

I hereby certify that this correspondence is being deposited with the United States Postal Service with sufficient postage as first class mail in an envelope addressed to Commissioner of Patents, Washington D.C. 20231 on:

(Date)

Commissioner of Patents  
 P.O. Box 1450  
 Alexandria, VA 22313-1450

**DECLARATION OF AVI ASHKENAZI, Ph.D UNDER 37 C.F.R. § 1.132**

I, Avi Ashkenazi, Ph.D. declare and say as follows: -

1. I am Director and Staff Scientist at the Molecular Oncology Department of Genentech, Inc., South San Francisco, CA 94080.
2. I joined Genentech in 1988 as a postdoctoral fellow. Since then, I have investigated a variety of cellular signal transduction mechanisms, including apoptosis, and have developed technologies to modulate such mechanisms as a means of therapeutic intervention in cancer and autoimmune disease. I am currently involved in the investigation of a series of secreted proteins over-expressed in tumors, with the aim to identify useful targets for the development of therapeutic antibodies for cancer treatment.
3. My scientific Curriculum Vitae, including my list of publications, is attached to and forms part of this Declaration (Exhibit A).
4. Gene amplification is a process in which chromosomes undergo changes to contain multiple copies of certain genes that normally exist as a single copy, and is an important factor in the pathophysiology of cancer. Amplification of certain genes (e.g., Myc or Her2/Neu)

gives cancer cells a growth or survival advantage relative to normal cells, and might also provide a mechanism of tumor cell resistance to chemotherapy or radiotherapy.

5. If gene amplification results in over-expression of the mRNA and the corresponding gene product, then it identifies that gene product as a promising target for cancer therapy, for example by the therapeutic antibody approach. Even in the absence of over-expression of the gene product, amplification of a cancer marker gene - as detected, for example, by the reverse transcriptase TaqMan<sup>®</sup> PCR or the fluorescence *in situ* hybridization (FISH) assays - is useful in the diagnosis or classification of cancer, or in predicting or monitoring the efficacy of cancer therapy. An increase in gene copy number can result not only from intrachromosomal changes but also from chromosomal aneuploidy. It is important to understand that detection of gene amplification can be used for cancer diagnosis even if the determination includes measurement of chromosomal aneuploidy. Indeed, as long as a significant difference relative to normal tissue is detected, it is irrelevant if the signal originates from an increase in the number of gene copies per chromosome and/or an abnormal number of chromosomes.

6. I understand that according to the Patent Office, absent data demonstrating that the increased copy number of a gene in certain types of cancer leads to increased expression of its product, gene amplification data are insufficient to provide substantial utility or well established utility for the gene product (the encoded polypeptide), or an antibody specifically binding the encoded polypeptide. However, even when amplification of a cancer marker gene does not result in significant over-expression of the corresponding gene product, this very absence of gene product over-expression still provides significant information for cancer diagnosis and treatment. Thus, if over-expression of the gene product does not parallel gene amplification in certain tumor types but does so in others, then parallel monitoring of gene amplification and gene product over-expression enables more accurate tumor classification and hence better determination of suitable therapy. In addition, absence of over-expression is crucial information for the practicing clinician. If a gene is amplified but the corresponding gene product is not over-expressed, the clinician accordingly will decide not to treat a patient with agents that target that gene product.

7. I hereby declare that all statements made herein of my own knowledge are true and that all statements made on information or belief are believed to be true, and further that these statements were made with the knowledge that willful false statements and the like so

made are punishable by fine or imprisonment, or both, under Section 1001 of Title 18 of the United States Code and that such willful statements may jeopardize the validity of the application or any patent issued thereon.

By: Avi Ashkenazi  
Avi Ashkenazi, Ph.D.

Date: 9/15/03

## **CURRICULUM VITAE**

**Avi Ashkenazi**

**July 2003**

### **Personal:**

Date of birth: 29 November, 1956  
Address: 1456 Tarrytown Street, San Mateo, CA 94402  
Phone: (650) 578-9199 (home); (650) 225-1853 (office)  
Fax: (650) 225-6443 (office)  
Email: aa@gene.com

### **Education:**

1983: B.S. in Biochemistry, with honors, Hebrew University, Israel  
1986: Ph.D. in Biochemistry, Hebrew University, Israel

### **Employment:**

1983-1986: Teaching assistant, undergraduate level course in Biochemistry  
1985-1986: Teaching assistant, graduate level course on Signal Transduction  
1986 - 1988: Postdoctoral fellow, Hormone Research Dept., UCSF, and  
Developmental Biology Dept., Genentech, Inc., with J. Ramachandran  
1988 - 1989: Postdoctoral fellow, Molecular Biology Dept., Genentech, Inc.,  
with D. Capon  
1989 - 1993: Scientist, Molecular Biology Dept., Genentech, Inc.  
1994 -1996: Senior Scientist, Molecular Oncology Dept., Genentech, Inc.  
1996-1997: Senior Scientist and Interim director, Molecular Oncology Dept.,  
Genentech, Inc.  
1997-1990: Senior Scientist and preclinical project team leader, Genentech, Inc.  
1999 -2002: Staff Scientist in Molecular Oncology, Genentech, Inc.  
2002-present: Staff Scientist and Director in Molecular Oncology, Genentech, Inc.

### **Awards:**

1988: First prize, The Boehringer Ingelheim Award

**Editorial:**

Editorial Board Member: *Current Biology*

Associate Editor, Clinical Cancer Research.

Associate Editor, Cancer Biology and Therapy.

**Refereed papers:**

1. Gertler, A., Ashkenazi, A., and Madar, Z. Binding sites for human growth hormone and ovine and bovine prolactins in the mammary gland and liver of the lactating cow. *Mol. Cell. Endocrinol.* 34, 51-57 (1984).
2. Gertler, A., Shamay, A., Cohen, N., Ashkenazi, A., Friesen, H., Levanon, A., Gorecki, M., Aviv, H., Hadari, D., and Vogel, T. Inhibition of lactogenic activities of ovine prolactin and human growth hormone (hGH) by a novel form of a modified recombinant hGH. *Endocrinology* 118, 720-726 (1986).
3. Ashkenazi, A., Madar, Z., and Gertler, A. Partial purification and characterization of bovine mammary gland prolactin receptor. *Mol. Cell. Endocrinol.* 50, 79-87 (1987).
4. Ashkenazi, A., Pines, M., and Gertler, A. Down-regulation of lactogenic hormone receptors in Nb2 lymphoma cells by cholera toxin. *Biochemistry Internatl.* 14, 1065-1072 (1987).
5. Ashkenazi, A., Cohen, R., and Gertler, A. Characterization of lactogen receptors in lactogenic hormone-dependent and independent Nb2 lymphoma cell lines. *FEBS Lett.* 210, 51-55 (1987).
6. Ashkenazi, A., Vogel, T., Barash, I., Hadari, D., Levanon, A., Gorecki, M., and Gertler, A. Comparative study on in vitro and in vivo modulation of lactogenic and somatotrophic receptors by native human growth hormone and its modified recombinant analog. *Endocrinology* 121, 414-419 (1987).
7. Peralta, E., Winslow, J., Peterson, G., Smith, D., Ashkenazi, A., Ramachandran, J., Schimerlik, M., and Capon, D. Primary structure and biochemical properties of an M2 muscarinic receptor. *Science* 236, 600-605 (1987).
8. Peralta, E., Ashkenazi, A., Winslow, J., Smith, D., Ramachandran, J., and Capon, D. J. Distinct primary structures, ligand-binding properties and tissue-specific expression of four human muscarinic acetylcholine receptors. *EMBO J.* 6, 3923-3929 (1987).
9. Ashkenazi, A., Winslow, J., Peralta, E., Peterson, G., Schimerlik, M., Capon, D., and Ramachandran, J. An M2 muscarinic receptor subtype coupled to both adenylyl cyclase and phosphoinositide turnover. *Science* 238, 672-675 (1987).

10. Pines, M., Ashkenazi, A., Cohen-Chapnik, N., Binder, L., and Gertler, A. Inhibition of the proliferation of Nb2 lymphoma cells by femtomolar concentrations of cholera toxin and partial reversal of the effect by 12-o-tetradecanoyl-phorbol-13-acetate. *J. Cell. Biochem.* 37, 119-129 (1988).
11. Peralta, E., Ashkenazi, A., Winslow, J., Ramachandran, J., and Capon, D. Differential regulation of PI hydrolysis and adenylyl cyclase by muscarinic receptor subtypes. *Nature* 334, 434-437 (1988).
12. Ashkenazi, A., Peralta, E., Winslow, J., Ramachandran, J., and Capon, D. Functionally distinct G proteins couple different receptors to PI hydrolysis in the same cell. *Cell* 56, 487-493 (1989).
13. Ashkenazi, A., Ramachandran, J., and Capon, D. Acetylcholine analogue stimulates DNA synthesis in brain-derived cells via specific muscarinic acetylcholine receptor subtypes. *Nature* 340, 146-150 (1989).
14. Lammare, D., Ashkenazi, A., Fleury, S., Smith, D., Sekaly, R., and Capon, D. The MHC-binding and gp120-binding domains of CD4 are distinct and separable. *Science* 245, 743-745 (1989).
15. Ashkenazi, A., Presta, L., Marsters, S., Camerato, T., Rosenthal, K., Fendly, B., and Capon, D. Mapping the CD4 binding site for human immunodeficiency virus type 1 by alanine-scanning mutagenesis. *Proc. Natl. Acad. Sci. USA.* 87, 7150-7154 (1990).
16. Chamow, S., Peers, D., Byrn, R., Mulkerrin, M., Harris, R., Wang, W., Bjorkman, P., Capon, D., and Ashkenazi, A. Enzymatic cleavage of a CD4 immunoadhesin generates crystallizable, biologically active Fd-like fragments. *Biochemistry* 29, 9885-9891 (1990).
17. Ashkenazi, A., Smith, D., Marsters, S., Riddle, L., Gregory, T., Ho, D., and Capon, D. Resistance of primary isolates of human immunodeficiency virus type 1 to soluble CD4 is independent of CD4-rgp120 binding affinity. *Proc. Natl. Acad. Sci. USA.* 88, 7056-7060 (1991).
18. Ashkenazi, A., Marsters, S., Capon, D., Chamow, S., Figari, I., Pennica, D., Goddard, D., Palladino, M., and Smith, D. Protection against endotoxic shock by a tumor necrosis factor receptor immunoadhesin. *Proc. Natl. Acad. Sci. USA.* 88, 10535-10539 (1991).
19. Moore, J., McKeating, J., Huang, Y., Ashkenazi, A., and Ho, D. Virions of primary HIV-1 isolates resistant to sCD4 neutralization differ in sCD4 affinity and glycoprotein gp120 retention from sCD4-sensitive isolates. *J. Virol.* 66, 235-243 (1992).

20. Jin, H., Oksenberg, D., Ashkenazi, A., Peroutka, S., Duncan, A., Rozmahel, R., Yang, Y., Mengod, G., Palacios, J., and O'Dowd, B. Characterization of the human 5-hydroxytryptamine<sub>1B</sub> receptor. *J. Biol. Chem.* 267, 5735-5738 (1992).
21. Marsters, A., Frutkin, A., Simpson, N., Fendly, B. and Ashkenazi, A. Identification of cysteine-rich domains of the type 1 tumor necrosis receptor involved in ligand binding. *J. Biol. Chem.* 267, 5747-5750 (1992).
22. Chamow, S., Kogan, T., Peers, D., Hastings, R., Byrn, R., and Ashkenazi, A. Conjugation of sCD4 without loss of biological activity via a novel carbohydrate-directed cross-linking reagent. *J. Biol. Chem.* 267, 15916-15922 (1992).
23. Oksenberg, D., Marsters, A., O'Dowd, B., Jin, H., Havlik, S., Peroutka, S., and Ashkenazi, A. A single amino-acid difference confers major pharmacologic variation between human and rodent 5-HT<sub>1B</sub> receptors. *Nature* 360, 161-163 (1992).
24. Haak-Frendscho, M., Marsters, S., Chamow, S., Peers, D., Simpson, N., and Ashkenazi, A. Inhibition of interferon  $\gamma$  by an interferon  $\gamma$  receptor immunoadhesin. *Immunology* 79, 594-599 (1993).
25. Penica, D., Lam, V., Weber, R., Kohr, W., Basa, L., Spellman, M., Ashkenazi, A. Shire, S., and Goeddel, D. Biochemical characterization of the extracellular domain of the 75-kd tumor necrosis factor receptor. *Biochemistry* 32, 3131-3138. (1993).
26. Barford, L., Zheng, Y., Kuang, W., Hart, M., Evans, T., Cerione, R., and Ashkenazi, A. Cloning and expression of a human CDC42 GTPase Activating Protein reveals a functional SH3-binding domain. *J. Biol. Chem.* 268, 26059-26062 (1993).
27. Chamow, S., Zhang, D., Tan, X., Mhtre, S., Marsters, S., Peers, D., Byrn, R., Ashkenazi, A., and Yunghans, R. A humanized bispecific immunoadhesin-antibody that retargets CD3<sup>+</sup> effectors to kill HIV-1-infected cells. *J. Immunol.* 153, 4268-4280 (1994).
28. Means, R., Krantz, S., Luna, J., Marsters, S., and Ashkenazi, A. Inhibition of murine erythroid colony formation in vitro by interferon  $\gamma$  and correction by interferon  $\gamma$  receptor immunoadhesin. *Blood* 83, 911-915 (1994).
29. Haak-Frendscho, M., Marsters, S., Mordenti, J., Gillet, N., Chen, S., and Ashkenazi, A. Inhibition of TNF by a TNF receptor immunoadhesin: comparison with an anti-TNF mAb. *J. Immunol.* 152, 1347-1353 (1994).

30. Chamow, S., Kogan, T., Venuti, M., Gadek, T., Peers, D., Mordenti, J., Shak, S., and Ashkenazi, A. Modification of CD4 immunoadhesin with monomethoxy-PEG aldehyde via reductive alkylation. *Bioconj. Chem.* 5, 133-140 (1994).
31. Jin, H., Yang, R., Marsters, S., Bunting, S., Wurm, F., Chamow, S., and Ashkenazi, A. Protection against rat endotoxic shock by p55 tumor necrosis factor (TNF) receptor immunoadhesin: comparison to anti-TNF monoclonal antibody. *J. Infect. Diseases* 170, 1323-1326 (1994).
32. Beck, J., Marsters, S., Harris, R., Ashkenazi, A., and Chamow, S. Generation of soluble interleukin-1 receptor from an immunoadhesin by specific cleavage. *Mol. Immunol.* 31, 1335-1344 (1994).
33. Pitti, B., Marsters, M., Haak-Frendscho, M., Osaka, G., Mordenti, J., Chamow, S., and Ashkenazi, A. Molecular and biological properties of an interleukin-1 receptor immunoadhesin. *Mol. Immunol.* 31, 1345-1351 (1994).
34. Oksenberg, D., Havlik, S., Peroutka, S., and Ashkenazi, A. The third intracellular loop of the 5-HT<sub>2</sub> receptor specifies effector coupling. *J. Neurochem.* 64, 1440-1447 (1995).
35. Bach, E., Szabo, S., Dighe, A., Ashkenazi, A., Aguet, M., Murphy, K., and Schreiber, R. Ligand-induced autoregulation of IFN- $\gamma$  receptor  $\beta$  chain expression in T helper cell subsets. *Science* 270, 1215-1218 (1995).
36. Jin, H., Yang, R., Marsters, S., Ashkenazi, A., Bunting, S., Marra, M., Scott, R., and Baker, J. Protection against endotoxic shock by bactericidal/permeability-increasing protein in rats. *J. Clin. Invest.* 95, 1947-1952 (1995).
37. Marsters, S., Penica, D., Bach, E., Schreiber, R., and Ashkenazi, A. Interferon  $\gamma$  signals via a high-affinity multisubunit receptor complex that contains two types of polypeptide chain. *Proc. Natl. Acad. Sci. USA.* 92, 5401-5405 (1995).
38. Van Zee, K., Moldawer, L., Oldenburg, H., Thompson, W., Stackpole, S., Montegut, W., Rogy, M., Meschter, C., Gallati, H., Schiller, C., Richter, W., Loetcher, H., Ashkenazi, A., Chamow, S., Wurm, F., Calvano, S., Lowry, S., and Lesslauer, W. Protection against lethal *E. coli* bacteremia in baboons by pretreatment with a 55-kDa TNF receptor-Ig fusion protein, Ro45-2081. *J. Immunol.* 156, 2221-2230 (1996).
39. Pitti, R., Marsters, S., Ruppert, S., Donahue, C., Moore, A., and Ashkenazi, A. Induction of apoptosis by Apo-2 Ligand, a new member of the tumor necrosis factor cytokine family. *J. Biol. Chem.* 271, 12687-12690 (1996).

40. Marsters, S., Pitti, R., Donahue, C., Rupert, S., Bauer, K., and Ashkenazi, A. Activation of apoptosis by Apo-2 ligand is independent of FADD but blocked by CrmA. *Curr. Biol.* 6, 1669-1676 (1996).
41. Marsters, S., Skubatch, M., Gray, C., and Ashkenazi, A. Herpesvirus entry mediator, a novel member of the tumor necrosis factor receptor family, activates the NF- $\kappa$ B and AP-1 transcription factors. *J. Biol. Chem.* 272, 14029-14032 (1997).
42. Sheridan, J., Marsters, S., Pitti, R., Gurney, A., Skubatch, M., Baldwin, D., Ramakrishnan, L., Gray, C., Baker, K., Wood, W.I., Goddard, A., Godowski, P., and Ashkenazi, A. Control of TRAIL-induced apoptosis by a family of signaling and decoy receptors. *Science* 277, 818-821 (1997).
43. Marsters, S., Sheridan, J., Pitti, R., Gurney, A., Skubatch, M., Baldwin, D., Huang, A., Yuan, J., Goddard, A., Godowski, P., and Ashkenazi, A. A novel receptor for Apo2L/TRAIL contains a truncated death domain. *Curr. Biol.* 7, 1003-1006 (1997).
44. Marsters, A., Sheridan, J., Pitti, R., Brush, J., Goddard, A., and Ashkenazi, A. Identification of a ligand for the death-domain-containing receptor Apo3. *Curr. Biol.* 8, 525-528 (1998).
45. Rieger, J., Naumann, U., Glaser, T., Ashkenazi, A., and Weller, M. Apo2 ligand: a novel weapon against malignant glioma? *FEBS Lett.* 427, 124-128 (1998).
46. Pender, S., Fell, J., Chamow, S., Ashkenazi, A., and MacDonald, T. A p55 TNF receptor immunoadhesin prevents T cell mediated intestinal injury by inhibiting matrix metalloproteinase production. *J. Immunol.* 160, 4098-4103 (1998).
47. Pitti, R., Marsters, S., Lawrence, D., Roy, Kischkel, F., M., Dowd, P., Huang, A., Donahue, C., Sherwood, S., Baldwin, D., Godowski, P., Wood, W., Gurney, A., Hillan, K., Cohen, R., Goddard, A., Botstein, D., and Ashkenazi, A. Genomic amplification of a decoy receptor for Fas ligand in lung and colon cancer. *Nature* 396, 699-703 (1998).
48. Mori, S., Marakami-Mori, K., Nakamura, S., Ashkenazi, A., and Bonavida, B. Sensitization of AIDS Kaposi's sarcoma cells to Apo-2 ligand-induced apoptosis by actinomycin D. *J. Immunol.* 162, 5616-5623 (1999).
49. Gurney, A. Marsters, S., Huang, A., Pitti, R., Mark, M., Baldwin, D., Gray, A., Dowd, P., Brush, J., Heldens, S., Schow, P., Goddard, A., Wood, W., Baker, K., Godowski, P., and Ashkenazi, A. Identification of a new member of the tumor necrosis factor family and its receptor, a human ortholog of mouse GITR. *Curr. Biol.* 9, 215-218 (1999).

50. Ashkenazi, A., Pai, R., Fong, s., Leung, S., Lawrence, D., Marsters, S., Blackie, C., Chang, L., McMurtrey, A., Hebert, A., DeForge, L., Khoumenis, I., Lewis, D., Harris, L., Bussiere, J., Koeppen, H., Shahrokh, Z., and Schwall, R. Safety and anti-tumor activity of recombinant soluble Apo2 ligand. *J. Clin. Invest.* 104, 155-162 (1999).
51. Chuntharapai, A., Gibbs, V., Lu, J., Ow, A., Marsters, S., Ashkenazi, A., De Vos, A., Kim, K.J. Determination of residues involved in ligand binding and signal transmissiion in the human IFN- $\alpha$  receptor 2. *J. Immunol.* 163, 766-773 (1999).
52. Johnsen, A.-C., Haux, J., Steinkjer, B., Nonstad, U., Egeberg, K., Sundan, A., Ashkenazi, A., and Espevik, T. Regulation of Apo2L/TRAIL expression in NK cells - involvement in NK cell-mediated cytotoxicity. *Cytokine* 11, 664-672 (1999).
53. Roth, W., Isenmann, S., Naumann, U., Kugler, S., Bahr, M., Dichgans, J., Ashkenazi, A., and Weller, M. Eradication of intracranial human malignant glioma xenografts by Apo2L/TRAIL. *Biochem. Biophys. Res. Commun.* 265, 479-483 (1999).
54. Hymowitz, S.G., Christinger, H.W., Fuh, G., Ultsch, M., O'Connell, M., Kelley, R.F., Ashkenazi, A. and de Vos, A.M. Triggering Cell Death: The Crystal Structure of Apo2L/TRAIL in a Complex with Death Receptor 5. *Molec. Cell* 4, 563-571 (1999).
55. Hymowitz, S.G., O'Connel, M.P., Utsch, M.H., Hurst, A., Totpal, K., Ashkenazi, A., de Vos, A.M., Kelley, R.F. A unique zinc-binding site revealed by a high-resolution X-ray structure of homotrimeric Apo2L/TRAIL. *Biochemistry* 39, 633-640 (2000).
56. Zhou, Q., Fukushima, P., DeGraff, W., Mitchell, J.B., Stetler-Stevenson, M., Ashkenazi, A., and Steeg, P.S. Radiation and the Apo2L/TRAIL apoptotic pathway preferentially inhibit the colonization of premalignant human breast cancer cells overexpressing cyclin D1. *Cancer Res.* 60, 2611-2615 (2000).
57. Kischkel, F.C., Lawrence, D. A., Chuntharapai, A., Schow, P., Kim, J., and Ashkenazi, A. Apo2L/TRAIL-dependent recruitment of endogenous FADD and Caspase-8 to death receptors 4 and 5. *Immunity* 12, 611-620 (2000).
58. Yan, M., Marsters, S.A., Grewal, I.S., Wang, H., \*Ashkenazi, A., and \*Dixit, V.M. Identification of a receptor for BlyS demonstrates a crucial role in humoral immunity. *Nature Immunol.* 1, 37-41 (2000).

59. Marsters, S.A., Yan, M., Pitti, R.M., Haas, P.E., Dixit, V.M., and Ashkenazi, A. Interaction of the TNF homologues BLyS and APRIL with the TNF receptor homologues BCMA and TACI. *Curr. Biol.* 10, 785-788 (2000).
60. Kischkel, F.C., and Ashkenazi, A. Combining enhanced metabolic labeling with immunoblotting to detect interactions of endogenous cellular proteins. *Biotechniques* 29, 506-512 (2000).
61. Lawrence, D., Shahrokh, Z., Marsters, S., Achilles, K., Shih, D., Mounho, B., Hillan, K., Totpal, K., DeForge, L., Schow, P., Hooley, J., Sherwood, S., Pai, R., Leung, S., Khan, L., Gliniak, B., Bussiere, J., Smith, C., Strom, S., Kelley, S., Fox, J., Thomas, D., and Ashkenazi, A. Differential hepatocyte toxicity of recombinant Apo2L/TRAIL versions. *Nature Med.* 7, 383-385 (2001).
62. Chuntharapai, A., Dodge, K., Grimmer, K., Schroeder, K., Marsters, S.A., Koeppen, H., Ashkenazi, A., and Kim, K.J. Isotype-dependent inhibition of tumor growth in vivo by monoclonal antibodies to death receptor 4. *J. Immunol.* 166, 4891-4898 (2001).
63. Pollack, I.F., Erff, M., and Ashkenazi, A. Direct stimulation of apoptotic signaling by soluble Apo2L/tumor necrosis factor-related apoptosis-inducing ligand leads to selective killing of glioma cells. *Clin. Cancer Res.* 7, 1362-1369 (2001).
64. Wang, H., Marsters, S.A., Baker, T., Chan, B., Lee, W.P., Fu, L., Tumas, D., Yan, M., Dixit, V.M., \*Ashkenazi, A., and \*Grewal, I.S. TACI-ligand interactions are required for T cell activation and collagen-induced arthritis in mice. *Nature Immunol.* 2, 632-637 (2001).
65. Kischkel, F.C., Lawrence, D. A., Tinel, A., Virmani, A., Schow, P., Gazdar, A., Blenis, J., Arnott, D., and Ashkenazi, A. Death receptor recruitment of endogenous caspase-10 and apoptosis initiation in the absence of caspase-8. *J. Biol. Chem.* 276, 46639-46646 (2001).
66. LeBlanc, H., Lawrence, D.A., Varfolomeev, E., Totpal, K., Morlan, J., Schow, P., Fong, S., Schwall, R., Sinicropi, D., and Ashkenazi, A. Tumor cell resistance to death receptor induced apoptosis through mutational inactivation of the proapoptotic Bcl-2 homolog Bax. *Nature Med.* 8, 274-281 (2002).
67. Miller, K., Meng, G., Liu, J., Hurst, A., Hsei, V., Wong, W-L., Ekert, R., Lawrence, D., Sherwood, S., DeForge, L., Gaudreault, G., Keller, G., Sliwkowski, M., Ashkenazi, A., and Presta, L. Design, Construction, and analyses of multivalent antibodies. *J. Immunol.* 170, 4854-4861 (2003).

68. Varfolomeev, E., Kischkel, F., Martin, F., Wanh, H., Lawrence, D., Olsson, C., Tom, L., Erickson, S., French, D., Schow, P., Crewal, I. and Ashkenazi, A. Immune system development in APRIL knockout mice. Submitted.

Review articles:

1. Ashkenazi, A., Peralta, E., Winslow, J., Ramachandran, J., and Capon, D., J. Functional role of muscarinic acetylcholine receptor subtype diversity. *Cold Spring Harbor Symposium on Quantitative Biology*. LIII, 263-272 (1988).
2. Ashkenazi, A., Peralta, E., Winslow, J., Ramachandran, J., and Capon, D. Functional diversity of muscarinic receptor subtypes in cellular signal transduction and growth. *Trends Pharmacol. Sci.* Dec Supplement, 12-21 (1989).
3. Chamow, S., Duliege, A., Ammann, A., Kahn, J., Allen, D., Eichberg, J., Byrn, R., Capon, D., Ward, R., and Ashkenazi, A. CD4 immunoadhesins in anti-HIV therapy: new developments. *Int. J. Cancer* Supplement 7, 69-72 (1992).
4. Ashkenazi, A., Capon, and D. Ward, R. Immunoadhesins. *Int. Rev. Immunol.* 10, 217-225 (1993).
5. Ashkenazi, A. and Peralta, E. Muscarinic Receptors. In *Handbook of Receptors and Channels*. (S. Peroutka, ed.), CRC Press, Boca Raton, Vol. I, p. 1-27, (1994).
6. Krantz, S. B., Means, R. T., Jr., Lina, J., Marsters, S. A., and Ashkenazi, A. Inhibition of erythroid colony formation in vitro by gamma interferon. In *Molecular Biology of Hematopoiesis* (N. Abraham, R. Shadduck, A. Levine F. Takaku, eds.) Intercept Ltd. Paris, Vol. 3, p. 135-147 (1994).
7. Ashkenazi, A. Cytokine neutralization as a potential therapeutic approach for SIRS and shock. *J. Biotechnology in Healthcare* 1, 197-206 (1994).
8. Ashkenazi, A. and Chamow, S. M. Immunoadhesins: an alternative to human monoclonal antibodies. *Immunomethods: A companion to Methods in Enzymology* 8, 104-115 (1995).
9. Chamow, S., and Ashkenazi, A. Immunoadhesins: Principles and Applications. *Trends Biotech.* 14, 52-60 (1996).
10. Ashkenazi, A. and Chamow, S. M. Immunoadhesins as research tools and therapeutic agents. *Curr. Opin. Immunol.* 9, 195-200 (1997).
11. Ashkenazi, A. and Dixit, V. Death receptors: signaling and modulation. *Science* 281, 1305-1308 (1998).
12. Ashkenazi, A. and Dixit, V. Apoptosis control by death and decoy receptors. *Curr. Opin. Cell. Biol.* 11, 255-260 (1999).

13. Ashkenazi, A. Chapters on Apo2L/TRAIL; DR4, DR5, DcR1, DcR2; and DcR3. Online Cytokine Handbook ([www.apnet.com/cytokinereference/](http://www.apnet.com/cytokinereference/)).
14. Ashkenazi, A. Targeting death and decoy receptors of the tumor necrosis factor superfamily. *Nature Rev. Cancer* 2, 420-430 (2002).
15. LeBlanc, H. and Ashkenazi, A. Apoptosis signaling by Apo2L/TRAIL. *Cell Death and Differentiation* 10, 66-75 (2003).
16. Almasan, A. and Ashkenazi, A. Apo2L/TRAIL: apoptosis signaling, biology, and potential for cancer therapy. *Cytokine and Growth Factor Reviews* 14, 337-348 (2003).

**Book:**

Antibody Fusion Proteins (Chamow, S., and Ashkenazi, A., eds., John Wiley and Sons Inc.) (1999).

**Talks:**

1. Resistance of primary HIV isolates to CD4 is independent of CD4-gp120 binding affinity. UCSD Symposium, HIV Disease: Pathogenesis and Therapy. Greenelefe, FL, March 1991.
2. Use of immuno-hybrids to extend the half-life of receptors. IBC conference on Biopharmaceutical Half-life Extension. New Orleans, LA, June 1992.
3. Results with TNF receptor Immunoadhesins for the Treatment of Sepsis. IBC conference on Endotoxemia and Sepsis. Philadelphia, PA, June 1992.
4. Immunoadhesins: an alternative to human antibodies. IBC conference on Antibody Engineering. San Diego, CA, December 1993.
5. Tumor necrosis factor receptor: a potential therapeutic for human septic shock. American Society for Microbiology Meeting, Atlanta, GA, May 1993.
6. Protective efficacy of TNF receptor immunoadhesin vs anti-TNF monoclonal antibody in a rat model for endotoxic shock. 5th International Congress on TNF. Asilomar, CA, May 1994.
7. Interferon- $\gamma$  signals via a multisubunit receptor complex that contains two types of polypeptide chain. American Association of Immunologists Conference. San Francisco, CA, July 1995.
8. Immunoadhesins: Principles and Applications. Gordon Research Conference on Drug Delivery in Biology and Medicine. Ventura, CA, February 1996.

9. Apo-2 Ligand, a new member of the TNF family that induces apoptosis in tumor cells. Cambridge Symposium on TNF and Related Cytokines in Treatment of Cancer. Hilton-Head, NC, March 1996.
10. Induction of apoptosis by Apo2 Ligand. American Society for Biochemistry and Molecular Biology, Symposium on Growth Factors and Cytokine Receptors. New Orleans, LA, June, 1996.
11. Apo2 ligand; an extracellular trigger of apoptosis. 2nd Clontech Symposium, Palo Alto, CA, October 1996.
12. Regulation of apoptosis by members of the TNF ligand and receptor families. Stanford University School of Medicine, Palo Alto, CA, December 1996.
13. Apo-3: a novel receptor that regulates cell death and inflammation. 4th International Congress on Immune Consequences of Trauma, Shock, and Sepsis. Munich, Germany, March 1997.
14. New members of the TNF ligand and receptor families that regulate apoptosis, inflammation, and immunity. UCLA School of Medicine, LA, CA, March 1997.
15. Immunoadhesins: an alternative to monoclonal antibodies. 5th World Conference on Bispecific Antibodies. Volendam, Holland, June 1997.
16. Control of Apo2L signaling. Cold Spring Harbor Laboratory Symposium on Programmed Cell Death. Cold Spring Harbor, New York. September, 1997.
17. Chairman and speaker, Apoptosis Signaling session. IBC's 4th Annual Conference on Apoptosis. San Diego, CA., October 1997.
18. Control of Apo2L signaling by death and decoy receptors. American Association for the Advancement of Science. Philadelphia, PA, February 1998.
19. Apo2 ligand and its receptors. American Society of Immunologists. San Francisco, CA, April 1998.
20. Death receptors and ligands. 7th International TNF Congress. Cape Cod, MA, May 1998.
21. Apo2L as a potential therapeutic for cancer. UCLA School of Medicine. LA, CA, June 1998.
22. Apo2L as a potential therapeutic for cancer. Gordon Research Conference on Cancer Chemotherapy. New London, NH, July 1998.
23. Control of apoptosis by Apo2L. Endocrine Society Conference, Stevenson, WA, August 1998.
24. Control of apoptosis by Apo2L. International Cytokine Society Conference, Jerusalem, Israel, October 1998.

25. Apoptosis control by death and decoy receptors. American Association for Cancer Research Conference, Whistler, BC, Canada, March 1999.
26. Apoptosis control by death and decoy receptors. American Society for Biochemistry and Molecular Biology Conference, San Francisco, CA, May 1999.
27. Apoptosis control by death and decoy receptors. Gordon Research Conference on Apoptosis, New London, NH, June 1999.
28. Apoptosis control by death and decoy receptors. Arthritis Foundation Research Conference, Alexandria GA, Aug 1999.
29. Safety and anti-tumor activity of recombinant soluble Apo2L/TRAIL. Cold Spring Harbor Laboratory Symposium on Programmed Cell Death. Cold Spring Harbor, NY, September 1999.
30. The Apo2L/TRAIL system: therapeutic potential. American Association for Cancer Research, Lake Tahoe, NV, Feb 2000.
31. Apoptosis and cancer therapy. Stanford University School of Medicine, Stanford, CA, Mar 2000.
32. Apoptosis and cancer therapy. University of Pennsylvania School of Medicine, Philadelphia, PA, Apr 2000.
33. Apoptosis signaling by Apo2L/TRAIL. International Congress on TNF. Trondheim, Norway, May 2000.
34. The Apo2L/TRAIL system: therapeutic potential. Cap-CURE summit meeting. Santa Monica, CA, June 2000.
35. The Apo2L/TRAIL system: therapeutic potential. MD Anderson Cancer Center. Houston, TX, June 2000.
36. Apoptosis signaling by Apo2L/TRAIL. The Protein Society, 14<sup>th</sup> Symposium. San Diego, CA, August 2000.
37. Anti-tumor activity of Apo2L/TRAIL. AAPS annual meeting. Indianapolis, IN Aug 2000.
38. Apoptosis signaling and anti-cancer potential of Apo2L/TRAIL. Cancer Research Institute, UC San Francisco, CA, September 2000.
39. Apoptosis signaling by Apo2L/TRAIL. Kenote address, TNF family Minisymposium, NIH. Bethesda, MD, September 2000.
40. Death receptors: signaling and modulation. Keystone symposium on the Molecular basis of cancer. Taos, NM, Jan 2001.
41. Preclinical studies of Apo2L/TRAIL in cancer. Symposium on Targeted therapies in the treatment of lung cancer. Aspen, CO, Jan 2001.

42. Apoptosis signaling by Apo2L/TRAIL. Weizmann Institute of Science, Rehovot, Israel, March 2001.
43. Apo2L/TRAIL: Apoptosis signaling and potential for cancer therapy. Weizmann Institute of Science, Rehovot, Israel, March 2001.
44. Targeting death receptors in cancer with Apo2L/TRAIL. Cell Death and Disease conference, North Falmouth, MA, Jun 2001.
45. Targeting death receptors in cancer with Apo2L/TRAIL. Biotechnology Organization conference, San Diego, CA, Jun 2001.
46. Apo2L/TRAIL signaling and apoptosis resistance mechanisms. Gordon Research Conference on Apoptosis, Oxford, UK, July 2001.
47. Apo2L/TRAIL signaling and apoptosis resistance mechanisms. Cleveland Clinic Foundation, Cleveland, OH, Oct 2001.
48. Apoptosis signaling by death receptors: overview. International Society for Interferon and Cytokine Research conference, Cleveland, OH, Oct 2001.
49. Apoptosis signaling by death receptors. American Society of Nephrology Conference. San Francisco, CA, Oct 2001.
50. Targeting death receptors in cancer. Apoptosis: commercial opportunities. San Diego, CA, Apr 2002.
51. Apo2L/TRAIL signaling and apoptosis resistance mechanisms. Kimmel Cancer Research Center, Johns Hopkins University, Baltimore MD. May 2002.
52. Apoptosis control by Apo2L/TRAIL. (Keynote Address) University of Alabama Cancer Center Retreat, Birmingham, Ab. October 2002.
53. Apoptosis signaling by Apo2L/TRAIL. (Session co-chair) TNF international conference. San Diego, CA. October 2002.
54. Apoptosis signaling by Apo2L/TRAIL. Swiss Institute for Cancer Research (ISREC). Lausanne, Switzerland. Jan 2003.
55. Apoptosis induction with Apo2L/TRAIL. Conference on New Targets and Innovative Strategies in Cancer Treatment. Monte Carlo. February 2003.
56. Apoptosis signaling by Apo2L/TRAIL. Hermelin Brain Tumor Center Symposium on Apoptosis. Detroit, MI. April 2003.
57. Targeting apoptosis through death receptors. Sixth Annual Conference on Targeted Therapies in the Treatment of Breast Cancer. Kona, Hawaii. July 2003.
58. Targeting apoptosis through death receptors. Second International Conference on Targeted Cancer Therapy. Washington, DC. Aug 2003.

**Issued Patents:**

1. Ashkenazi, A., Chamow, S. and Kogan, T. Carbohydrate-directed crosslinking reagents. US patent 5,329,028 (Jul 12, 1994).
2. Ashkenazi, A., Chamow, S. and Kogan, T. Carbohydrate-directed crosslinking reagents. US patent 5,605,791 (Feb 25, 1997).
3. Ashkenazi, A., Chamow, S. and Kogan, T. Carbohydrate-directed crosslinking reagents. US patent 5,889,155 (Jul 27, 1999).
4. Ashkenazi, A. APO-2 Ligand. US patent 6,030,945 (Feb 29, 2000).
5. Ashkenazi, A., Chuntharapai, A., Kim, J., APO-2 ligand antibodies. US patent 6,046,048 (Apr 4, 2000).
6. Ashkenazi, A., Chamow, S. and Kogan, T. Carbohydrate-directed crosslinking reagents. US patent 6,124,435 (Sep 26, 2000).
7. Ashkenazi, A., Chuntharapai, A., Kim, J., Method for making monoclonal and cross-reactive antibodies. US patent 6,252,050 (Jun 26, 2001).
8. Ashkenazi, A. APO-2 Receptor. US patent 6,342,369 (Jan 29, 2002).
9. Ashkenazi, A., Fong, S., Goddard, A., Gurney, A., Napier, M., Tumas, D., Wood, W. A-33 polypeptides. US patent 6,410,708 (Jun 25, 2002).
10. Ashkenazi, A. APO-3 Receptor. US patent 6,462,176 B1 (Oct 8, 2002).
11. Ashkenazi, A. APO-2L1 and APO-3 polypeptide antibodies. US patent 6,469,144 B1 (Oct 22, 2002).
12. Ashkenazi, A., Chamow, S. and Kogan, T. Carbohydrate-directed crosslinking reagents. US patent 6,582,928B1 (Jun 24, 2003).